FINITE ELEMENT ANALYSES AND EXPERIMENTAL TESTING OF HYBRID COMPOSITE/METAL JOINTS SUBJECTED TO FULLY REVERSED FLEXURE FATIGUE LOADING

Project Report:

Structural Response of Hybrid Ship Connections Subject To Fatigue Loads

by

Douglas Dow, Graduate Research Assistant,

Vincent Caccese, PhD. P.E, Professor and Principal Investigator

Senthil S. Vel, PhD, Associate Professor and Co-Principal Investigator

Prepared for:

Office of Naval Research

800 N Quincy St.

Arlington VA. 22217-5660

Grant No. N00014-05-1-0735

Dr. Roshdy G.S. Barsoum,

Program Manager

University of Maine

Department of Mechanical Engineering

Orono, ME 04469-5711

August 30, 2009

Report No. C-2004-015-RPT-06

FINITE ELEMENT ANALYSES AND EXPERIMENTAL TESTING OF HYBRID COMPOSITE/METAL JOINTS SUBJECTED TO FULLY REVERSED FLEXURE FATIGUE LOADING

Abstract

Glass Reinforced Polymers (GRP's) have good potential for use in naval structures due to their inherent characteristics. High strength, low weight, corrosion resistance, minimal electromagnetic signature, and elaborate forming capabilities are properties which make GRP's advantageous in marine applications. Previous studies have shown that GRP's alone lack the overall stiffness that is necessary for medium to long length ships, however, a ship with a metallic skeleton and composite outer shell could solve this issue. This type of design would require the incorporation of hybrid composite/metal connections, of which a comprehensive study is needed to ensure that structural failures are avoided. Naval vessels must be able to withstand the random and harsh nature of wave loading, which is why a fatigue response evaluation is vital. Special attention must be paid to material connections because this is where failure most often occurs. The goal in this research is to accurately assess the fatigue life of hybrid composite/metal connections focusing upon bolted joints used in removable panels. Experimental testing in flexure fatigue was performed as part of this effort and is essential for fatigue life evaluation. In addition, analytical studies were performed using finite element analysis. Existing finite element modeling software offers a robust method for assessing the structural integrity of proposed hybrid connections. ANSYS™, a finite element modeling program, was used to study the response of two hybrid connection configurations subjected to fully-reversed flexure fatigue loading. A through-the-thickness stress investigation at critical locations in the connection was developed. Variables in the hybrid connection were altered in a parametric study and effects on flexibility and stress were observed. Through the use of various models, a method for predicting the fatigue life in hybrid joints is proposed.

ACKNOWLEDGEMENTS

The authors would like to gratefully acknowledge the funding for this project through the Office of Naval Research under grant number N00014-05-1-0735. The cognizant program officer is Dr. Roshdy G.S. Barsoum. The assistance of UMaine students Brendan Owen, Jacob Folz, Alex Booth, Jeffrey Tifft, Yuezhong Feng and graduate students Radek Glaser and Serdar Yorulmaz was also a major contributing factor to the completion of this work and their help is much appreciated. Also, the support of the UMaine Advanced Manufacturing Center under the direction of John Belding is gratefully acknowledged.

TABLE OF CONTENTS

Page

FINITE ELEMENT ANALYSES AND EXPERIMENTAL TESTING OF HYBRID COMPOSITE/METAL JOINTS SUBJECTED TO FULLY REVERSED FLEXURE FATIGUE LOADING

1. INTRODUCTION

The U.S. Navy currently has an objective to develop higher-speed, stealthier ships to contest existing threats and to enhance future littoral combat capabilities. GRP's (Glass Reinforced Polymers) in particular have built-in characteristics which could help the Navy achieve this goal. Safety of crew members is a primary concern, so prevention of structural failures is essential. When at sea, ships are exposed to harsh oceanic forces and environmental durability of connections and material interfaces is critical because this is where failures are most likely to occur. Fatigue of structural materials is one primary limiting factor in design. Traditional hull construction materials have constrained the ability to build the complex shapes needed for high-speed military support vessels in a cost-effective manner. For these reasons, use of advanced materials in ship construction has been a primary focus of naval research. Although a large ship made completely out of composite material would lack necessary stiffness, a hybrid construction where a steel inner core and composite outer hull exists is a viable alternative.

Extensive fatigue testing of hybrid composite/metal connections must be executed in order to quantify the fatigue life of this type of design and validate its practicality. Fatigue testing, however, is time consuming, and finite element modeling software presents a time-saving way to evaluate the stresses which would occur at the boundary between the two material bodies. Hence the focus of this research is to integrate experimental fatigue testing with finite element modeling to predict the fatigue life of various geometries.

The major goal of this research program is to quantify the fatigue life of hybrid composite/metal joints to be used in complex hydrodynamic hull-forms. Past Office of Naval Research (ONR) funded projects led to the implementation of the work which this paper is focused on. One of these, the Modular Advanced Composite Hull Form (MACH) project, was centered on providing a method for attaching removable composite

panels using hybrid composite/metal connections. A connection arrangement that can hold up to flexural loading is needed for this work, as out-of-plane dynamic loading is a primary concern in that case. A shortage of fatigue data on flexural response of hybrid composite metal connections was disclosed at the projects' completion, and therefore initiated the current work. Corriveau et al. (2008) carried out fully reversed bending fatigue tests at the University of Maine for two baseline hybrid connection configurations: standard bolted, and clamped. A recommendation to execute bolted fatigue tests with different thickness of composites and with higher grade steel is given, with the expectation that those experimental results will be particularly valuable when compared to the standard bolted data already gathered.

An in-depth study of fatigue response of hybrid connections is essential to insure that newly emerging hybrid ship designs will have a high degree of structural integrity. The need for robust methods to evaluate fatigue life in the proposed hybrid joints is evident when the time span required for experimental testing is taken into consideration. Finite element modeling methodologies are executed using ANSYS and outlined to provide the reader with straightforward instructions for successful hybrid joint fatigue analysis.

1.1 Background

Stealth, speed, and lightweight structures have become important concerns in current naval ship designs (Black, 2003). Cost is a major driver in naval vessel design, as with most large structures. The U.S. Navy has a particular interest in how advanced materials can contribute to the robust construction of lightweight vessels to increase structural resistance and overall performance in a cost-efficient manner. Although lighter in weight than steel, issues arise with building a ship completely out of GRP's. The lower natural frequencies associated with the composite would effect the design of sensitive equipment and instrumentation which must be anchored onboard. Additionally, the overall stiffness of the ship would be reduced to potentially unworkable magnitudes. Alm (1983) estimated that a 50m naval ship would be 2.4 times less stiff than its steel counterpart. Maknien et al. (1988) came to virtually the same conclusion in that the deflections would be 3 times greater. A practical solution to these problems is the construction of hybrid

vessels that combine GRP's and steel. One proposed design, and the one which this report is concerned with, is a ship that uses a composite outer shell attached to a metallic skeleton (Barsoum, 2003). This way, equipment which is readily secured to a metal foundation can be, and the steel center can provide the essential overall structural stiffness. Speed and performance can be improved not only by decreasing the overall weight of the ship, but also through the incorporation of modern hydrodynamic shapes in the hull-form. One of the principal cost drivers in developing advanced hull-forms with conventional techniques is in the metal forming of complex shapes. The inherent complex-forming capabilities of composites with little increased cost when compared to flat-panel forming makes them a desirable alternative to metals.

1.1.1 Prior Work Completed at UMaine

The background of the hybrid structures effort at the University of Maine is described in Kabche et al. (2006). The initial studies focused mainly upon development of a watertight hybrid connection. Monotonic and cyclic tests of the joint were used for evaluations. Corriveau et al. (2008) gathered experimental flexure fatigue response data for two hybrid joint configurations: clamped and standard bolted. Figures 1.1 and 1.2 each show the experimental test fixture for the clamped and bolted cases, respectively. Cyclic tests to failure, fatigue tests, intermediate cyclic tests, and residual strength tests were carried out in fully reversed bending fashion for both attachment arrangements. Finite element analyses were carried out to calculate the moment and shear forces that a typical hybrid joint would be subjected to, as part of designing the experimental test setup. Evaluating the composite and metal materials in separate tests would not capture the interactions that occur when the two components are joined together and tested as one body. These differences are primarily due to the type of connection present and the effect of the design details on strength. Corriveau et al. (2008) investigated flexural loading of the connections, since this is one of the principal types of loading that a hybrid panel system in a hull would undergo. A guideline for future studies was established at that project's completion, giving direction for the current research. Additional fatigue testing of the full composite-metal connection is needed to ensure sufficient fatigue response data results.

Figure 1.1 – Clamped Joint Apparatus, Corriveau et al. 2008)

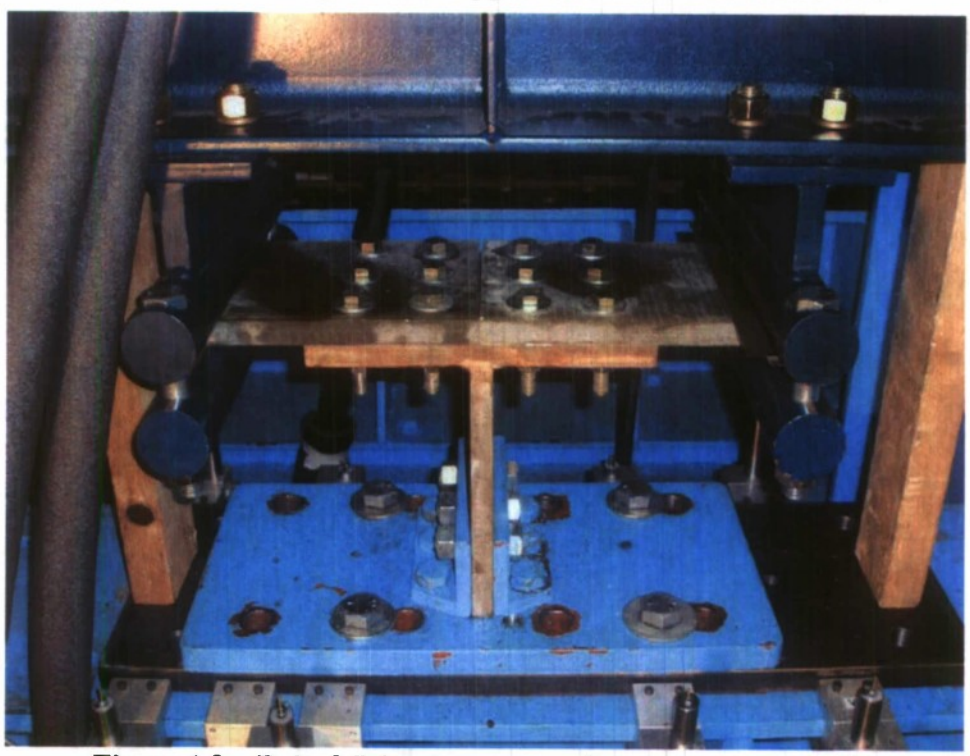

Figure 1.2 – Bolted Joint Apparatus, Corriveau et al. (2008)

Initially, the experimental work by Corriveau et al. (2008) involved determining a representative moment arm length to employ during testing of the connections, which would also lead to more practical geometric detailing of the test articles. The connection arrangement, shown in Figure 1.3, shows the load location, L_p, which controls the ratio of shear force to moment. This ratio will vary at each critical section; which includes the end of the steel-T and the boltline. To establish this needed value, finite element models of representative flat ship hull sections were analyzed, with pressure loading applied to various panel sizes. Figure 1.4 is a depiction of a hydrodynamic lifting body, marking the hybrid panel testing region. Two panel sizes were modeled in ANSYS; a 6'x6' section as well as a 10'x10' section using a similar hybrid shell model. The primary dimensions for the symmetric panel are shown in Figure 1.5. In both instances three parallel stiffeners were included and their rigidities were altered, as they were the primary variable in the evaluation. The stiffeners in the 6'x6' panel had length l_s of 4', while the 10'x10' panel had stiffener lengths l_s of 8'. Three boundary condition cases were studied by Corriveau et al. (2008): a composite plate simply supported at the boundary, a composite plate clamped at the boundary, and a hybrid plate (steel border) clamped at the boundary.

A pressure of 12 psi was applied to the plates in all instances. The results from this analysis gave possible lever arm lengths ranging from 6.23 to 8.85 inches. With the reasoning that shear stresses are typically lower than bending and axial stresses in the hull of a vessel out at sea, the decision was made to use a moment arm value of 8.5in, which was at the upper end of the applicable lever arm range and should yield a conservative strength.

Several styles of testing were executed by Corriveau et al. (2008) on the clamped standard bolted specimens. One cyclic test to failure was performed for each connection type to determine the magnitude at which the fatigue tests would be run. The cyclic test to failure is displacement-controlled, and the joint must endure 3 cycles of positive and negative movement before the displacement level is raised. The GRP Panels tested were

nearly quasi-isotropic with 42 unidirectional layers resulting in ¾" thick laminates, and were attached to a steel tee which had a ¾" thickness. Using ASTM Standard D6507-00 (2005), the particular layup of the composite is denoted as:

$$\left[\left(\pm 45/0/90/\mp 45/90/0\right)_2\left(\pm 45/0/90\right)\overline{(90/0)}\right]_S$$

The maximum loads that the bolted and clamped connections withstood in these tests were 16.2kip and 17.83kip, respectively.

Fatigue tests were carried out in both connection setups for several load amplitudes. A fully reversed harmonic load with a peak value of ±8 kips, approximately 50% of the peak load value, was chosen for the magnitude of the first fatigue test in the bolted configuration. Each bolted fatigue test thereafter was run at fully reversed levels of 7, 6, 5, and 4 kip force values. Based on results from the bolted tests, the clamped fatigue tests were run at fully reversed levels of 8, 7, 6, 6.5, 6, and 5 kip load levels. Results for the cycles to failure for each fatigue test are shown in Table 1.1 quantified by peak load. Prior to and throughout the length of fatigue tests, single-cycle intermediate cyclic tests were carried out by Corriveau (2007). These were load-controlled evaluations run at the fatigue test load magnitude to follow the progressive damage experienced by the connection. In the instance where a particular specimen lasted more than 2 million cycles in a fatigue test, a residual strength test was executed to evaluate the remaining strength left in the hybrid connection. The only instance where 2 million cycles was reached was in the case of the 5 kip clamped joint test.

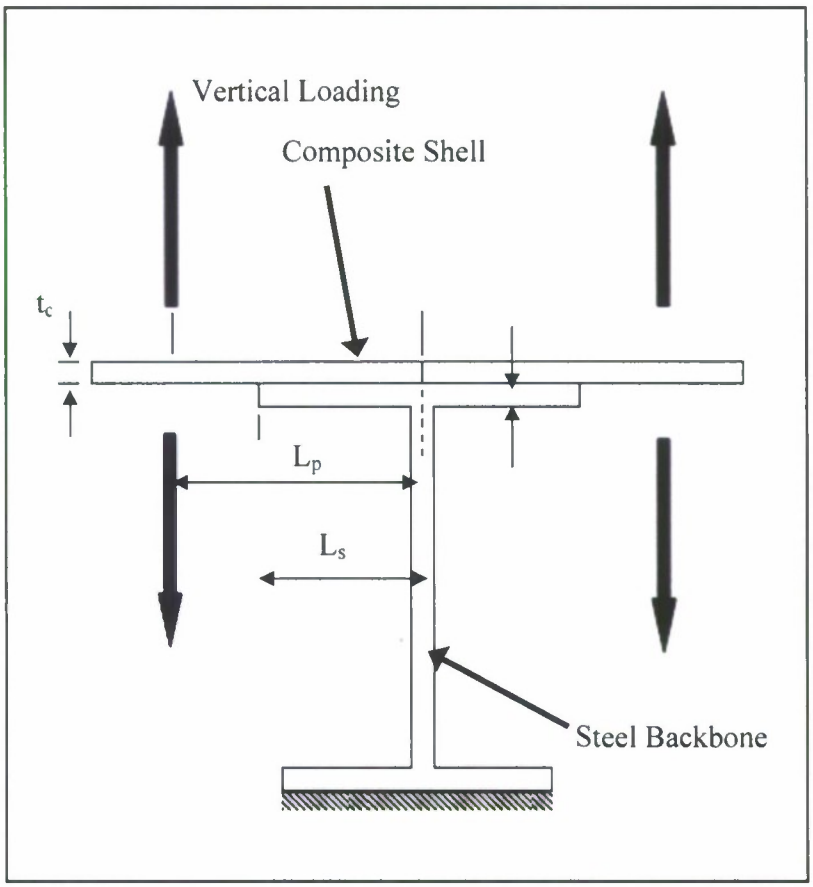

Figure 1.3 – Hybrid Connection

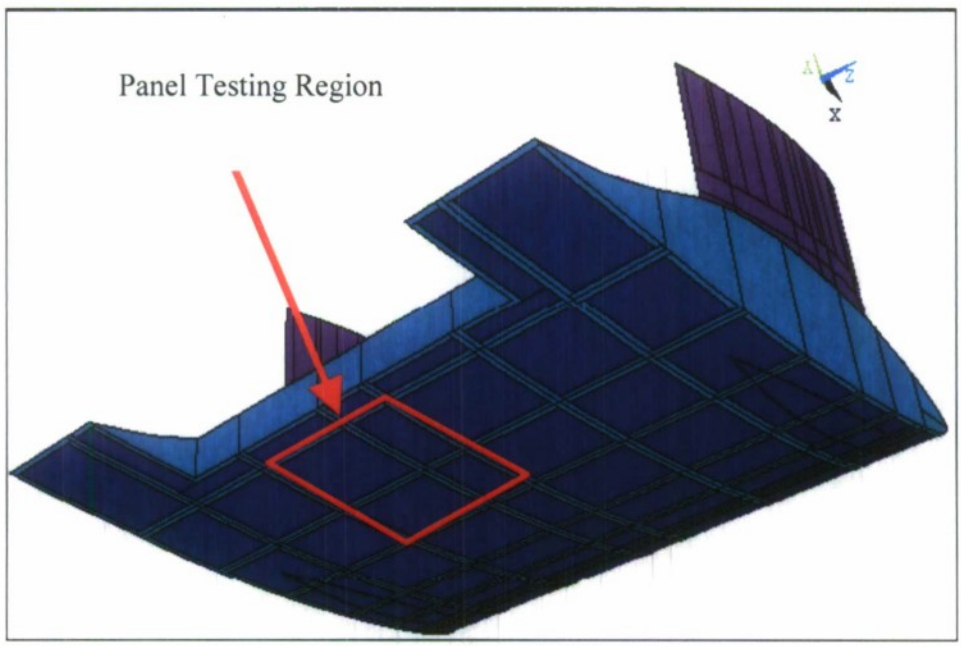

Figure 1.4 – Underwater Lifting Body Showing Panel Testing Region, (Corriveau et al. , 2008)

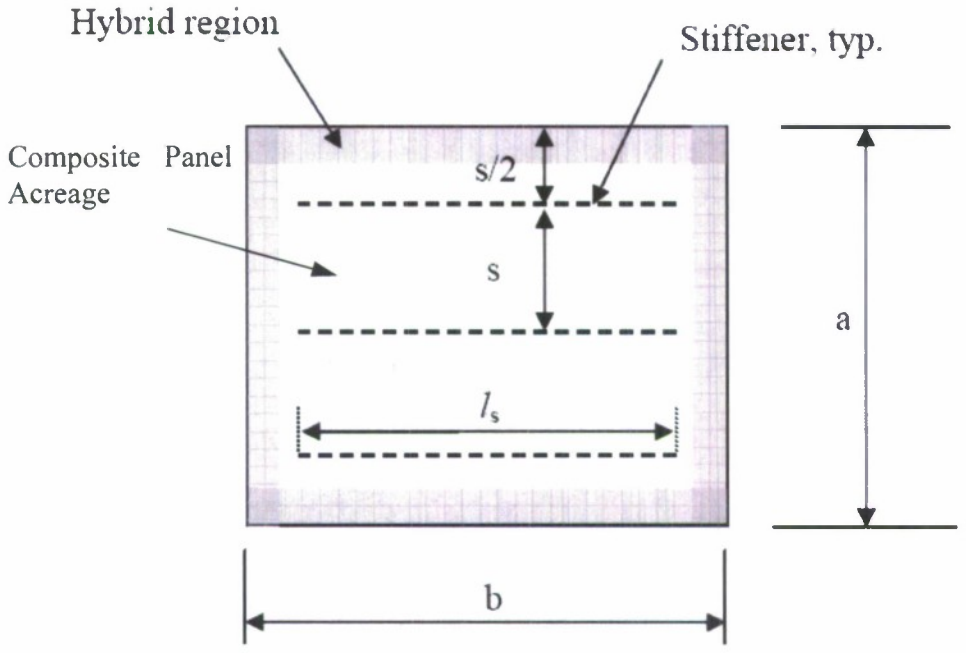

Figure 1.5 – Panel Dimensions Used in Finite Element Model, Corriveau et al. (2008)

Table 1.1 – Cycles to Failure for all Fatigue Tests, Corriveau et al. (2008)

Test Designation	Joint Style	Load Freq. (Hz)	Peak Load (kips)	Cycles to Failure
FC-S1-BP-050-75-001	Bolted	0.50	± 8	7,200
FC-S1-BP-050-75-002	Bolted	0.55	± 7	16,500
FC-S1-BP-050-75-003	Bolted	0.61	± 6	32,500
FC-S1-BP-050-75-004	Bolted	0.67	± 5	170,000
FC-S1-BP-050-75-005	Bolted	0.71	± 4	425,000
FC-S1-CL-000-75-001	Clamped	0.75	± 8	13,500
FC-S1-CL-000-75-002	Clamped	0.75	± 7	75,000
FC-S1-CL-000-75-003	Clamped	0.65	± 6.5	112,000
FC-S1-CL-000-75-004	Clamped	0.75	± 6	550,000
FC-S1-CL-000-75-005	Clamped	0.80	± 5	>2,000,000

Corriveau et al. (2008) used the nominal stress to determine an S-N curve for these joints where the nominal stress computation treats the composite as isotropic. Although not a mathematically correct evaluation of the peak stress, this approach can be used to provide

an indication of fatigue life and is easy to implement. The resulting S-N curves are shown in Figure 1.6.

It is recommended that a more detailed investigation of the stress state be performed and that geometric and material properties be studied. The objective of the current research is to perform a more comprehensive evaluation of the structural response and stress computation and to use computer models to make fatigue life predictions.

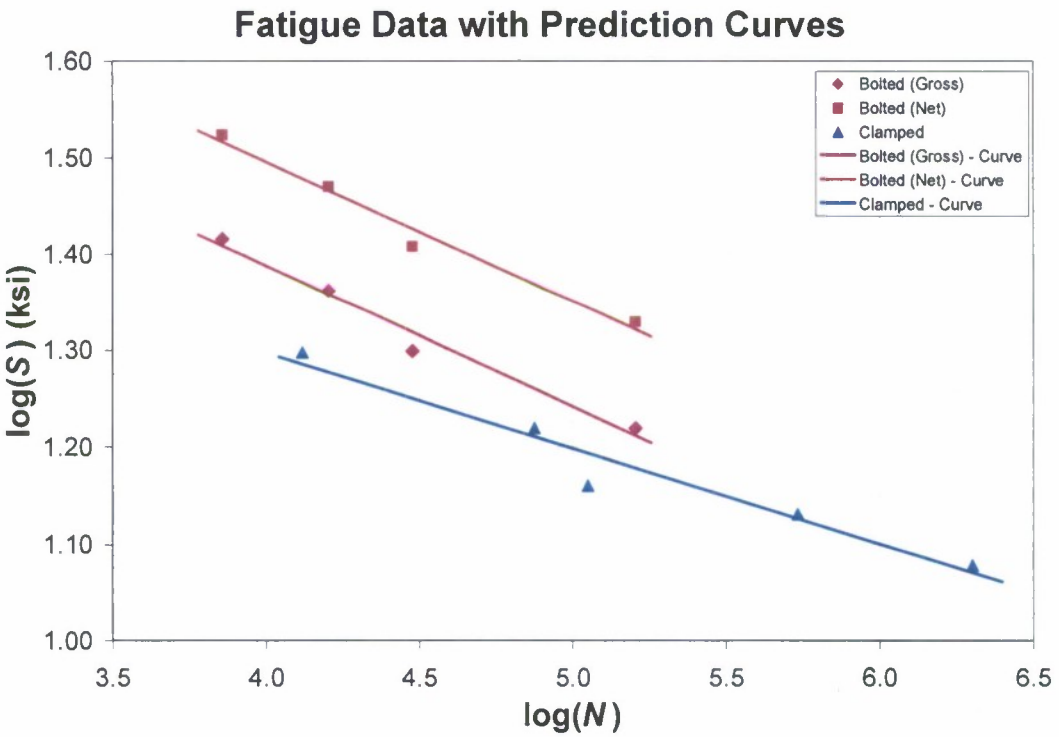

Figure 1.6 – *S-N* Prediction Curves with Fatigue Test Data, Corriveau et al. (2008)

1.2 Objectives

The focus of this research is the out-of-plane fatigue characterization of hybrid composite to metal connections. The principal goal of this research effort is to develop and analyze the fatigue performance of hybrid composite/metallic structural systems and hybrid connection concepts for use in naval ship hulls via finite element analysis. Techniques

for optimization of the geometric and structural parameters of the connections and composite specimens will be developed using ANSYS finite element software. As a secondary objective, experimental research will be implemented to further supplement data gathered by Corriveau et al. (2008) which quantifies the fatigue life of various hybrid joints.

The specific research objectives of this work are:

1. Perform a comprehensive evaluation of the structural response and stress of the composite/metal hybrid joints using computer models to make predictions.

2. Vary geometric and material parameters and observe their effect on fatigue resistance and structural integrity using finite element analysis.

3. Perform a supplemental experimental study of the fatigue response of metal-GRP hybrid connections focusing on bolted connections.

1.3 Scope of Work

Subsequent to this portion of Chapter 1 will be a literature review which encapsulates work done previously in relation to the current work. Experimental data will be presented in Chapter 2, along with an explanation of the experimental test setup, including dimensions, materials, and test types. Instructions for the finite element modeling of each setup using ANSYS will be discussed in Chapter 3. A parametric study with results will be assessed in Chapter 4 which will vary geometric and material properties of the hybrid connection.

1.4 Literature Review

1.4.1 Fatigue of Composite Materials

The damage modes of composite laminates become particularly complex when they are subjected to low cycle fatigue (LCF). Harik and Bogetti (2003) investigated polymer-matrix laminates and the distinctive characteristics of their LCF behavior. For any particular composite material design, experimental data is essential to have confidence in

the predictive capability of any associated fatigue-behavior model. In particular, it has been shown that the fatigue-life predictions that are based on the engineering S–N curves may systematically under-predict the lifespan of composite based structures under LCF loads, which may result in significant errors (i.e., thousands of loading cycles) in structural designs, maintenance/repair planning and structural-safety monitoring (Harik and Bogetti, 2003). That stated, this may result in heavier, "over-designed" structural components, making construction more costly than is necessary and giving larger-than-needed factors of safety.

There are many traditional models for predicting the fatigue life of composite laminates. These are typically based on the idea of measuring the damage accumulation in the material properties, such as residual strength, stiffness and life, which are reliable indications of fatigue life. Whitworth (2000) proposes a mathematical model to investigate the strength degradation based on the residual stiffness degradation. Utilizing this model, a distribution function is obtained and used to predict the residual strength statistical distribution for constant amplitude fatigue loading. The process starts with an equation relating residual stiffness to fatigue life:

$$E(n) = E(N)\left[-h \cdot \ln(n+1) + \left(\frac{E(0)}{E(N)}\right)^{m}\right]^{1/m} \qquad \text{(Eq. 1.1)}$$

where E(n) is the residual stiffness after n fatigue cycles, E(N) is the stiffness at failure, N is the number of cycles to reach failure, and h and m are variables that depend on the applied stress, fatigue loading frequency and environmental conditions. A strain failure criterion, where the stress strain response is assumed to remain linear to failure, is introduced to replace the failure stiffness E(N). Initial stiffness of the specimen before any loading occurs can be expressed as

$$E(0) = \frac{S_U}{\varepsilon_U} \qquad \text{(Eq. 1.2)}$$

where S_U is the ultimate strength and ε_U is the ultimate static strain. The failure stiffness can be expressed as

$$E(N) = \frac{S}{\varepsilon_f} \qquad \text{(Eq. 1.3)}$$

where S is the maximum induced stress and ε_f is the fatigue failure strain. By combining Equations 1.2 and 1.3, the relation can be modified to include nonlinear effects and defined as

$$\frac{S}{S_U} = c_1 \cdot \left[\frac{E(N)}{E(0)}\right]^{c_2} \qquad \text{(Eq. 1.4)}$$

where c_1 and c_2 are constants to be determined experimentally. At failure, n=N and Equation 1.1 can be expressed as

$$E(N) = E(N)\left[-h \cdot \ln(N+1) + \left(\frac{E(0)}{E(N)}\right)^m\right]^{1/m} \qquad \text{(Eq. 1.5)}$$

By substituting Equations 1.4 into Equation 1.5, the following relation may result:

$$N = \exp\left\{\frac{1}{h}\left[\left(\frac{c_1 \cdot S_U}{S}\right)^{m/c_2} - 1\right]\right\} - 1 \qquad \text{(Eq. 1.6)}$$

Equation 1.6 has been proven to predict the fatigue life of AS4-3501-6 graphite/epoxy laminates fairly well. Previous work has shown that the residual strength degradation can be related to fatigue life by the following mathematical model:

$$S_R^{\gamma}(n) = S_U^{\gamma} - g(S) \cdot n \qquad \text{(Eq. 1.7)}$$

where after n cycles $S_R(n)$ is the residual strength, g(S) is a function of the maximum cyclic stress, S, and γ is a constant. At fracture,

$$S_R(n) = S \quad \text{and} \quad n = N \qquad \text{(Eq. 1.8)}$$

and g(S) is expressed as follows:

$$g(S) = \frac{S_U^\gamma - S^\gamma}{N} \qquad \text{(Eq. 1.9)}$$

Using Equations 1.9 and 1.6, Equation 1.7 can be written as

$$S_R^\gamma = S_U^\gamma - J(S_U) \cdot n \qquad \text{(Eq. 1.10)}$$

where

$$J(S_U) = \frac{S_U^\gamma - S^\gamma}{\exp\left\{\frac{1}{h}\left[\left(\frac{c_1 S_U}{S}\right)^{m/c_2} - 1\right]\right\} - 1} \qquad \text{(Eq. 1.11)}$$

A two-parameter Weibull distribution can represent the statistical variable of ultimate strength reasonably well, given by:

$$\begin{aligned} F_{S_U}(y) &= P[S_U \le y] \\ &= 1 - \exp\left[-\left(\frac{y}{\beta}\right)^\alpha\right], y \ge 0 \end{aligned} \qquad \text{(Eq. 1.12)}$$

where $F_{S_U}(y)$ represents the probability that S_U is less than a value y, and α and β denote the shape and scale parameters, respectively. By transforming Equations 1.10 and 1.11, the statistical distribution of residual strength can be denoted as follows:

$$F_{SR}(z) = P[S_R \le z] = P[S_U \le y] = F_{SU}(y) \qquad \text{(Eq. 1.13)}$$

where y and z represent the ultimate and residual strength, respectively. By substituting y and z into Equations 1.10 and 1.11, they are related as follows:

$$z^\gamma = y^\gamma - J(y) \cdot n \qquad \text{(Eq. 1.14)}$$

$$J(y) = \frac{y^\gamma - S^\gamma}{\exp\left\{\frac{1}{h}\left[\left(\frac{c_1 y}{S}\right)^{m/c_2} - 1\right]\right\} - 1} \qquad \text{(Eq. 1.15)}$$

Then from Equations 1.12 and 1.13, the ultimate strength can be denoted as

$$y = \left\{-\ln\left[1 - F_{SR}(z)\right]\right\}^{1/\alpha} \qquad \text{(Eq. 1.16)}$$

where the parameters γ, h, m, c_1, and c_2 are determined experimentally, and Equations 1.14-1.16 have been normalized using the Weibull scale parameter β. Residual strength data and the distribution function denoted by Equation 1.14 is shown in Figure 1.7. The fatigue life prediction made by the model shows there is good agreement with experimental data.

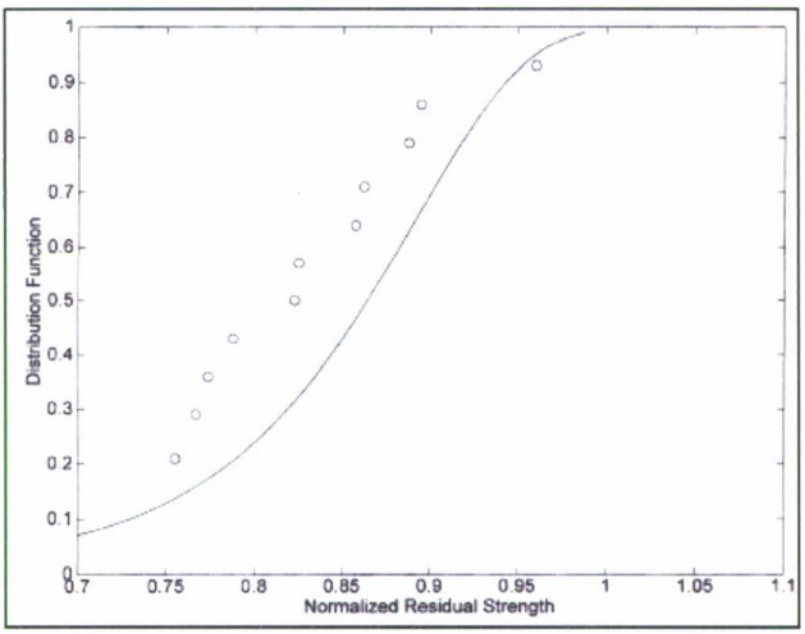

Figure 1.7 – Distribution Function and Corresponding Residual Strength Data Plot, (Whitworth, 2000).

In the analysis of composite plates and beams, transverse shear strain plays an important role. An analysis based on first-order shear deformation theories (FSDT) requires the use of shear correction factors. While accurate as a means of analysis, it can be difficult to determine the shear correcting factors, the determination of which is still a topic of debate. Shi et al. (1998) proposed to use higher-order shear deformation theories (HSDT) as a means of analysis, which requires no shear correcting factors, leading to a model that has the accuracy of the FSDT but is more accessible to use. A difference,

between the FSDT and HSDT modeling analyses, which obtain similarly accurate results, is that the HSDT requires more nodal degrees of freedom, even in the case where the displacement variables are the same. When modeling with HSDT, different strain expressions can be derived, which lead to finite elements involving different nodal variables, changing the accuracy. The author proposes that this difference in the accuracy stems from the order difference on the approximations of element bending strains interpolated from the given nodal variables. Deriving the means for picking out the proper strain expression that typically uses the most accurate elements is a primary purpose, given the number of degrees of freedom that ultimately obtain the most accurate results. This is done through a series of examples that formulate composite beam elements. However, it should be noted that this can be extended to composite plate and shell elements. The conclusion is that in both the analytical results and the numerical results, using an element based on the linear bending strain gives more accurate results, while using the same nodal degrees of freedom. From this, Shi et al. (1998) postulate that based on the data, the expression to be chosen should be the one with the higher order of bending strain interpolation, when using a finite element model based on HSDT.

Composite materials are becoming increasingly more important in many industries and this is especially true, for example, in both the aerospace and naval industries. With a wide range of applications, the strength and stiffness of composite materials are well known to be high. However, it is not yet possible to adequately predict fatigue life for each specific application without actual experimental testing. The objective of work done by Paepegem and Degrieck (2001) is to establish an adequate methodology for numerically modeling the fatigue of composites, in order to save time and money that is traditionally spent on gathering the experimental data. The results in Figure 1.9 were obtained from experimental testing performed on plain-woven glass/epoxy composite panels; the experimental setup for this testing is shown in Figure 1.8. In the figure, the variable L is the distance from point A to B, u_{max} and u_{min} are the maximum and minimum bending-displacements and R_d is the ratio u_{max}/u_{min}. The testing consisted of conducting displacement controlled bending fatigue tests on specimens with the dimensions 2.72mm x 30mm x 145mm with both 0° and 45° layups, respectively. The composite specimen was fixed on one end (as in the case of a cantilever) with the testing

apparatus clamped to the other end, bending the panel at a rate of 2.2 Hz. The data was ascertained using a strain-gauge and the digital phase-shift shadow Moiré method. It can be concluded that by using the digital phase-shift Moiré technique, Paepegem and Degrieck (2001) were able to demonstrate that there is considerable difference between the 0° and 45° stacking sequences. The results of these tests are ostensibly different, with the 45° specimen degrading at a more gradual rate as shown in Figure 1.9. A residual stiffness model is adopted to numerically simulate the fatigue damage behavior. Next, a finite element model is designed with the goals in mind of effectively modeling the residual stiffness degradation while keeping in mind that the model needs to be chronologically economical and efficient. In order to achieve these goals, a cycle-jump approach is used. The cycle-jump principle refers to using not all of the cyclic data, but only specifically chosen intervals. Each Gauss-point, in addition to being assigned the damage variable D, is also assigned the state variable NJUMP1, which is the number of cycles that can be skipped over without losing accuracy for that particular point. Next, looping over all Gauss-point a cumulative relative frequency distribution is developed and the overall cycle jump is determined as a percentile of this frequency distribution. The graph by Paepegem and Degrieck (2001) in Figure 1.10 shows single-sided bending data, obtained using the experimental setup in Figure 1.8, and computer-modeled data comparison. Upon comparing the experimental results with the computer-modeled data, it follows that they agree closely and that this method appears valid.

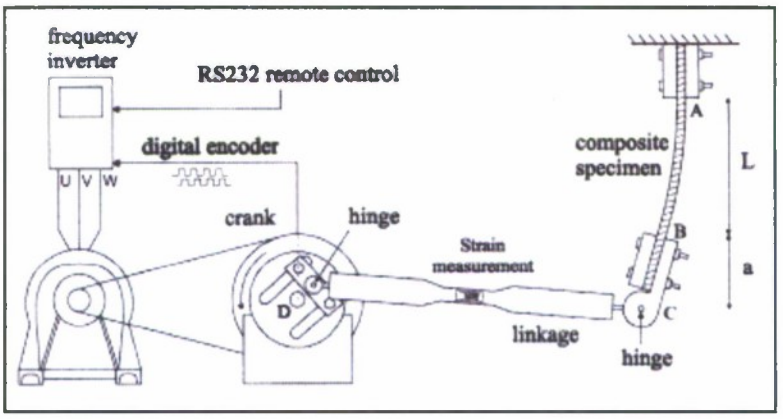

Figure 1.8 – Experimental Setup for Bending Fatigue Tests, (Paepegem & Degrieck, 2001)

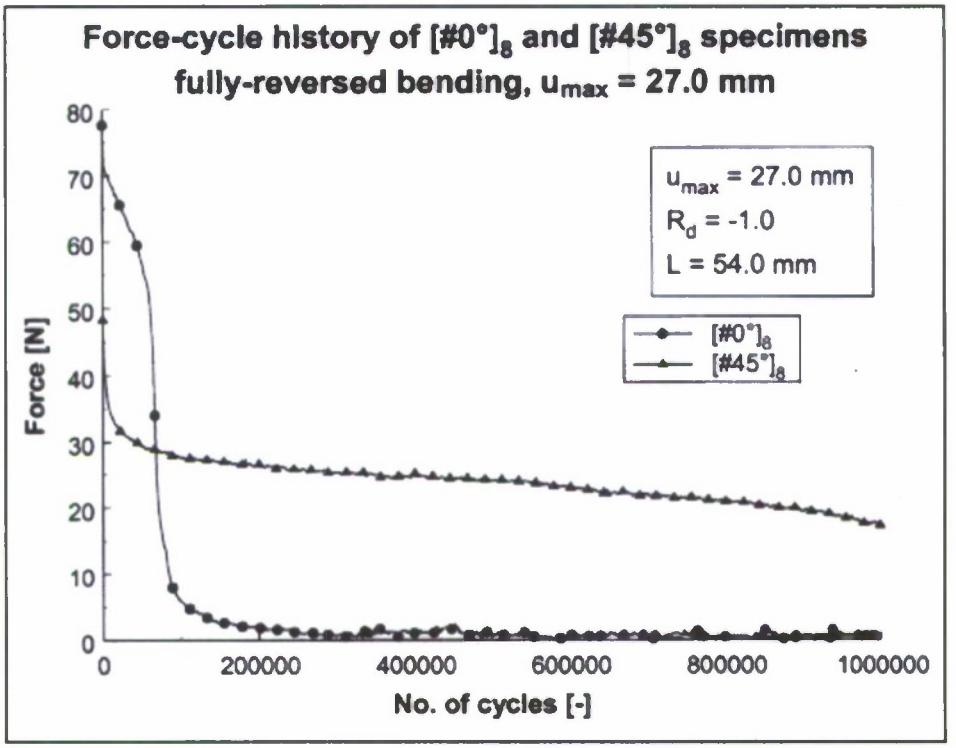

Figure 1.9 – Fully-Reversed Bending Experimental Fatigue Data, (Paepegem & Degrieck, 2001)

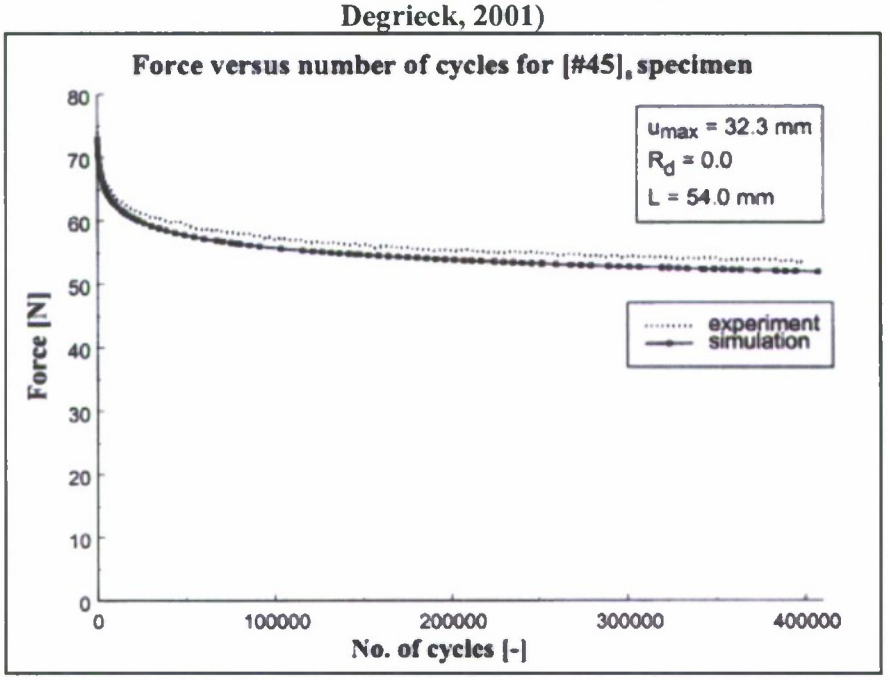

Figure 1.10 – Single-Sided Bending Experimental and Computer-Modeled Fatigue Data, (Paepegem & Degrieck, 2001)

1.4.2 Fatigue of Steel Connections

There has been much research performed on the fatigue life of steel connections, and there are several methods when it comes to predicting fatigue life. Some of the methods include:

- Nominal stress approach.
- Classification according to joint detail.
- Hot spot-stress approach.
- Notch-stress approach.
- Fracture mechanics approach

Approaches that deal with the crack initiation phase of fatigue use the S-N curve for prediction of fatigue life. Kendrick (2005) and Fricke and Kahl (2005) show some of the S-N curve approaches used for crack initiation. Predictive curves for the fatigue life of a connection are constructed based on the number of cycles (N) and the stress level (S). The fatigue response is computed as:

$$N \cdot S^m = A \qquad \text{(Eq. 1.17)}$$

where N is the number of cycles, S is the stress level at the location of ultimate failure, and m and A are constants which determined from results. Linear curves are created by taking the logarithms of both sides of the equation:

$$\log(N) + m\log(S) = \log(A) \qquad \text{(Eq. 1.18)}$$

which can then used to predict fatigue life in comparable connection designs. Miners rule, as described by Kendrick (2005), provides the following model for fatigue prediction:

$$\sum \frac{n_i}{N_i} = 1 \qquad \text{(Eq. 1.19)}$$

where N_i is the number of cycles when ultimate failure occurs for a constant stress amplitude, and n_i is the number of cycles actually experienced. Miner's rule attempts to provide a means by which to quantify the load history of a component by using the constant amplitude data. With load paths that are constantly changing, constant amplitude fatigue tests will never accurately model variable loading no matter how involved the statistical method may be. Geometric parameters vary among connections as well, making the stress level choice to characterize a connection a very difficult task.

The far-field stress, S_{nom}, is used in the nominal stress approach, at the location where cracking may occur, for the S in Equation 1.17. Using experimental fatigue test data from specific joints, the constants m and A are calculated for the specific nominal stress approach. The more subtle geometric differences that are bound to exist between specimens (due to differences in welds, etc...) are not captured directly by this technique, because the data-curve characterizes the specific specimen tested. Munse et al. (1983) used the nominal stress approach and extensively researched available information on the fatigue of welded joints, presenting the *S-N* data for 53 welded joint arrangements. Weld details of six configurations Munse et al. analyzed are shown in Figure 1.11, and the connection used in the present research is shown in Figure 1.12. The *S-N* data for these connections is found in Table 1.2 and plotted in Figure 1.13.

Table 1.2 – *S-N* Data for Joint Details, Munse et al. (1983)

Detail	m	Log_{10}Ã (ksi)
5	3.278	9.65
12	4.398	14.12
13	4.229	12.12
14A	Data scatter makes evaluation questionable	
32B	3.533	9.71
42	7.358	16.98

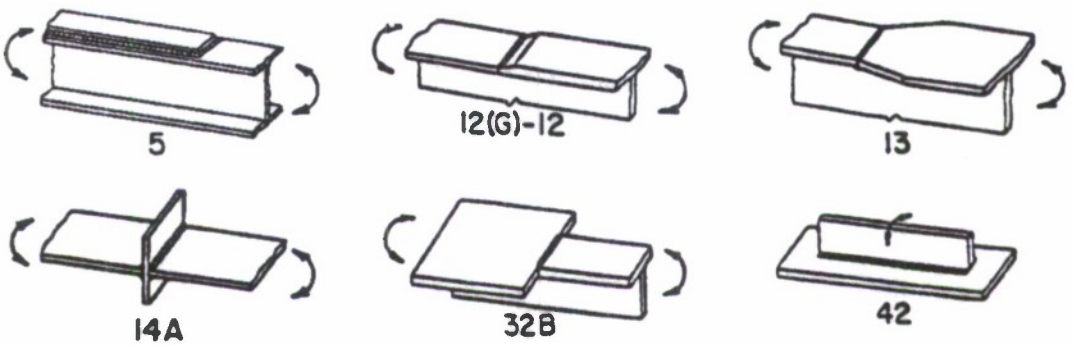

Figure 1.11 – Six Welded Joint Configurations Studied by Munse et al. (1983)

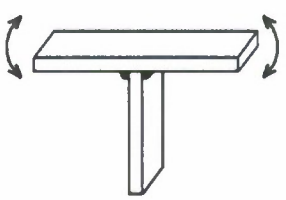

Figure 1.12 – Steel-T Part of the Connection Under Evaluation in Present Research, Corriveau et al. (2008)

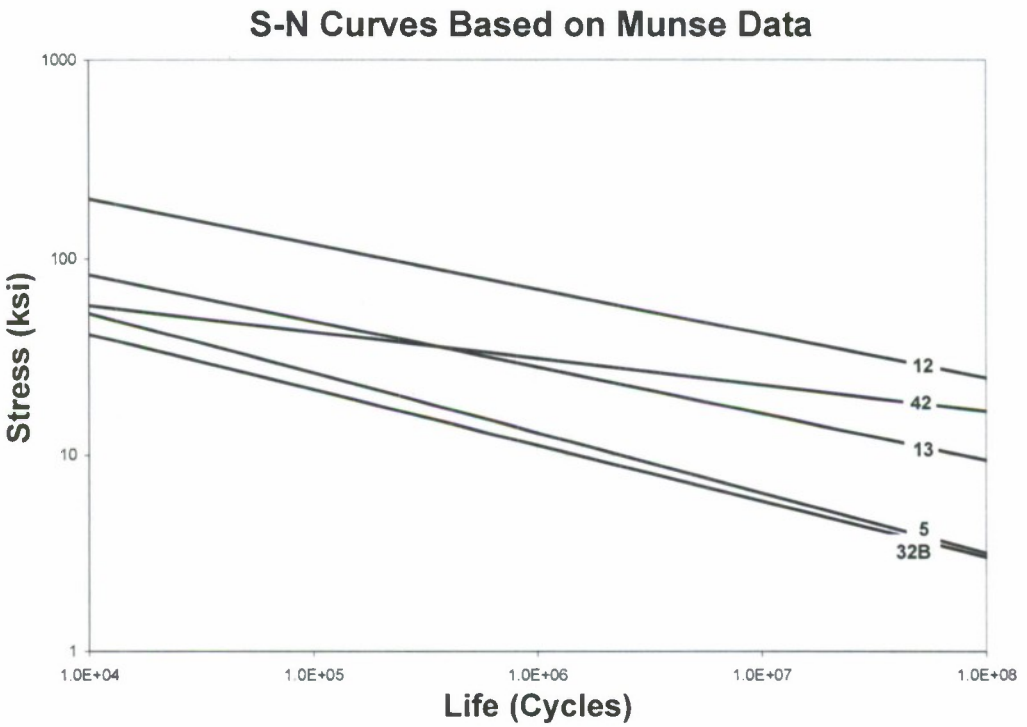

Figure 1.13 – Munse et al. (1983) Weld Detail Fatigue Curves

A variation of the nominal stress approach, called the abbreviated joint classification approach, is provided by Munse et. al (1996) as is shown in the welded joint fatigue curve classifications in Table 1.3 developed by the British. The abbreviated nominal stress approach is more conservative than the specific nominal stress approach, and takes into account the subtle geometric differences that are present in each test specimen of the same joint. Using this method, the probability of a test article failing before the predicted fatigue life is much smaller. The joint classifications provided by Mansour et al. (1996) were comprehensively analyzed by replacing S with S_{nom} in Equations 1.17 and 1.18, and descriptions of each category are given in Table 1.3. The *S-N* data values of m and A for these connections are provided in Table 1.4 and the corresponding *S-N* curves are provided in Figure 1.14. Gurney (1976) describes the British-classification design rules

and how they should be used. He explains that the joint category specified accounts for the differences present in each weld pattern, and the named stress magnitude in no way refers to the stress concentrations resulting from these. The quoted stress levels are a combination of resulting shear and bending effects. Fricke and Kahl (2005) outline a fatigue classification system, designated as FAT, similar to that which was established by the British. This particular system specifies the calculated stress level, in MPa, that a specific joint will fail at 2 million cycles. The curves developed by this classification method can be applied to those created by the British by pin-pointing the location where the curve intersects the 2 million cycle line.

Table 1.3 - British Standard Joint Classification (Mansour et al., 1996)

Class	m	Design Curve (A_0)	
		MPa	ksi
B	4.0	1.01×10^{15}	4.47×10^{11}
C	3.5	4.23×10^{13}	4.91×10^{10}
D	3.0	1.52×10^{12}	4.64×10^{9}
E	3.0	1.04×10^{12}	3.17×10^{9}
F	3.0	6.30×10^{11}	1.92×10^{9}
F2	3.0	4.30×10^{11}	1.31×10^{9}
G	3.0	2.50×10^{11}	7.63×10^{8}
W	3.0	1.60×10^{11}	2.88×10^{8}

Table 1.4 – *S-N* Data for British Standard Joint Details (Mansour et al., 1996)

Class	Description
B	Plain steel in the as-rolled condition, or with cleaned surfaces, but with no flame cut edges or re-entrant corners. Full penetration butt welds, parallel to the direction of applied stress, with the weld overfill dressed flush with the surface and finish-machined in the direction of stress, and with the weld proved free from significant defects by non-destructive examination.
C	Butt or fillet welds, parallel to the direction of applied stress, with the welds made by an automatic submerged or open arc process and with no stop-start positions within the length. Transverse butt welds with the weld overfill dressed flush with the surface and with the weld proved free from significant defects by non-destructive examination.
D	Transverse butt welds with the welds made in the shop either manually or by an automatic process other than submerged arc, provided all runs are made in the flat position.
E	Transverse butt welds that are not class C or D.
F	Load-carrying fillet welds with the joint made with full penetration welds with any undercutting at the corners of the member dressed out by local grinding.
F2	Load-carrying fillet welds with the joint made with partial penetration or fillet welds with any undercutting at the corners of the member dressed out by local grinding (*The standard bolted joints under evaluation in the present research fall into his category*).
G	Parent metal at the ends of load-carrying fillet welds which are essentially parallel to the direction of applied stress
W	Weld metal in load-carrying joints made with fillet or partial penetration welds, with the welds either transverse or parallel to the direction of applied stress (based on nominal shear stress on the minimum weld throat area).

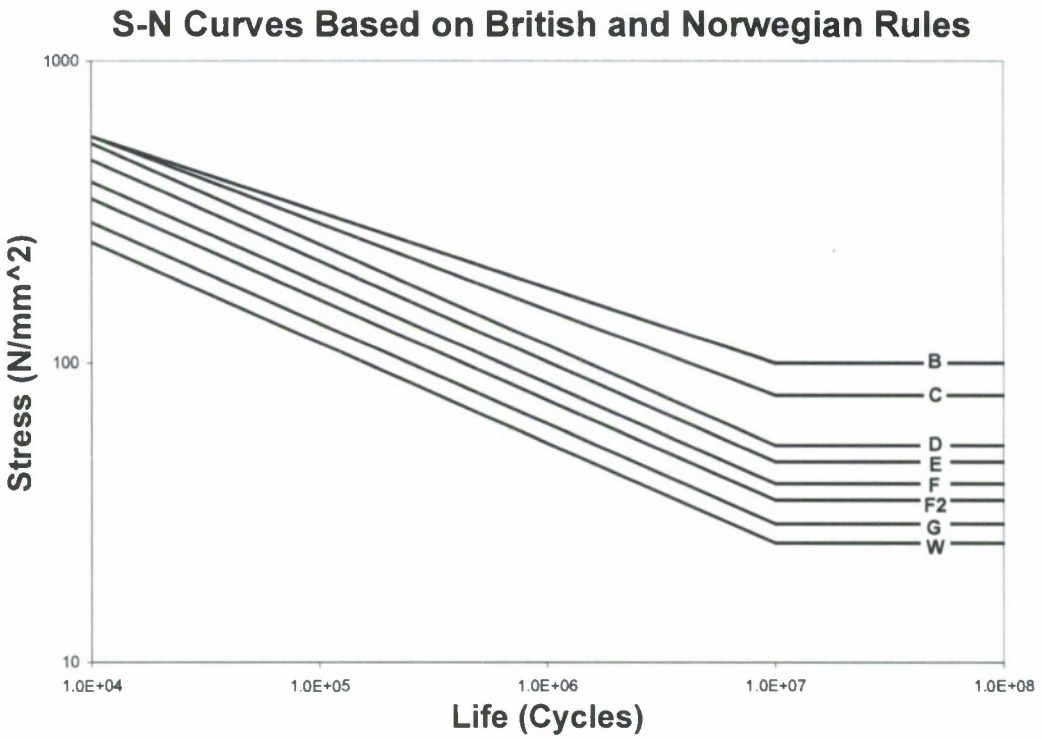

Figure 1.14 – British Standard Weld Detail Fatigue Curves, Mansour et al. (1996)

Fricke (2002) and Fricke and Kahl (2005) use a hot spot stress approach which utilizes finite element analysis to pinpoint the maximum stress location, designated as S_{hs}. An accurate prediction using this technique must begin with a geometrically sound, FEA representation of the connection. The issues that typically arise from using this method stem from the mathematical singularity present at critical locations, causing an increase in stresses with decreasing mesh size. Reference points that are a specified distance away, calculated using the joint thickness, can be used to deduce the hot spot stress. Mesh refinement at the hot spot stress location and computing the stress at a specified distance from the hot spot location is another technique that is used for stress prediction. The hot spot stress can then be related to the nominal stress using a stress concentration factor K_g, as shown in Equation 1.20. Prediction curves are developed by replacing S

with S_{hs} in Equations 1.17 and 1.18.

$$S_{hs} = K_g \cdot S_{nom} \qquad \text{(Eq. 1.20)}$$

The notch-stress approach uses experimental data and S_{nom}, and then adds the effects of notches that are actually present by including several stress concentration factors. The factors attempt to account for the various geometric imperfections that are present in reality. The notch-stress approach is utilized by Kendrick (2005) with the following equations,

$$S_{notch} = K_g \cdot K_w \cdot S_{nom} \qquad \text{(Eq. 1.21)}$$

$$S_{notch} = K_g \cdot K_w \cdot K_{te} \cdot K_{t\alpha} \cdot K_n \cdot S_{nom} \qquad \text{(Eq. 1.22)}$$

where K_g is the gross geometry stress concentration factor, K_w is the weld geometry stress concentration factor, K_{te} the eccentricity tolerance stress concentration factor (for plate connections), $K_{t\alpha}$ is the angular mismatch stress concentration factor, (for plate connections), and K_n is a concentration factor for un-symmetrical stiffeners on laterally loaded panels (when S_{nom} is derived from simple beam analyses).

2. EXPERIMENTAL INVESTIGATION

Tests performed by Corriveau et al (2008) were supplemented in this study by performing additional tests using other laminate thicknesses and with the addition of adhesive bonding. The successful production of test specimens at nominally 1/2 inch and 7/8 inch thickness led to the continuation of experimental work by Corriveau et al. (2008) in flexure fatigue. The new test articles were fabricated with a 21-layer or 48-layer bidirectional laminate mounted on a ¾" thick steel tee. The out-of-plane configuration would remain the fatigue loading type for this investigation. The new bolted hybrid joint fatigue tests also makes use of an alternative, stronger HSLA-65, steel as the metal backbone.

2.1 Fatigue Testing Apparatus

The test fixture used in this study was based upon most of the test setup components that were used previously by Corriveau et al. (2008). The fixture which was currently set up for the fatigue tests included a 165-kip, ± 3-inch actuator. The decision was made to switch to a lower capacity 22-kip, ± 3-inch actuator for these tests. The reaction frame beams needed to be shifted with respect to one another to accommodate the smaller dimensions of the replacement actuator. The load could then be transferred from the actuator via a hydraulic grip plate and load transfer beam to the test specimens.

The test setup, shown in Figure 2.1, consists of three main parts. The first part is the 22-kip actuator with hydraulic grip plate, which allows attachment to the second part: the load transfer beam. The third part is the hybrid composite/steel tee component which is joined to the load transfer beam via two grippers. Each gripper uses two 0.75" grade 8 steel bolts to clamp the test articles. The steel tee base is secured to the reaction frame beam using eight 0.875" grade 5 steel bolts. The laminates are attached to the steel tee by either the clamped or bolted method, as previously discussed. A complete description of the experimental test setup with all dimension details is outlined by Corriveau et al. (2008). The reader should take note that a stronger, HSLA-65 (High Strength Low Alloy) steel tee of 0.125" thinner thickness is used in the current work for the 28-ply, bolted-connection fatigue testing; the data gathered by Corriveau et al. (2008) used a mild

steel tee which was 0.75" thick.

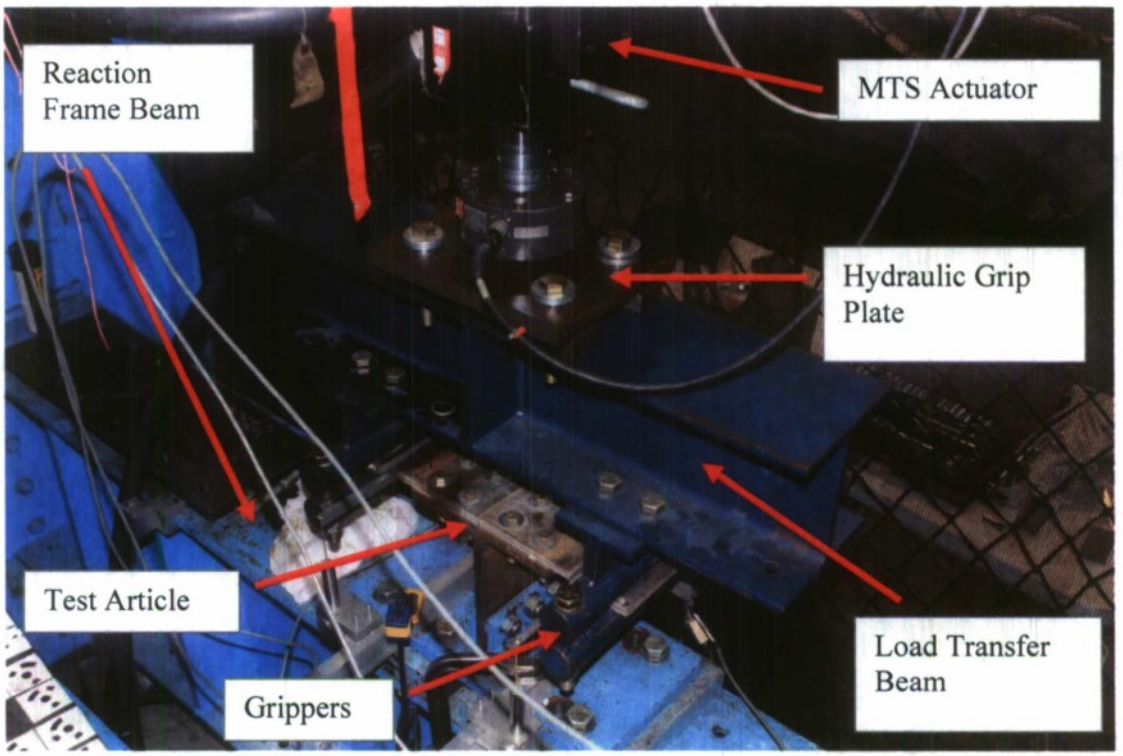

Figure 2.1 – Photograph of Fixture Gripping Test Article

2.2 Specimens

Specimens tested are summarized in Table 2.1 and include clamped cyclic tests (CC designation), bolted cyclic tests (BC), bolted fatigue tests (BF), and bolted/bonded fatigue tests (BB). A range of fatigue loads was provided from 2.5 kips to 7 kips. The bolted/bonded specimens were tested at only one load level of 3.5 kips due to time and cost constraints. Composite materials were fabricated using the same procedures as discussed by Corriveau et al. (2008). Composite panels were post cured in a kiln for nine hours at 280 degrees Fahrenheit. In the case of bolted/bonded panels, once the composite panels were post cured, they were bonded to an HSLA-65 steel tee with the adhesive Loctite 9340 using the following procedure. First, the surfaces of the composite panel and the steel tee were prepared for bonding by sanding the bonding surface of the composite panel and sandblasting the bonding surface of the steel tee. Next, the adhesive was applied according to the manufacturer's procedures. Once the adhesive was applied

to both surfaces, they were immediately bolted together under a torque of 80 foot-pounds. Clamps were then attached to the outside corners of the steel tee edge in order to prevent peeling. Prior to testing, the specimen was then set aside for a minimum of one week to allow the adhesive to cure.

Table 2.1 – Test Specimen Thickness and Width Dimensions (inches)

				Left Side		Right Side		Steel	
# Plies	Test Name	Test Style	Test Type	t	w	t	w	t	w
48	CC002	Clamped	Cyclic	0.826	6.75	0.824	6.79	N/A	N/A
48	BF001	Bolted	6-kip Fatigue	0.913	6.79	0.915	6.78	0.635	6.78
28	CC001	Clamped	Cyclic	0.55	6.68	0.554	6.79	N/A	N/A
28	BC001	Bolted	Cyclic	0.485	6.75	0.505	6.74	0.760	6.82
28	BF005	Bolted	3.5-kip Fatigue	0.550	6.62	0.545	6.62	0.635	6.78
28	BF006	Bolted	5-kip Fatigue	0.485	6.77	0.485	6.77	0.635	6.78
28	BF007	Bolted	5-kip Fatigue	0.484	6.76	0.485	6.79	0.635	6.78
28	BF008	Bolted	5-kip Fatigue	0.480	6.71	0.480	6.82	0.635	6.78
28	BF002	Bolted	7-kip Fatigue	0.545	6.85	0.550	6.76	0.635	6.78
28	BF003	Bolted	7-kip Fatigue	0.545	6.75	0.549	6.78	0.635	6.78
28	BF004	Bolted	7-kip Fatigue	0.555	6.60	0.551	6.58	0.635	6.78
28	BF009	Bolted	5-kip Fatigue	0.477	6.83	0.489	6.85	0.635	6.78
28	BF010	Bolted	5-kip Fatigue	0.475	6.72	0.485	6.82	0.635	6.78
28	BF011	Bolted	3.5-kip Fatigue	0.487	6.74	0.482	6.75	0.631	6.77
28	BF012	Bolted	3.5-kip Fatigue	0.471	6.61	0.485	6.70	0.635	6.78
28	BF013	Bolted	3.5-kip Fatigue	0.494	6.67	0.492	6.70	0.635	6.78
28	BF014	Bolted	3.5-kip Fatigue	0.482	6.53	0.488	6.58	0.635	6.78
28	BF015	Bolted	2.5-kip Fatigue	0.460	6.64	0.488	6.76	0.631	6.77
28	BF016	Bolted	2.5-kip Fatigue	0.461	6.62	0.472	6.63	0.631	6.77
28	BF017	Bolted	2.5-kip Fatigue	0.472	6.69	0.467	6.67	0.631	6.77
28	BF018	Bolted	3.5-kip Fatigue	0.468	6.72	0.473	6.78	0.631	6.77
28	BB001	Bolted/ Bonded	3.5-kip Fatigue	0.492	6.60	0.482	6.70	0.635	6.78
28	BB002	Bolted/ Bonded	3.5-kip Fatigue	0.478	6.58	0.488	6.75	0.631	6.77
28	BB003	Bolted/ Bonded	3.5-kip Fatigue	0.487	6.55	0.493	6.70	0.635	6.78
28	BB004	Bolted/ Bonded	3.5-kip Fatigue	0.497	6.62	0.487	6.65	0.631	6.77

2.3 Testing Controls

The experimental testing for this work was conducted using an MTS universal test control system. A computer equipped with DAQFl software communicates with the MTS system and outputs the desired analog signals to the actuator. The DAQFI software also records the load and displacement data which the load cell and transducer on the actuator output. A detailed description of the complete test control system used for the current research is outlined by Corriveau et al. (2008).

2.4 Experimental Results

2.4.1 Cyclic Testing

Cyclic tests to failure were performed for both clamped and bolted configurations. The results of clamped cyclic to failure tests on two different laminate thicknesses can be found in Figures 2.2 and 2.3. Results of bolted cyclic to failure tests are provided in Figures 2.4 and 2.5. Progressive failure and close-up photos of failure for all cyclic tests are shown in Figures 2.6-2.10. Peak loads and their corresponding displacements for all tests are given in Table 2.2.

Peak load when moving upward in the 28-ply clamped case is 14.7 kips, compared to 8.86 kips for the 28-ply bolted joint case. This significant difference in load amplitude is clearly due to the larger moment arm present in the bolted configuration when the connection is loaded up. An unexpected outcome was that ultimate failure occurred along the steel tee edge and not along the bolt line, as was seen in a similar 42-ply cyclic test performed by Corriveau et al. (2008). The 48-ply clamped test did not reach failure due to the maximum load output by the actuator being insufficient.

Table 2.2 – Peak Loads and Corresponding Displacements in Cyclic Tests

Test Style	# Plies	Peak Load Up (kip)	Peak Load Down (kip)	Displ. @ Peak Up (in)	Displ. @ Peak Down (in)
*Clamped	48	-21.19	21.75	-0.443	0.407
*Bolted	48	-20.93	21.13	-0.902	0.938
Clamped	28	-14.70	16.48	-0.547	0.547
Bolted	28	-8.86	13.61	-1.017	0.714

Note: *These tests did not reach failure.

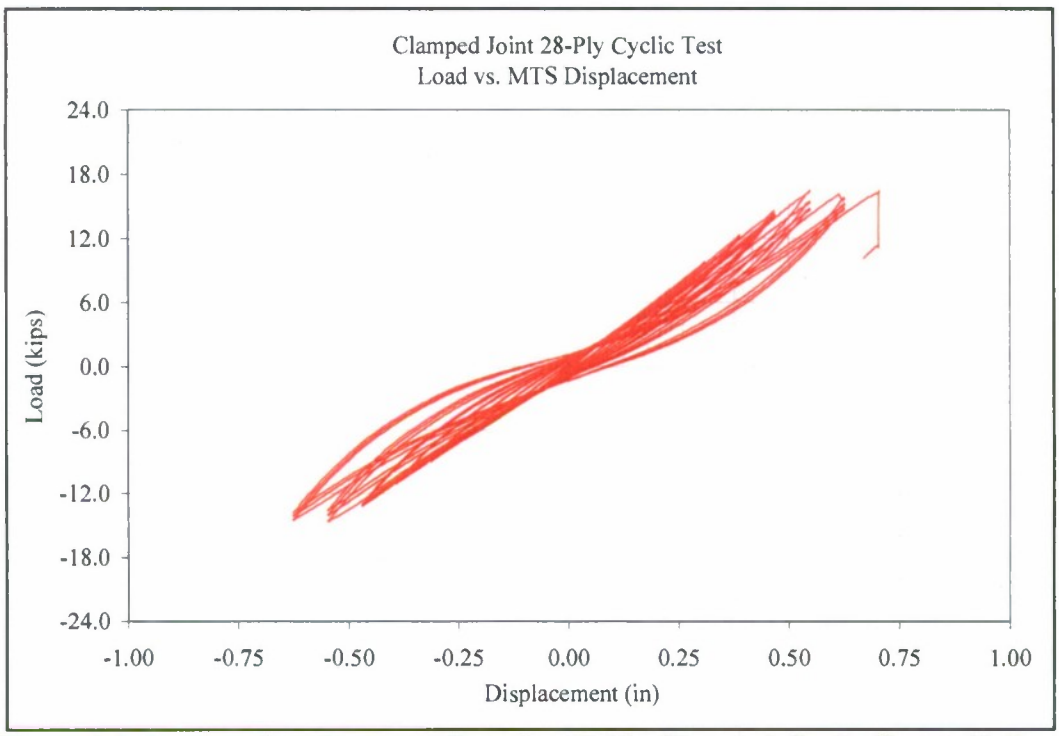

Figure 2.2–Load vs. Displacement Data for 28-Ply Clamped Cyclic Test to Failure

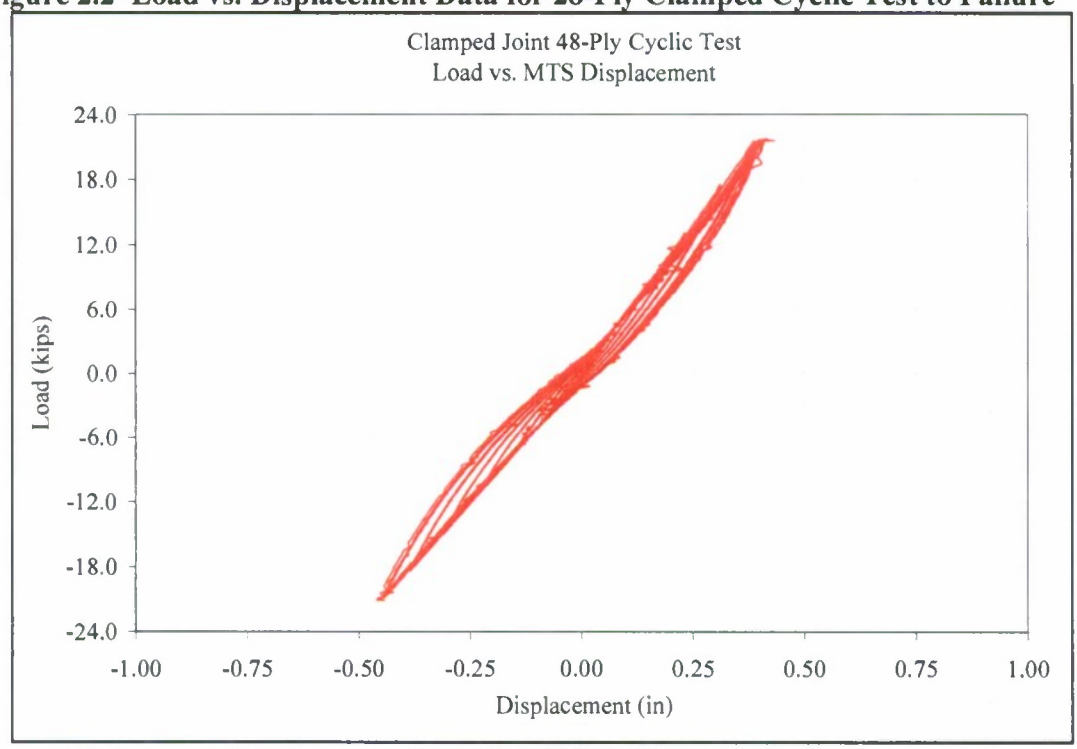

Figure 2.3–Load vs. Displacement Data for 48-Ply Clamped Cyclic Test to Failure

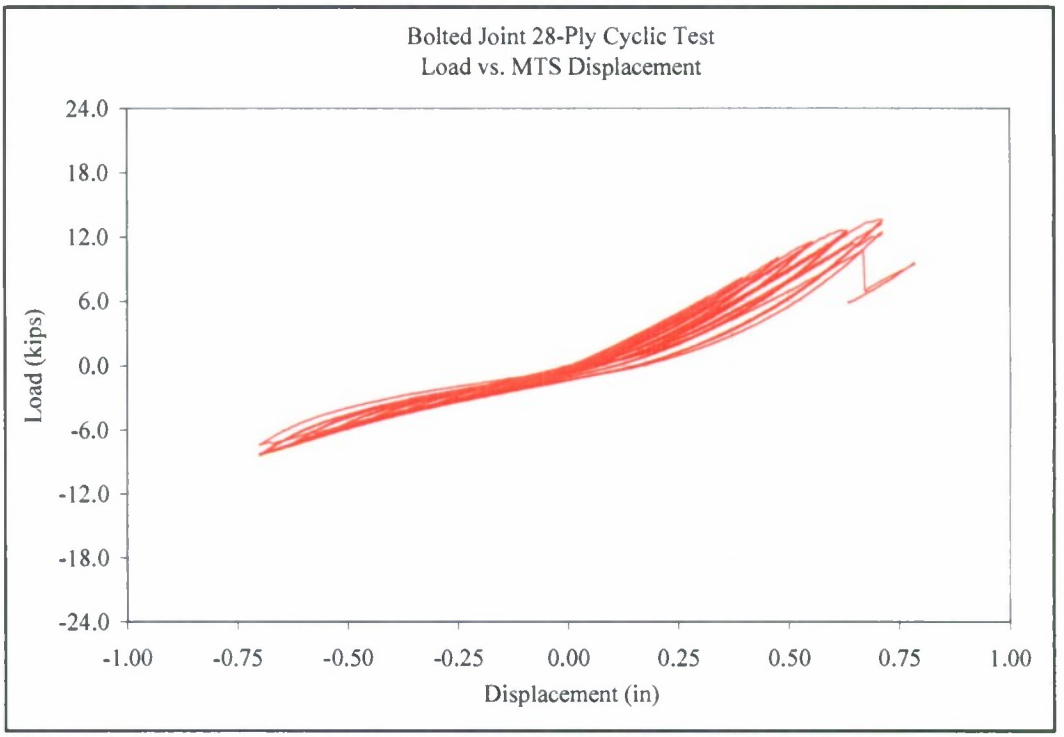

Figure 2.4–Load vs. Displacement Data for 28-Ply Bolted Cyclic Test to Failure

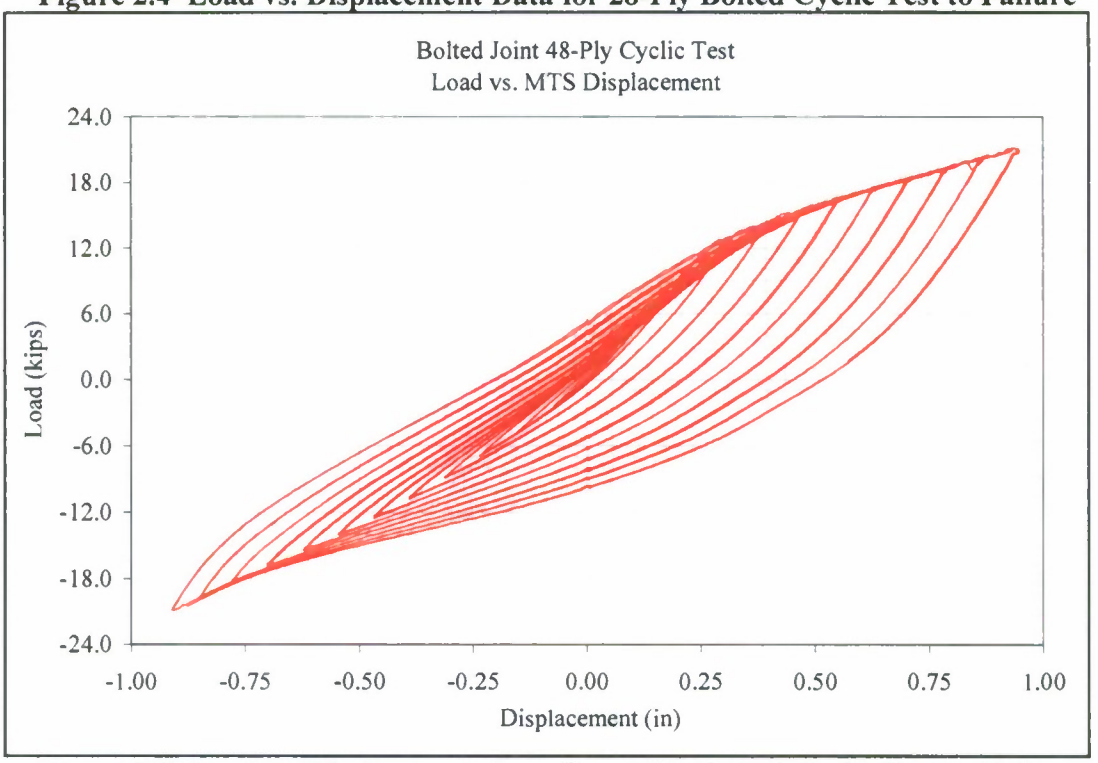

Figure 2.5–Load vs. Displacement Data for 48-Ply Bolted Cyclic Test to Failure

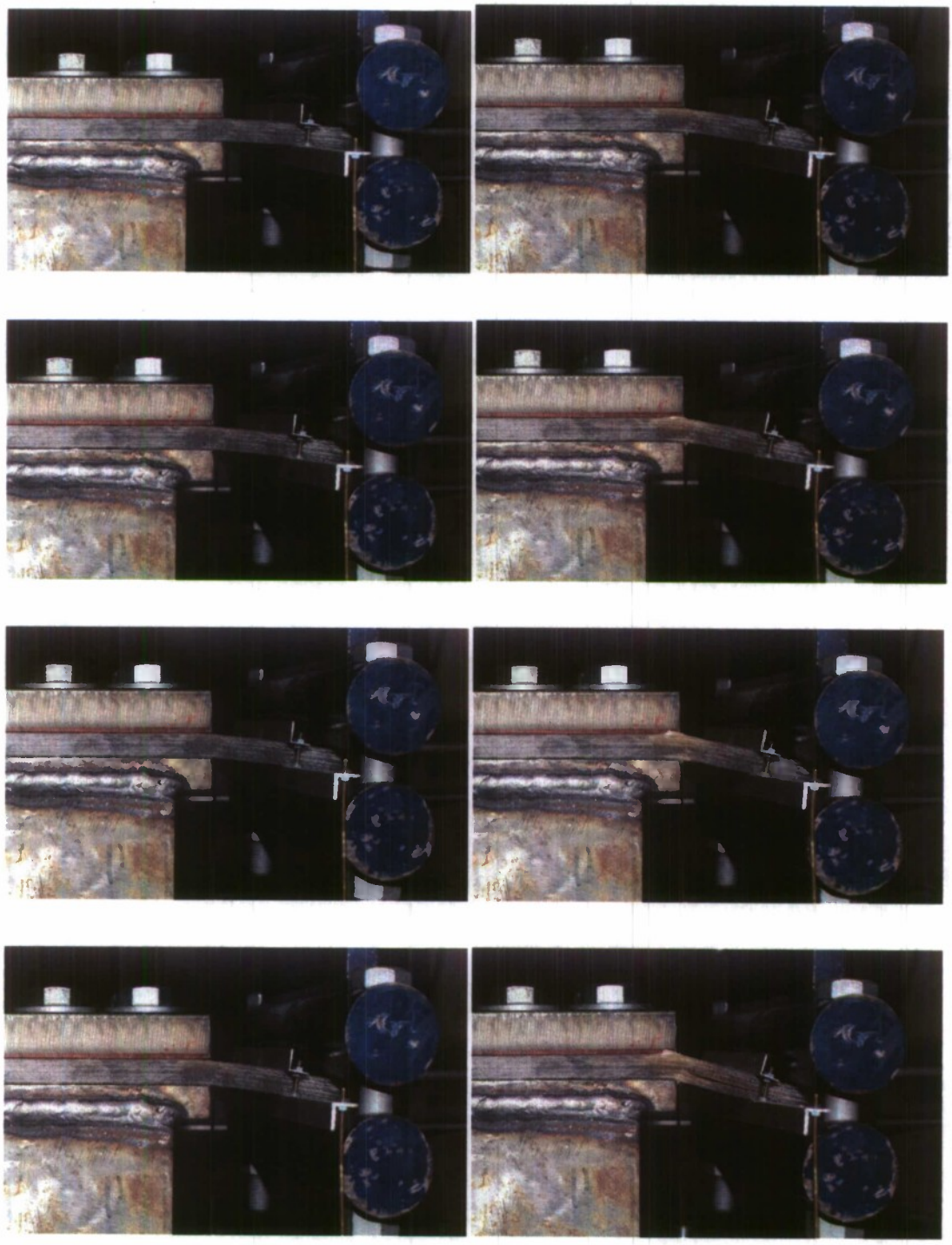

Figure 2.6 – 28-Ply Clamped Joint Cyclic Test Progressive Failure

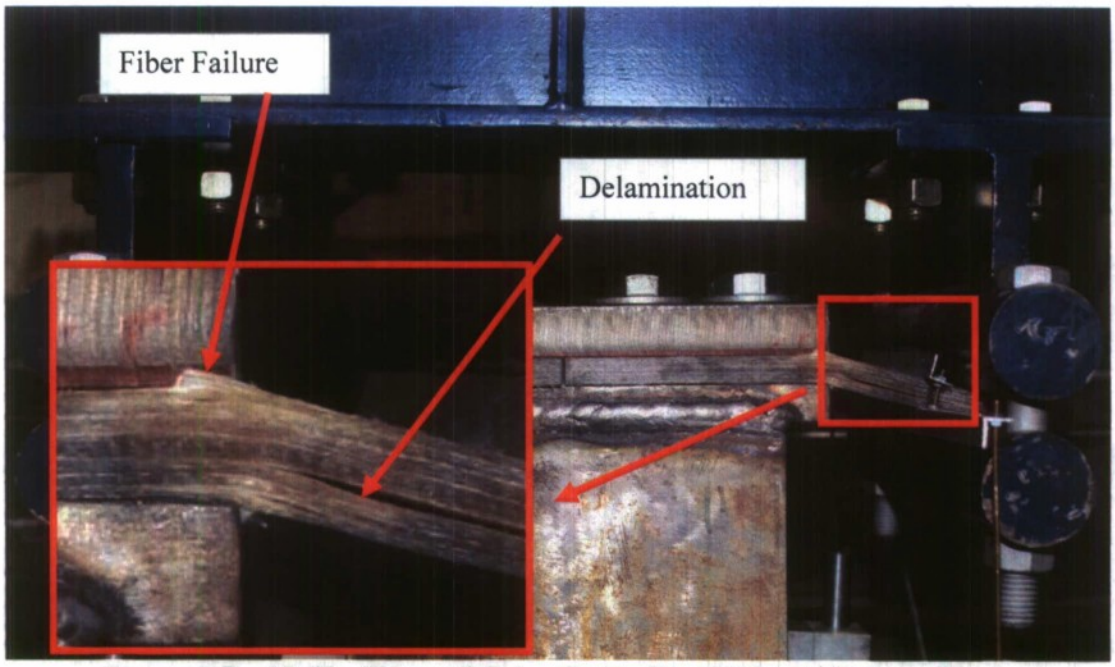

Figure 2.7 – 28-Ply Clamped Joint Cyclic Test Ultimate Failure Photo

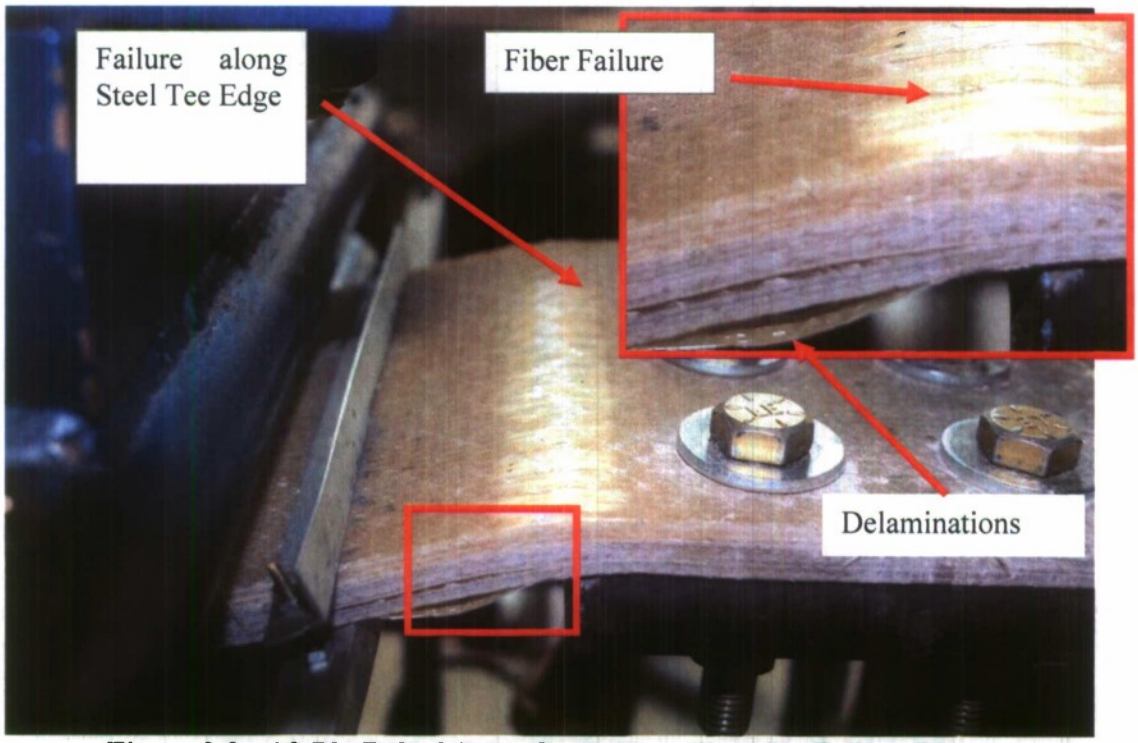

Figure 2.8 – 28-Ply Bolted Joint Cyclic Test Close-Up Failure Photo

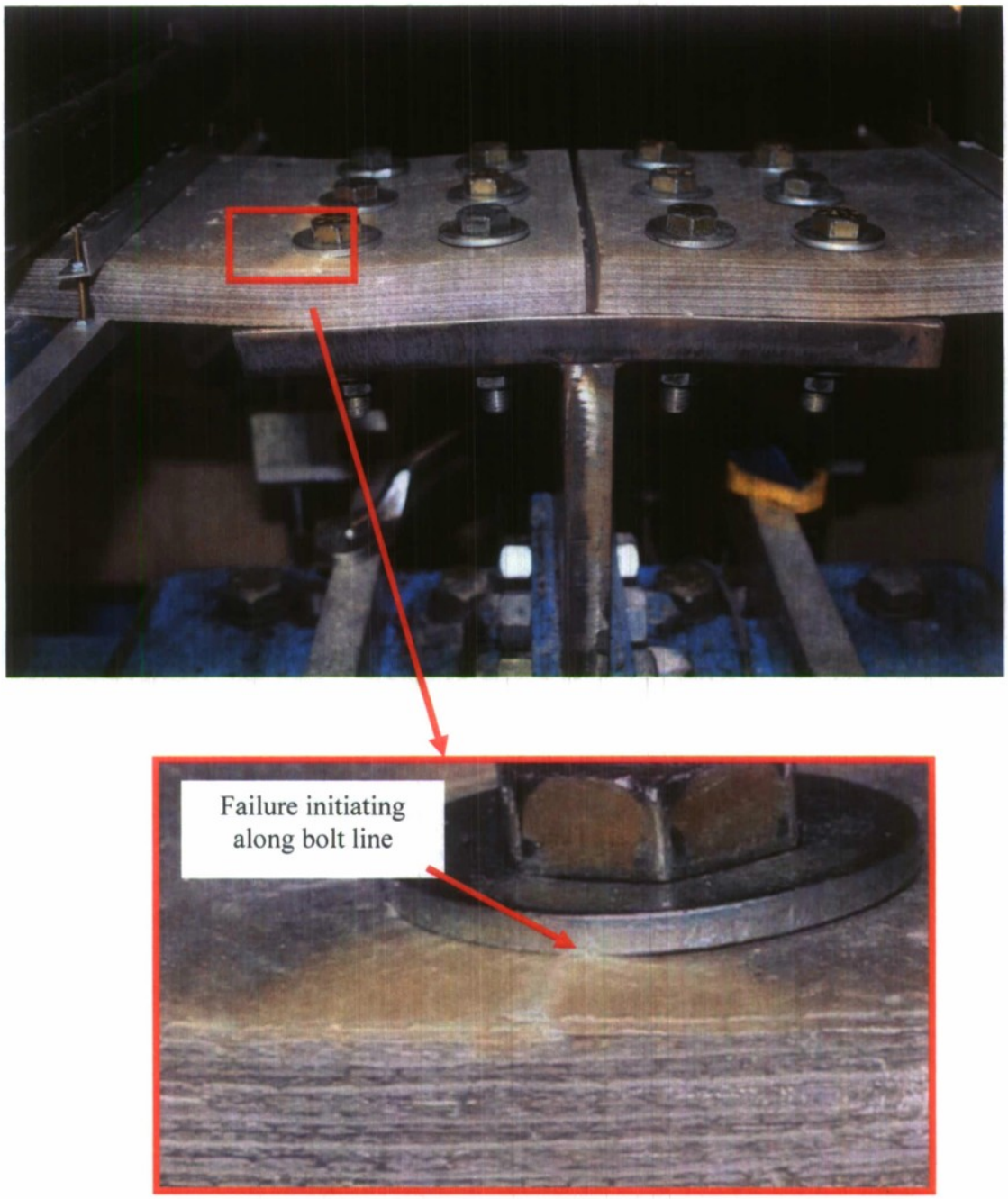

Figure 2.9 – 48-Ply Bolted Joint Cyclic Test, Upward-Load Photo

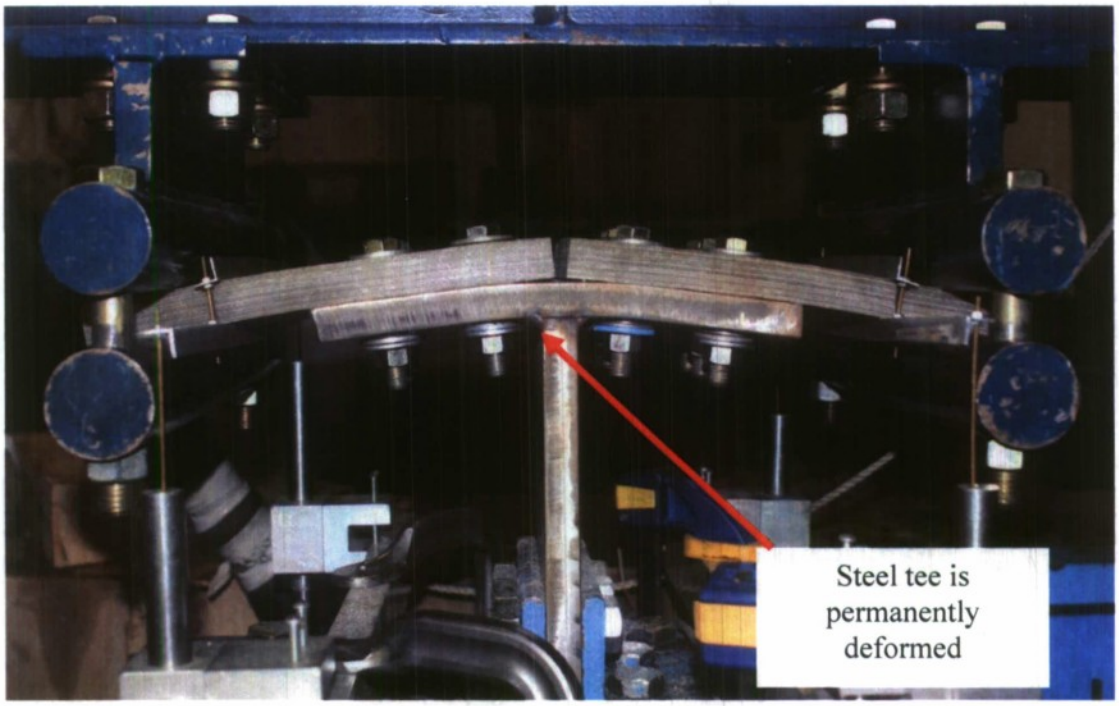

Figure 2.10 – 48-Ply Bolted Joint Cyclic Test, Downward-Load Photo

2.4.2 Fatigue Testing

Results of the fatigue tests performed are summarized in Table 2.3. The fatigue graphs for these tests with corresponding intermediate cyclic test plots are given in Appendix A. A fatigue S-N curve for the ½ inch thick specimens is presented in Figure 2.11 on a log-log scale. The nominal stress used in this plot is the bending stress assuming linear-elastic homogeneous isotropic conditions. Although this is not the actual stress in the composite material it is used at this point to assess the fidelity of the fatigue results. The critical section is assumed to be across the bolt line and the bending moment is assumed distributed over the net width ($W - 3*D_b$). Stress is computed as $6*M/t_c^2$. Where M is the moment per unit width and t_c is the total composite material thickness. The line on this figure represents the best fit to the data which occurs with m=7.19 and log(A)=16.42 in ksi.

The primary mode of failure for the fatigue tests was delamination and fiber failure. One exception was the 6 kip, 48-ply bolted joint fatigue test which failed at the steel tee as

shown in Figures 2.12, with no observable damage present in the laminate. The steel failure was attributed to the strong stiff laminate and stress concentrations at the weldment. In consideration of the failure mode, time and cost, additional testing at this laminate thickness was not undertaken.

Figure 2.11 also presents the results of the adhesively bonded/bolted specimens compared to the bonded only version. This comparison is at the +/- 3.5 kip load level only due to time constraints. The geometric mean of the number of cycles to failure was found to be 140,400 cycles for the bolted only specimens compared to 229,100 for the bonded/bolted version. This demonstrates a significant increase in fatigue life due to the bonding.

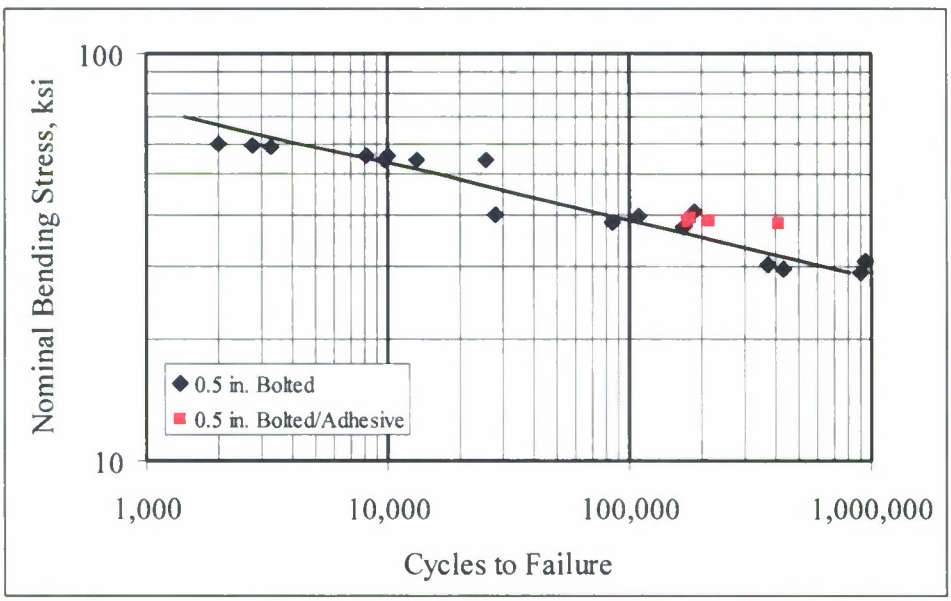

Figure 2.11 – Nominal Bending Stress vs. Cycles to Failure for the Hybrid Bolted Connection with 0.5 inch Thick Composite.

Table 2.3 – Cycles to Failure for Bolted Joint Fatigue Tests

Test Name	# Plies	Laminate Thickness (in)	Laminate Width (in)	Peak Load (kips)	Cycles to Failure	Remarks
BF001	48	0.914	6.78	± 6	195,000	Steel tee failed at weld toe
BF002	28	0.548	6.81	± 7	2,000	Fiber failure at bolt line
BF003	28	0.547	6.76	± 7	2,750	Fiber failure at bolt line
BF004	28	0.553	6.59	± 7	3,300	Fiber failure at bolt line
BF005	28	0.548	6.62	± 3.5	947,000	Fiber failure at gripper
BF006	28	0.485	6.77	± 5	25,540	Fiber failure at bolt line
BF007	28	0.485	6.78	± 5	13,160	Fiber failure at bolt line
BF008	28	0.480	6.77	±5	8,160	Fiber failure at bolt line
BF009	28	0.483	6.84	± 5	9,760	Fiber failure at bolt line
BF010	28	0.480	6.77	±5	10,000	Fiber failure at bolt line
BF011	28	0.485	6.75	± 3.5	85,500	Fiber failure at bolt line
BF012	28	0.478	6.65	± 3.5	27,890	Fiber failure at bolt line
BF013	28	0.493	6.69	± 3.5	166,770	Fiber failure at bolt line
BF014	28	0.485	6.56	± 3.5	110,000	Fiber failure at bolt line
BF015	28	0.474	6.70	± 2.5	900,250	Fiber failure at bolt line
BF016	28	0.466	6.63	± 2.5	372,310	Fiber failure at bolt line
BF017	28	0.470	6.68	± 2.5	434,930	Fiber failure at bolt line
BF018	28	0.471	6.75	± 3.5	185,000	Fiber failure at bolt line
BB001	28	0.487	6.65	± 3.5	213,380	Fiber failure at bolt line
BB002	28	0.483	6.66	± 3.5	179,840	Fiber failure at bolt line
BB003	28	0.490	6.62	± 3.5	174,350	Fiber failure at bolt line
BB004	28	0.492	6.64	± 3.5	412,050	Fiber failure at bolt line

Photos of ultimate fiber failure at the bolt line for the 28-ply 7 kip bolted joint fatigue tests 1, 2, and 3 are provided in Figures 2.13 -2.15. A photo of ultimate fiber failure at the bolt line for the 28-ply 5 kip bolted joint fatigue test 3 is provided in Figures 2.16. Photos showing delamination prior to complete failure in the 28-ply 3.5kip bolted joint fatigue test are shown in Figure 2.17. During this test, at approximately 700,000 cycles,

the actuator started leaking oil, which was then soaked into the composite specimen and more than likely affected the outcome of the test. Ultimate failure occurred where the rollers grip the test specimen, as seen in Figure 2.18, where the end of the laminate detached completely. Figure 2.19 shows a combined failure mode which includes delamination and fiber failure. Figure 2.20 presents the response of the bolted/bonded specimens at increasing number of cycles. The photographs were taken at the peak of the intermittent cyclic tests. It is noted that after 110,000 cycles the joint is in essentially the same condition as a non bonded joint as the adhesive has failed to the point where there is little if any resistance to peel. Complete adhesive failure apparently occurred between 85,000 and 110,000 cycles.

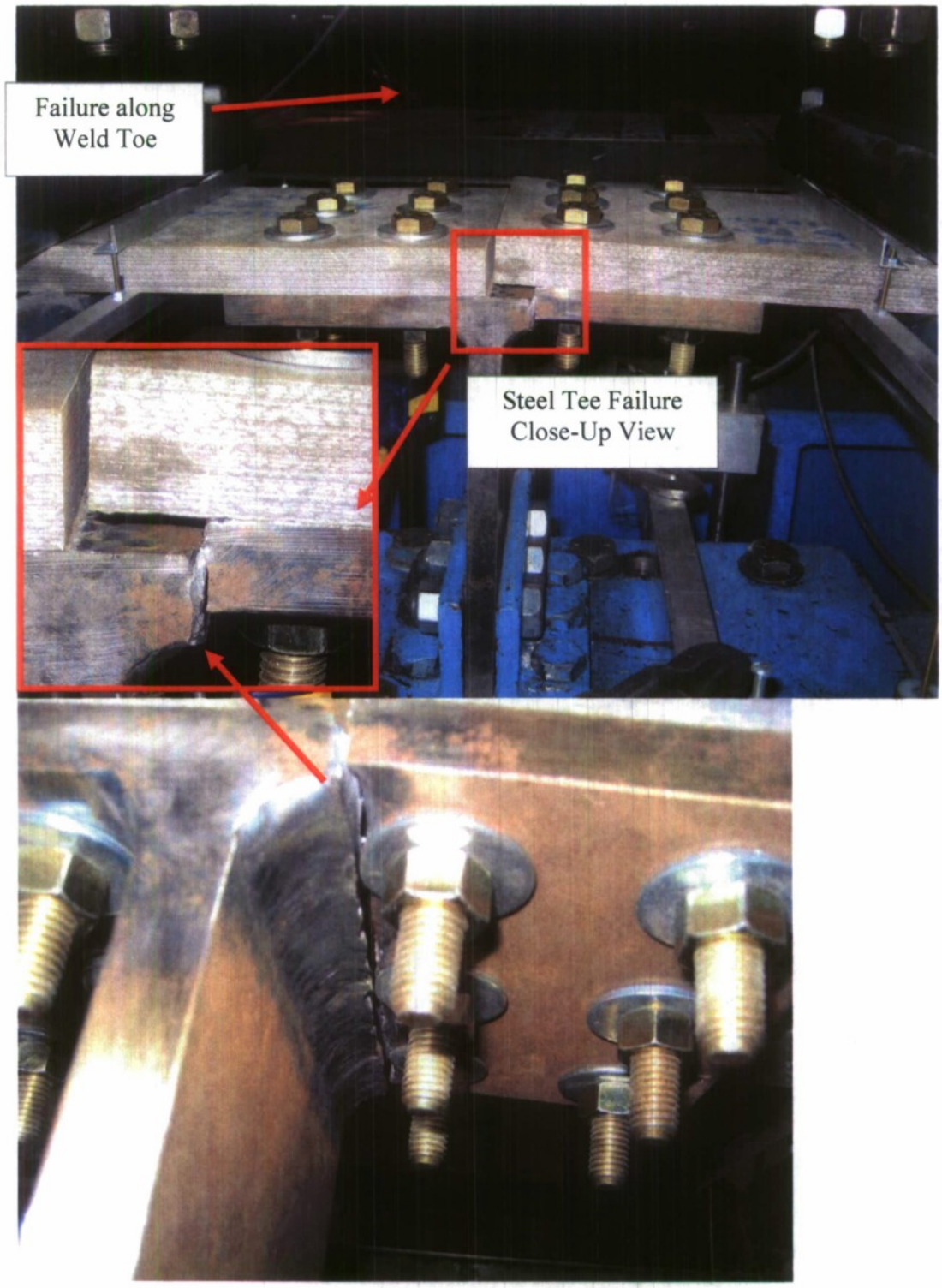

Figure 2.12 – 48-Ply Bolted Joint 6kip Fatigue Test Failure Photos

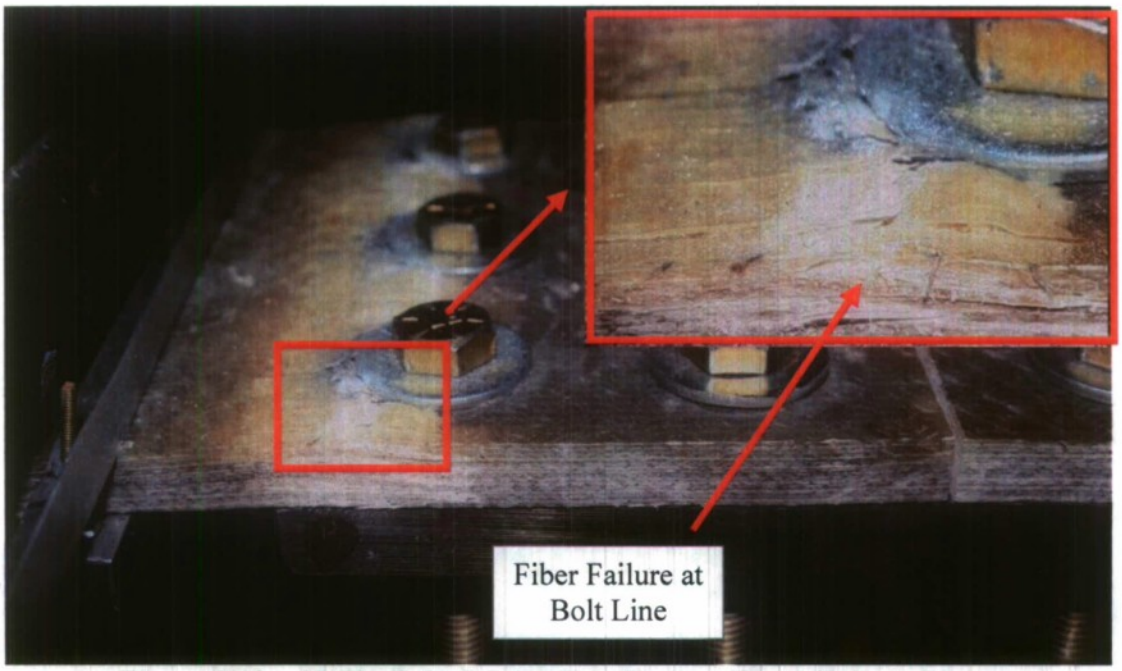

Figure 2.13 – 28-Ply Bolted Joint 7kip Fatigue Test 1 Failure Photo

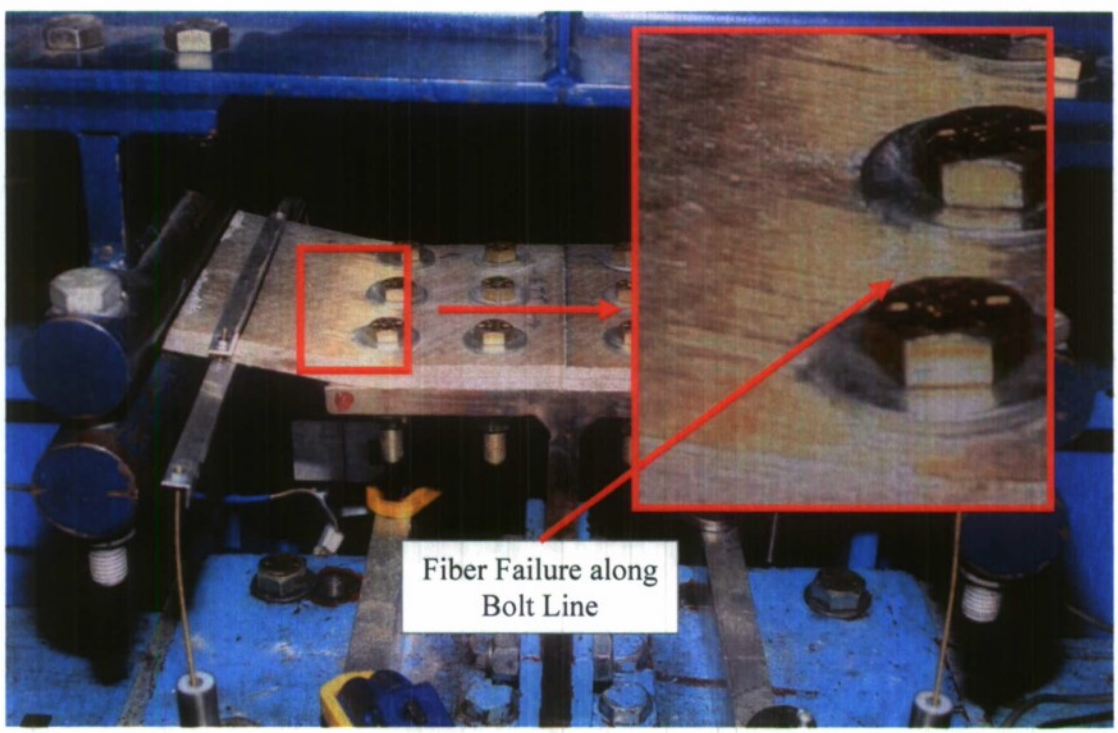

Figure 2.14 – 28-Ply Bolted Joint 7kip Fatigue Test 2 Failure Photo

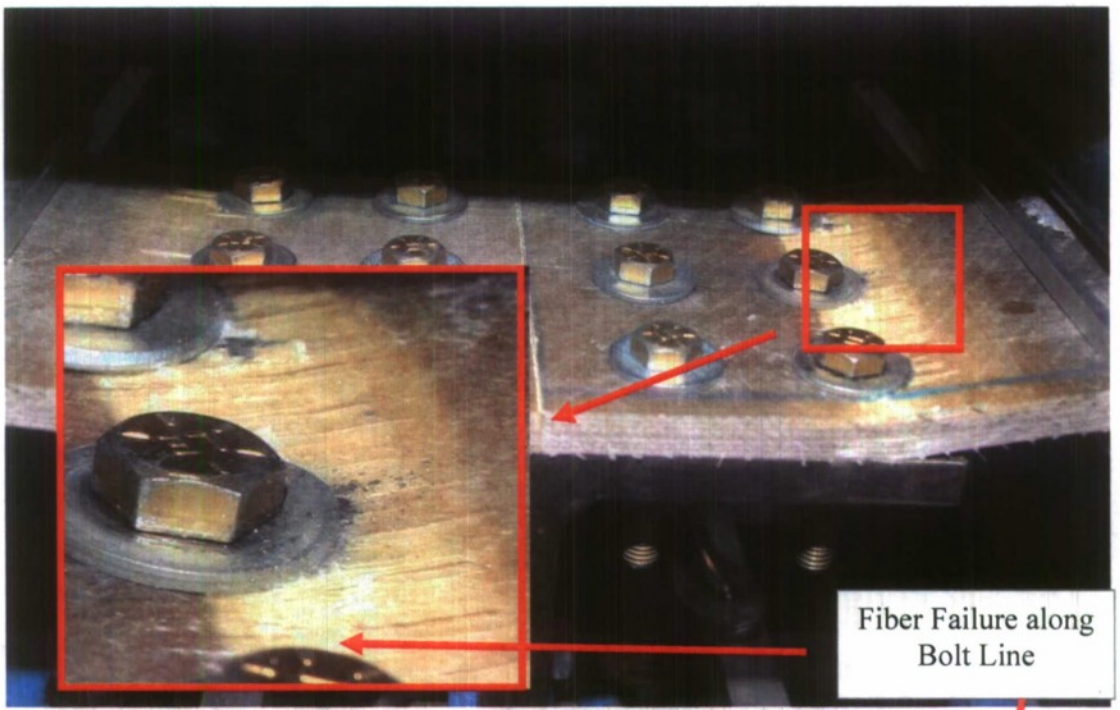

Figure 2.15 – 28-Ply Bolted Joint 7kip Fatigue Test 3 Failure Photo

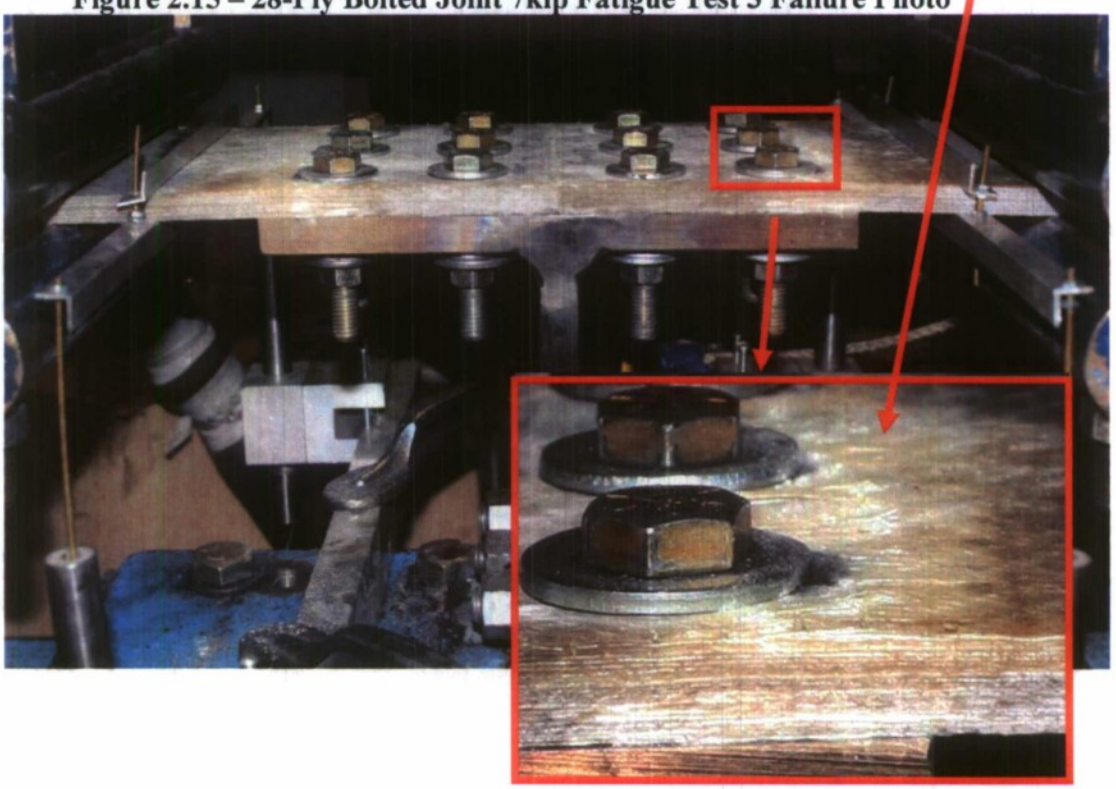

Figure 2.16 – 28-Ply Bolted Joint 5kip Fatigue Test 3 Failure Photo

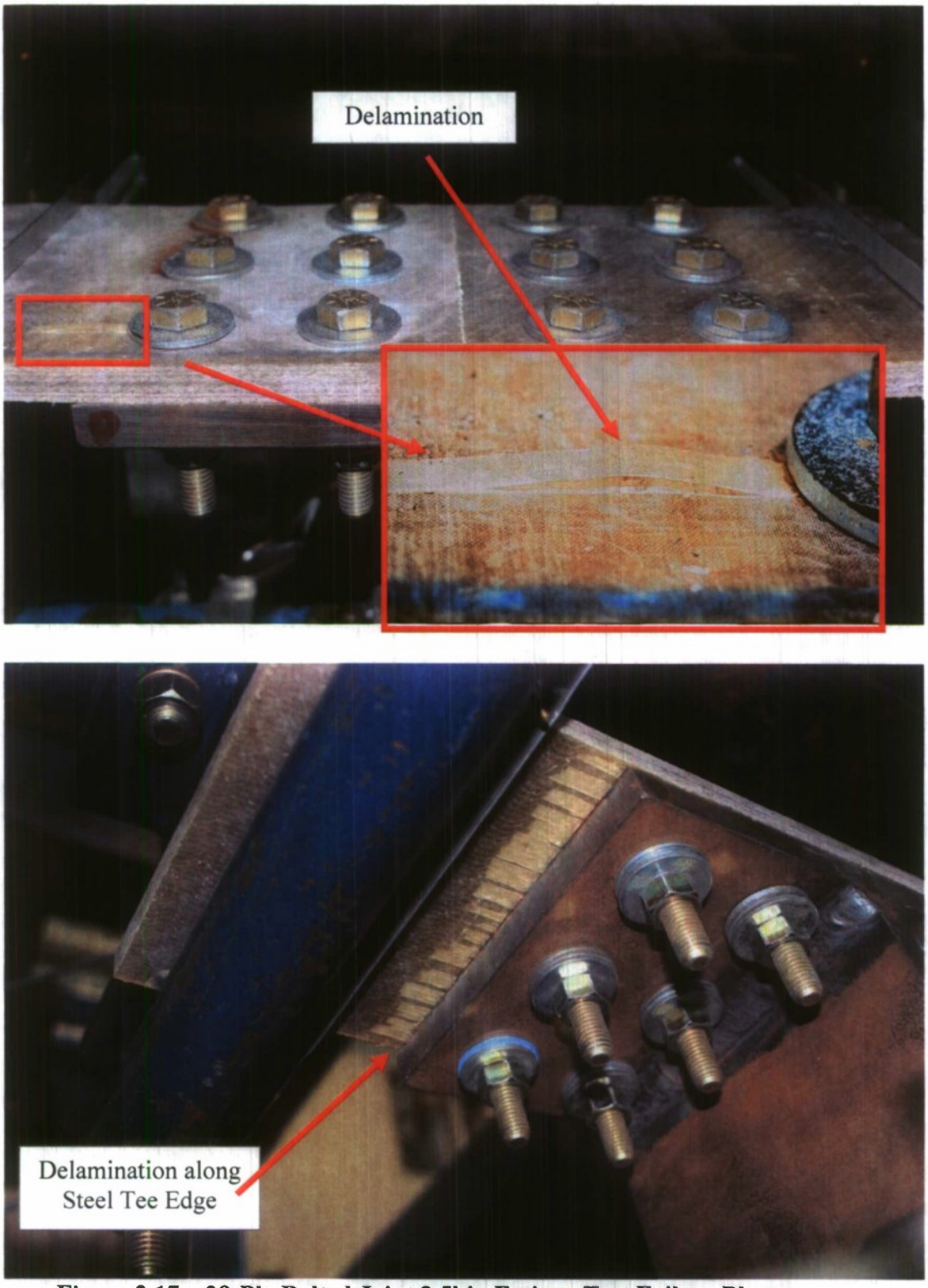

Figure 2.17 – 28-Ply Bolted Joint 3.5kip Fatigue Test Failure Photos

Figure 2.18 – 28-Ply Bolted Joint Failure at Gripper

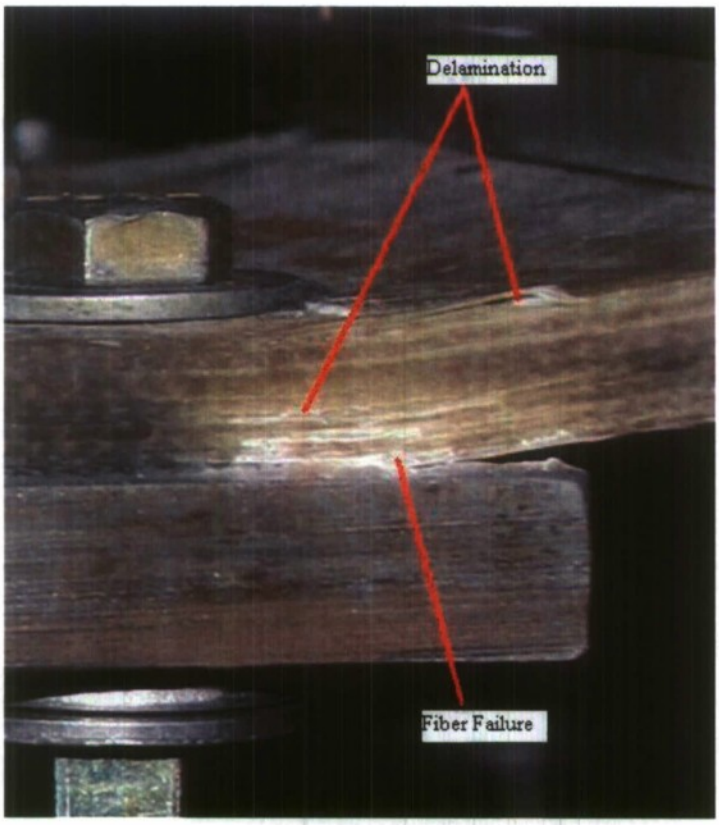

Figure 2.19 – Bolted Joint Fiber Failure at Base of Joint with Delamination

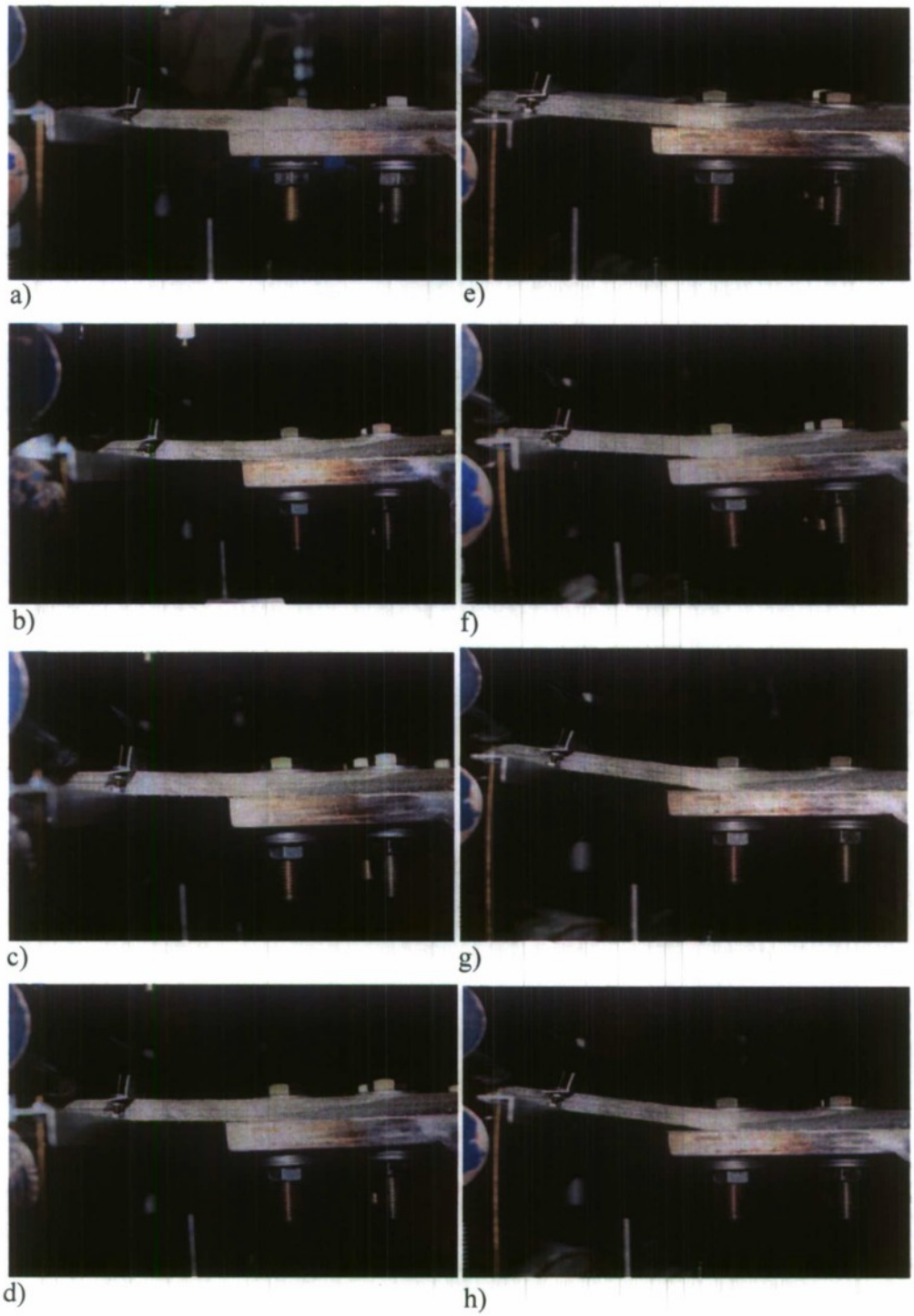

Figure 2.20 – 28-Ply Bolted/Bonded Fatigue Test Progressive Failure
a) 10,000 cycles, b) 35,000 cycles, c) 60,000 cycles, d) 85,000 cycles, e) 110,000 cycles, f) 135,000 cycles, g) 160,000 cycles, h) 180,000 cycles

3. FINITE ELEMENT MODELING TECHNIQUES USING ANSYS

ANSYS software offers a robust tool for the finite element modeling of a wide array of structures. It can be used to analyze specific details of a particular connection. The following subsections include step-by-step instructions for shell, plane-strain, and solid modeling techniques and how to accurately construct and analyze the connection configuration using ANSYS. This entire section describing the modeling techniques will limit the description to the instance where the laminate consists of 42 plies. As already mentioned, using ASTM Standard D6507-00 (2005) this particular layup of fiber is denoted as:

$$\left[(\pm 45/0/90/\mp 45/90/0)_2(\pm 45/0/90)\overline{(90/0)}\right]_S .$$

The plane strain analysis will include a 2-D construction of the complete experimental connection and was chosen since a joint as implemented is typically long compared to its other dimensions, resulting in a case of plane strain. Plane strain elements are employed in the majority of the geometry, while link elements are used for the bolts so that a preload may be defined. Contact elements are applied to all material interfaces. The presence of symmetry about the center of the test article allows accurate results to be achieved when modeling half of the hybrid connection. Although not a complete 3-dimensional representation of the experimental setup, this model is robust tool in performing a comprehensive parametric study of the connection. Some components in the model are not consistent across the width of the specimen (i.e. the bolts, washers, etc…) and certain specified properties and dimensions in the geometry are altered so that an accurate interpretation of the experiment may result.

The shell model will use orthotropic-layered and isotropic shell elements to model the hybrid composite/metal connection. This finite element construction will include the portion of the connection that includes the composite, and the hybrid section of the steel tee which is connected to the composite. This finite element model has low fidelity for this localized application, and is more practical in global model analysis of entire ship structures and far field stress prediction. This approach was demonstrated by Kabche et

al. (2006) and then by Corriveau et al. (2008).

The solid analysis is by far the most complex of the three techniques shown in this work with the least amount of assumptions required. Solid elements are utilized for the modeling all of the experimental setup geometries, including the bolts, washers, steel tee with clamping plate, composite, as well as all through-holes to accommodate the bolts. Contact elements are applied at all material interfaces in an effort to capture the full experimental effects of the GRP-metal union. The presence of symmetry allows the modeling of a quarter-section of the composite-steel connection without any loss of integrity in results. The solid model constructed in this work is too stiff as is designed currently and fine tuning this analysis is outside the scope of this thesis. For this reason, the instructions for modeling the clamped configuration will be provided in Appendix D and no results will be provided.

3.1 Plane Strain Analysis

The more simplified case of modeling the hybrid connection using shell elements is understood from prior work, so the new task at hand is to build and solve a more detailed plane-strain model. This 2-D analysis of the hybrid connection is presented before the shell modeling and more complex solid finite element modeling, and Figure 3.1 shows a diagram of the modeling plan. As with any finite element modeling project, element choice is crucial. The objective of this task is to provide step-by-step instructions on how to create and solve plane-strain models of the bolted, adhesive-bolted, and clamped cases. More than one element type fits this particular application. The ANSYS element PLANE42 was selected for this investigation and the geometry for this is shown in Figure 3.2. All dimensions are in inches.

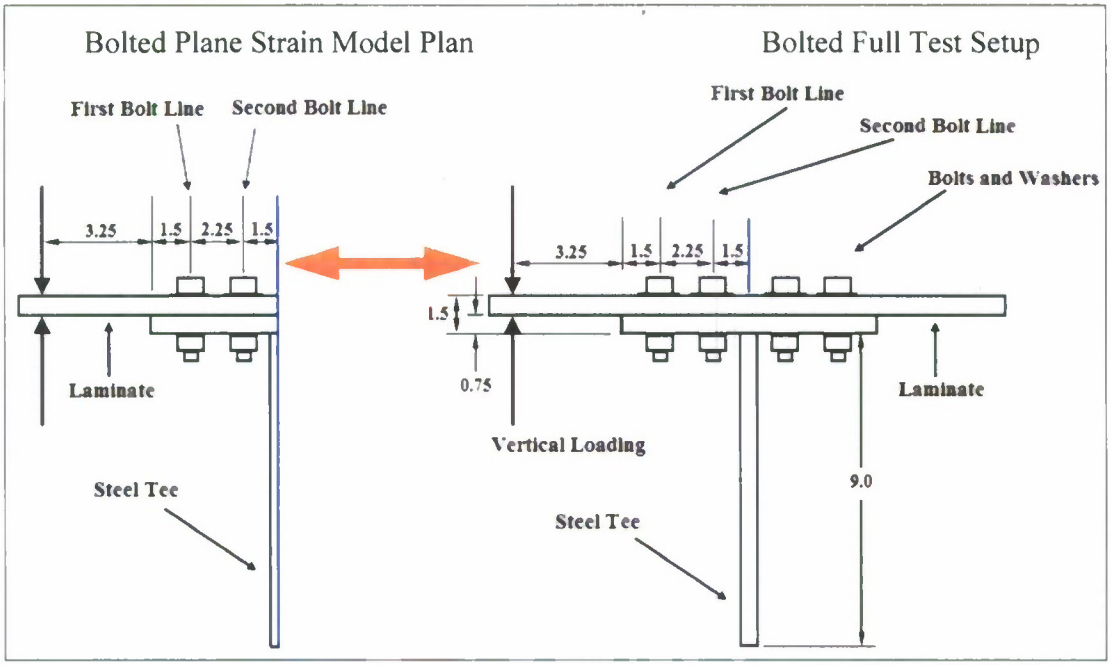

Figure 3.1 – Plane Strain Model Schematic

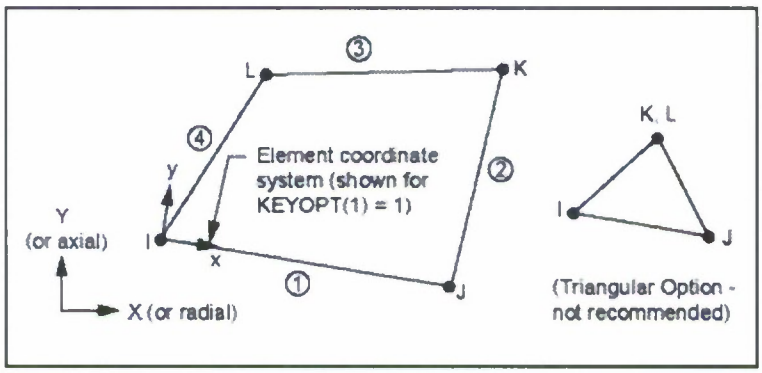

Figure 3.2 - PLANE42 Element Geometry, ANSYS Inc. (2007)

3.1.1 Bolted Case Modeling Instructions

Step 1 – Choose all Element Types Needed:

The element is chosen with the ability to connect isotropic materials with orthotropic materials and run a contact, plane-strain analysis which agrees well with experimental

results. The connection between the composite and steel tee will be made with LINK elements, representing the bolts. Element descriptions can be found in the ANSYS 11.0 Utility Menu by going to: **Help>Help Topics> Contents>Release 11.0 Documentation for ANSYS>Elements>Reference>Element Library**.

Step 2 – Choose an Analysis Type and Element:

For this part, two element types must be defined; one for the composite, steel tee, bolt heads, washers, and nuts, and the other for the bolts. The LINK1 element is used for the bolts and the PLANE42 element is applied to the remaining components.

a) In the ANSYS Main Menu find the Graphical User Interface (GUI), shown in Figure 3.3 below, and click on *"Preferences"*. In the *"Preferences for GUI Filtering"* window, select the *"Structural"* checkbox under *"Individual discipline(s) to show in the GUI"*.

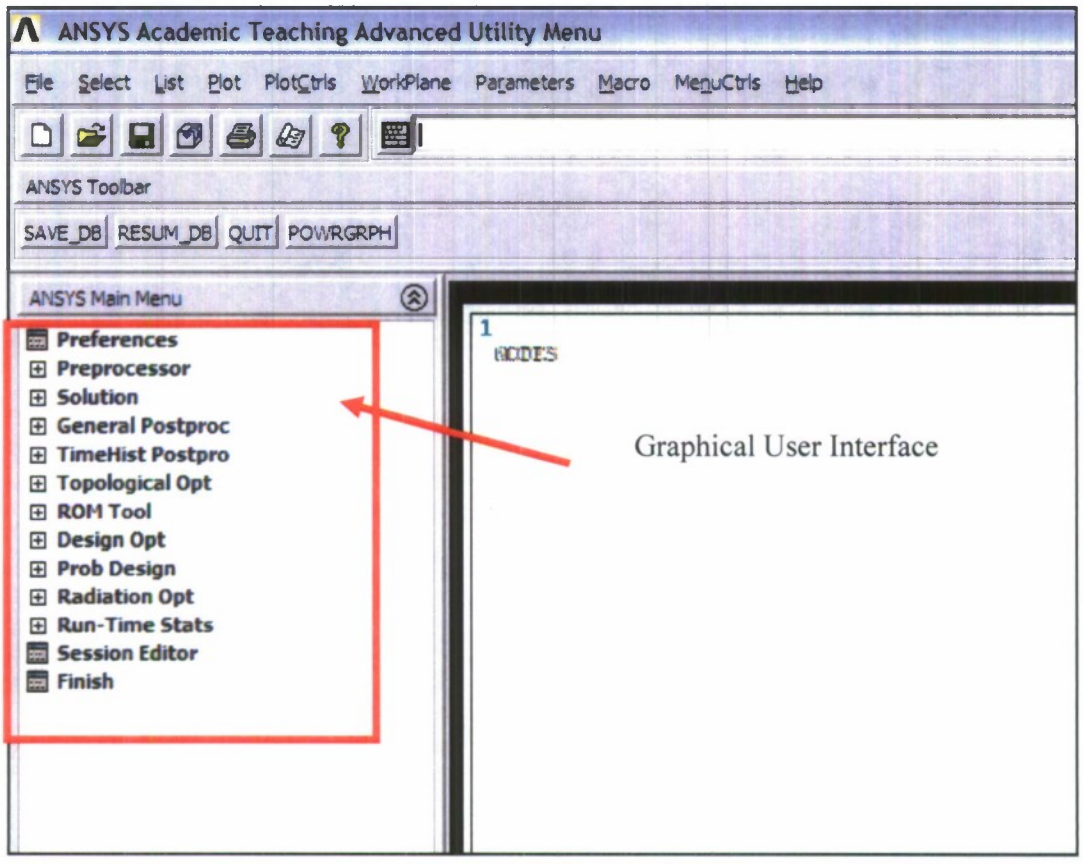

Figure 3.3 – ANSYS Home Screen Showing Graphical User Interface

b) Go to: **Preprocessor>Element Type>Add/Edit/Delete**. When the *"Element Type"* dialog box appears, choose *"Add"*.

c) In the *"Library of Element Types"* dialog box, choose *"Solid"*, then *"Quad 4node 42"*. This is the PLANE42 element.

d) In the *"Element Type"* window, choose *"Add"* once again.

e) In the *"Library of Element Types"* window, choose *"Link"*, then *"2D spar 1"*. This is the LINK1 element.

Step 3 – Set Element Options and Real Constants:

The LINK1 element requires a cross-sectional area and initial strain to be defined. This is an axial element with stiffness k = AE/L. Since this is a 2D model, a representative value, A_l, for the cross-sectional area per unit width of the bolts is needed. This is calculated by taking the cross-sectional area of one row of bolts (there are 3 total), and dividing by the width of the specimen, w, as follows:

$$A_b = \pi \cdot r_b^2 \qquad \text{(Eq. 3.1)}$$

$$A_{row} = 3 \cdot A_b \qquad \text{(Eq. 3.2)}$$

$$A_l = \frac{A_{row}}{w} \qquad \text{(Eq. 3.3)}$$

The strain which results from a bolt preload, P_b, that, for example, is equivalent to 50% of the ultimate tensile strength of the bolt (σ_u =1.5x10^5 psi) is computed as follows:

$$\sigma_{allow} = 0.5 \cdot \sigma_u \qquad \text{(Eq. 3.4)}$$

$$P_b = \sigma_{allow} \cdot A_s \qquad \text{(Eq. 3.5)}$$

$$\varepsilon_b = \frac{P_b}{A_b \cdot E_b} \qquad \text{(Eq. 3.6)}$$

a) In the *"Element Types"* window, highlight *"PLANE42"* and choose *"Options"*. The *"PLANE42 element type options"* dialog box pops up, shown in Figure 3.4. Under the *"Element Behavior K3"* tab, set to *"Plane Strain"*. Close the "*Element Types*" window.

b) In the GUI, go to: **Preprocessor>Real Constants>Add/Edit/Delete**. Click *"Add"*, then highlight *"Type 2 LINK1"* and click *"OK"* in the "*Real Constants"* window. Set *"Real Constant Set No."* to 1, *"Cross- sectional area"* to 0.08727, and *"Initial strain"* to 0.0026. Close the *"Real Constants"* window.

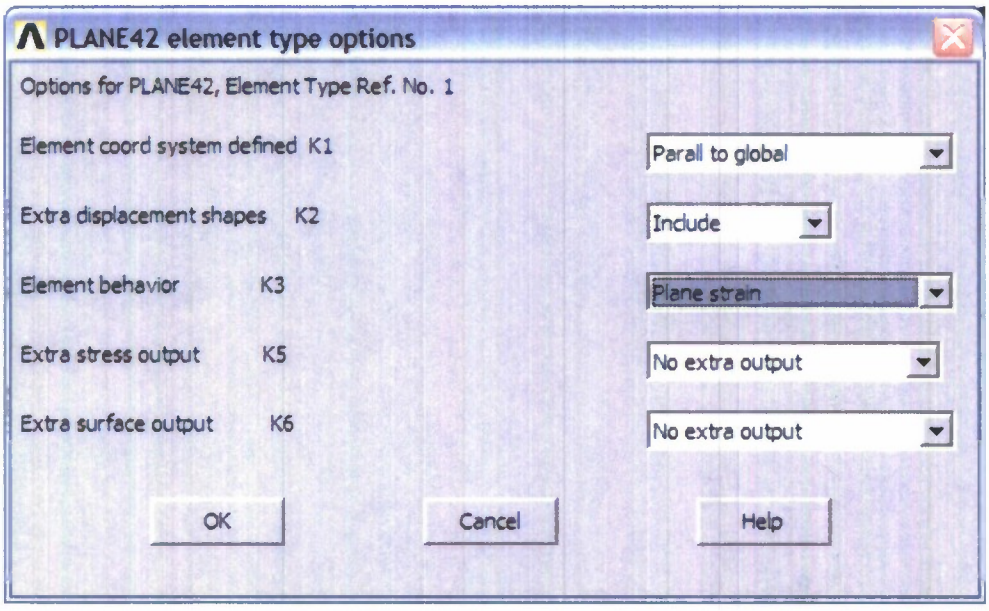

Figure 3.4 – PLANE42 Element Type Options Window

Step 4 – Defining Material Properties:

For this segment, six sets of material properties must be defined; one set for the steel tee and bolts, four sets representing each of the four different orientations for the laminate, and another set for the bolt heads, nuts, and washers. The reason a separate material definition is needed for the bolt heads, nuts, and washers is the 2-D construction does not allow for the modeling of each individual component. In order to capture an equivalent representation of the experimental response, the elastic modulus E_s of the steel bolt heads, nuts, and washers are smeared across the width of the apparatus to calculate an effective elastic modulus, E_m. The areas of 3 washers are calculated using its radius (see Figure

3.5):

$$A_w = 3\pi \cdot \left(r_w^2 - r_h^2\right) \qquad \text{(Eq. 3.7)}$$

The area of the section made by stretching the washer diameter across one-third the width of the specimen (since there are 3 washers in each row) is calculated as follows:

$$A_s = 2 \cdot \left(r_w - r_h\right) \cdot w \qquad \text{(Eq. 3.8)}$$

The washer area ratio is used to find the representative elastic modulus for the bolt heads, nuts, and washers as follows:

$$R_w = \frac{A_w}{A_s} \qquad \text{(Eq. 3.9)}$$

$$E_m = R_w \cdot E_s \qquad \text{(Eq. 3.10)}$$

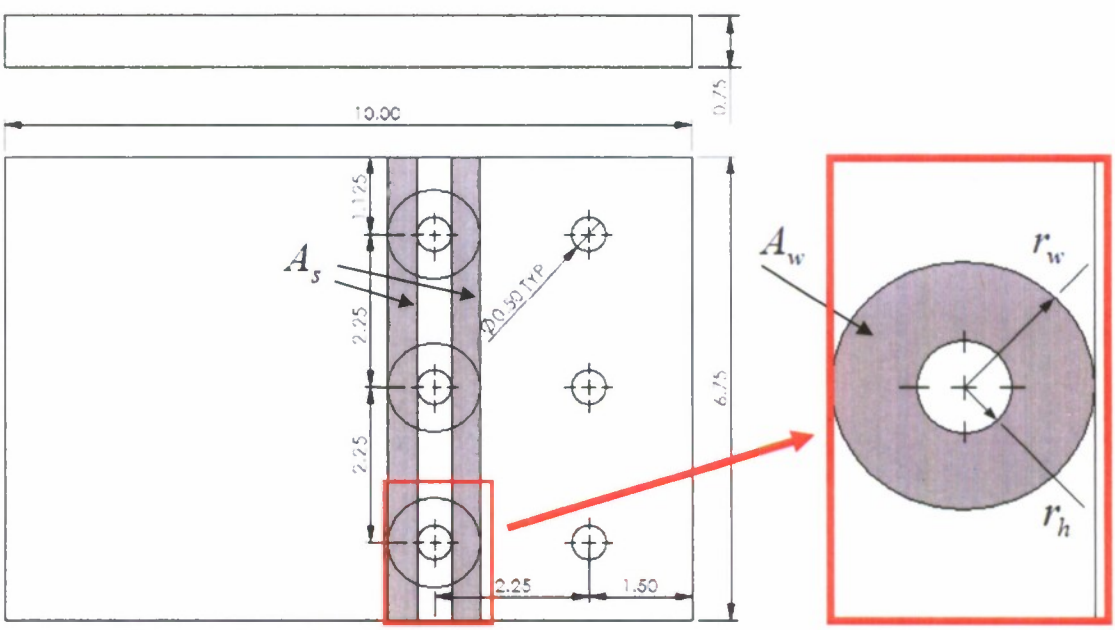

Figure 3.5 – Top View of Laminate Showing Washer Area Ratio

The six material definitions are input as follows:

a) In the GUI, go to: Preprocessor>Material Props>Material Models.

b) In the *"Define Material Model Behavior"* window, as seen in Figure 3.6, navigate to: **Structural>Linear>Elastic>Isotropic**. The material properties for the steel tee and bolts are input in the *"Linear Isotropic Properties for Material Number 1"* window; define an elastic modulus of 2.9×10^7 psi and a Poisson's Ratio of 0.3.

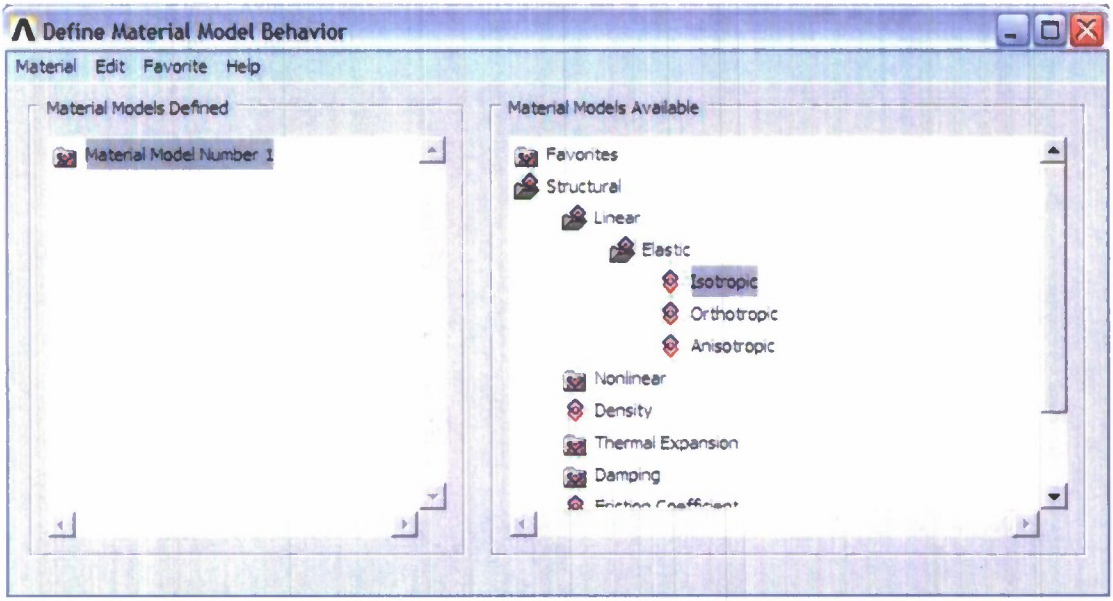

Figure 3.6 – Material Model Window

c) In the same *"Define Material Model Behavior"* window menu, go to: **Material>New Model**. This will allow for a new material definition for the composite with an *"ID"* of 2. Follow the path: **Structural>Linear>Elastic>Orthotropic,** and define the material properties for the 0° composite plies as: *"EX"*=5.6e6, *"EY"*=1.563e6, *"EZ"*=1.563e6, *"PRXY"*=0.2882, *"PRYZ"*=0.435, *"PRXZ"*=0.2882, *"GXY"*=4.74e5, *"GYZ"*=3.335e5, and *"GXZ"*=3.335e5".

d) Create another set of material properties with an "*ID"* of 3 for the 45° composite layers as in the previous step with the following values assigned: *"EX"*=1.416e6, *"EY"*=1.416e6, *"EZ"*=1.563e6, *"PRXY"*=0.4935, *"PRYZ"*=0.2335, *"PRXZ"*=0.2335, *"GXY"*=1.085e6, *"GYZ"*=3.915e5, and *"GXZ"*=3.915e5".

e) For the 90° composite layers enter the following values with an "*ID"* of 4:

"EX"=1.563e6, *"EY"*=5.6e6, *"EZ"*=1.563e6, *"PRXY"*=0.08044, *"PRYZ"*=0.2882, *"PRXZ"*=0.435, *"GXY"*=4.745e5, *"GYZ"*=4.745e5, and *"GXZ"*=3.335e5".

f) Enter the following values for the -45° composite plys, with an *"ID"* of 5: *"EX"*=1.416e6, *"EY"*=1.416e6, *"EZ"*=1.563e6, *"PRXY"*=0.4935, *"PRYZ"*=0.2335, *"PRXZ"*=0.2335, *"GXY"*=1.085e6, *"GYZ"*=3.915e5, and *"GXZ"*=3.915e5".

g) Define the sixth material model for the bolt heads, nuts, and washers with an *"ID"* of 6 by navigating to: **Structural>Linear>Elastic>Isotropic**. Set an elastic modulus of 1.961×10^7 psi and a Poisson's Ratio of 0.3 for this material model.

Step 5 – Building the Steel Tee Geometry:

There is only a need to build half of the actual experimental apparatus in ANSYS, since there is symmetry about the center of the steel tee. Dimensions for the bolted experimental setup are shown in Figure 3.2. For the following steps, rectangles will be constructed using the GUI by going to: **Preprocessor>Modeling> Create>Areas> Rectangle>By 2 Corners**.

a) To create the bottom of the steel tee, enter the following: *"WP X"*=0, *"WP Y"*=0, *"Width"*=-0.375, *"Height"*=9.0.

b) For the top portion of the tee and enter: *"WP X"*=0, *"WP Y"*=9, *"Width"*=-5.25, *"Height"*=0.75.

Step 6 – Building the Laminate Geometry:

Each ply of the 42-layer composite material is modeled in two parts: one set of areas are to be connected directly to the steel tee, and the other set provides a location to apply the vertical load.

a) To model the first set of composite areas, go to: **Preprocessor>Modeling> Create>Areas> Rectangle>By 2 Corners**. For the first layer enter: *"WP X"*=0, *"WP Y"*=9.75, *"Width"*=-8.25, *"Height"*=0.01786. Each of the 41 layers that follow have the same input values, except for *"WP Y"*, which requires that each successive layer entry

have a value of 0.01786 higher in magnitude than the preceding one. For example, the second layer has the values: "*WP X*"=0, "*WP Y*"=9.76786, "*Width*"=-8.25, "*Height*"=0.01786. Complete the rectangles for all 42 plies.

b) The second set of composite areas is under the load application point and is created using the same procedure as in the previous step. For the first layer enter: "*WP X*"=-8.25, "*WP Y*"=9.75, "*Width*"=-0.5, "*Height*"=0.01786. Each of the 41 layers that follow have the same input values, except for "*WP Y*", which requires that each successive layer entry have a value of 0.01786 higher in magnitude than the preceding one. For example, the second layer has the values: "*WP X*"=-8.25, "*WP Y*"=9.76786, "*Width*"=-0.5, "*Height*"=0.01786. Complete the rectangles for all 42 plies.

Step 7 – Gluing the Composite Layers:

Before creating the areas needed to complete the model of the whole apparatus, it is necessary to glue all of the laminate areas together.

a) In the GUI, go to: Preprocessor>Modeling>Operate>Booleans>Glue>Areas.

b) In the "*Glue Areas*" window set the method for gluing to "Box", draw a box around the entire laminate, and click "*OK*". **Be sure not to select any part of the steel tee in this step.**

Step 8 – Creating the Washers:

The washers are modeled as rectangles, each part representing half of one washer. There are two rows of washers, bolts and nuts. Using the same procedure as the previous steps, enter the following data for each washer-half:

a) "*WP X*"=-0.8125, "*WP Y*"=10.50012, "*Width*"=-0.40625, "*Height*"=0.125

b) "*WP X*"=-1.78125, "*WP Y*"=10.50012, "*Width*"=- 0.40625, "*Height*"=0.125

c) "*WP X*"=-3.0625, "*WP Y*"=10.50012, "*Width*"=-0.40625, "*Height*"=0.125

d) "*WP X*"=-4.03125, "*WP Y*"=10.50012, "*Width*"=-0.40625, "*Height*"=0.125

e) "*WP X*"=-0.8125, "*WP Y*"=8.875, "*Width*"=-0.40625, "*Height*"=0.125

f) *"WP X"*=-1.78125, *"WP Y"*=8.875, *"Width"*=- 0.40625, *"Height"*=0.125

g) *"WP X"*=-3.0625, *"WP Y"*=8.875, *"Width"*=-0.40625, *"Height"*=0.125

h) *"WP X"*=-4.03125, *"WP Y"*=8.875, *"Width"*=-0.40625, *"Height"*=0.125

Step 9 – Creating the Bolt Heads and Nuts:

The bolt heads and nuts are each divided into to areas in order to create "keypoints" that the LINK elements can attach to. Input the subsequent data for the bolt heads:

a) *"WP X"*=-1.125, *"WP Y"*=10.62512, *"Width"*=-0.375, *"Height"*=0.25

b) *"WP X"*=-1.5, *"WP Y"*=10.62512, *"Width"*=-0.375, *"Height"*=0.25

c) *"WP X"*=-3.375, *"WP Y"*=10.62512, *"Width"*=-0.375, *"Height"*=0.25

d) *"WP X"*=-3.75, *"WP Y"*=10.62512, *"Width"*=-0.375, *"Height"*=0.25

For the nuts, enter:

e) *"WP X"*=-1.125, *"WP Y"*=8.625, *"Width"*=-0.375, *"Height"*=0.25

f) *"WP X"*=-1.5, *"WP Y"*=8.625, *"Width"*=-0.375, *"Height"*=0.25

g) *"WP X"*=-3.375, *"WP Y"*=8.625, *"Width"*=-0.375, *"Height"*=0.25

h) *"WP X"*=-3.75, *"WP Y"*=8.625, *"Width"*=-0.375, *"Height"*=0.25.

Figure 3.7 shows the full geometry of the model, with all entities labeled.

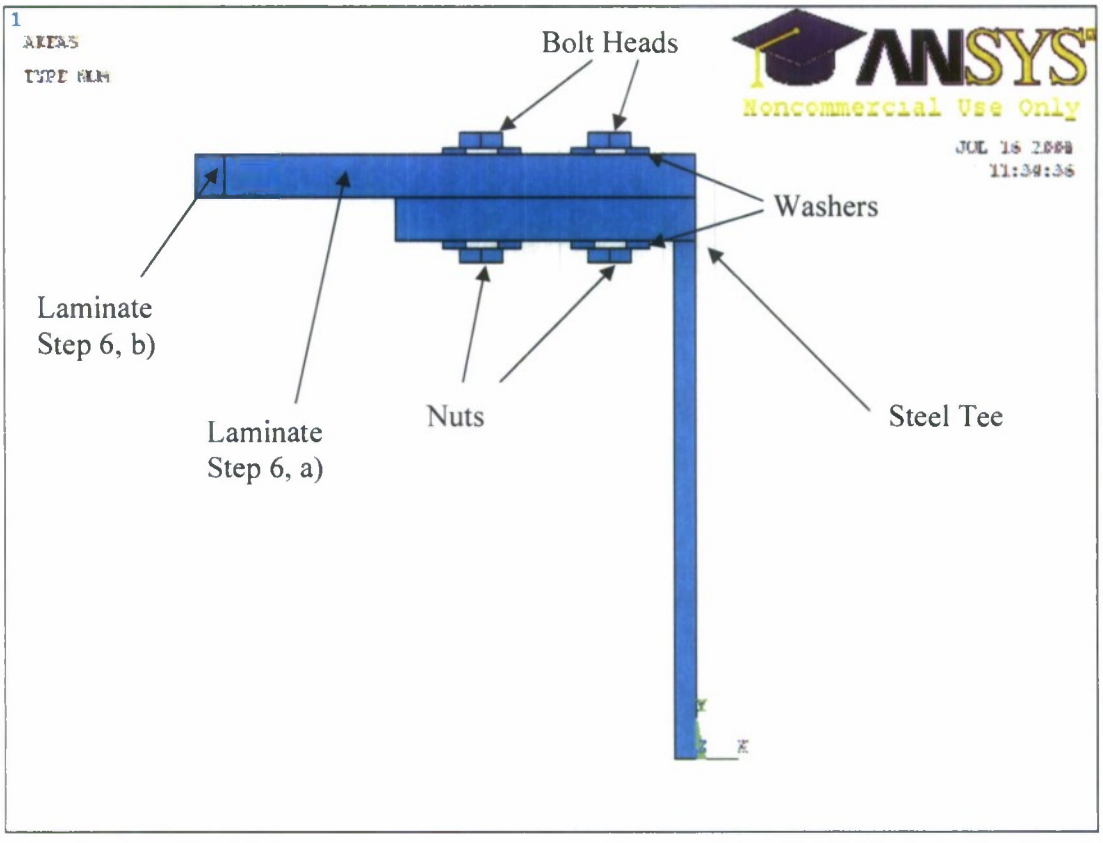

Figure 3.7 – ANSYS Bolted Model Geometry

Step 10 – Glue Bolt Heads and Nuts Areas:

a) In the GUI, go to: Preprocessor>Modeling>Operate>Booleans>Glue>Areas.

b) Choose both halves of each bolt head and nut by clicking on each area one-by-one. Once all the areas have been selected, as shown in Figure 3.8, click *"OK"*.

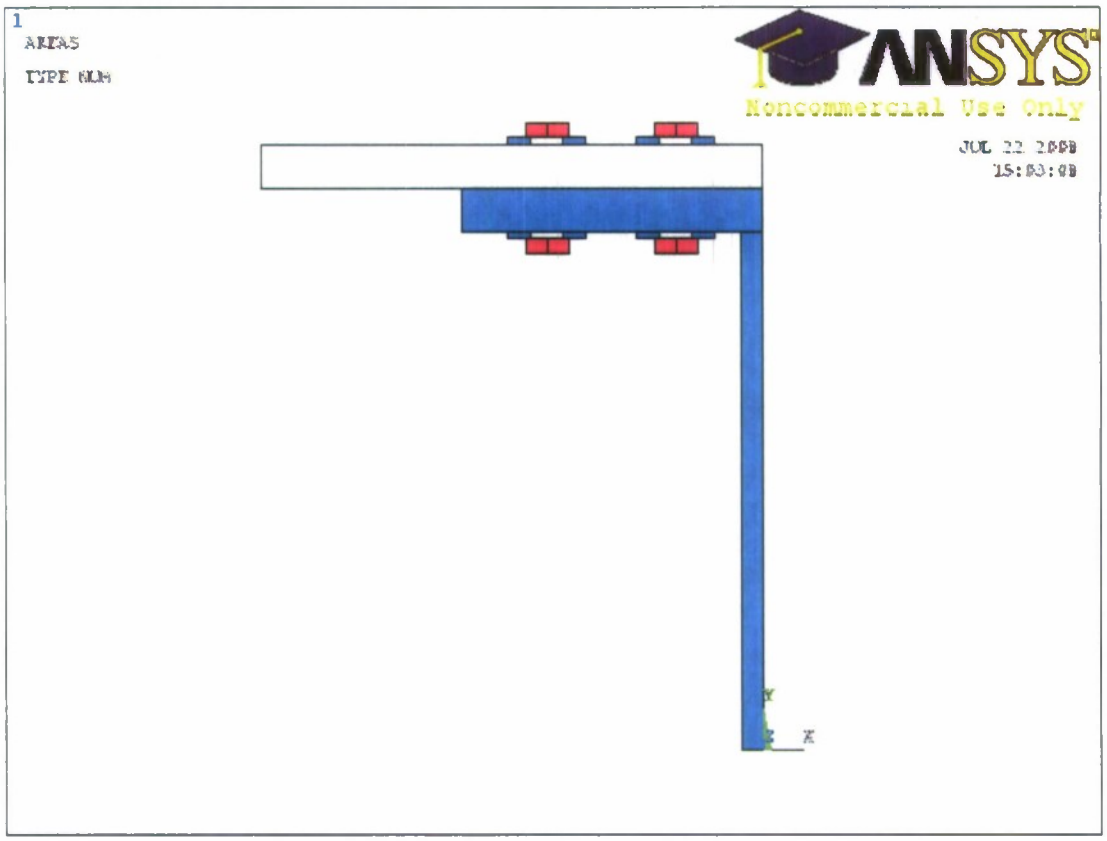

Figure 3.8 – Bolted Plane-Strain 2D ANSYS Model with Glued Areas Highlighted

Step 11 – Mesh Washers, Bolt Heads, and Nuts:

Before any area is meshed, a suitable mesh pattern should be decided upon and defined for each section.

a) Through the GUI, go to: **Preprocessor>Meshing>Meshtool**. In the *"Meshtool"* dialog box, set the *"Element Attributes"* tab to *"Global"* and Click *"Set"*.

b) In the "Meshing Attributes" window, set "Element type number" to 1 PLANE42 and "Material Number" to 6.

c) Under *"Size Controls: Areas"* in the *"Meshtool"* dialog box, click *"Set"*. Pick the areas which represent the bolt heads and nuts and click *"OK"*. Set the *"Element edge length"* to 0.125 in the *"Element Size at Picked Areas"*.

d) Under *"Size Controls: Lines"* in the *"Meshtool"* dialog box, click *"Set"*. Pick the 16 vertical lines that are part of the washers. Set *"No. of element divisions"* to 2. For the 16 horizontal lines which represent the washers, set *"No. of element divisions"* to 4.

e) Mesh the areas representing the bolts, nuts, and washers using the *"Meshtool"* window and by setting *"Mesh"* to "Areas", *"Shape"* to "Quad and Mapped". Click the *"Mesh"* button and pick the corresponding areas on the model.

Step 12 – Mesh the Steel Tee:

a) Through the GUI, go to: **Preprocessor>Meshing>Meshtool**. In the *"Meshtool"* dialog box, set the *"Element Attributes"* tab to *"Global"* and Click *"Set"*.

b) In the "Meshing Attributes" window, set "Element type number" to 1 PLANE42 and "Material Number" to 1.

c) Under *"Size Controls: Areas"* in the *"Meshtool"* dialog box, click *"Set"*. Pick the 2 areas which represent the steel tee and click *"OK"*. Set *"Element edge length"* to 0.125 in the *"Element Size at Picked Areas"* window.

e) Mesh the steel tee using the *"Meshtool"* window by setting *"Mesh"* to "Areas", *"Shape"* to "Quad and Mapped". Click the *"Mesh"* button and pick the applicable areas of the steel tee on the model.

Step 13 – Mesh the Laminate:

a) Through the GUI, go to: **Preprocessor>Meshing>Meshtool**. Under *"Size Controls: Areas"* in the *"Meshtool"* dialog box, click *"Set"*.

b) Using the "*Box*" option, pick all 84 areas which represent the composite (zooming in may make this task easier) and click *"OK"*. Set *"Element edge length"* to 0.01786 in the *"Element Size at Picked Areas"* window.

c) In the "Meshtool" dialog box, set the "Element Attributes" tab to "Global" and Click "Set". In the "Meshing Attributes" window, set "Element type number" to 1 PLANE42

and "Material Number" to 2.

d) Using the zoom tool, enlarge the area which makes up the location on the laminate for the load to be applied, as shown in Figure 3.9. Mesh the 0° composite plies using the *"Meshtool"* window and by setting *"Mesh"* to "Areas", *"Shape"* to "Quad and

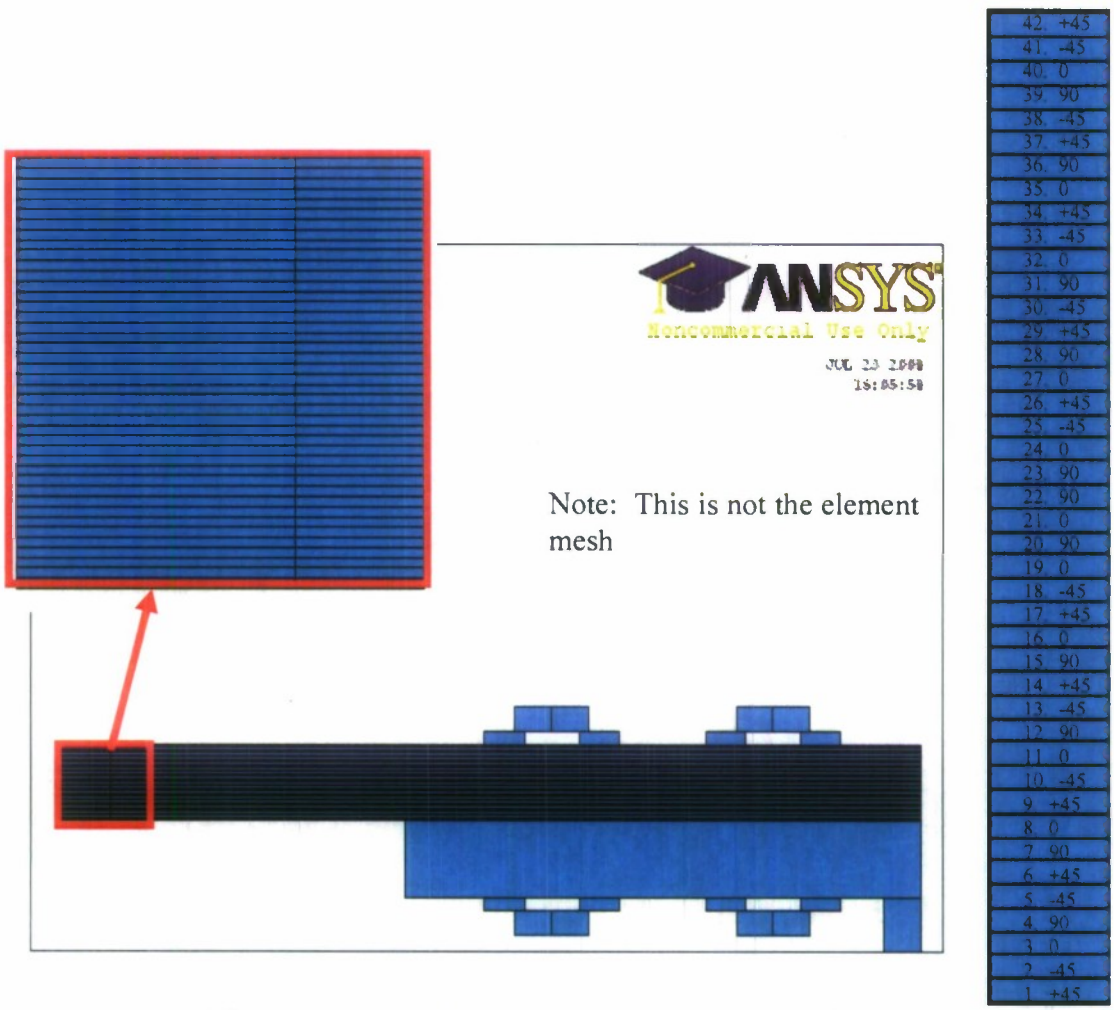

Figure 3.9 – Zoomed-In View of the Composite Layers

Mapped". Click the "*Mesh*" button and pick the 0° laminate layers on the model, as they are labeled in Figure 3.10, then click "*OK*".

e) Repeat Step 12 c), and change the "*Material Number*" to 3. Follow Step 12 d), however this time be sure to mesh the 45° layers.

f) Repeat Step 12 c), and change the "*Material Number*" to 4. Follow Step 12 d), and this time be sure to mesh the 90° layers.

g) Repeat Step 12 c), and change the "*Material Number*" to 5. Follow the procedure in Step 12 d) to mesh the -45° layers.

h) Using the procedure outlined in steps c) through g), mesh the other section of the composite which is attached directly to the steel tee.

Step 14 – Create Lines for LINK Elements and Mesh:

a) In the GUI, go to: **Preprocessor>Modeling>Create>Lines>Lines> Straight Line**. On the left bolt pick the keypoint in the middle of the bolt head on the top surface, then pick the keypoint in the middle of the nut head

Figure 3.10 – Layer Numbers and Orientations

on the bottom surface. Do the same for the bolt furthest to the right side of the model. There should now be 2 lines for the bolts.

b) Through the GUI, go to: **Preprocessor>Meshing>Meshtool**. In the *"Meshtool"* dialog box, set the *"Element Attributes"* tab to *"Global"* and Click *"Set"*.

c) In the "Meshing Attributes" window, set "Element type number" to 2 LINK1, "Material number" to 1, and "Real constant" to 1.

d) Under *"Size Controls: Lines"* in the *"Meshtool"* dialog box, click *"Set"*. Pick the 2 lines which represent the bolts and click *"OK"*. Set *"No. of element divisions"* to 1 in the *"Element Sizes on Picked Lines"* window.

e) Using the *"Meshtool"* window set *"Mesh"* to "Lines". Click the "*Mesh*" button and select the 2 bolt-lines on the model. The entire model is now meshed and is shown in Figure 3.10 below.

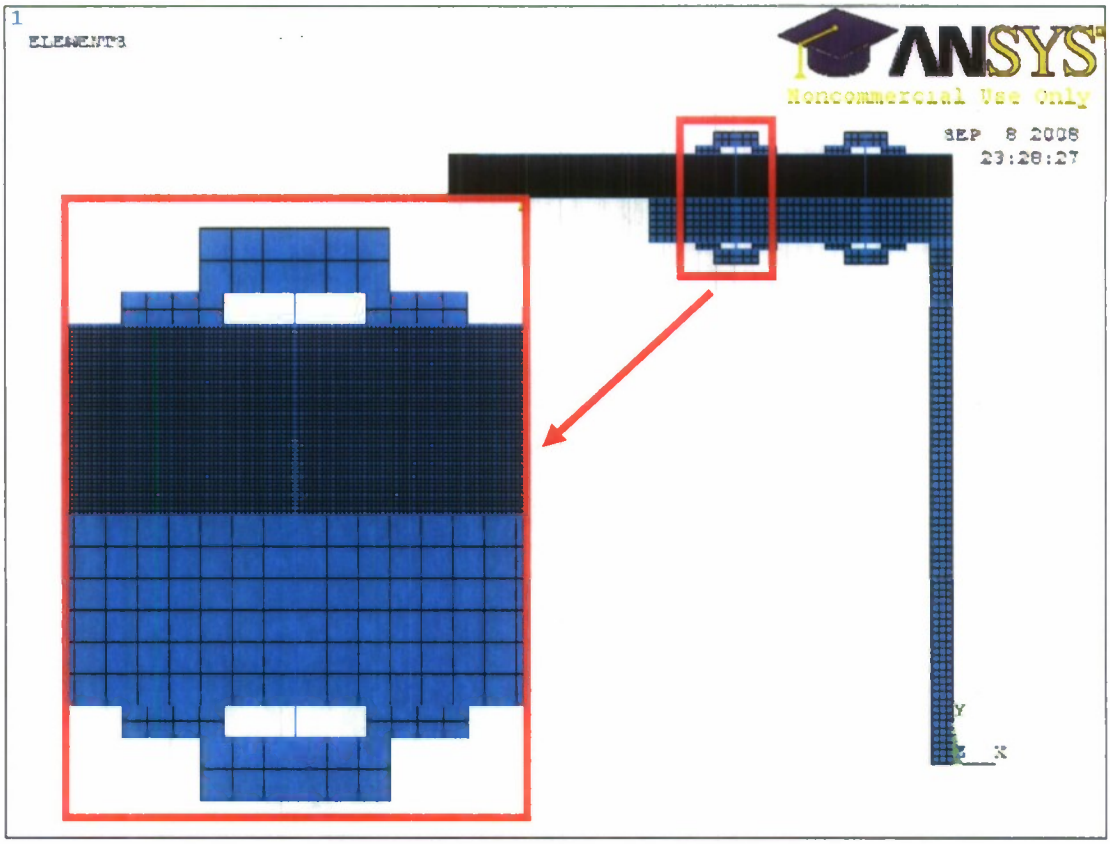

Figure 3.10 – Bolted Model Mesh

Step 15 – Define Boundary Conditions:

a) In the GUI, navigate to: **Preprocessor>Loads>Define Loads>Apply>Structural> Pressure>On Lines**. Select the line which lies on the very top of the laminate where the load is to be applied, as shown in Figure 3.12, and click *"OK"*. Note: This pressure corresponds to the occurrence of the laminate being pushed downward in the actual experimental test. To mimic the upward deflection, this pressure must be applied to the line on the bottom of the laminate, directly under the line specified above.

b) In the "Apply PRES on lines" window, select "Constant value" under "Apply PRES on lines as a". Set "Load PRES value" to 1185.19.

c) Go to: Preprocessor>Loads>Define Loads>Apply>Structural>

Displacement>On Lines. Choose the line at the bottom of the steel tee, as shown in

Figure 3.12, and click *"OK"*.

d) In the *"Apply U, ROT on Lines"* window, set *"DOF's to be constrained"* to ALL DOF. This action will constrain the displacements UX and UY, and will not apply any rotational restriction.

e) Go to: **Preprocessor>Loads>Define Loads>Apply>Structural> Displacement>On Lines**. Choose the 2 vertical lines that make up the center of the steel tee along the right side of the model, as shown in Figure 3.12, and click *"OK"*.

f) Set "DOF's to be constrained" to UX.

g) Follow: **Preprocessor>Loads>Define Loads>Apply>Structural> Displacement> On Keypoints**. On the composite, choose the bottom right keypoint which lies along the right side of the model, as shown in Figure 3.12, and click *"OK"*.

h) Set "DOF's to be constrained" to UX.

Step 16 – Contact Surfaces for Washers, Bolt Heads, and Nuts:

a) In the Utility Menu at the top of the ANSYS Home Screen, click the *"Contact*

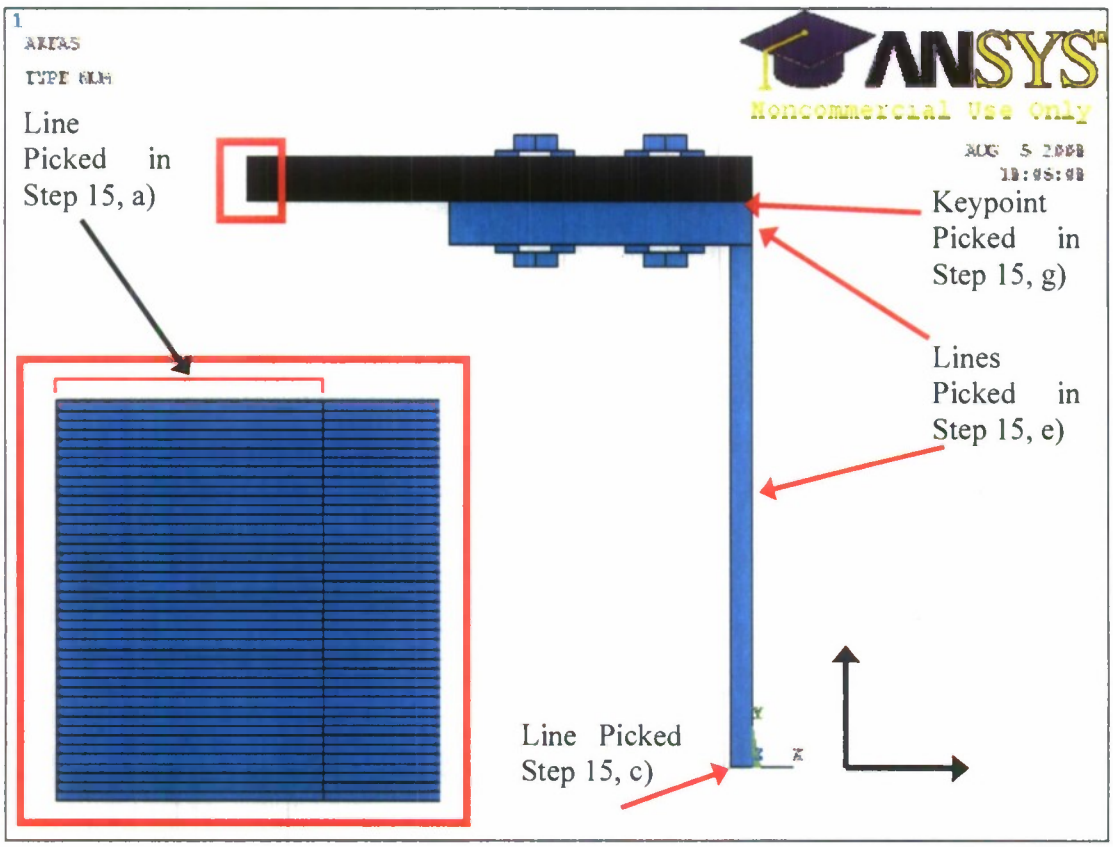

Figure 3.11 – Boundary Conditions Locations

Manager" button. In the dialog box that pops up, click the *"Contact Wizard"* button.

b) In the *"Contact Wizard"* window, the following settings must be correct:

Target Surface: Set to "*Lines*".

Target Type: Set to "*Flexible*".

c) Click "*Pick Target*".

d) Select the 8 horizontal lines on the washers where they come in contact with either a nut or a bolt head, then click "*Apply*".

e) In the *"Contact Wizard"* window, click "*Next*". In the new window, the following settings must be correct:

Contact Surface: Set to "*Lines*".

Contact Element Type: Set as "*Surface-to-Surface*".

f) Click "*Pick Contact*"

g) Select the 8 horizontal lines on the bolts and nuts where they come in contact with the washers, then click "*Apply*".

h) In the *"Contact Wizard"* window, click "*Next*". In the new window, the following settings must be correct:

Check the box next to "Include initial penetration".

Friction>Material ID: Set to 6.

i) Click "Optional settings". In the "Contact Properties" window under the "Basic" tab, set "Normal Penalty Stiffness" to 10 and set "Behavior of contact surface" to "Bonded (always)".

j) In the same window under the *"Friction"* tab, set *"Stiffness Matrix"* to *"Unsymmetric"* and click *"OK"*.

k) Create the contact surfaces by clicking *"Create"* in the contact wizard window.

Step 17 – Creating Contact Where Steel Tee and Washers Meet:

a) As in Step 16, open the Contact Wizard.

b) Repeat Step 16, b).

c) Click "*Pick Target*".

d) Select the horizontal line on the steel tee where it meets the washers, then click "*Apply*".

e) Repeat Step 16, e).

f) Click "*Pick Contact*"

g) Select the 4 horizontal lines on the washers where they come in contact with the steel tee, then click "*Apply*".

h) In the *"Contact Wizard"* window, click "*Next*". In the new window, the following settings must be correct:

Check the box next to "Include initial penetration".

Friction>Material ID: Set to 1.

i) Follow i) through k) in Step 16.

Step 18 – Creating Contact Between Two Steel T Areas:

a) Open the Contact Wizard.

b) Repeat Step 16, b).

c) Click "*Pick Target*".

d) Select the horizontal line as in Step 17, d) and click "*Apply*".

e) Repeat Step 16, e).

f) Click "*Pick Contact*"

g) On the remaining steel tee section, select the horizontal line located at the top of the area, then click "*Apply*".

h) In the *"Contact Wizard"* window, click "*Next*". In the new window, the following settings must be correct:

Check the box next to "Include initial penetration".

Friction>Material ID: Set to 1.

i) Follow i) through k) in Step 16.

Step 19 – Creating Contact Between the Steel Tee and Composite:

a) Open the Contact Wizard.

b) Repeat Step 16, b).

c) Click "*Pick Target*".

d) Select the horizontal line on the bottom side of the laminate, then click "*Apply*".

e) Repeat Step 16, e).

f) Click "Pick Contact…"

g) Select the horizontal line on the top side of the steel tee, then click "*Apply*".

h) In the *"Contact Wizard"* window, click "*Next*". In the new window, the following settings must be correct:

Check the box next to "Include initial penetration".

Friction>Material ID: Set to 1.

i) Click "Optional settings". In the "Contact Properties" window under the "Basic" tab, set "Normal Penalty Stiffness" to 0.1 and set "Behavior of contact surface" to "Standard".

j) In the same window under the *"Friction"* tab, set *"Stiffness Matrix"* to *"Unsymmetric"* and click *"OK"*.

k) Create the contact surfaces by clicking *"Create"* in the contact wizard window.

Step 20 – Creating Contact Between Top of Composite and Washers:

a) Open the Contact Wizard.

b) Repeat Step 16, b).

c) Click "*Pick Target*".

d) Select the horizontal line on the top side of the laminate, then click "*Apply*".

e) Repeat Step 16, e).

f) Click "*Pick Contact*"

g) Select the 4 horizontal lines on the washers where they come in contact with the laminate, then click "*Apply*".

h) In the *"Contact Wizard"* window, click "*Next*". In the new window, the following settings must be correct:

Check the box next to "Include initial penetration".

Friction>Material ID: Set to 6.

i) Follow i) through k) in Step 16.

Step 21 –Solve the Model:

In the GUI, go to: **Solution>Solve>Current LS**. Click "*OK*" in the *"Solve Current Load Step"* window.

Step 22 –Obtain the Displacement Contour Plot:

To qualitatively verify that the analysis is accurate, a contour plot of the nodal displacement, as shown in Figure 3.13, can be acquired by navigating to: **General Postproc>Plot Results>Contour Plot>Nodal Solu.** In the *"Contour Nodal Solution Data"* window, go to: **Nodal Solution>DOF Solution>Displacement Vector Sum**, and click "*OK*".

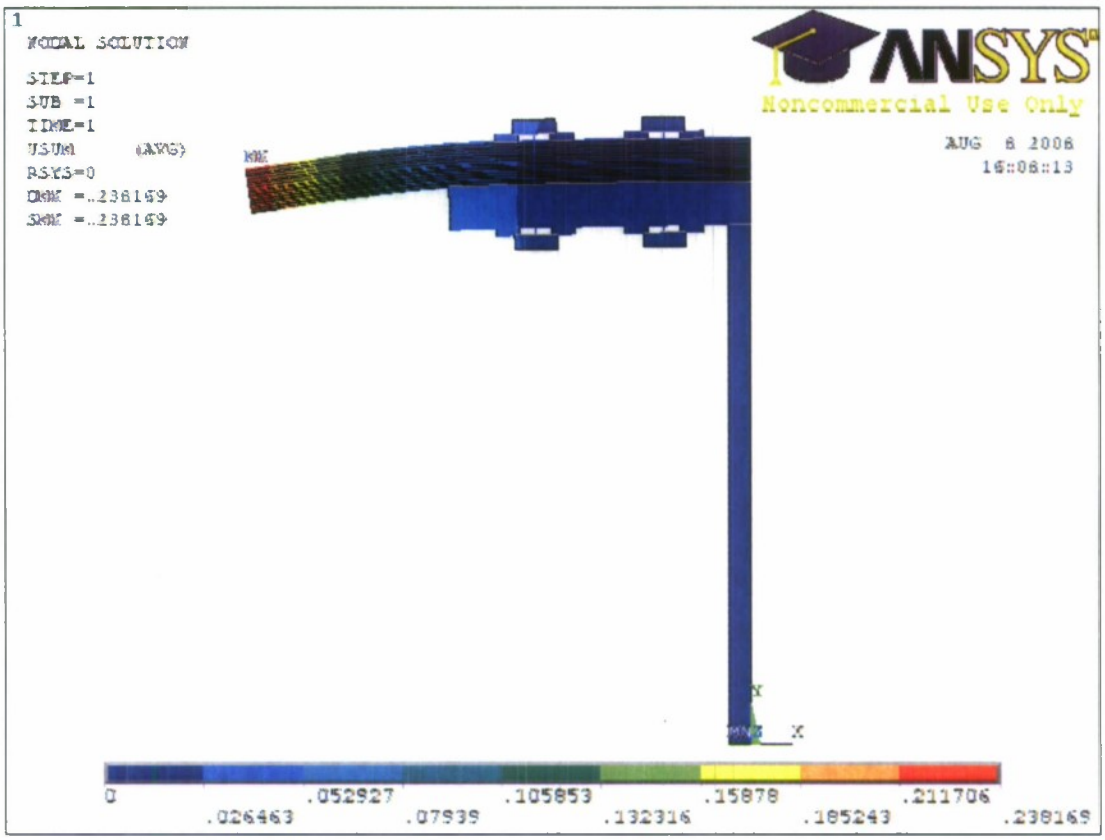

Figure 3.12 – Displacement Contour Plot

Step 23 –Obtain the MTS Displacement Plot:

An MTS displacement plot is needed to determine how well the analysis agrees with experimental response data. Begin by going to **Plot>Elements** in the Utility Menu, then for the following steps go to **General Postproc>Path Operations** in the GUI.

a) Go to **Define Path>By Nodes**. Using the zoom tool, enlarge the area where the load is applied. With the cursor, pick the 14th node from the end of the laminate, as shown in Figure 3.14.

b) Using the zoom tool, enlarge the area at the top right corner of the composite. Pick the top right corner node on the laminate, as shown in Figure 3.14, then click "*Apply*".

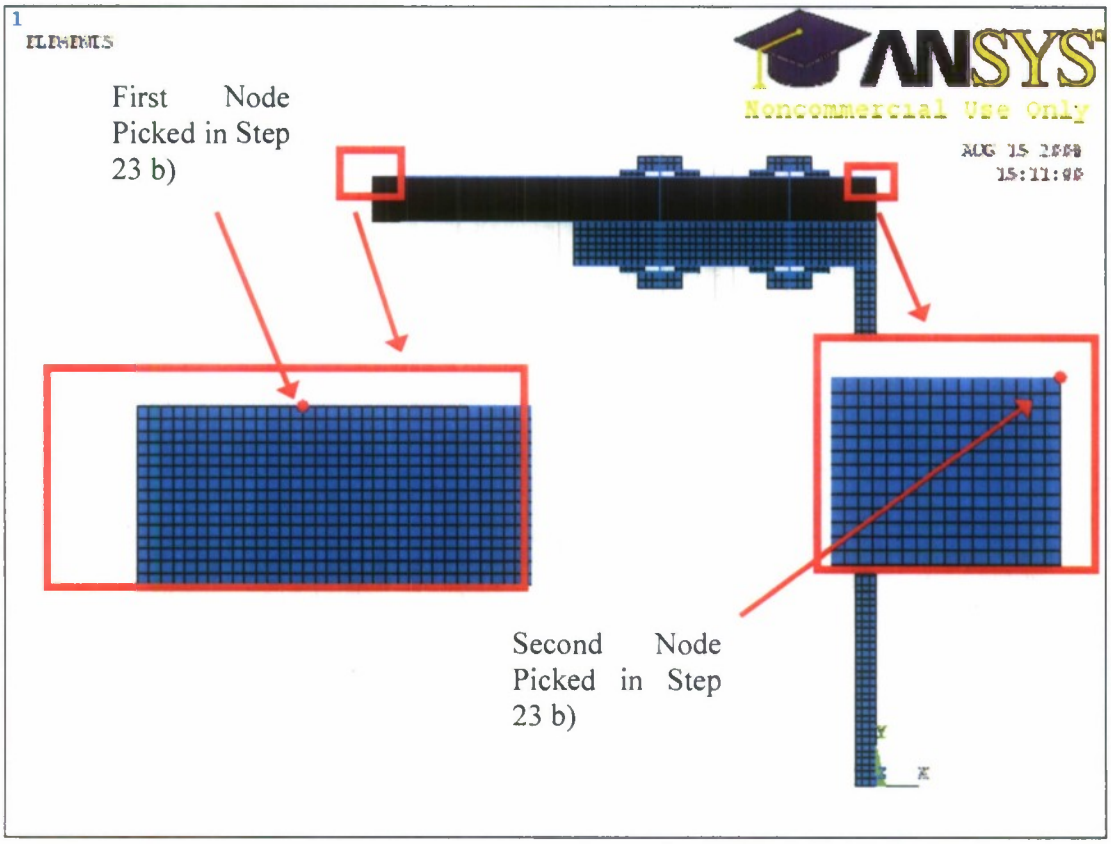

Figure 3.13 – Zoomed-in View of MTS Displacement Area

c) In the "*By Nodes*" dialog box, input the following:

Set "Define Path Name" to UY.

Set "*Number of Data Sets*" to 30 (This is the default value).

Set "*Number of Divisions*" to 50 and click "*OK*".

d) Navigate to **Map onto Path**. In the *"Map Result Items onto Path"* window, set *"User Label for Item"* to UY1, then select "*DOF solution>Translation UY*" and click "*OK*".

e) Go to **Plot Path Item>On Graph**. Select "*UY1*" and click "*OK*". The resulting plot is shown in Figure 3.15.

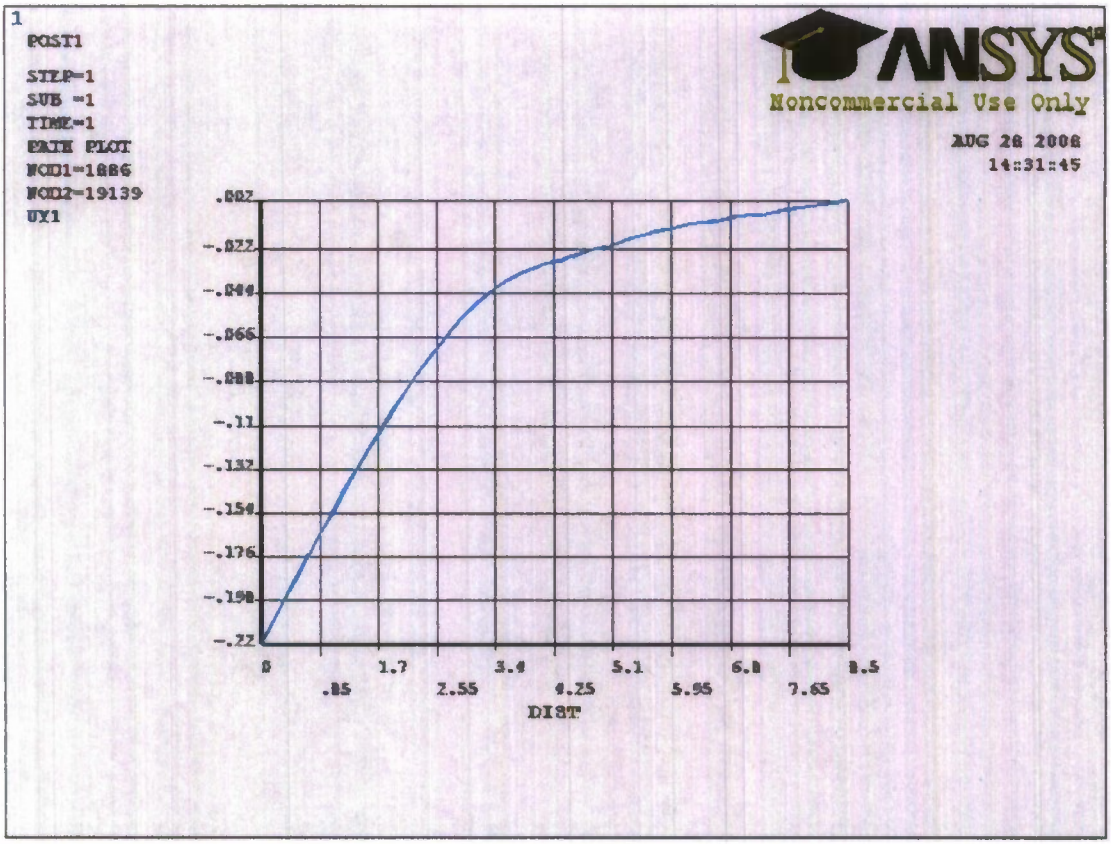

Figure 3.15 – Bolted MTS Displacement Plot

Step 24 –Obtain the Laminate σ_x Plot at the Steel Tee Edge:

A graph which shows σ_x layer-by-layer is a useful tool for stress analysis of the hybrid connection. Begin by going to **Plot>Elements** in the Utility Menu, then for the following steps go to **General Postproc>Path Operations** in the GUI:

a) Go to **Define Path>By Nodes**. Using the zoom tool, enlarge the area of the composite which is directly above the steel tee edge. Pick the node closest to the left edge of the steel tee, then directly above pick the node on the top side of the laminate, as shown in Figure 3.16, then click "*Apply*".

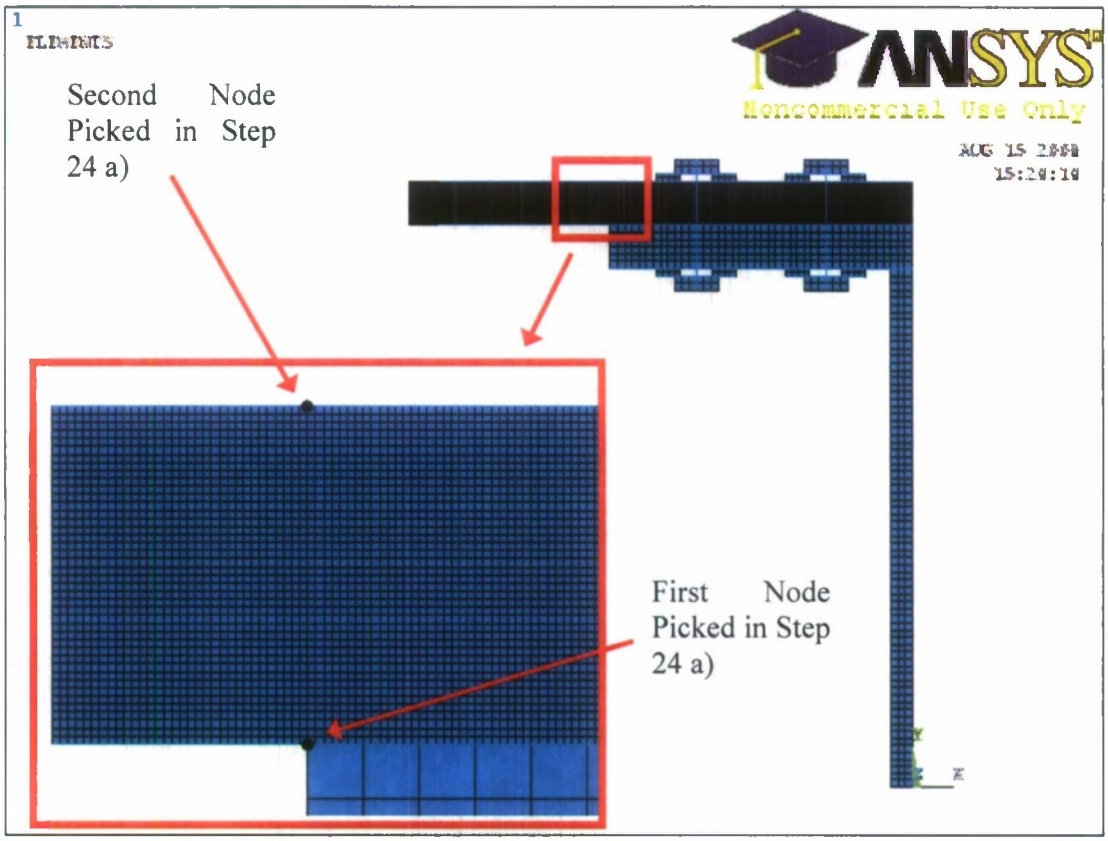

Figure 3.16 – Zoomed-in View of Maximum Stress Region

c) In the "*By Nodes*" dialog box, input the following:

Set "Define Path Name" to SX.

Set "*Number of Data Sets*" to 30 (This is the default value).

Set "*Number of Divisions*" to 10000 and click "*OK*".

d) Navigate to **Map onto Path**. In the *"Map Result Items onto Path"* window, set *"User Label for Item"* to SX1, then select "*Stress>X-direction SX*". Uncheck the box next to "*Average result across element*", and click "*OK*".

e) Go to **Plot Path Item>On Graph**. Select "*SX1*" and click "*OK*". The resulting plot is shown in Figure 3.17.

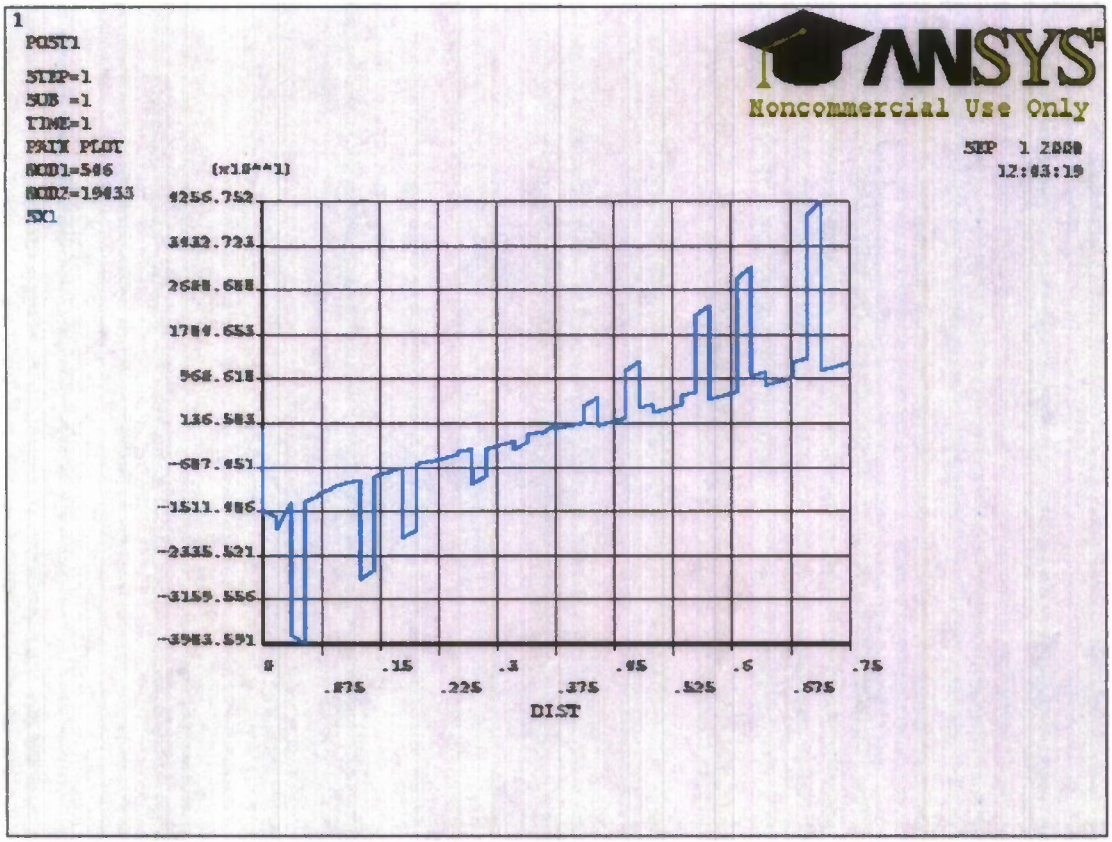

Figure 3.17 – Bolted σ_x Plot at Steel Tee Edge

3.1.2 Clamped Case Modeling Instructions

The instructions for modeling the clamped case are very much the same as for the bolted case, with a few differences in geometries, as shown in Figure 3.18 below, and input values. To perform an accurate analysis of the clamped specimen, follow the bolted case procedure with the following modifications made to the specified steps below:

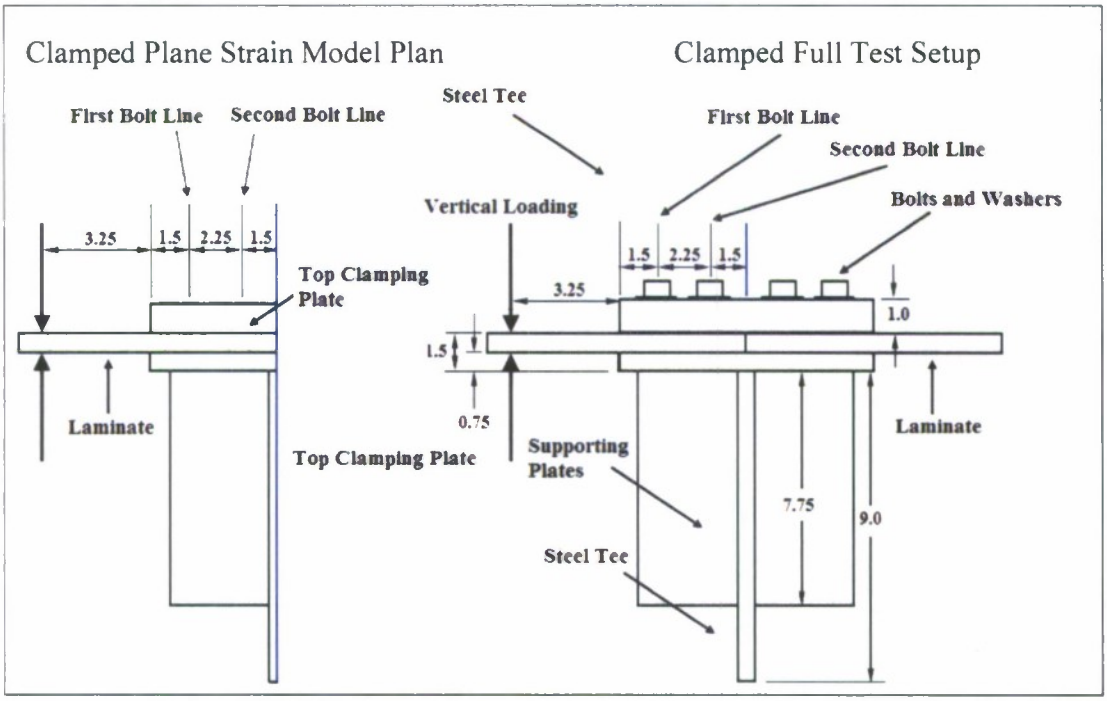

Figure 3.18 – Clamped Plane Strain Model Schematic

Step 3 – Set Element Options and Real Constants:

The LINK1 element for this configuration requires a new cross-sectional area per unit width, A_l, and initial strain to be defined for the bolts. This is calculated by taking the cross-sectional area of one row of bolts (there are 3 total), and dividing by the width of the specimen. Since the width of the composite, w_c, is different from the steel tee, w_s, an effective width is calculated using the elastic modulus of each component as follows:

$$\frac{E_c}{E_s} = R_e \qquad \text{(Eq. 3.11)}$$

$$w_{eff} = w_c - (R_e \cdot (w_s - w_c)) \qquad \text{(Eq. 3.12)}$$

Using this new effective width and the larger bolt radius r_b of 0.375", the new cross sectional area per unit width of the bolts can be found using the equations shown in the bolted case. The strain computation here uses a lower σ_{allow} of $1.2\text{x}10^5$ psi, along with the total bolt area for one row of bolts, A_{row}.

b) In the "Real Constants" window, set "Cross- sectional area" to 0.19705, and "Initial strain" to 0.0021.

Step 4 – Defining Material Properties:

The inclusion of bolt heads, nuts, and washers is not necessary, so sub-step g) need not be carried out. There is a need for a material model definition designated for the supporting plates which are welded to the steel tee. So, sub-step g) below should be switched with the bolted case. This effective elastic modulus is found by multiplying the supporting plate/steel tee width-ratio by the elastic modulus of steel.

g) Define the sixth material model for the supporting plates with an "*ID*" of 6 by navigating to: **Structural>Linear>Elastic>Isotropic**. Set an elastic modulus of $2.0\text{x}10^6$ psi and a Poisson's Ratio of 0.3.

Step 5 – Building the Steel Tee Geometry:

The top portion of the steel tee will be constructed in three pieces in order to generate the keypoints which the link elements for the bolts can be attached to.

b) For the three geometries denoting the top portion of the tee enter:

"*WP X*"=0, "*WP Y*"=9, "*Width*"=-1.5, "*Height*"=0.75.

"*WP X*"=-1.5, "*WP Y*"=9, "*Width*"=-2.25, "*Height*"=0.75

"*WP X*"=-3.75, "*WP Y*"=9, "*Width*"=0.625, "*Height*"=0.75

"*WP X*"=-4.375, "*WP Y*"=9, "*Width*"=0.875, "*Height*"=0.75

Step 7- Glue the Composite Layers and Generate Clamping and Supporting Plates:

In addition to completing the sub-steps a) and b), complete the following sub-steps c) and d); c) will generate the top clamping plate via three adjacent rectangles and d), the supporting plate. Again, the purpose of making three separate areas for c) is to produce keypoints for link element attachment. These rectangles are made through the GUI by going to: **Preprocessor>Modeling>Create>Areas>Rectangle>By 2 Corners** and entering the following values:

c) For the top clamping plate and enter:

"*WP X*"=0, "*WP Y*"=10.50012, "*Width*"=-1.5, "*Height*"=1.0.

"*WP X*"=-1.5, "*WP Y*"= 10.50012, "*Width*"=-2.25, "*Height*"=1.0

"*WP X*"=-3.75, "*WP Y*"= 10.50012, "*Width*"=-1.5, "*Height*"=1.0

d) For the supporting plate:

"*WP X*"=-0.375, "*WP Y*"=2, "*Width*"=-4.25, "*Height*"=9.

This completes the geometry for this arrangement and Figure 3.19 shows the full geometry of the model, with all entities labeled.

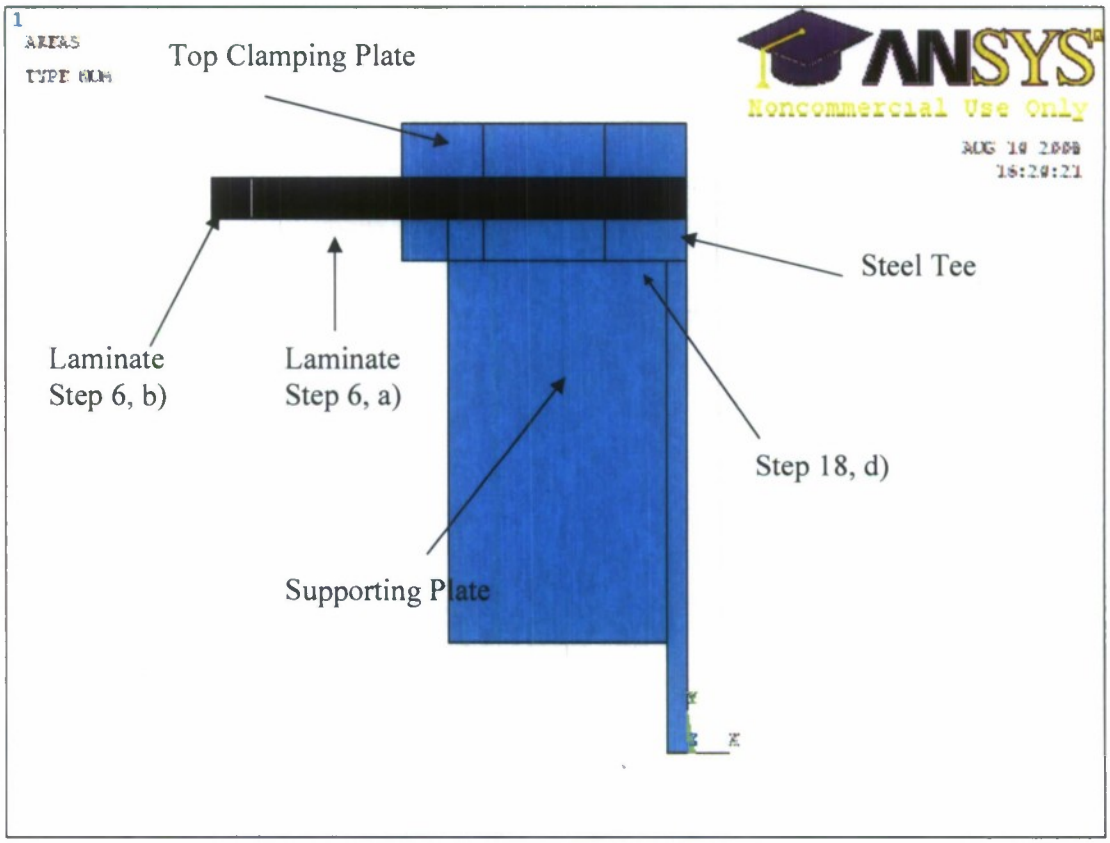

Figure 3.19 – ANSYS Clamped Model Geometry

Omit Steps 8 through 11

Before Step 12 – Glue the Steel Tee and Top Clamping Plate:

Before beginning the execution of this step, the steel tee and top clamping plate must be glued in the following manner.

a) In the GUI to: **Preprocessor>Modeling>Operate> Booleans> Glue>Areas**. Pick the 4 areas that make up the horizontal part of the steel tee that touches the laminate, and click "*Apply*".

b) Pick the 3 areas that make up the top clamping plate, and click "*OK*".

Step 12 – Mesh the Steel Tee *and Top Clamping Plate*:

c) Be sure to pick all 8 areas which represent the steel tee and top clamping plate when setting the element edge length to 0.125.

e) Pick the applicable areas of the steel tee and the top clamping plate when meshing in this step.

Before Step 15 – Mesh the Supporting Plate:

a) Through the GUI, go to: **Preprocessor>Meshing>Meshtool**. In the *"Meshtool"* dialog box, set the *"Element Attributes"* tab to *"Global"* and Click *"Set"*.

b) In the "Meshing Attributes" window, set "Element type number" to 1 PLANE42 and "Material Number" to 6.

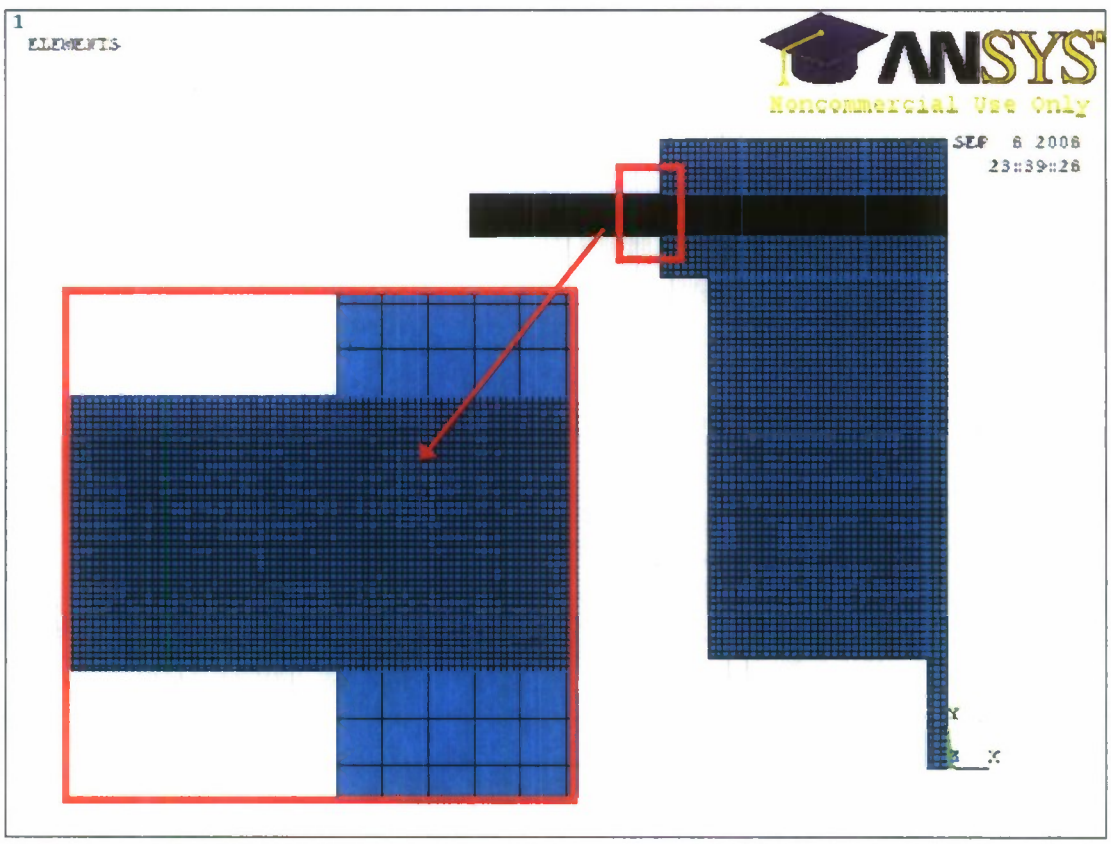

Figure 3.20 – Clamped Model Mesh

c) Under *"Size Controls: Areas"* in the *"Meshtool"* dialog box, click *"Set"*. Pick the

area which represents the supporting plate and click *"OK"*. Set *"Element edge length"* to 0.125 in the *"Element Size at Picked Areas"* window.

e) Mesh the supporting plate using the *"Meshtool"* window by setting *"Mesh"* to "Areas", *"Shape"* to "Quad and Mapped". Click the "*Mesh"* button and pick the applicable areas on the model. The mesh of the model is now complete and is shown below in Figure 3.20.

Step 15 – Define Boundary Conditions:

The effective width, w_{eff}, is used to obtain the desired pressure value, equivalent to 4kips:

b) Set *"Load PRES value"* to 1189.41.

e) Choose the 3 vertical lines that make up the center of the steel tee and top clamping plate, along the right side of the model, and click *"OK"*.

Omit Steps 16 and 17

Step 18 – Creating Contact Between Two Steel T Areas:

d) Select the horizontal line as shown in Figure 3.20, and click "*Apply"*.

g) Select the horizontal line located at the top of the area which makes up the vertical portion of the steel tee, then click "*Apply*".

Step 19 – Creating Contact Between the Steel Tee and Composite:

g) Select the 4 horizontal lines on the top side of the steel tee, then click "*Apply*".

Step 20 – Creating Contact between Top of Composite and *Clamping Plate*:

g) Select the 3 horizontal lines on the top clamping plate where they come in contact with the laminate, then click "*Apply*".

h) >ii. Friction>Material ID: Set to 1.

i) Click "Optional settings". In the "Contact Properties" window under the "Basic" tab, set "Normal Penalty Stiffness" to 0.1 and set "Behavior of contact surface" to "Standard". **Note: For the case of upward-flexure, the "Normal Penalty Stiffness" must be set to 0.01.**

Before Step 21 – Creating Contact between Supporting Plate and Steel Tee:

a) Open the Contact Wizard.

b) In the *"Contact Wizard"* window, the following settings must be correct:

Target Surface: Set to "*Lines*".

Target Type: Set to "*Flexible*".

c) Click "*Pick Target*".

d) Select the horizontal line and vertical line that make up the top and right side of the supporting plate, respectively, and then click "*Apply*".

e) In the *"Contact Wizard"* window, click "*Next*". In the new window, the following settings must be correct:

Contact Surface: Set to "*Lines*".

Contact Element Type: Set as "*Surface-to-Surface*".

f) Click "*Pick Contact*"

g) Select the 4 lines on the steel tee where it comes in contact with the supporting plate, then click "*Apply*".

h) In the *"Contact Wizard"* window, click "*Next*". In the new window, the following settings must be correct:

Check the box next to "Include initial penetration".

Friction>Material ID: Set to 6.

i) Click "Optional settings". In the "Contact Properties" window under the "Basic" tab, set "Normal Penalty Stiffness" to 10 and set "Behavior of contact surface" to "Bonded (always)".

j) In the same window under the *"Friction"* tab, set *"Stiffness Matrix"* to *"Unsymmetric"* and click *"OK"*.

k) Create the contact surfaces by clicking *"Create"* in the contact wizard window.

i) Follow i) through k) in Step 16 for the bolted case. The model is now ready to be solved.

3.2 Shell Analysis

The shell model, which is more practical for large-ship analysis, is the next ANSYS procedure that will be shown. A schematic is provided in Figure 3.21 which illustrates the part of the bolted hybrid connection that will be modeled in Ansys. Although localized stress concentrations will not be the strongpoint of this analysis, overall ship response and far field stress prediction is the primary focus for this model type. The shell model of the hybrid joint must be validated with other theoretical computations since this analysis plan does not take into account the complete experimental test setup. The theoretical computations for comparison are made with the composite analysis software COMPRO, as well as beam theory equations using the flexural modulus of the laminate used in the experimental testing. This smaller, localized model is constructed so that it may be applied to a global model of a large vessel; this could then be constructed completely out of shell and beam elements, first by creating the metal sub-frame with the

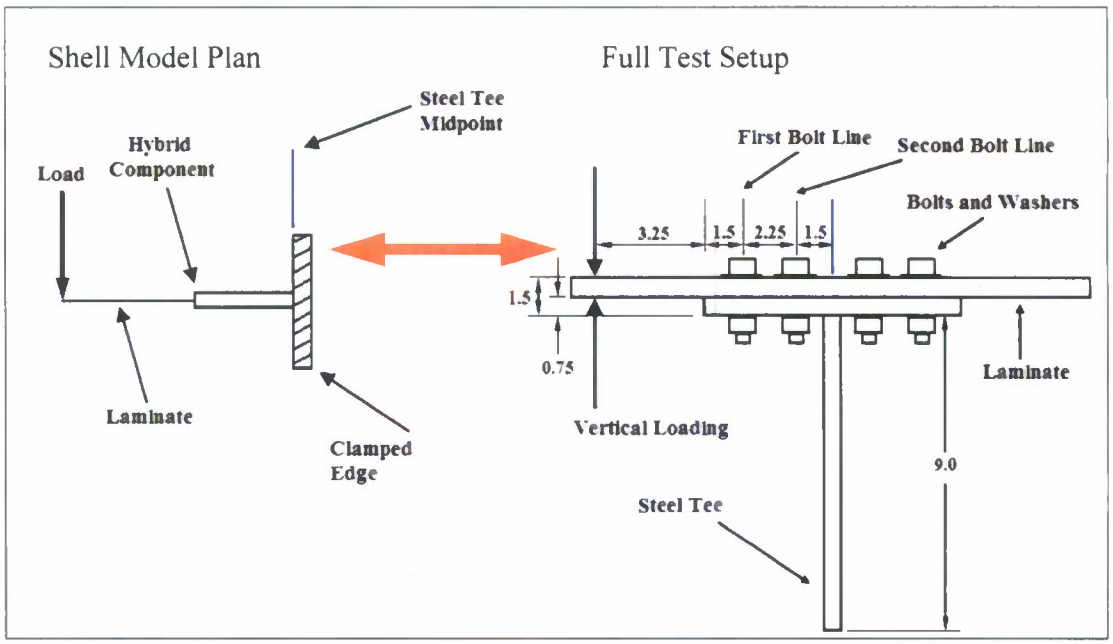

Figure 3.21 – Shell Model Schematic

appropriate beam properties defined. The gaps in the ship-hull skeleton can then be filled-in with the hybrid connections. A global analysis procedure has already been demonstrated previously in the MACH project.

This type of analysis, being fully comprised of shell and beam elements, results in a quick and practical computer evaluation. The intent of the beam-element metal skeleton is to provide the overall structural stiffness for the vessel. A global shell model also offers a robust method for conducting a far-field stress investigation, where a similar evaluation experimentally would be a sizeable task.

3.2.1 Local Shell Modeling Instructions for Bolted Hybrid Connection

Step 1 – Choose an Analysis Type and Element:

For this part, two element types must be defined; one for the composite and the other for the steel/composite hybrid section of the joint. The SHELL99 element is used for the composite as well as the hybrid component.

a) In the ANSYS Main Menu find the Graphical User Interface (GUI), shown in Figure

3.5 below, and click on *"Preferences"*. In the *"Preferences for GUI Filtering"* window, select the *"Structural"* checkbox under *"Individual discipline(s) to show in the GUI"*.

b) Go to: **Preprocessor>Element Type>Add/Edit/Delete**. When the *"Element Type"* dialog box appears, choose *"Add"*.

c) In the *"Library of Element Types"* dialog box, choose *"Shell"*, then *"Linear Layer 99"*. This is the SHELL99 element.

Step 2 – Set Element Options:

In the "Element Types" window, highlight "SHELL99" and choose "Options". The "SHELL99 element type options" dialog box pops up. Under the "Storage of Layer Data K8" tab, set to "All Layers". Close the "Element Types" window.

Step 3 – Set Real Constants for Laminate:

a) In the GUI, go to: **Preprocessor>Real Constants>Add/Edit/Delete**. Click *"Add"*, then highlight *"Type 1 SHELL99"* and click *"OK"* in the "*Real Constants"* window. Set *"Real Constant Set No."* to 1 and click *"OK"*. In the "*Real Constant Set Number 1, for SHELL99"* window, set "*Number of layers (250 max) NL"* to 42.

b) In the *"Real Constant Set Number 1, for SHELL99"* window, each layer must have a defined material number, x-axis rotation, and layer thickness. For all layers, set the material number to "1" and the thickness to "0.01786". Enter the layer orientations as indicated by Figure C1 in Appendix C for the 42-ply configuration.

Step 4 – Set Real Constants for Hybrid Section:

Using the bending rigidity equations and the material properties for steel and the laminate used in the current work, an effective thickness t_{eff} can be computed for the hybrid portion of the connection. The rigidity of the hybrid section is found by adding the rigidity of the individual sub-sections:

$$(E_s I_h)_{eff} = E_s \cdot I_s + E_c \cdot I_c \qquad \text{(Eq. 3.13)}$$

The moment of inertia for the hybrid section, when given a modulus of elasticity equal to steel, is then used to obtain t_{eff}:

$$I_h = \frac{1}{12} b t_{eff}^3 \qquad \text{(Eq. 3.14)}$$

$$t_{eff} = \sqrt[3]{\frac{12 \cdot (E_s \cdot I_h)_{eff}}{E_s \cdot b}} \qquad \text{(Eq. 3.15)}$$

Click "Add", then highlight "Type 1 SHELL99" and click "OK" in the "Real Constants" window. Set "Real Constant Set No." to 2 and click "OK". In the "Real Constant Set Number 1, for SHELL99" window, set "Number of layers (250 max) NL" to e) In the "Real Constant Set Number 1, for SHELL99" window, set the material number to "1", theta to "0", and the thickness to "0.771287".

Step 5 – Defining Material Properties:

a) In the GUI, go to: Preprocessor>Material Props>Material Models.

b) In the *"Define Material Model Behavior"* window, as seen in Figure 3.8, navigate to: **Structural>Linear>Elastic>Orthotropic**. The lamina material properties are input in the *"Linear Orthotropic Properties for Material Number 1"* window; define the material as follows: *"EX"*=5.6e6, *"EY"*=1.563e6, *"EZ"*=1.563e6, *"PRXY"*=0.2882, *"PRYZ"*=0.435, *"PRXZ"*=0.2882, *"GXY"*=4.74e5, *"GYZ"*=3.335e5, and *"GXZ"*=4.74e5".

c) In the same *"Define Material Model Behavior"* window menu, go to: **Material>New Model**. This will allow for a new material definition for the composite with an *"ID"* of 2. Follow the path: **Structural>Linear>Elastic>Isotropic**. Define an elastic modulus of 2.9×10^7 psi and a Poisson's Ratio of 0.3.

Step 6 – Building the Geometry:

For the following steps, rectangles will be constructed using the GUI by going to: **Preprocessor> Modeling>Create>Areas> Rectangle>By 2 Corners**.

a) To create the hybrid portion of the connection, enter the following: "*WP X*"=0, "*WP Y*"=-3.25, "*Width*"=5.25, "*Height*"=6.5.

b) For the part of the connection that contains only laminate material, enter: "*WP X*"=-5.25, "*WP Y*"=-3.25, "*Width*"=-3.2, "*Height*"=6.5.

c) Create the loading area by entering: "*WP X*"=-8.45, "*WP Y*"=-3.25, "*Width*"=-0.1, "*Height*"=6.5. The shell model geometry is now complete, and is shown in Figure 3.23 below.

Step 7 – Gluing the Areas:

a) In the GUI, go to: Preprocessor>Modeling>Operate>Booleans>Glue>Areas.

b) Select the 3 areas and click "*OK*".

Step 8 – Define Boundary Conditions:

a) In the GUI, navigate to: **Preprocessor>Loads>Define Loads>Apply>Structural>Pressure>On Areas**. Select the area as indicated in Figure 3.22, and click *"OK"*.

b) In the "Apply PRES on lines" window, select "Constant value" under "Apply PRES on areas as a". Set "Load PRES value" to 5925.93.

c) Go to: **Preprocessor>Loads>Define Loads>Apply>Structural>Displacement>On Lines**. Choose the line as shown in Figure 3.22, and click *"OK"*.

d) In the *"Apply U, ROT on Lines"* window, set *"DOF's to be constrained"* to ALL DOF. This action will constrain the displacements and rotations in all 3 dimensions.

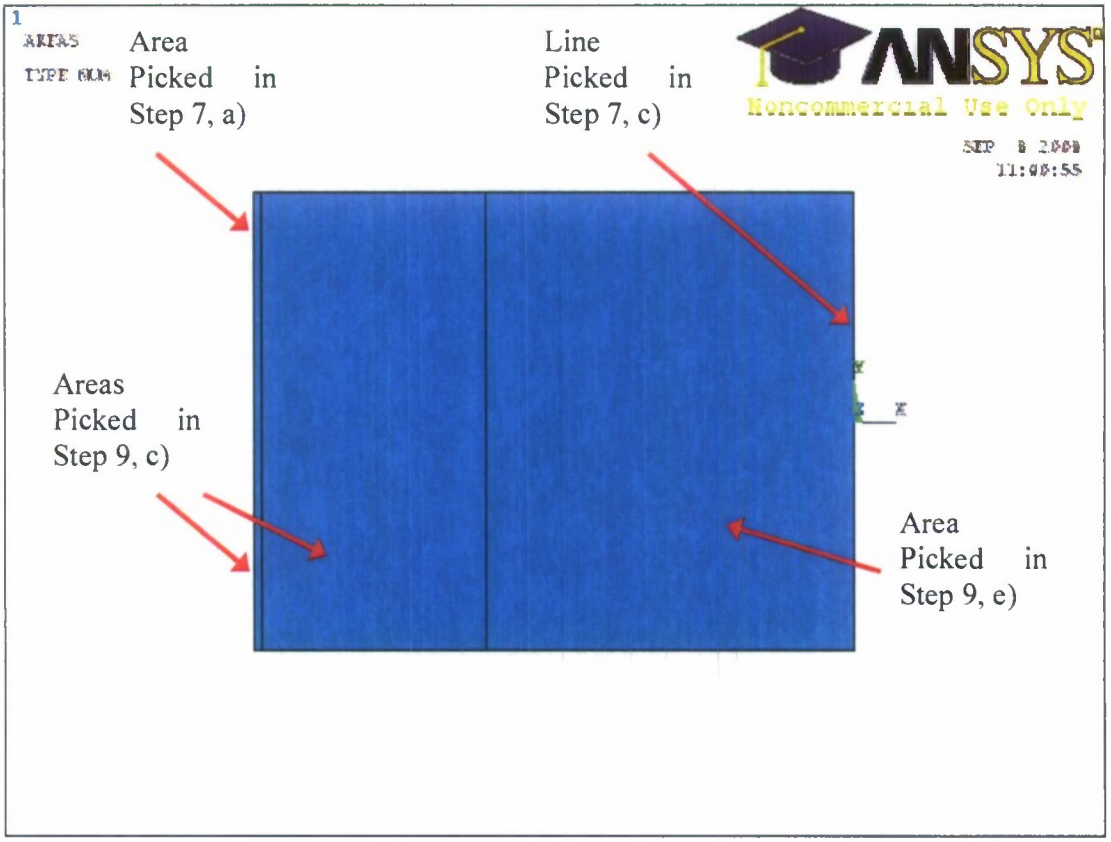

Figure 3.22 – Shell Model Geometry

Step 9 – Mesh Model:

a) Through the GUI, go to: **Preprocessor>Meshing>Meshtool**. Under *"Size Controls: Areas"* in the *"Meshtool"* dialog box, click *"Set"*. Pick the pressure location area and click *"OK"*. Set the *"Element edge length"* to 0.05 in the *"Element Size at Picked Areas"*. Using the same process, define the remaining areas to have an element edge length of 0.1.

b) In the "Meshtool" dialog box, set the "Element Attributes" tab to "Global" and Click "Set". In the "Meshing Attributes" window, set "Element type number" to 1 SHELL99, "Material Number" to 1, and "Real Constant Set Number" to 1.

c) Mesh the areas representing the laminate and pressure location, as shown in Figure 3.22, by using the *"Meshtool"* window and by setting *"Mesh"* to "Areas", *"Shape"* to

"Quad and Mapped". Click the *"Mesh"* button and pick the areas on the model.

d) In the "Meshtool" dialog box, set the "Element Attributes" tab to "Global" and Click "Set". In the "Meshing Attributes" window, set "Element type number" to 1 SHELL99, "Material Number" to 2, and "Real Constant Set Number" to 2.

e) Mesh the area representing the hybrid section of the model, as shown in Figure 3.22, by using the *"Meshtool"* window and by setting *"Mesh"* to "Areas", *"Shape"* to "*Quad and*

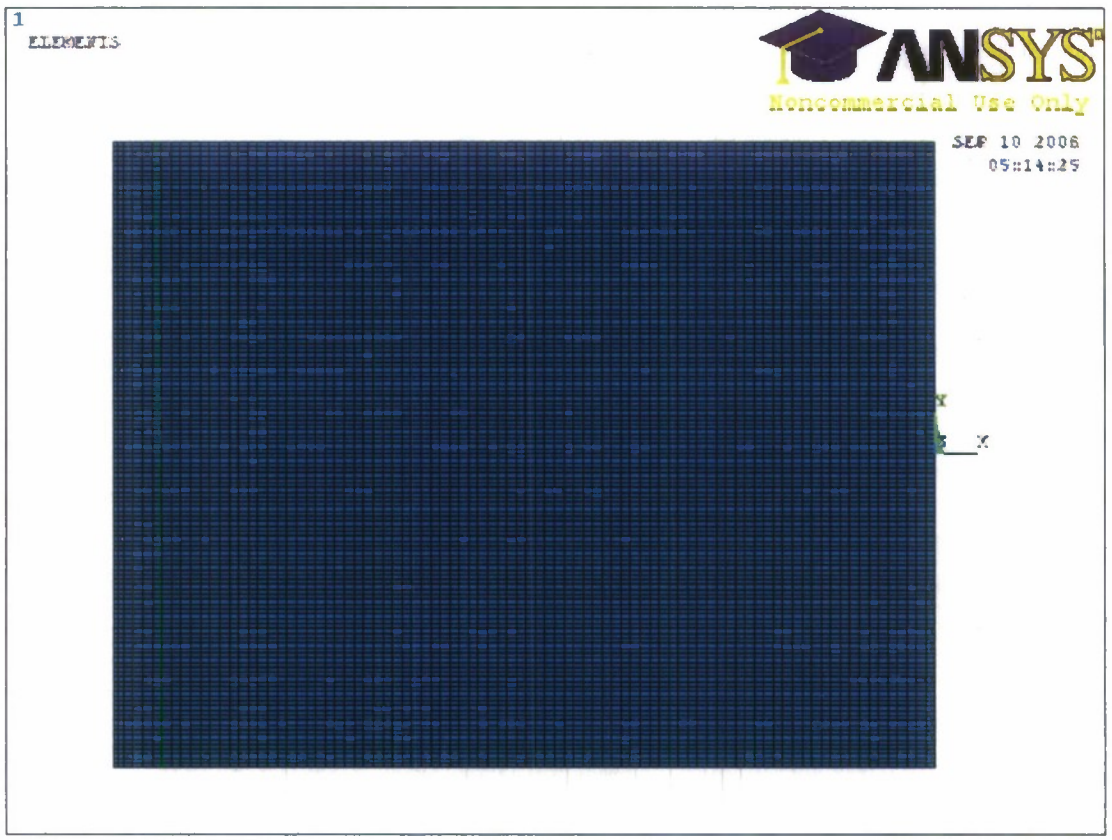

Figure 3.23 – Meshed Shell Model

Mapped". Click the *"Mesh"* button and pick the hybrid area on the model. The meshed model is shown in Figure 3.23.

Step 10 –Solve the Model:

In the GUI, go to: **Solution>Solve>Current LS**. Click "*OK*" in the *"Solve Current Load Step"* window.

Shell analysis results are provided in Section 4.2.

4. PARAMETRIC STUDY OF HYBRID JOINT

A typical joint configuration has adequate detail which makes a full 3-D analysis difficult, especially in the case where bolts are present. In the current work a simplified approach was selected. A typical connection has a longitudinal dimension that is quite large. Therefore, the connections analyzed were assumed to be in the condition of plane strain. The importance of making this decision is evident, because a 2-D model of the joint drastically simplifies the FEA. In contrast to a plane stress model, a plane strain model assumes the component being modeled is much longer in the z-direction when compared to the x and y directions. This is true of the connection but not quite true of the subcomponents tested in the current work. The strains that are associated with the z direction (the normal strain ε_{zz} and shear strains ε_{xz} and ε_{yz}) are assumed to be much smaller than the cross-sectional strains, as they are constrained. The non-zero stress σ_{zz} is needed to satisfy the zero-strain constraint assumed in the z direction, although it can be left out of the analysis so all that is left over are in-plane terms. In doing this, the 3-D model is reduced to a simplified 2-D case. Since it is likely that future studies in the field of the current work could involve FEA of connections that are much longer in the z direction, plane strain was selected as the approach for this analysis.

4.1 Plane Strain Analysis Results

Nonlinearity in the ANSYS™ FEA was limited to the contact and gap opening. A plane strain model is an efficient tool for performing a comprehensive parametric study of both connection configurations. Studies done with the 42-ply laminate makes up most of the experimental data tested by Corriveau et al. (2008), so this is used as the baseline in all parametric studies. One of the parameters, the bolt preload, was altered to varying degrees of its ultimate strength and the effect it had on the response of the model is observed for the bolted configuration. The degree of nonlinearity in the plane-strain, contact analysis is compared to that which is present in experimental test data. The influence of finite element mesh refinement on the model is evaluated by comparing stress and deflection results on the bolted and clamped connection arrangements for two mesh sizes. The laminate thickness is varied in another investigation of the hybrid joint;

the flexibility of the model is compared to available experimental response data and stress results are measured against a simplified computation that treats the laminate an as isotropic material. A force of 8 kips was chosen as the base load since this is approximately 50% of the ultimate failure load for the baseline composite thickness of 42 plies, and this point in the loading is where the joint experiences the characteristic nonlinear response of the connection.

4.1.1 Bolted Model Results, Influence of Bolt Clamp-Up Load and Stiffness

This subsection discusses the effect of bolt preload and bolt modulus on the response. Resulting deflections for several different bolt preloads on a bolted, 42-ply model with 8 kips of force applied to the connection are given in Table 4.1 below. The deflections down and up fluctuated by 3.2% and 11.1%, respectively, from the range of bolt pretensions induced. The bolt preload was altered to determine its effect on the hybrid connection stiffness, and the results show that the pre-strain can have a considerable effect on flexibility, especially when loaded up, and should not be ignored. This bolt prestrain influence is shown Figure 4.1, with the primary and secondary axis covering the same vertical range, and when the model is loaded upward the effect is more pronounced. The model was also solved with no applied load and a bolt pretension of $0.5\sigma_u$ in order to isolate the effect of bolt clamp-up load on deflection, the result of which is shown in Table 4.1. This bolt preload of $0.5\sigma_u$ is used for all of the bolted plane strain models for the remainder of this document; a preload of $0.9\sigma_u$ is used for the models of the clamped configuration.

Table 4.1 – Effect of Bolt Preload on Upward and Downward Deflections with Applied 8kip Load

		Deflection	
Bolt Stress in terms of ultimate bolt load, σ_u	Bolt Strain, ϵ_b	Loaded Down (in)	Loaded Up (in)
$0.1\sigma_u$	0.00052	0.225	0.320
$0.2\sigma_u$	0.00103	0.223	0.315
$0.3\sigma_u$	0.00155	0.222	0.310
$0.4\sigma_u$	0.00207	0.221	0.305
$0.5\sigma_u$	0.00259	0.220	0.301
$0.6\sigma_u$	0.00310	0.220	0.297
$0.7\sigma_u$	0.00362	0.219	0.294
$0.8\sigma_u$	0.00414	0.219	0.291
$0.9\sigma_u$	0.00466	0.218	0.288
*$0.5\sigma_u$	0.00259	Laminate Deflection Upward of 0.0024 in.	

* This is the effect of bolt load on the deflection with no load applied to the model

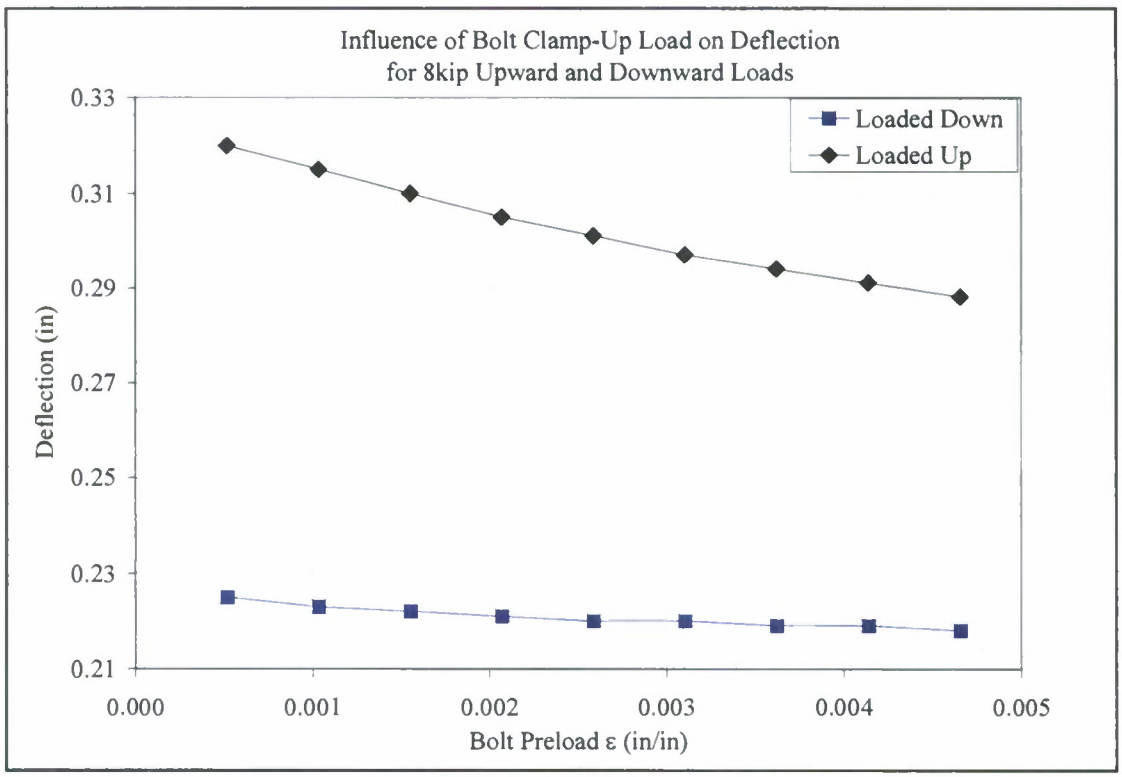

Figure 4.1 – Effect of Bolt Clamp-Up Load on Response

Resulting deflections due to varying bolt moduli on a bolted, 42-ply model with 8 kips of force applied to the connection are given in Table 4.2 below. The bolt modulus is varied over a range covering one degree of magnitude, and a plot of the response for the upward and downward loaded instances are provided in Figure 4.2. The plot shows how the response increases with decreasing bolt modulus values. The deflections down and up fluctuate by 217% and 138%, respectively, from the range of bolt moduli defined. Both upward and downward deflection magnitudes are approximately 20% apart, except for the case where the modulus is 2.9×10^6 psi where the difference drops to 2.5%, as shown in Figure 4.2.

Table 4.2 – Effect of Bolt Modulus on Upward and Downward Deflections with Applied 8kip Load

Bolt Modulus, E_b (psi)	Deflection, Loaded Down (in)	Deflection, Loaded Up (in)
2.9×10^6	0.697	0.715
9.5×10^6	0.349	0.425
16×10^6	0.274	0.355
22.5×10^6	0.24	0.321
29×10^6	0.22	0.301

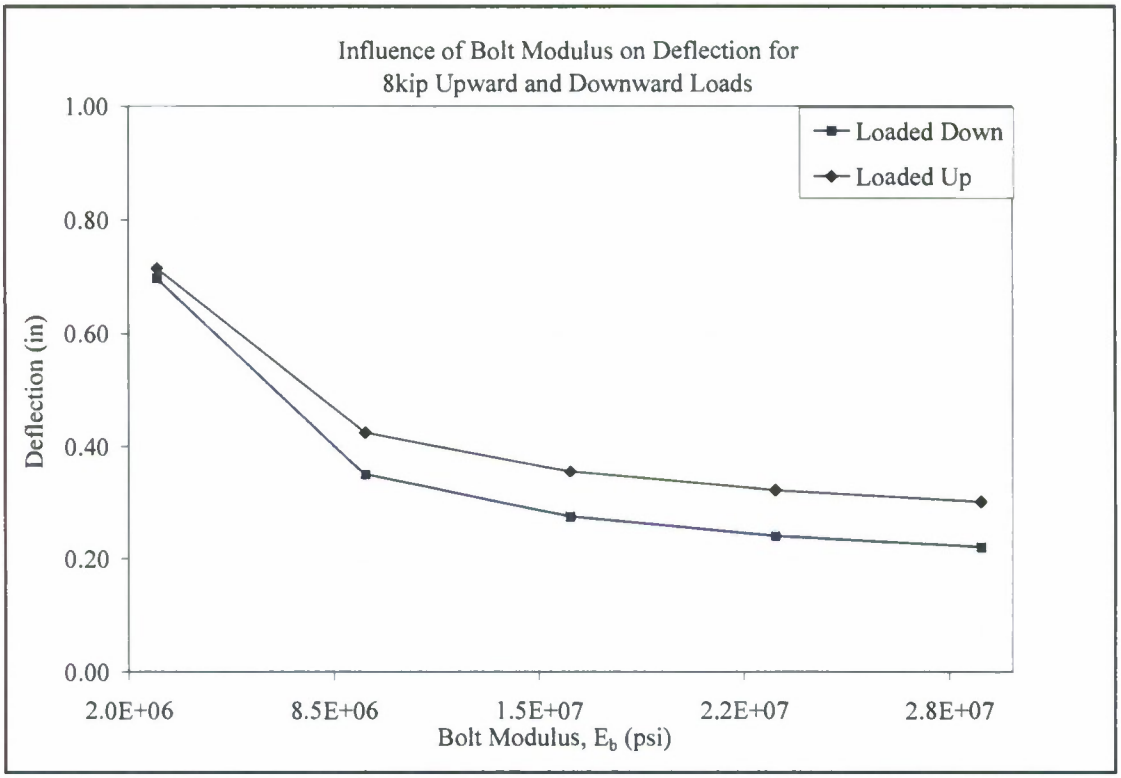

Figure 4.2 – Effect of Bolt Modulus E_b on Response

4.1.2 Degree of Nonlinearity of Contact Analysis

In this subsection the nonlinearity in the plane-strain, contact analysis is compared to that which is present in corresponding experimental test data for the case where the laminate is 42 layers thick. It is noted that this model does not include material nonlinearity. In Figures 4.2 and 4.3, the flexibility of the bolted connection in the experiment and the plane strain model are compared in downward and upward flexure for a peak load of ±8 kips. Figures 4.4 and 4.5 present the same comparison for the clamped configuration. The experimental data came from 8-kip, residual strength, load-controlled tests on 42-ply bolted and clamped connections; these strength tests are completed prior to any fatigue loading. The residual strength test starts gathering data at zero load and displacement and load is first steadily increased to a positive (down) +8 kip peak, then decreased (up) to a value of -8 kips, and finally brought back to zero load. When the bolted connection is loaded down the plane strain model maintains a linear response, however the experiment has a nonlinear response, as is seen in Figure 4.3 where the connection gains flexibility as

the load is increased. In the event of upward-bending in the bolted model, shown in Figure 4.4, there is a slight nonlinear effect from the contact analysis; however the experimental response is visibly much more pronounced. Although not as apparent as Figure 4.4, Figure 4.6 shows the same pattern of nonlinearity for the downward-loaded clamped model. From comparing the response of the experiment to ANSYS™ results the clamped model is too stiff, by 7.5%, at the maximum load of 8 kips, shown in Figure 4.4. The opposite effect of the downward loaded clamped case occurs in the experiment when the model is loaded upward, as is shown in Figure 4.5 when the experimental connection stiffness increases faintly with load. On the same plot for the first half of the loading amplitude, the model becomes more flexible, however for the remaining portion of the load the stiffness increases slightly. The clamped model is much too stiff when loaded up, by 24.4% at the maximum load of 8 kips. ANSYS™ flexibilities in this study show stiffer results than experimental findings in all cases; this is partially due to the damage occurring in the composite material, which is not included in the Ansys FEA.

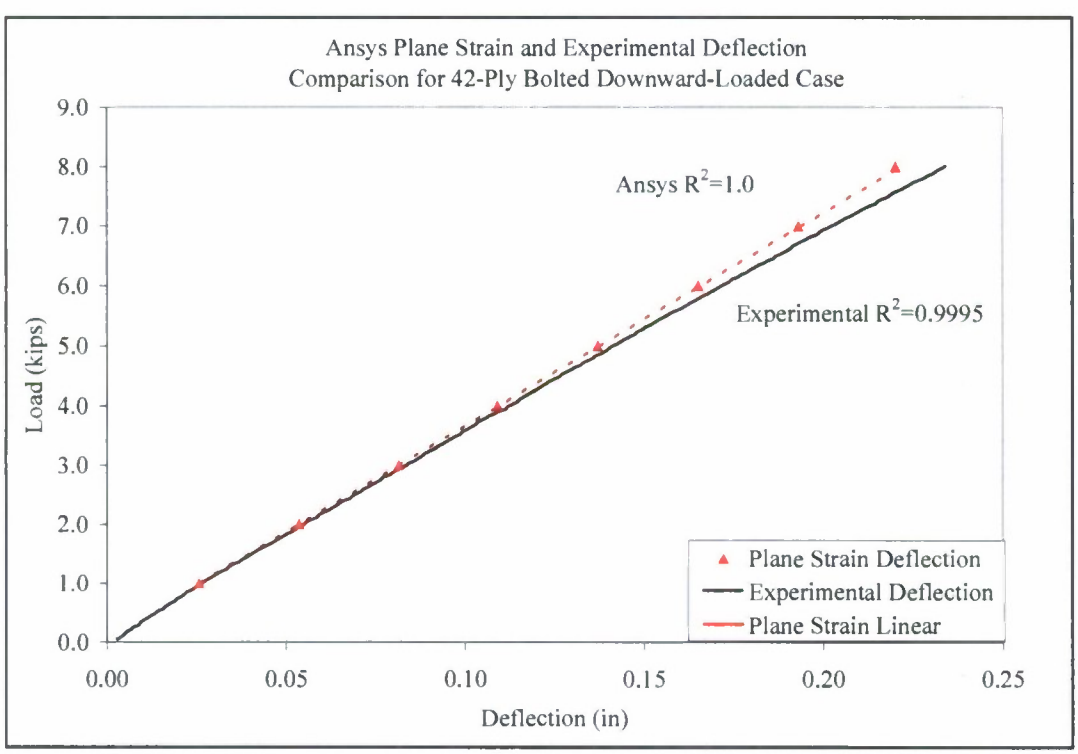

Figure 4.3 – Downward, Bolted 42-Ply Experimental & Ansys Model Comparison

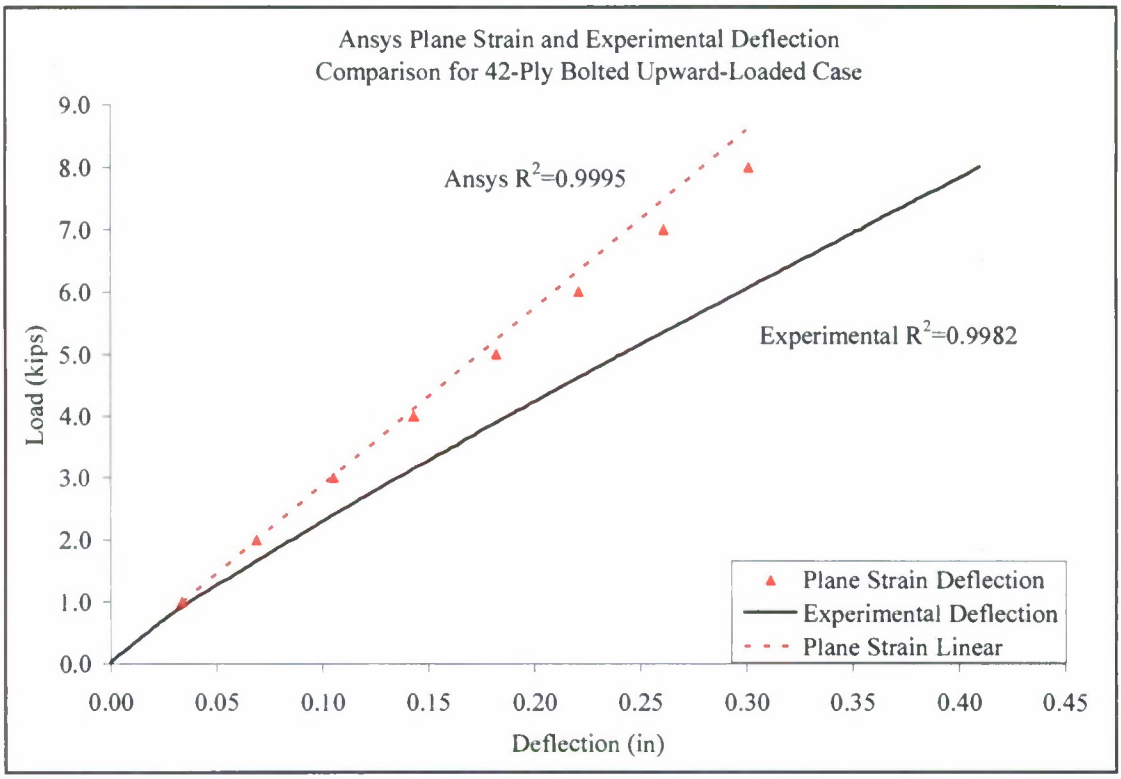

Figure 4.4 – Upward, Bolted 42-Ply Experimental & Ansys Model Comparison

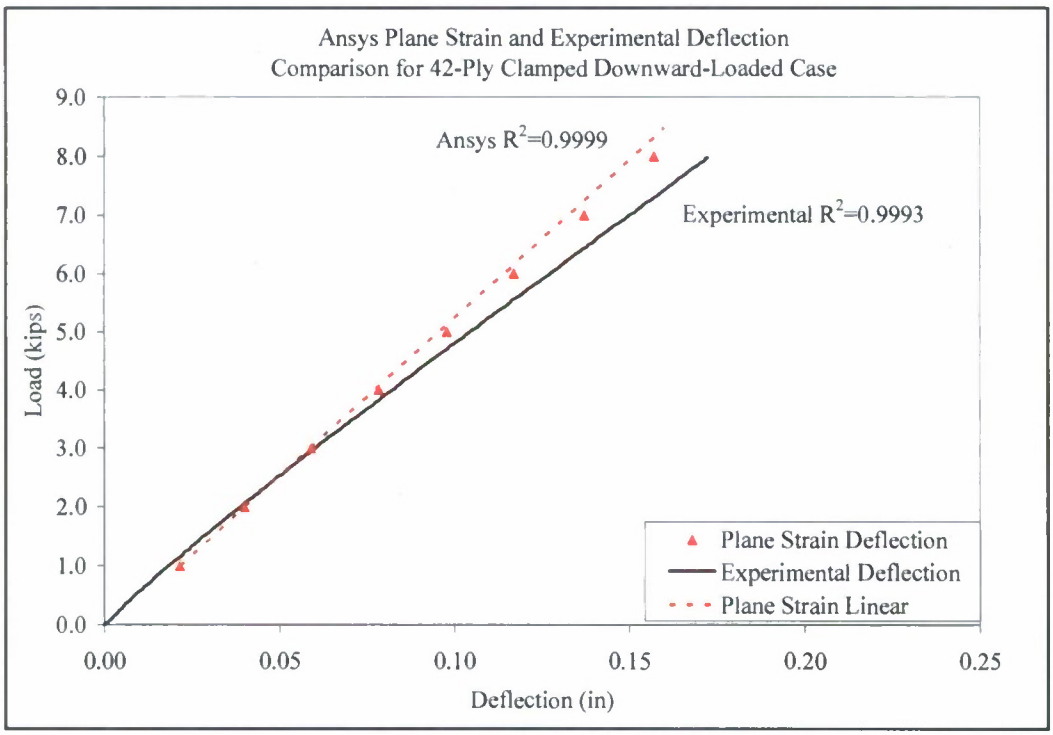

Figure 4.5 – Downward Clamped 42-Ply Experimental & Ansys Model Comparison

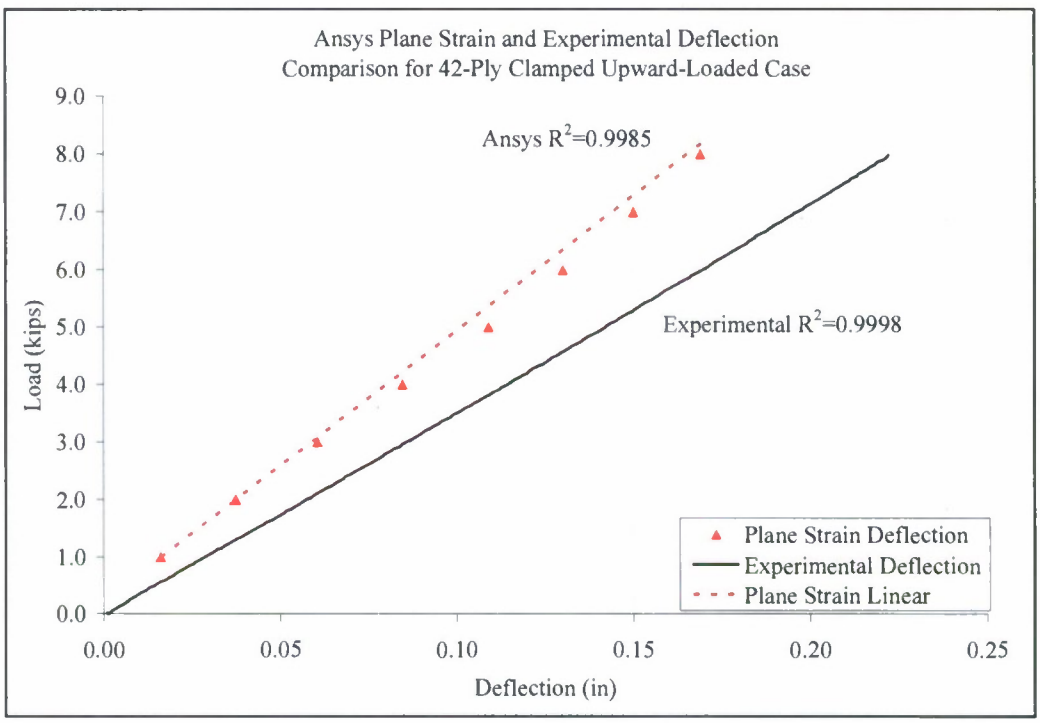

Figure 4.6 – Upward, Clamped 42-Ply Experimental and ANSYS™ Model Comparison

4.1.3 Influence of Finite Element Mesh

Effects on displacements and stresses from altering the finite element model mesh size are shown in this subsection for both connection configurations. Connections with a 42 layer laminate were used in this study and two meshes, which from now on will be denoted as "regular" and "refined", are used. Figures 3.12 and 3.21 show the regular mesh for the bolted and clamped connection arrangements. The refined meshes for the

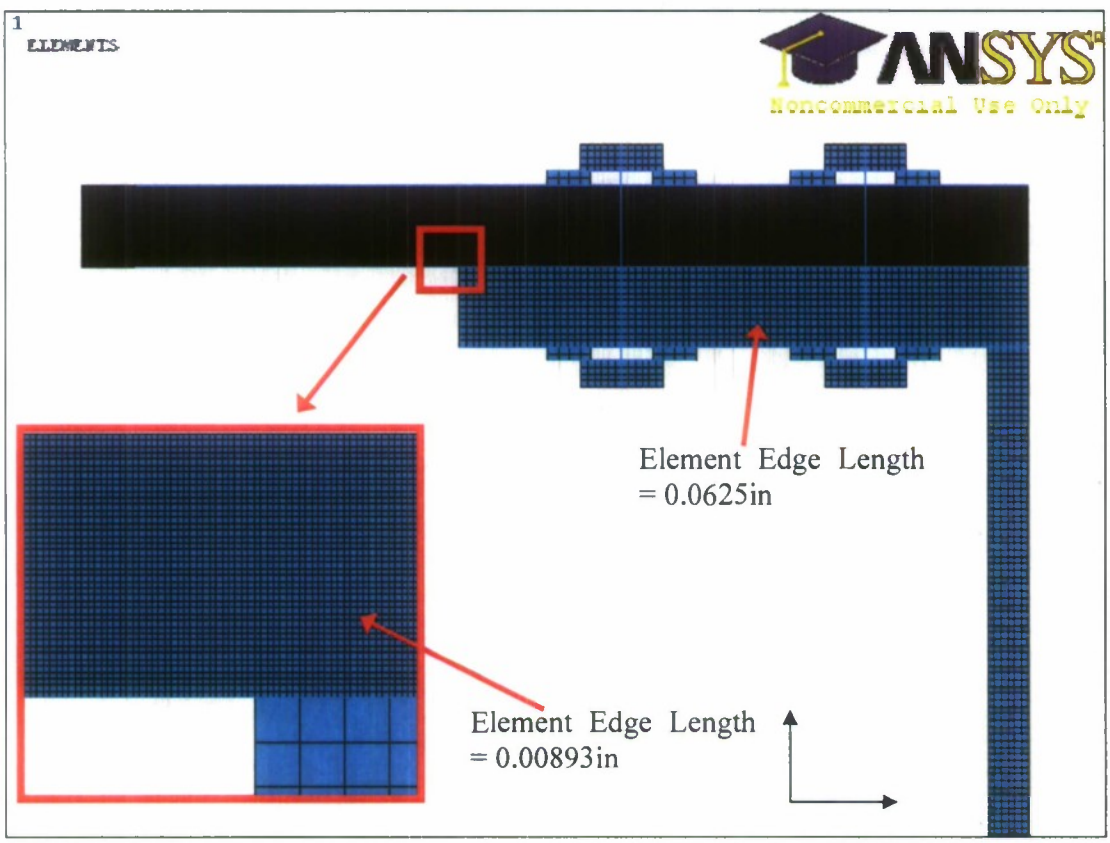

Figure 4.7 – Refined Mesh of Bolted Configuration

bolted and clamped models, shown in Figures 4.6 and 4.7, contain square elements which are half the size of those in the regular mesh; the laminate and steel tee elements have edge lengths of 0.00893 and 0.0625 inches, respectively. The location where peak stress values are gathered in this study for the clamped configuration is through the thickness of

the composite at the steel tee edge; this is also where stresses are obtained in the bolted model when there is downward load. Stress components for the case of upward flexure in the bolted model are gathered through the thickness of the laminate at the bolt line.

Table 4.2 summarizes ANSYS™ deflection and stress results with each mesh size for the case of 8 kips of load being applied to the connection. The x-direction is longitudinal to the joint and y-coordinate is the transverse direction as shown in Figure 4.8.

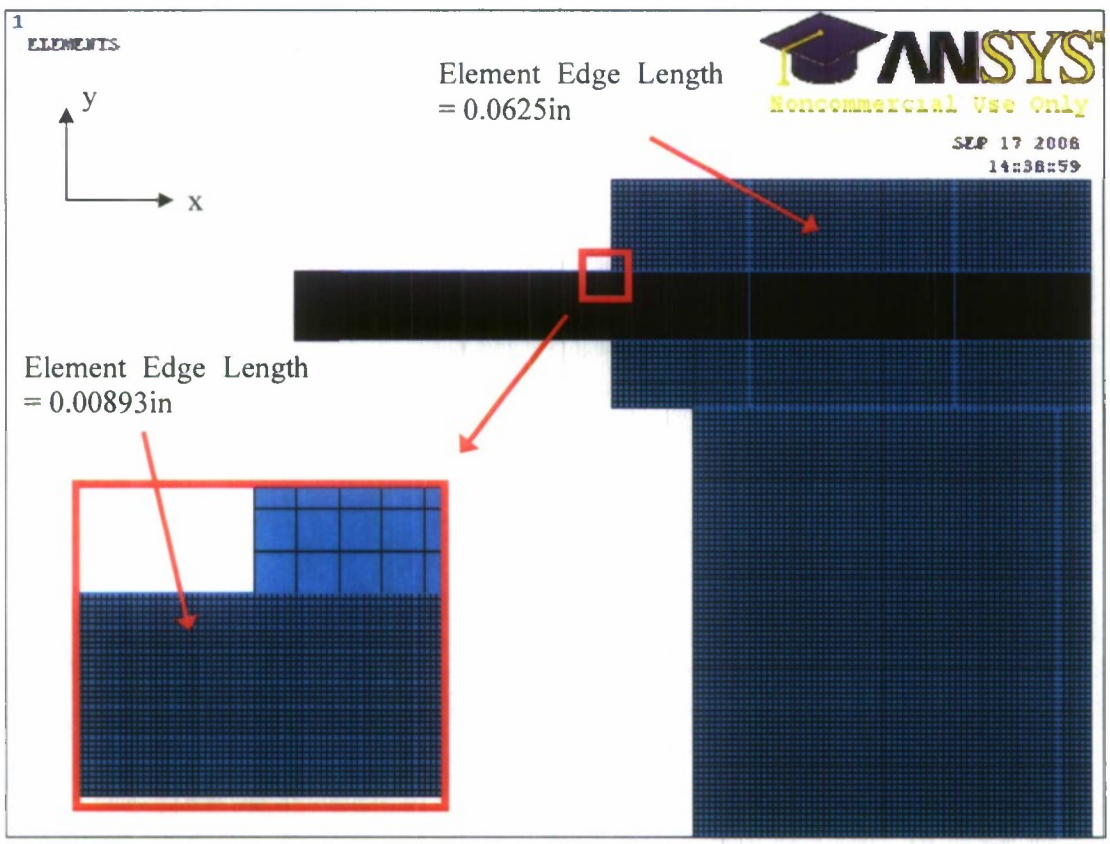

Figure 4.8 – Refined Mesh of Clamped Configuration

Table 4.3 summarizes the effect of mesh refinement on stress and deflection results with calculated percentage differences from the regular mesh results, calculated from Table 4.2. The mesh sizes used have little effect on deflection except for the case of clamped upward-bending where the magnitude is reduced by 13.6%. The cause of this inconsistency was found to be the Normal Penalty Stiffness setting of 0.01 for the contact between the top clamping plate and the composite; the clamped, upward-loaded situation

is the only instance where this contact value is altered from the default value of 0.1. The stress components τ_{xy}, σ_y, and σ_z are affected the most when the bolted model is loaded down, where the refining the mesh increases these values substantially. In the clamped model, the refined mesh causes transverse normal stress, σ_y, to increase significantly, by 21.5% and 34.9% for the downward and upward occurrences. The most critical stress in the analysis, namely the longitudinal stress, σ_x, is influenced the least overall by mesh refinement in this study.

Table 4.3 – Mesh Refinement Stress and Deflection Values Observed for 8kip Load on 42-Ply Plane Strain Model

Connection Configuration	Mesh Type	Force Direction	Deflection (in)	τ_{xy} (ksi)	σ_y (ksi)	σ_x (ksi)
Bolted	Base Mesh	Down	0.220	5.639	-10.850	-39.840
		Up	0.301	-11.851	-13.364	-68.550
	Refined Mesh	Down	0.218	12.425	-40.431	-40.271
		Up	0.303	-13.441	-13.817	-65.219
Clamped	Base Mesh	Down	0.157	5.903	-9.625	-40.239
		Up	0.169	-5.981	-10.228	-39.754
	Refined Mesh	Down	0.157	5.584	-11.696	-41.035
		Up	0.149	-6.492	-13.793	-40.528

4.1.4 Bolted Model Results, Laminate Thickness Varied

ANSYS flexibility results of the 8kip bolted configuration are given and compared to available experimental data in Table 4.4 for laminates of varying thickness; two different values of bolt preload are applied to the upward-loaded model and corresponding flexibility results are shown. The laminate orientations for all composite thicknesses in this section are specified in Appendix C. Analytical and experimental deflection results from Table 4.5 are plotted on the same graph for the downward and upward-load of 8 kips in Figures 4.9 and 4.10. These graphs show that analytical results are in good agreement with the available experimental response data, except when the upward-loaded bolted 28-ply model under-predicts experimental response by 34.5%. As can be deduced from Figure 4.10, this same characteristic is present for the 42-ply and 48-ply composite

thicknesses; there is a visible trend where this becomes more pronounced as the laminate gets thinner. Thin composites were not tested so the reader is cautioned in interpreting results in the 6-ply case. As the ratio of composite to steel thickness is reduced in the computer analysis, the model becomes subject to large deflections from the applied load of 8 kips, as is demonstrated by results for the 6-ply laminate; the resulting flexibility in Table 4.5 translates into 54.8 and 77.3 inch deflections when the hybrid connection is forced downward and upward with 8 kips of force, respectively. Figure 4.10 shows how the deflection of the connection increases in the model as the bolt preload is reduced from $0.5\sigma_u$ to $0.1\sigma_u$ (where $\sigma_u = 150$ ksi).

Table 4.4 – Percentage Differences Summarizing the Effect of Mesh Refinement on Stress and Deflection Results for 8kip Load on 42-Ply Laminate Model

	Force Direction	Deflection (in)	τ_{xy} (ksi)	σ_y (ksi)	σ_x (ksi)
Bolted	Down	-0.9%	120.3%	272.6%	1.1%
	Up	0.7%	13.4%	3.4%	-4.9%
Clamped	Down	0.0%	-5.4%	21.5%	2.0%
	Up	-11.8%	8.5%	34.9%	1.9%

Table 4.5 – ANSYS and Experimental Flexibility Computed at the 8kip Load Level

		Downward Loaded		Upward Loaded	
# Plies	ANSYS Flexibility (in/lb) Bolt $0.5\sigma_u$	Experimental Flexibility (in/lb)	ANSYS Deflection (in/lb) Bolt $0.5\sigma_u$	ANSYS Deflection (in/lb), Bolt $0.1\sigma_u$	Experimental Deflection (in/lb)
6	6.85E-03	-	9.66E-03	9.66E-03	-
14	3.34E-04	-	5.61E-04	5.64E-04	-
20	1.21E-04	-	2.36E-04	2.39E-04	-
28	5.30E-05	4.25E-05	8.25E-05	8.55E-05	1.26E-04
34	4.13E-05	-	6.01E-05	6.31E-05	-
42	2.75E-05	2.89E-05	3.76E-05	4.00E-05	5.00E-05
48	2.21E-05	2.37E-05	2.85E-05	3.06E-05	3.65E-05
56	1.78E-05	-	2.11E-05	2.30E-05	-

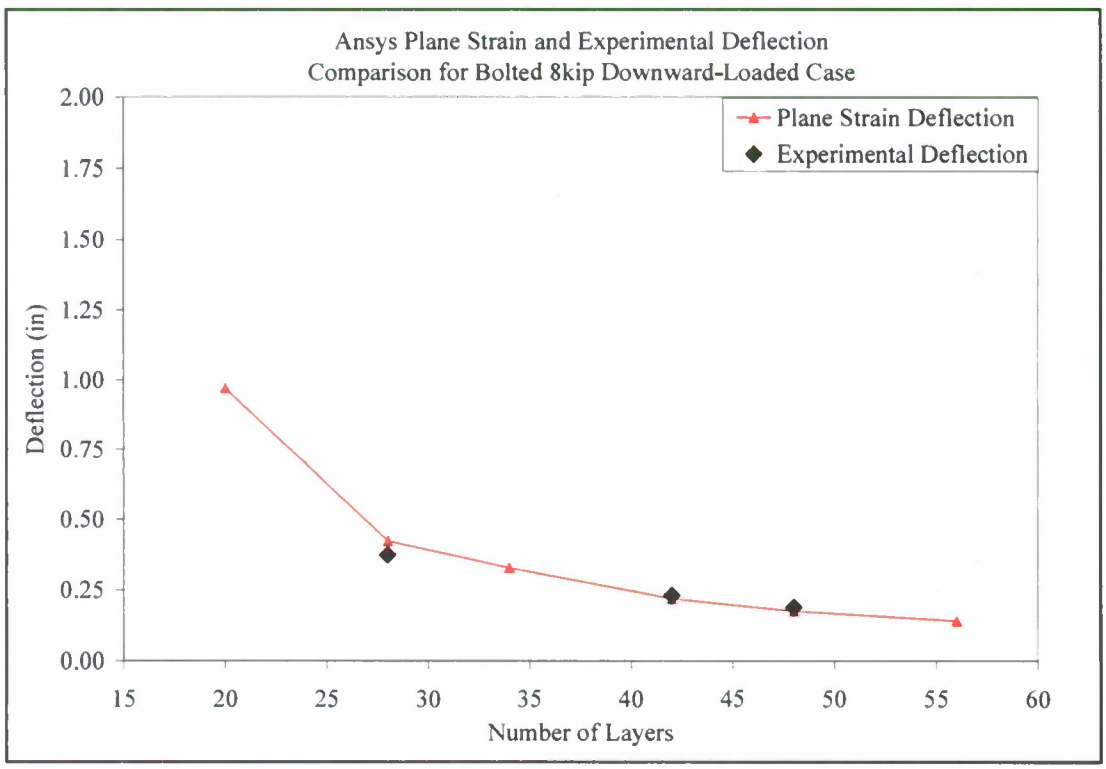

Figure 4.9 – ANSYS and Experimental Downward-Flexure Deflection Plot

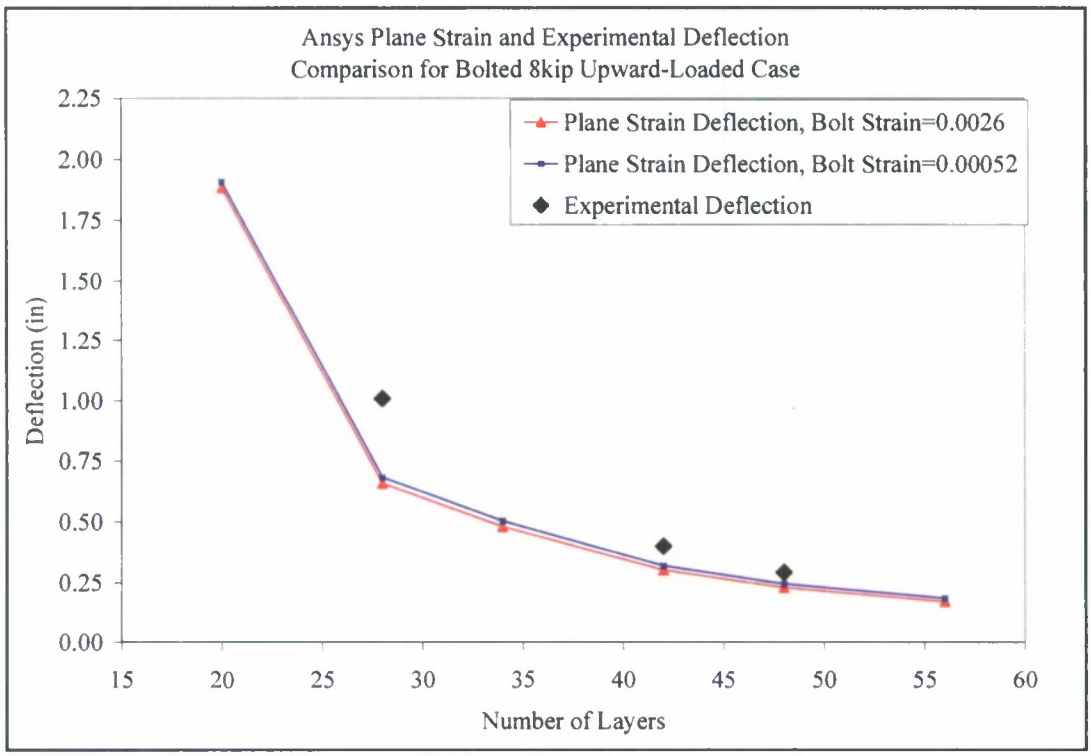

Figure 4.10 – ANSYS and Experimental Bolted Upward-Flexure Deflection Plot

Laminate peak stress through-the-thickness results for a nominal 1 kip downward and upward load on the bolted configuration are provided and compared to the simplified Gross method and Net method peak stress level calculations in Tables 4.6 and 4.7. Table 4.8 is a variation of Table 4.6 stress results, with the bolt preload reduced from $0.5\sigma_u$ to $0.1\sigma_u$. Differences in stress values from a change in bolt preload are minimal, with magnitudes in Table 4.8 being slightly greater than Table 4.7. Also included in these tables are the calculated ratios (σ_x-Ansys)/ (σ_x-Gross) and (τ_{xy}-Ansys)/ (σ_x-Gross) in Table 4.6, and (σ_x-Ansys)/ (σ_x-Net) and (τ_{xy}-Ansys)/ (σ_x-Gross) in Tables 4.7 and 4.8.

The Gross method uses the gross (i.e. total) width of the composite in the stress calculation and an isotropic-based strength of materials calculation is performed. The Net method uses the net width (i.e. the gross width minus the bolt hole diameters. In a

Table 4.6 – ANSYS Peak Stress Comparison for Bolted Nominal 1-kip Downward-Loaded Case, Bolt Preload = $0.5\sigma_u$

	ANSYS Analysis			Simplified Calculation		
# Plies	τ_{xy} (ksi)	σ_y (ksi)	σ_x (ksi)	Gross Method σ_x (ksi)	(σ_x-ANSYS)/ (σ_x-Gross)	(τ_{xy}-ANSYS)/ (σ_x-Gross)
6	1.11	-0.14	-135.20	-125.75	1.075	-0.009
14	6.24	-19.55	-34.19	-23.10	1.480	-0.270
20	2.68	-8.37	-18.54	-11.32	1.638	-0.237
28	0.98	-3.27	-12.72	-5.78	2.202	-0.169
34	0.89	-1.82	-7.30	-3.92	1.862	-0.228
42	0.71	-1.36	-4.98	-2.57	1.940	-0.275
48	0.60	-1.12	-3.89	-1.97	1.978	-0.305
56	0.50	-0.89	-2.92	-1.44	2.022	-0.344

Table 4.7 – ANSYS Peak Stress Comparison for Bolted Nominal 1-kip Upward-Loaded Case, Bolt Preload = $0.5\sigma_u$

	ANSYS Analysis			Simplified Calculation			
# Plies	τ_{xy} (ksi)	σ_y (ksi)	σ_x (ksi)	Gross Method σ_x (ksi)	Net Method σ_x (ksi)	(σ_x-ANSYS)/ (σ_x-Net)	(τ_{xy}-ANSYS)/ (σ_x-Net)
6	-14.39	-30.10	-146.64	-156.88	-201.75	0.727	0.071
14	-5.40	-8.96	-69.18	-28.82	-37.05	1.867	0.146
20	-5.14	-5.88	-28.09	-14.12	-18.15	1.547	0.283
28	-1.61	-1.72	-23.53	-7.20	-9.26	2.541	0.174
34	-2.17	-2.44	-12.04	-4.89	-6.28	1.917	0.346
42	-1.48	-1.67	-8.57	-3.20	-4.12	2.081	0.360
48	-1.16	-1.31	-6.89	-2.45	-3.15	2.185	0.369
56	-0.91	-1.03	-5.37	-1.80	-2.32	2.319	0.393

Table 4.8 – ANSYS Peak Stress Comparison for Bolted Nominal 1-kip Upward-Loaded Case, Bolt Preload = $0.1\sigma_u$

	ANSYS Analysis			Simplified Calculation			
# Plies	τ_{xy} (ksi)	σ_y (ksi)	σ_x (ksi)	Gross Method σ_x (ksi)	Net Method σ_x (ksi)	(σ_x-ANSYS)/ (σ_x-Net)	(τ_{xy}-ANSYS)/ (σ_x-Net)
6	-14.59	-31.92	-146.79	-156.88	-201.75	0.728	0.072
14	-5.42	-8.99	-69.19	-28.82	-37.05	1.867	0.146
20	-5.19	-5.95	-28.12	-14.12	-18.15	1.549	0.286
28	-1.65	-1.78	-23.65	-7.20	-9.26	2.554	0.178
34	-2.24	-2.53	-12.12	-4.89	-6.28	1.929	0.356
42	-1.54	-1.75	-8.64	-3.20	-4.12	2.097	0.374
48	-1.20	-1.37	-6.95	-2.45	-3.15	2.207	0.381
56	-0.94	-1.07	-5.41	-1.80	-2.32	2.333	0.404

similar calculation. Only the Gross method applies to the downward load since failure is in the gross section along the entire steel tee edge. The Net method is applied for upward load since failure is along the bolt line at the net section. All peak stress tensor components for upward and downward bending of the bolted connection were obtained in the laminate, through-the-thickness, at locations indicated by Figures 4.11 and 4.12, respectively. Figure 4.11 is a color-contour plot of the σ_x stress component when loaded down, with a close-up view of the area where the peak stresses in Table 4.6 are gathered in the laminate. The σ_x magnitudes are shown to be the highest at the steel tee weld area, pointed out in Figure 4.11, as well as some layers that are close to the top and bottom sides of the composite; these layers as one would expect are oriented at 0°. Figure 4.12 is the same plot as Figure 4.11, only the load on the model is up, so σ_x stresses are similar in magnitude but with opposite sign. The peak stresses in Table 4.7 are obtained for the upward-loaded model at the bolt line, through-the-thickness of the composite, as shown in Figure 4.12. This figure also shows the separation that occurs when the composite lifts off of the steel tee, and this is a critical step in the contact-aspect of the analysis at the connection interface.

Analytical and Gross method peak σ_x magnitudes in Table 4.6 are compared for the case of downward-flexure in Figure 4.11 for all layups except for the 6-ply laminate configuration. Analytical and Net method peak σ_x magnitudes in Table 4.7 are compared in the same way for the upward-bending instance in Figure 4.12. These figures show that as the number of layers is increased, the resulting stress level decreases for simplified Gross and Net method computations as well as ANSYS values for both upward and downward flexure. In Figures 4.13 and 4.14, the simplified Gross and Net method σ_x curves lay below the peak ANSYS σ_x curves. In other words, the Gross and Net method calculations for peak σ_x stress consistently underestimate the same values that are obtained in the plane strain model. The σ_x curves for the Gross and Net methods are smooth due to the isotropic-based nature of the calculation. The σ_x curves resulting from the ANSYS analysis would be smooth if not for the 28-ply result, as is noticeable in Figures 4.13 and 4.14.

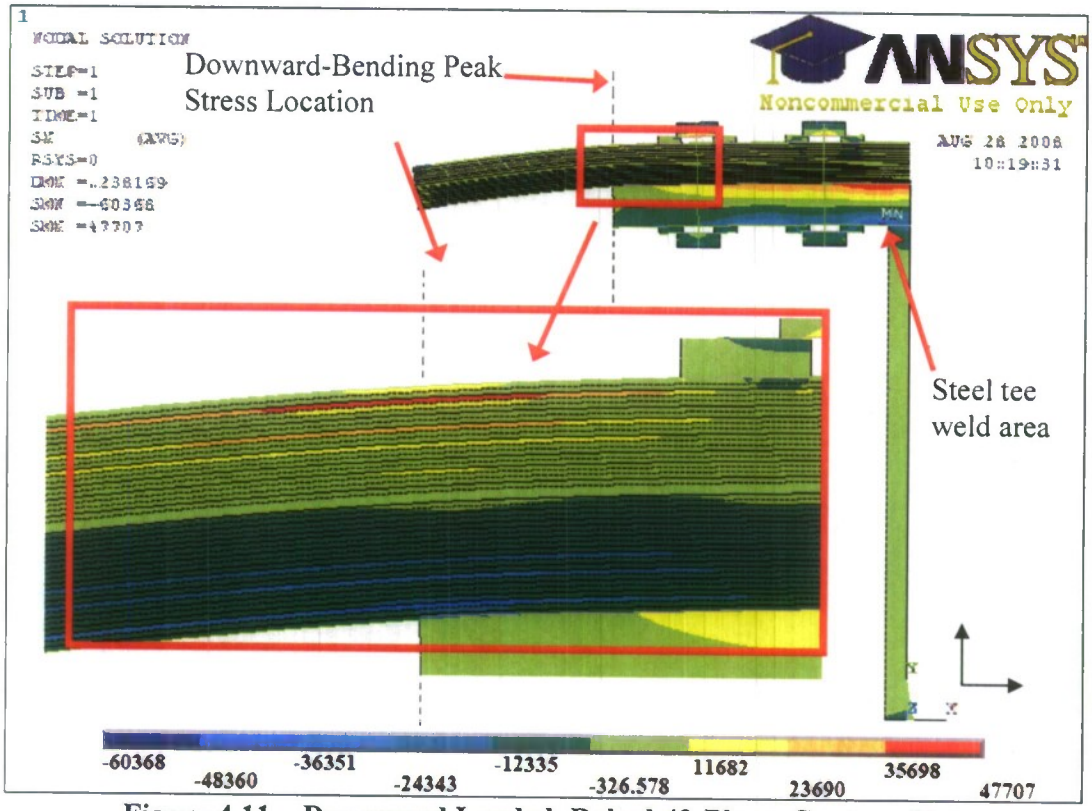

Figure 4.11 – Downward Loaded, Bolted 42-Ply σ_x Contour Plot

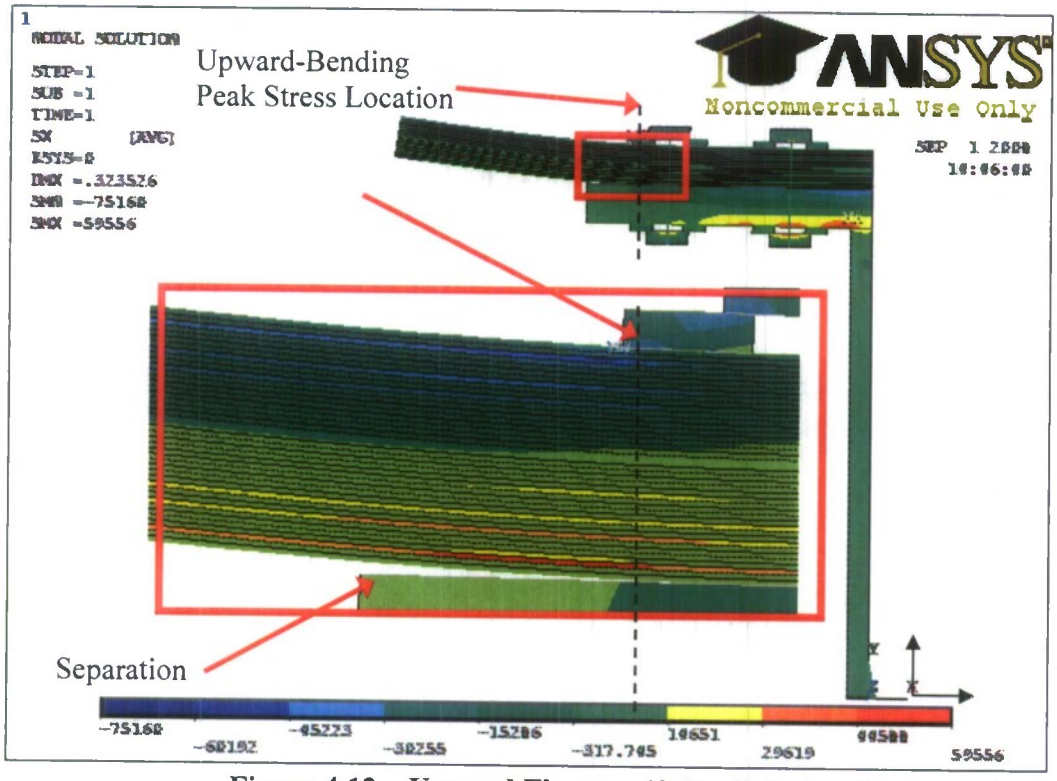

Figure 4.12 – Upward Flexure, 42-Ply Bolted σ_x Plot

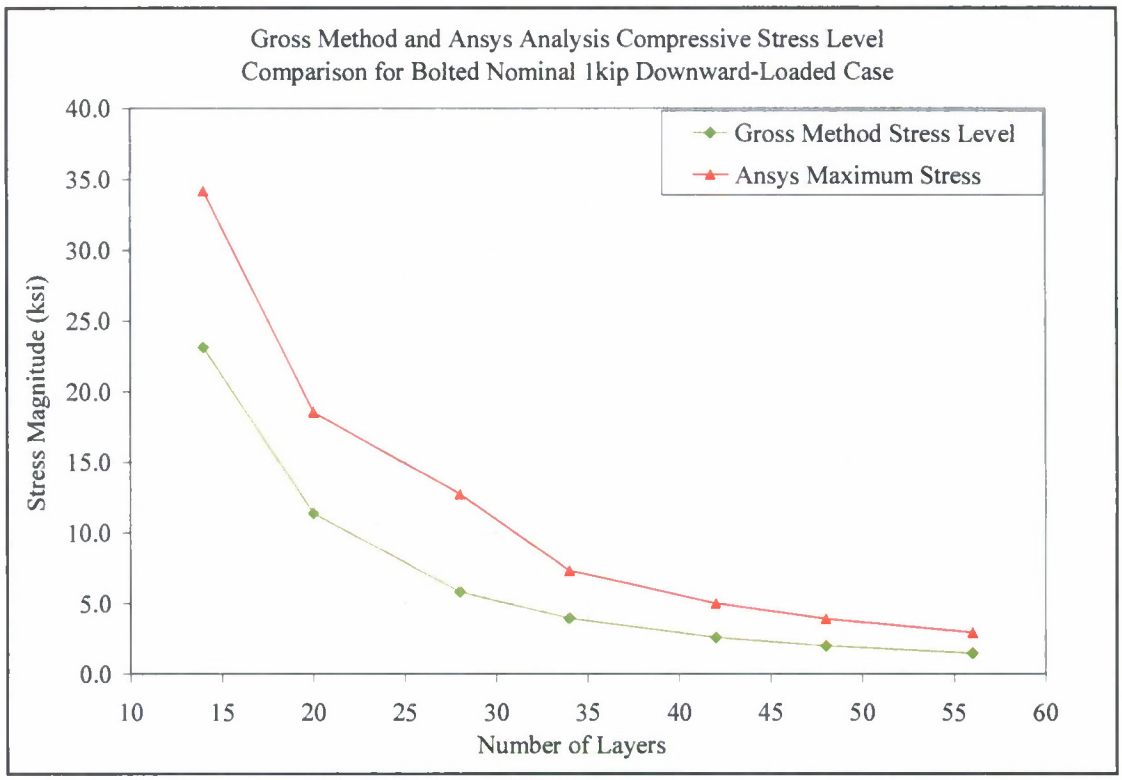

Figure 4.13 – Gross Method and ANSYS Bolted Maximum Stress Comparison

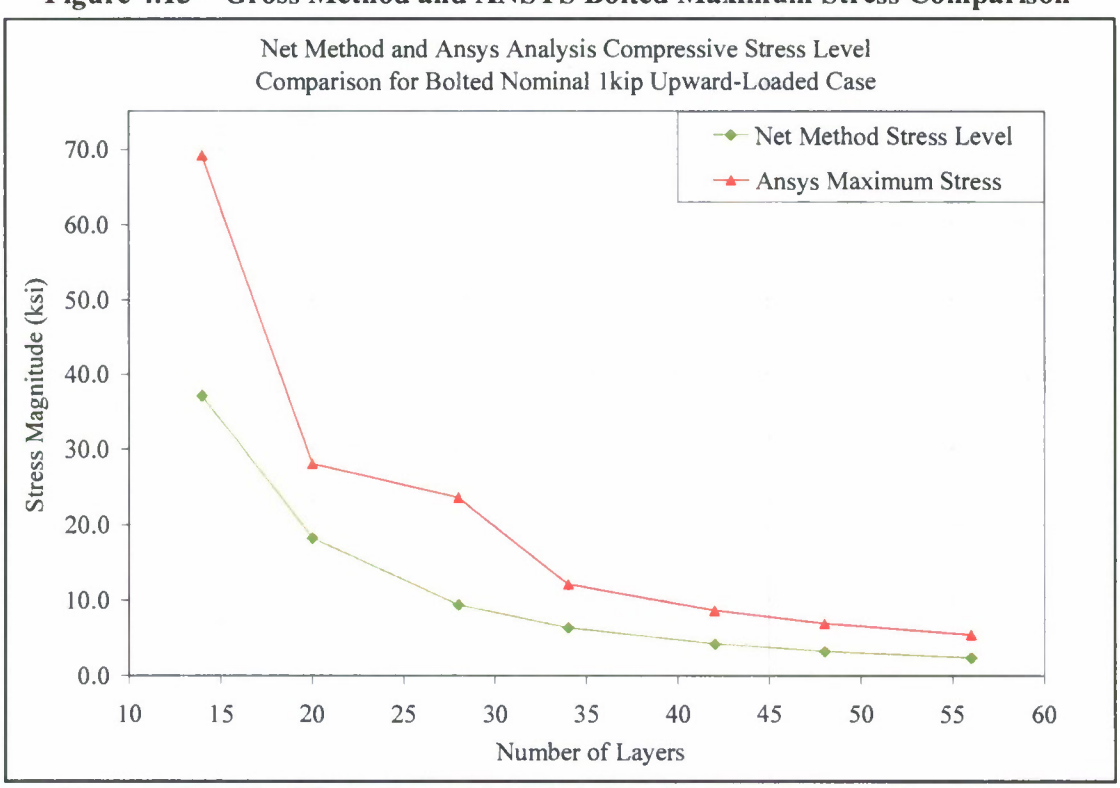

Figure 4.14 – Net Method and ANSYS Bolted Maximum Stress Comparison

This peak stress inconsistency with the trend set by other composite thicknesses can be explained by a characteristic difference in layer orientation for the 28-ply case, where it is the only layup with 0° layers on the top and bottom surfaces. Since these 0° orientations occupy the very top and bottom layers of the composite it is expected that the peak stress in those layers will be greater than a layup of the same thickness with 0° layers that are not located at the top and bottom faces of the laminate. Consequently there is a slight jump in the Ansys maximum stress curves in both figures for the 28-ply thickness. Peak σ_x value results are greater in magnitude when the connection is loaded upward as can be concluded by comparing Figures 4.13 and 4.14; this is due to the greater moment arm length used in the σ_x stress calculations which extends from the load to the bolt-line, as opposed to the steel tee edge when downward loading takes place.

Laminate through-the-thickness ANSYS™ σ_x stress plots for the 6, 28, and 48-ply thicknesses are shown for the case of nominal 1 kip downward load in Figures 4.15-4.17, respectively. The location where the stress magnitudes are obtained for all through-the thickness plots for the bolted downward-loaded model is shown in Figure 4.11, at the

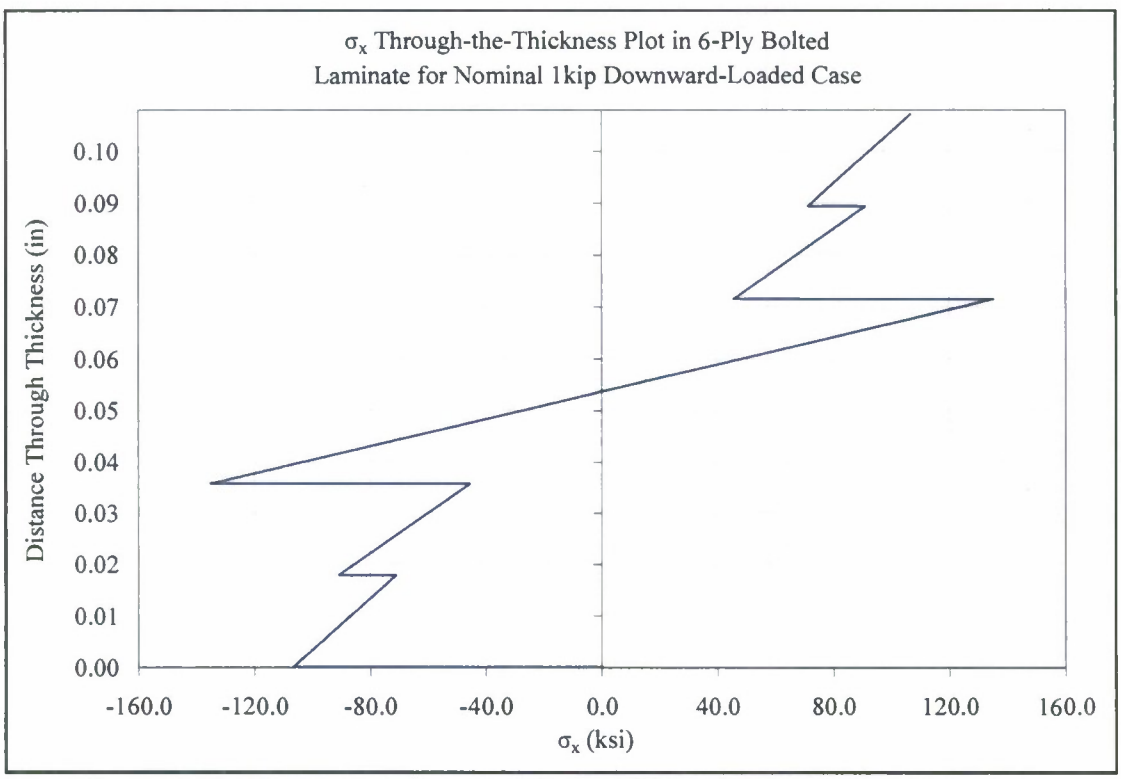

Figure 4.15 - Downward Loaded, Bolted 6-Ply σ_x Through-Thickness Plot

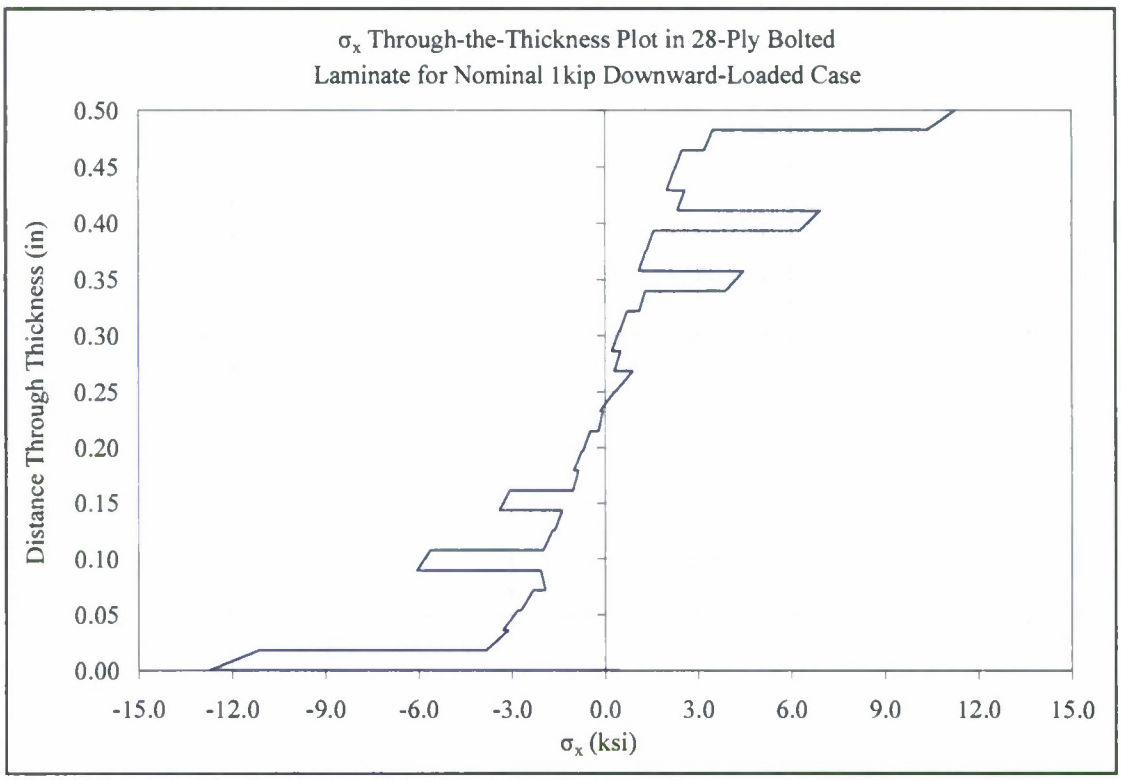

Figure 4.16 - Downward Loaded, Bolted 28-Ply σ_x Through-Thickness Plot

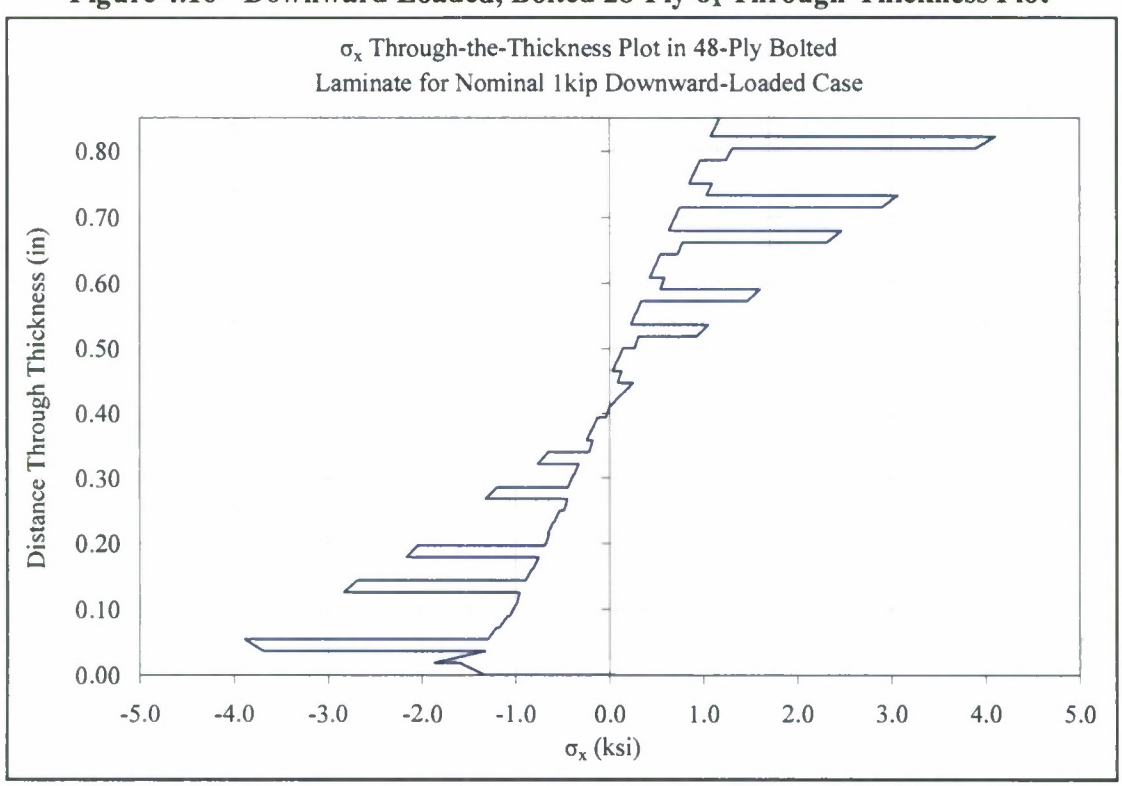

Figure 4.17 - Downward Loaded, Bolted 48-Ply σ_x Through-Thickness Plot

steel tee edge. In Figure 4.15, stresses in the composite thickness are negative (in compression) at the bottom half and positive (in tension) at the top half. The same pattern is evident in the 28-ply and 48-ply thicknesses in Figures 4.16 and 4.17. The 6-ply stress plot shows symmetry in stress magnitude at the halfway point through the thickness. Looking at each layer individually the decrease in magnitude of stress is evident as the middle of the composite is approached. The maximum compressive and tensile σ_x values for in the 6-ply laminate occur at the middle layers due to their orientation of 0°, and they both reach a magnitude of approximately 135 ksi. The reader should take note that this magnitude of stress would be unrealistic in an experiment since static failure for a composite plate with a quasi-isotropic layup, as is used in the current work, normally occurs in the range of 40-50 ksi. For this reason, results for the 6-ply instance are not plotted in Figures 4.13 and 4.14, which include the trends of analytical peak σ_x magnitudes for 7 different laminate thicknesses. If a 6-ply laminate were tested in fatigue using the experimental setup in this work, the load amplitude would need to be reduced significantly in order to obtain any useful fatigue data for that thickness. The degradation of the composite has not been included in the ANSYS model; the analysis will not show the catastrophic failure of a material that is subjected to large deflections, which would normally occur in an experimental test. The 28-ply and 48-ply plots in Figures 4.14 and 4.15 show that, as with the 6-ply case, the magnitude of stress generally decreases as the middle of the thickness is approached when looking at layers individually. There are a few instances, however, where this pattern is not followed. In the 28-ply graph, the 5th layer from the bottom shows an increase in stress magnitude as the middle of the laminate is approached; the same observation is made in the 48-ply plot at the 1st and 3rd layers from the bottom of the thickness. This irregularity could be due to the force of the steel tee edge against the laminate at that location. Although not perfect, there is a trend of symmetry of stress magnitude about the middle of the 28-ply and 48-ply laminates; the general pattern is that stresses increase as the outer layers become closer. The 0° plies in both of these layups exhibit the highest stresses magnitudes in comparison to the layers adjacent to them.

Through-the-thickness ANSYS™ τ_{xy} stress plots for the 6, 28, and 48-ply layups are

provided in Figures 4.18-4.20 when under a nominal 1 kip downward load. This plot represents the average transverse shear stress in each layer. Looking at each layer individually in Figures 4.18-4.20, the magnitude of τ_{xy} stays the same through-the-thickness of the ply, unlike the σ_x through-the-thickness stress plots. The 6-ply laminate, in Figure 4.18, displays increasing positive τ_{xy} stress values as the middle of the thickness is approached from the outer layers, and the maximum occurs at the middle 0° layers. The 28-ply plot in Figure 4.19 shows negative τ_{xy} stress values for the top half of the thickness and positive for the bottom half. The τ_{xy} stress values for the 48-ply case in Figure 4.20 are positive throughout the thickness, steadily increasing as the bottom of the laminate draws near. In the 28-ply and 48-ply instances the magnitude of τ_{xy} stress reaches a maximum at the 2nd layer from the bottom, both oriented at -45°. There is a large difference in magnitude of delamination stress τ_{xy} when comparing values close to the top and bottom surfaces of the composite, and this is most likely caused by the concentrated force of the steel tee edge.

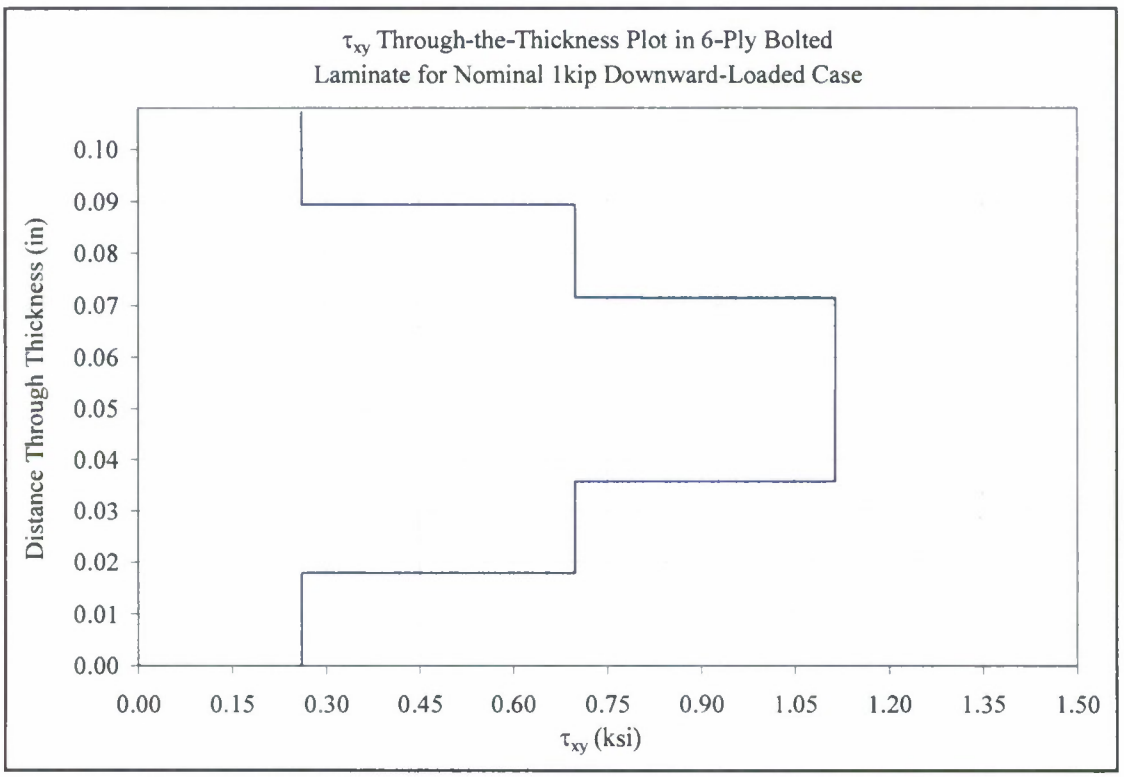

Figure 4.18 - Downward Loaded, Bolted 6-Ply τ_{xy} Through-Thickness Plot

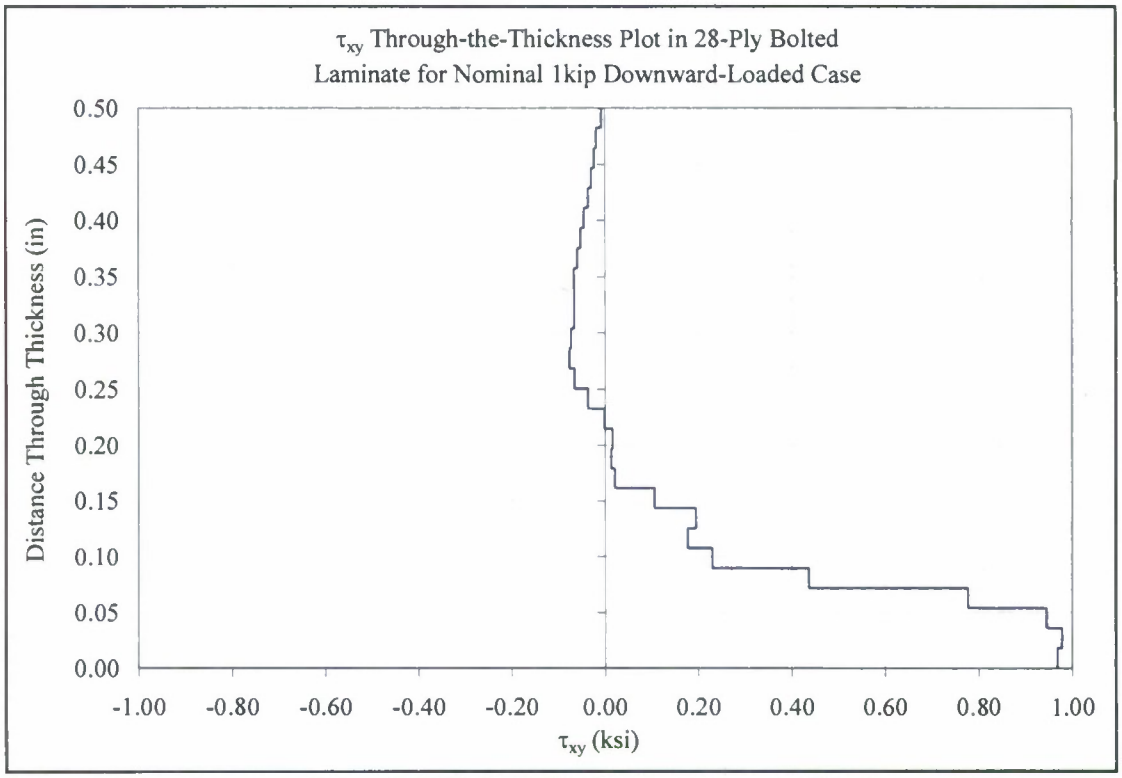

Figure 4.19 - Downward Loaded, Bolted 28- Ply τ_{xy} Through-Thickness Plot

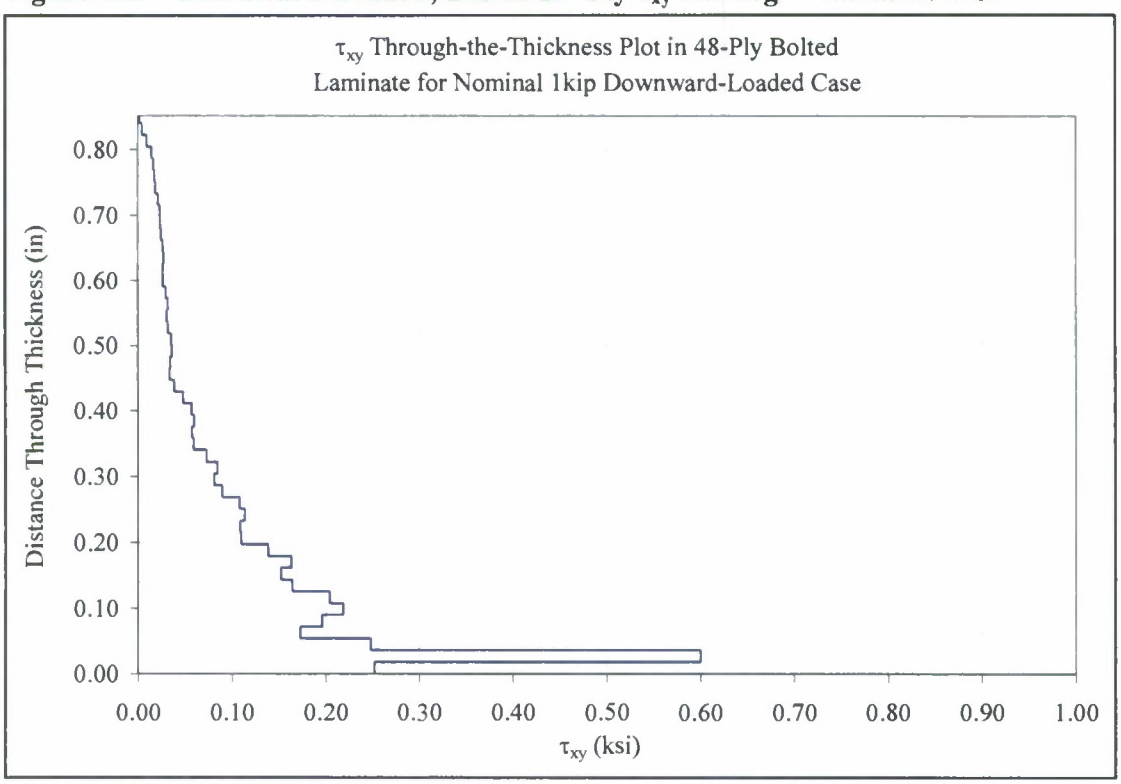

Figure 4.20 - Downward Loaded, Bolted 48-Ply τ_{xy} Through-Thickness Plot

Composite ANSYS™ σ_x through-the-thickness plots for the 6, 28, and 48-ply thicknesses are shown for the case of nominal 1 kip upward load in Figures 4.21-4.23, respectively. The location where the stress magnitudes are obtained for all bolted, through-the-thickness plots when the model is loaded up is shown in Figure 4.12, at the bolt line. In the 6-ply case, shown in Figure 4.21, stress values are compressive at the top half and tensile at the bottom half; opposite of when the load on the model is directed down. This trend exists for the 28-ply and 48-ply layups as well, as shown in Figures 4.22 and 4.23. The value of σ_x reaches a maximum magnitude about 147 ksi at two locations in the layup; at the lower 0° layer at the top surface of the composite. The top layer attains this high of a stress probably because of the concentrated force cause by the bolt in the model. This same stress increase is present in the 28-ply and 48-ply plots, where a significantly greater magnitude of stress is achieved as compared to the rest of the thickness.

Through-the-thickness ANSYS™ τ_{xy} stress plots for the 6, 28, and 48-ply layups are provided in Figures 4.24-4.26 when under a nominal 1 kip upward load. Unlike the case of downward load, values for τ_{xy} are negative in the 6-ply laminate, shown in Figure 4.24; this takes place in the top two plies. The 2nd layer from the top is the location of maximum shear stress for all three layups. All three layups also display positive τ_{xy} values in the bottom half of the laminate thickness and then a rapid decrease and change in sign of those values as the top side of the laminate becomes closer.

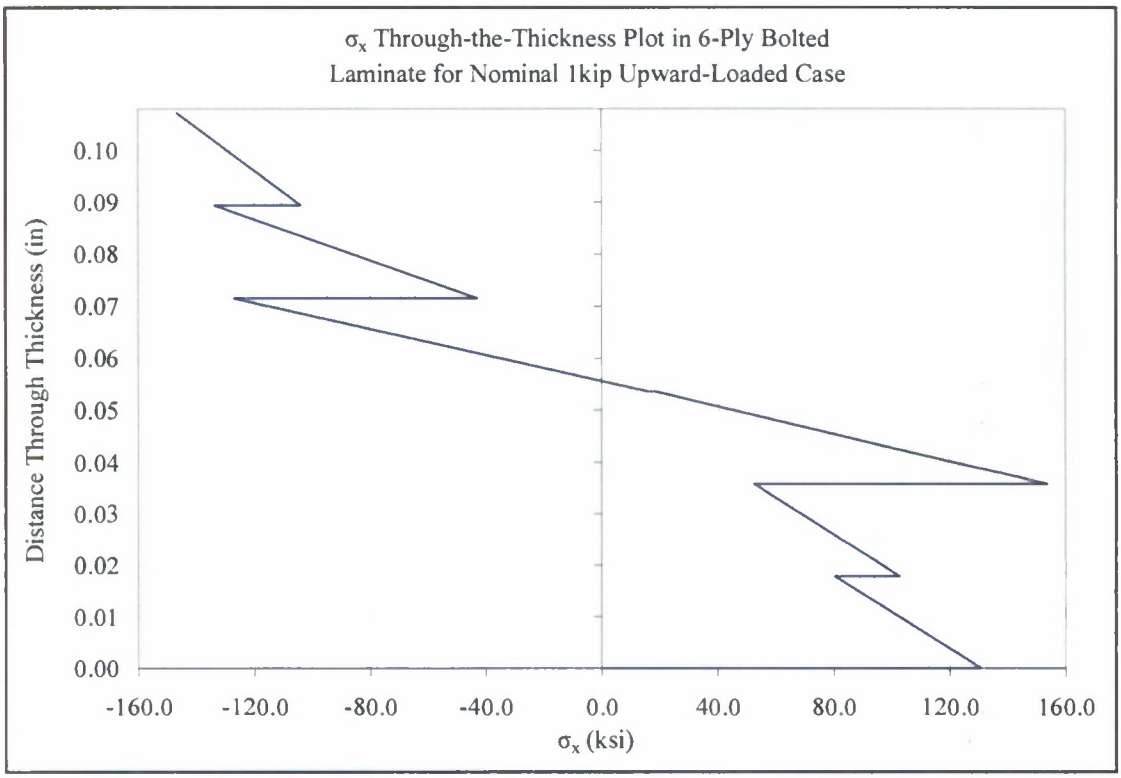

Figure 4.21 - Upward Loaded, Bolted 6-Ply σ_x Through-Thickness Plot

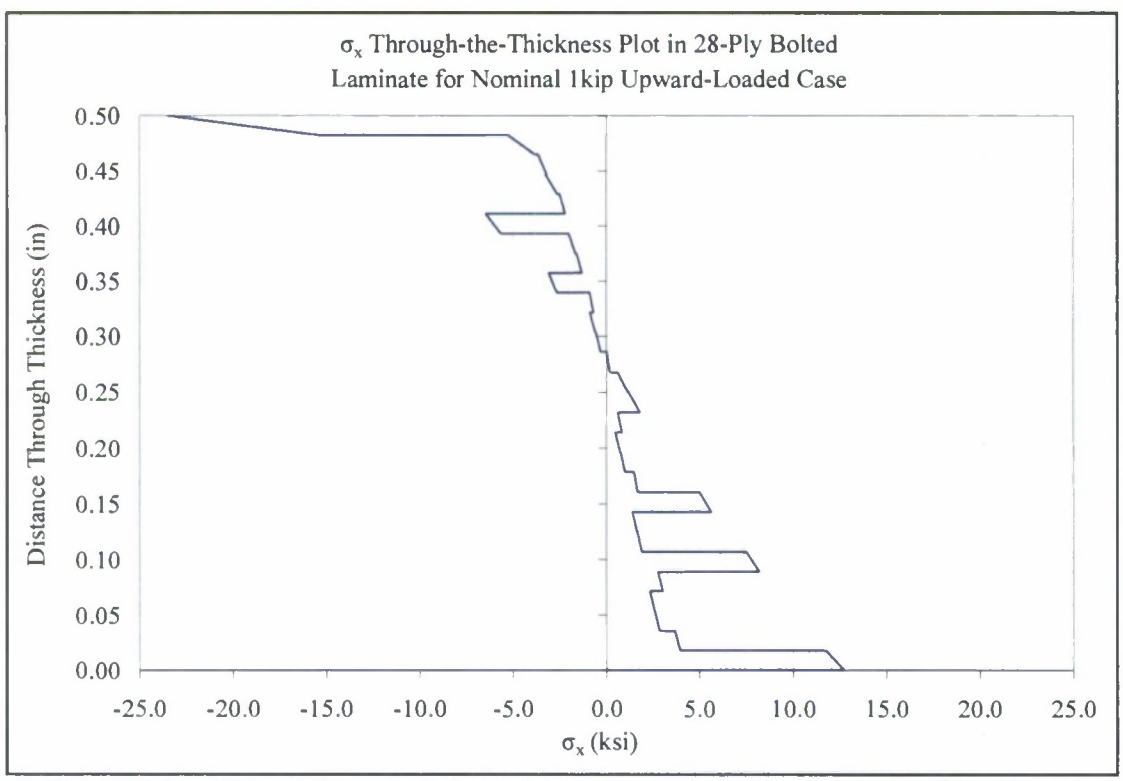

Figure 4.22 - Upward Loaded, Bolted 28-Ply σ_x Through-Thickness Plot

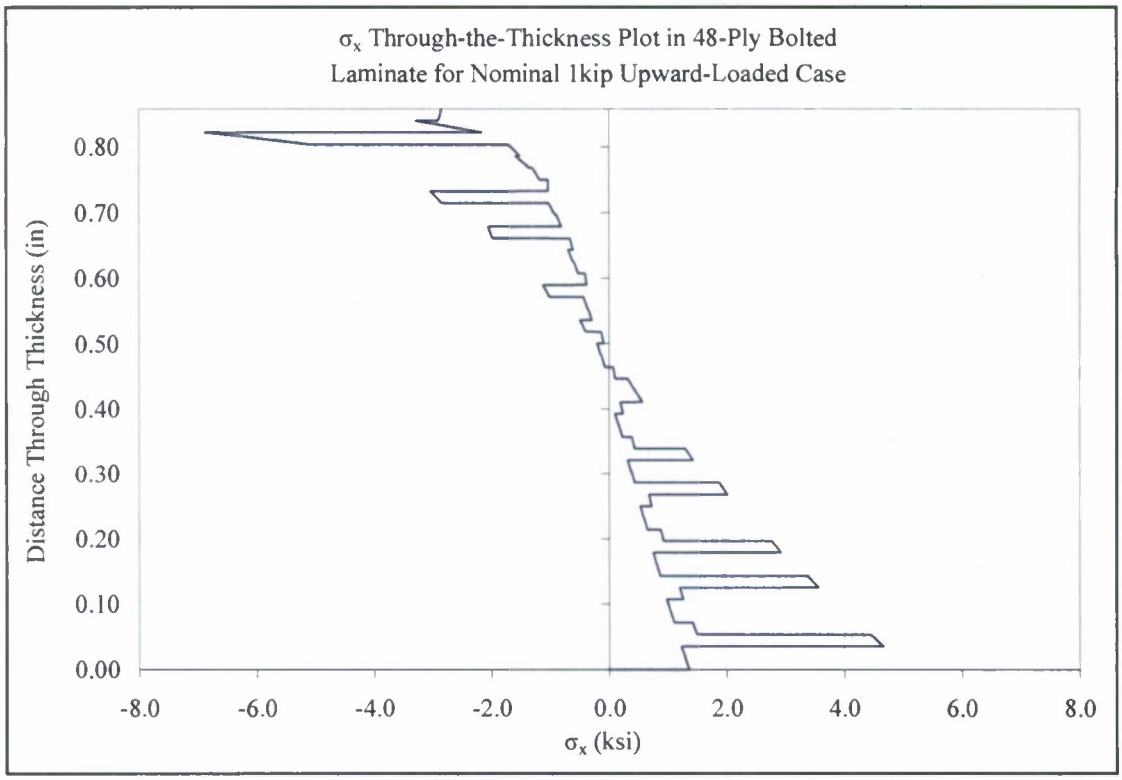

Figure 4.23 - Upward Loaded, Bolted 48-Ply σ_x Through-Thickness Plot

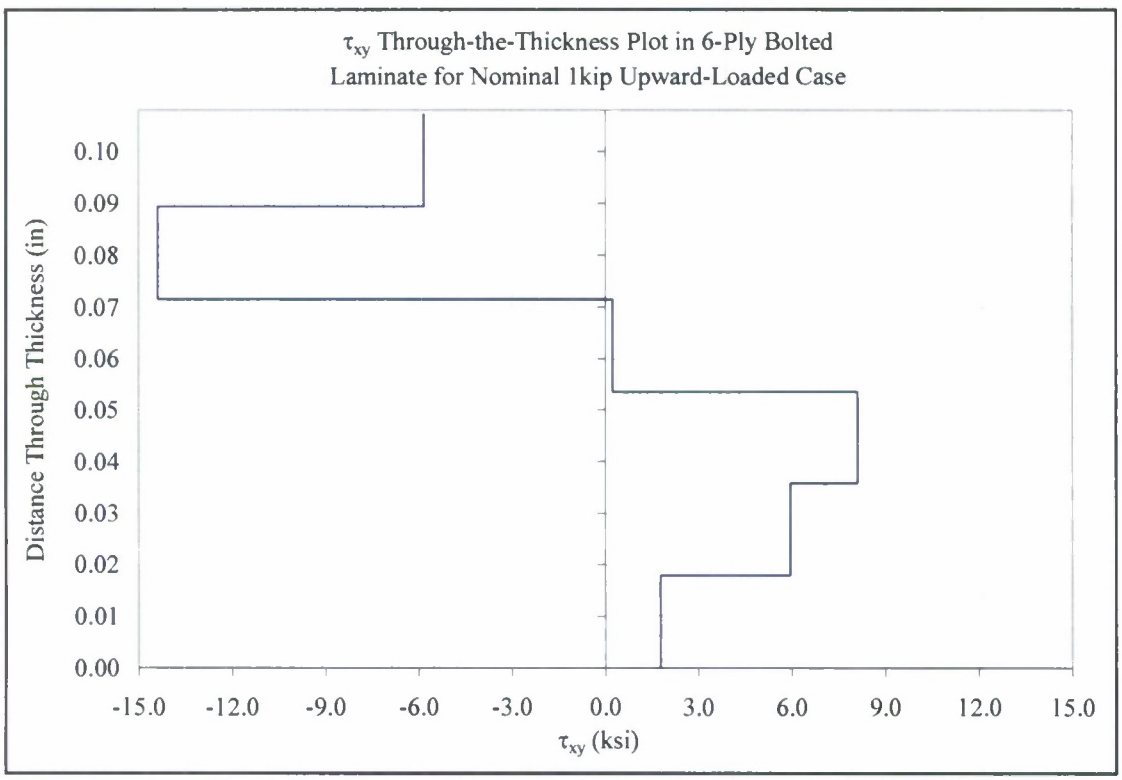

Figure 4.24 - Upward Loaded, Bolted 6-Ply τ_{xy} Through-Thickness Plot

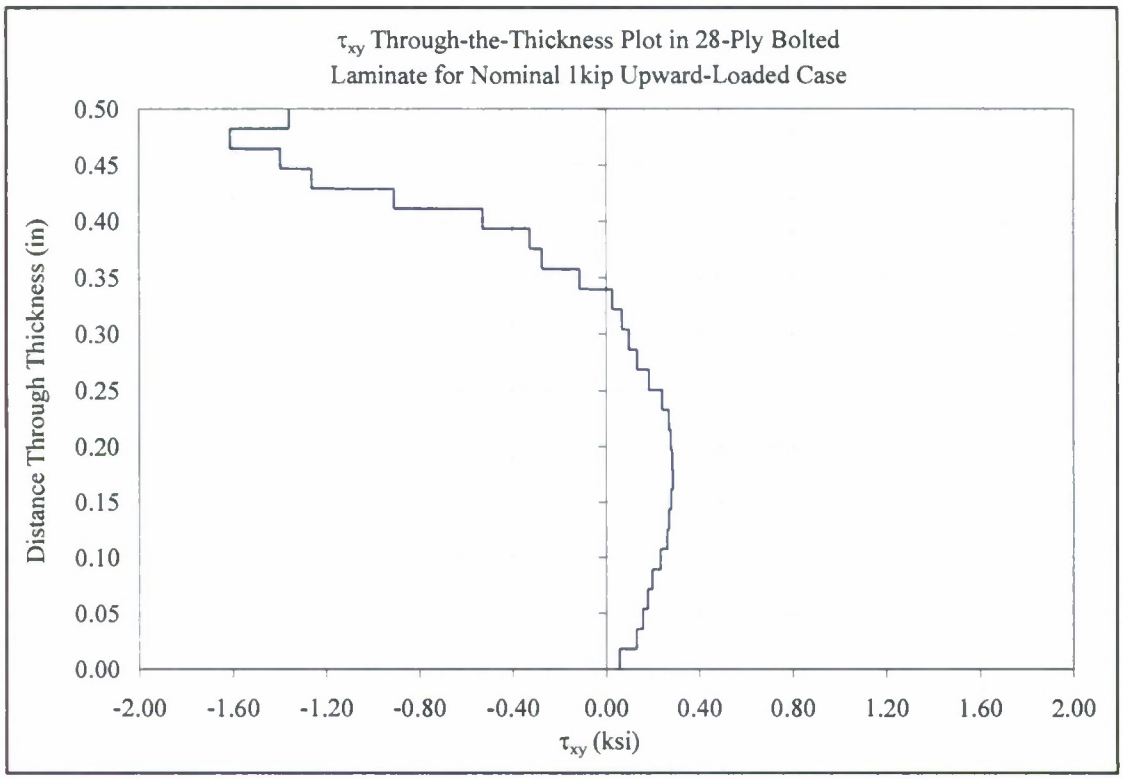

Figure 4.25 - Upward Loaded, Bolted 28-Ply τ_{xy} Through-Thickness Plot

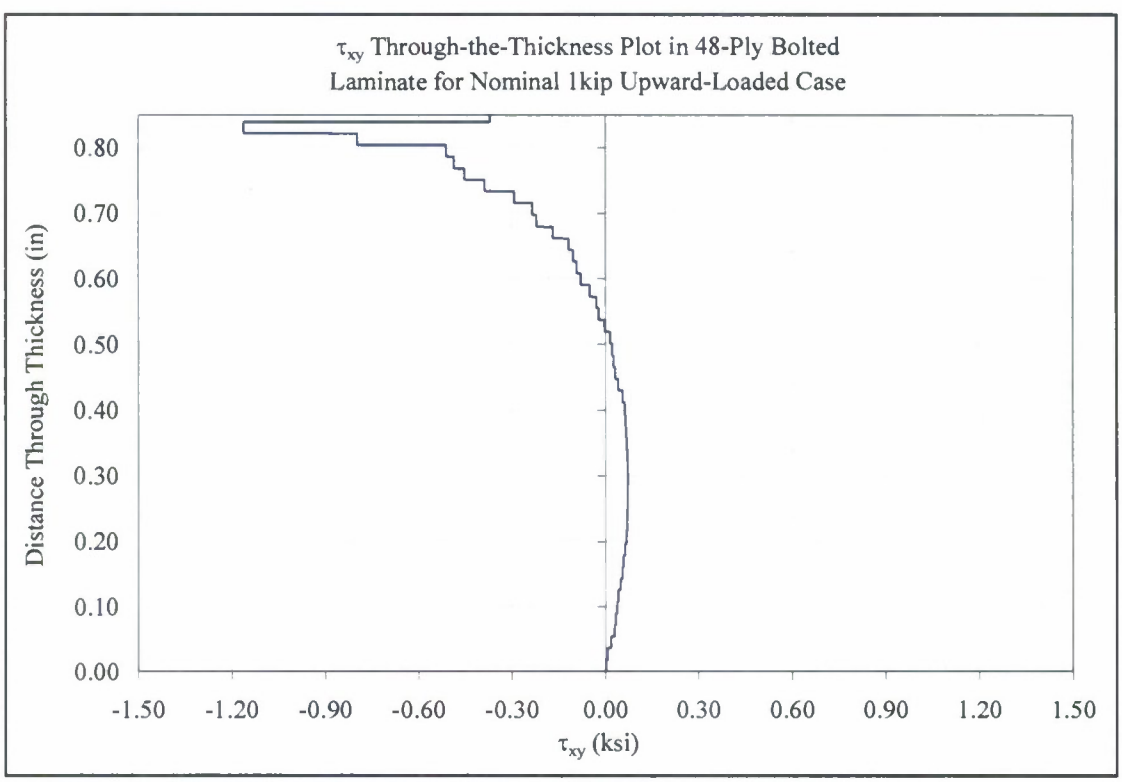

Figure 4.26 - Upward Loaded, Bolted 48-Ply τ_{xy} Through-Thickness Plot

4.1.5 Clamped Model Results, Laminate Thickness Varied

ANSYS flexibility results of the clamped configuration are given and compared to available experimental data in Table 4.9; two different values of bolt preload are applied to the upward-loaded model and corresponding flexibility results are shown. Analytical and experimental deflection results are plotted on the same graph for the downward and upward-loaded instances in Figures 4.27 and 4.28, respectively. As with the bolted configuration, when only 6 plies are modeled the ANSYS analysis becomes valid for only small amounts of force. Analytical results match available experimental data fairly well, except for the 28-ply layup where the Ansys flexibility deviation from experimental response for downward-bending and upward-bending response becomes 32.3 and 30.7 percent, respectively. This discrepancy may be attributed to the difference in outer-layer

Table 4.9 – ANSYS and Experimental Flexibility Computed at the 8kip Load Level

Laminate Thickness		Downward Loaded		Upward Loaded		
Inches	# Plies	ANSYS Flexibility (in/lb)	Experimental Flexibility (in/lb)	ANSYS Deflection (in/lb) Bolt $\varepsilon=0.9\sigma_u$	ANSYS Deflection (in/lb) Bolt $\varepsilon=0.1\sigma_u$	Experimental Deflection (in/lb)
0.107	6	4.98E-03	-	4.98E-03	4.99E-03	-
0.250	14	3.12E-04	-	3.13E-04	3.20E-04	-
0.357	20	1.36E-04	-	1.36E-04	1.40E-04	-
0.500	28	4.46E-05	3.37E-05	4.89E-05	5.16E-05	3.74E-05
0.607	34	3.50E-05	-	3.60E-05	3.88E-05	-
0.750	42	1.96E-05	2.12E-05	2.11E-05	2.38E-05	2.79E-05
0.857	48	1.43E-05	1.80E-05	1.56E-05	1.83E-05	2.09E-05
1.000	56	1.00E-05	-	1.11E-05	1.35E-05	-

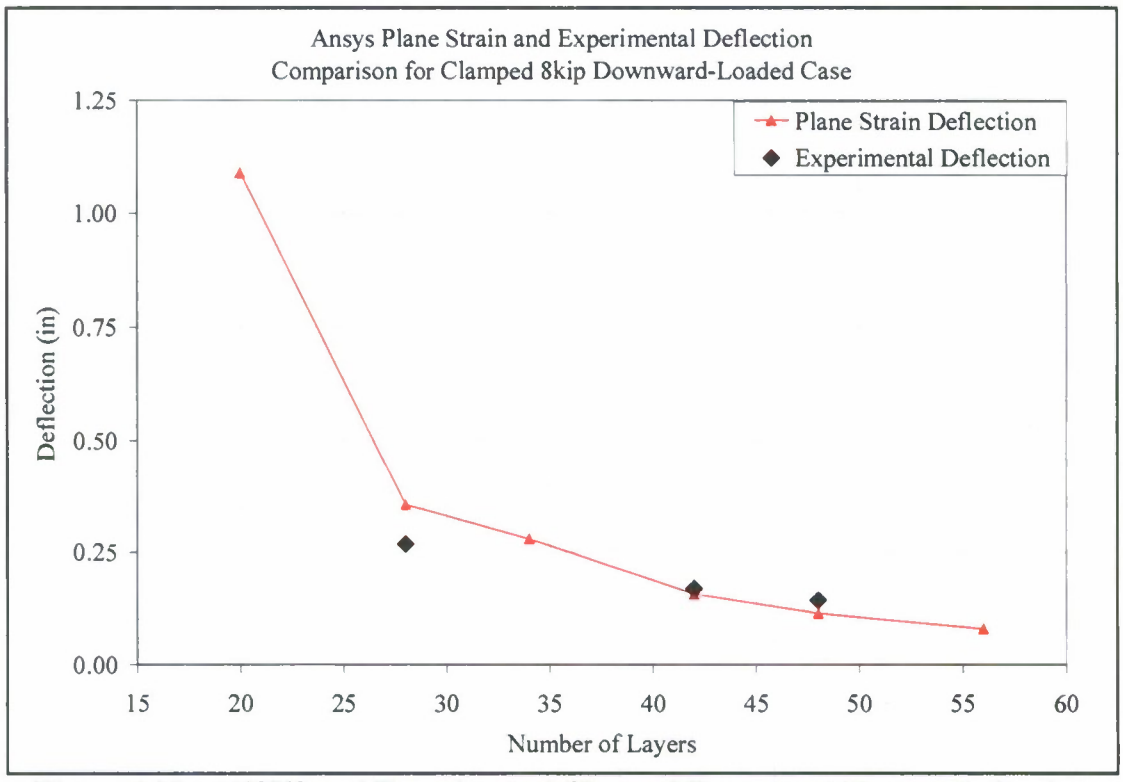

Figure 4.27 - ANSYS and Experimental Clamped Downward-Flexure Deflection

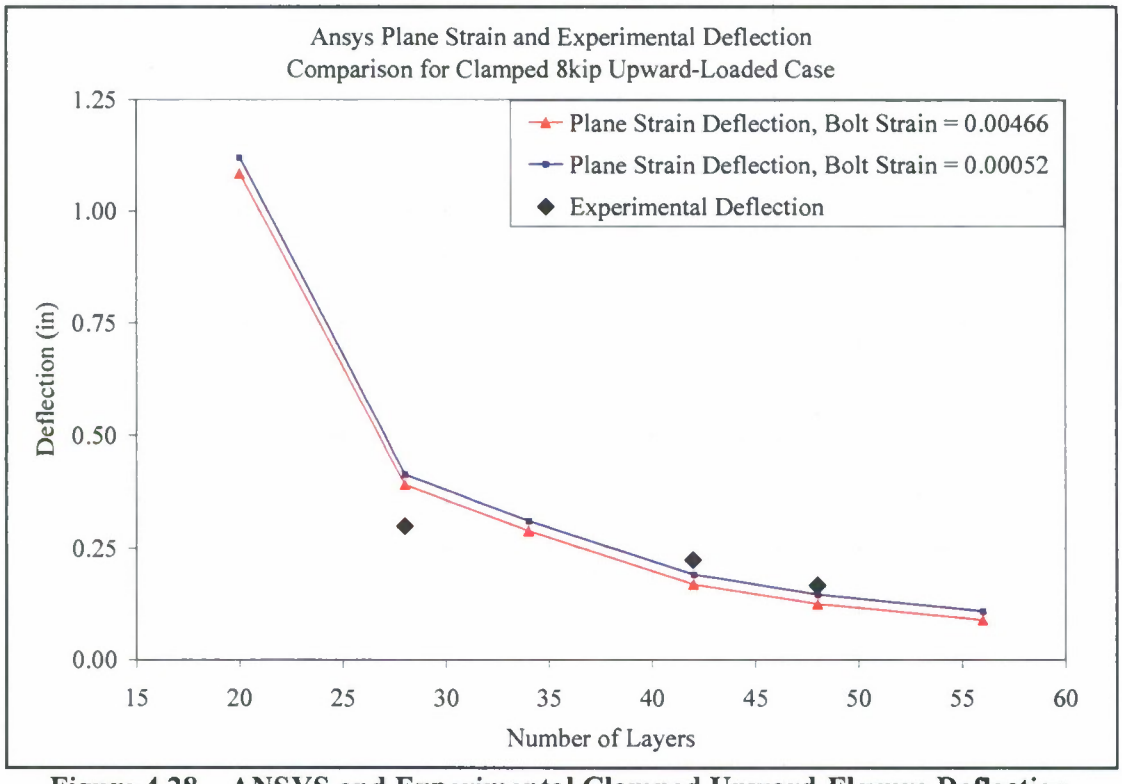

Figure 4.28 – ANSYS and Experimental Clamped Upward-Flexure Deflection

orientation in the layup design as compared to all the other laminates, details of which are summarized in Appendix C. Figure 4.28 shows how the deflection of the connection increases in the model as the bolt preload is reduced from $0.9\sigma_u$ to $0.1\sigma_u$ (where $\sigma_u = 150$ ksi).

Peak stress through-the-thickness results for a nominal 1 kip downward and upward load on the clamped configuration are provided and compared to the simplified Gross method peak stress level calculations in Tables 4.10 and 4.11. Table 4.12 is a variation of Table 4.11 stress results, with the bolt preload reduced from $0.9\sigma_u$ to $0.1\sigma_u$; differences in stress values due to a change in bolt preload are minimal. Also included in these tables are the calculated ratios (σ_x- ANSYS)/ (σ_x-Gross) and (τ_{xy}- ANSYS)/ (σ_x-Gross). ANSYS™ and Gross method peak σ_x magnitudes are compared on the same graph for the case of downward and upward flexure in Figures 4.31 and 4.32 for all layups except for the 6-ply laminate configuration. All the peak stress tensor components in Tables 4.9 and 4.10 were obtained in the laminate, through-the-thickness, at the location specified by Figures 4.29 and 4.30.

Table 4.10 – ANSYS Stress Comparison for Clamped Nominal 1-kip Downward-Loaded Case

	ANSYS Analysis			Simplified Calculation		
# Plies	τ_{xy} (ksi)	σ_y (ksi)	σ_x (ksi)	Gross Method σ_x (ksi)	(σ_x-ANSYS)/ (σ_x-Gross)	(τ_{xy}-ANSYS)/ (σ_x-Gross)
6	-16.42	-3.69	-101.70	-125.75	0.809	0.131
14	6.05	-17.22	-35.31	-23.10	1.528	-0.262
20	1.87	-5.10	-18.97	-11.32	1.675	-0.165
28	0.99	-1.89	-11.90	-5.78	2.060	-0.171
34	1.03	-1.81	-7.31	-3.92	1.867	-0.262
42	0.74	-1.20	-5.03	-2.57	1.959	-0.287
48	0.59	-0.93	-3.93	-1.97	1.999	-0.298
56	0.46	-0.71	-2.94	-1.44	2.036	-0.320

Table 4.11 – ANSYS Stress Comparison for Clamped Nominal 1-kip Upward-Loaded Case, Bolt Preload = $0.9\sigma_u$

	ANSYS Analysis			Simplified Calculation		
# Plies	τ_{xy} (ksi)	σ_y (ksi)	σ_x (ksi)	Gross Method σ_x (ksi)	(σ_x-ANSYS)/ (σ_x-Gross)	(τ_{xy}-ANSYS)/ (σ_x-Gross)
6	16.42	-3.46	-101.95	-125.75	0.811	-0.131
14	-5.69	-16.96	-34.56	-23.10	1.496	0.246
20	-1.83	-4.94	-18.98	-11.32	1.677	0.162
28	-0.50	-1.14	-11.31	-5.78	1.958	0.086
34	-1.03	-1.85	-7.32	-3.92	1.869	0.263
42	-0.75	-1.28	-4.97	-2.57	1.935	0.291
48	-0.59	-0.93	-3.95	-1.97	2.008	0.302
56	-0.32	-0.52	-2.89	-1.44	2.004	0.221

Table 4.12 – ANSYS Stress Comparison for Clamped Nominal 1-kip Upward-Loaded Case, Bolt Preload = $0.1\sigma_u$

	ANSYS Analysis			Simplified Calculation		
# Plies	τ_{xy} (ksi)	σ_y (ksi)	σ_x (ksi)	Gross Method σ_x (ksi)	(σ_x-ANSYS)/ (σ_x-Gross)	(τ_{xy}-ANSYS)/ (σ_x-Gross)
6	15.77	-2.87	-103.51	-125.75	0.823	-0.125
14	-6.13	-19.08	-34.24	-23.10	1.482	0.265
20	-2.48	-7.51	-18.66	-11.32	1.648	0.219
28	-0.49	-1.47	-11.75	-5.78	2.033	0.085
34	-0.90	-1.86	-7.32	-3.92	1.866	0.229
42	-0.70	-1.28	-4.97	-2.57	1.933	0.270
48	-0.55	-0.99	-3.86	-1.97	1.957	0.280
56	-0.22	-0.37	-2.92	-1.44	2.026	0.149

Figure 4.29 is a color-contour plot of the σ_x stress component when loaded down and Figure 4.30 is the same plot for an upward load. The close-up views in these two figures show that σ_x stress intensities in the laminate are equivalent in degree but their values are opposite in sign when the load direction switches from down to up. The σ_x magnitudes are shown to be the highest in the laminate, without values reaching a similar magnitude in the steel tee, at the weld, as with the bolted model; there is a support plate, pointed out

in Figures 4.29 and 4.30, which is "welded" to the steel tee in the model. Much of the load on the model is distributed across the top of this support plate, and the test setup was designed in this way in order to isolate the composite in the experiment. In Figures 4.29 and 4.30, the layers close to the top and bottom sides of the composite that show the highest stress levels are oriented at 0°.

ANSYS™ and Gross method peak σ_x magnitudes in Table 4.10 are compared for the case of downward-flexure in Figure 4.31 for all layups except for the 6-ply laminate configuration. The same comparison is made in Figure 4.32 for the upward-bending

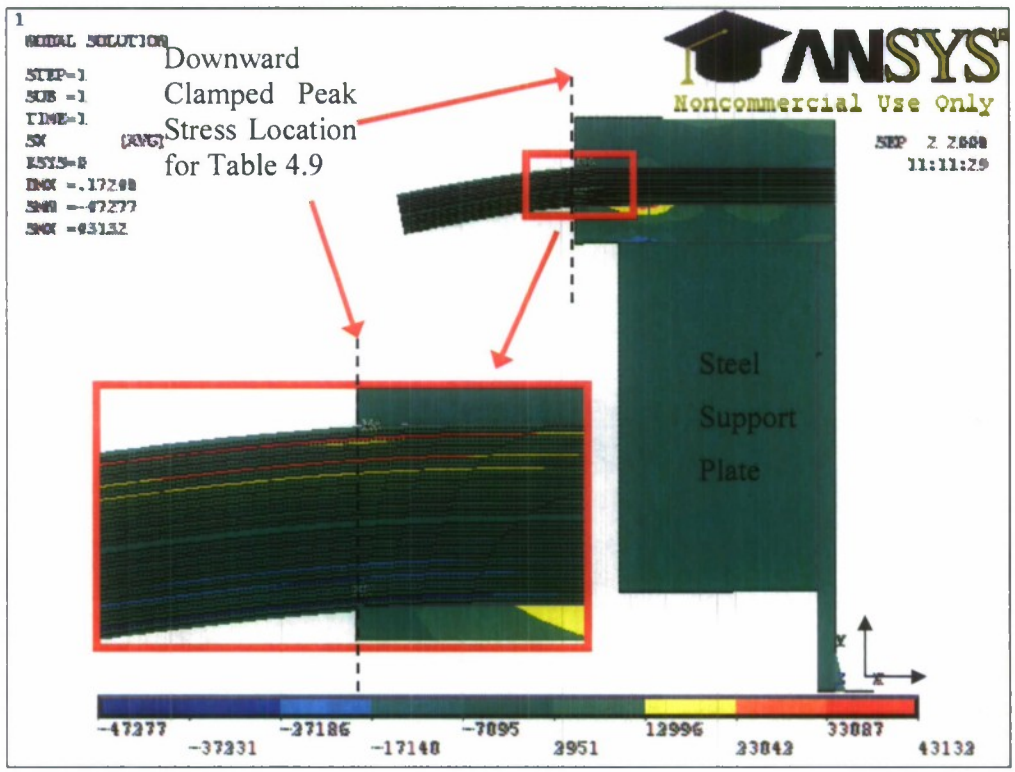

Figure 4.29 – Downward Flexure, 42-Ply Clamped σ_x Plot

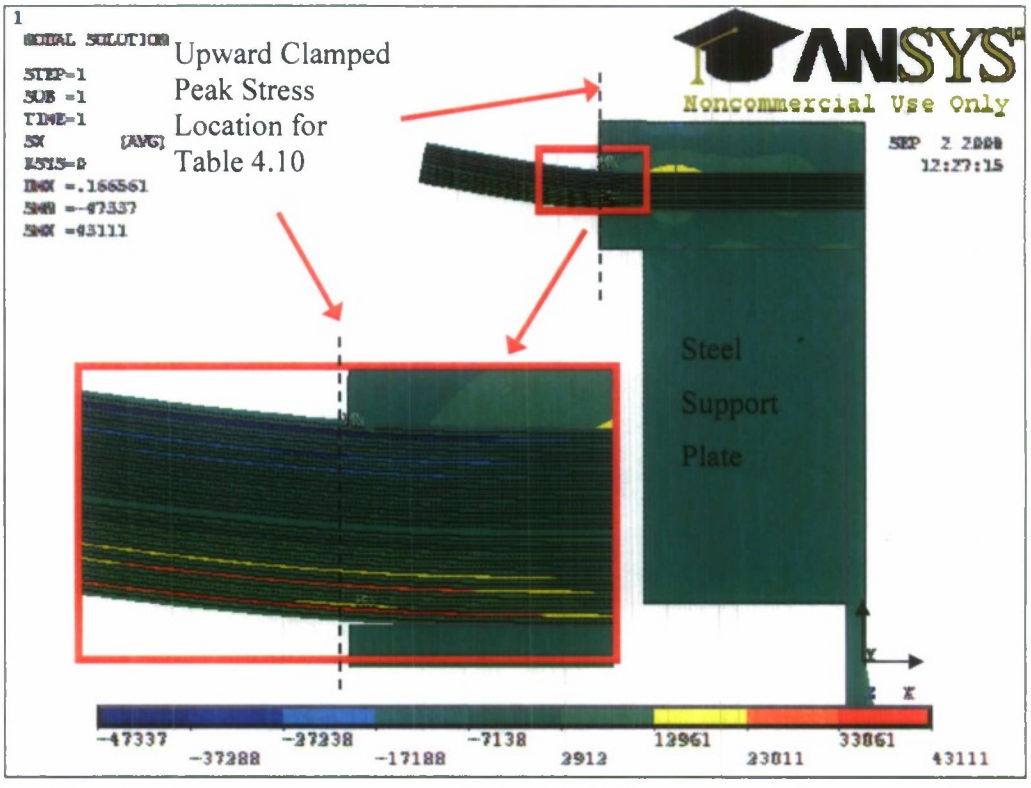

Figure 4.30 – Upward Flexure, 42-Ply Clamped σ_x Plot

instance, using peak σ_x magnitudes from Table 4.11. As with the bolted configuration, these figures show that as the number of layers is increased the resulting level of peak σ_x stress decreases for all computational methods. In Figures 4.31 and 4.32, the simplified Gross method σ_x curves lay below the peak ANSYS™ σ_x curves, as was observed in the bolted connection results. Peak σ_x value results are similar in magnitude for both upward and downward load situations, unlike the bolted model results, as can be concluded by comparing Figures 4.31 and 4.32; the moment arms used in the σ_x stress calculations for upward and downward load are the same length, both extending from the load to the same horizontal position at the steel tee edge.

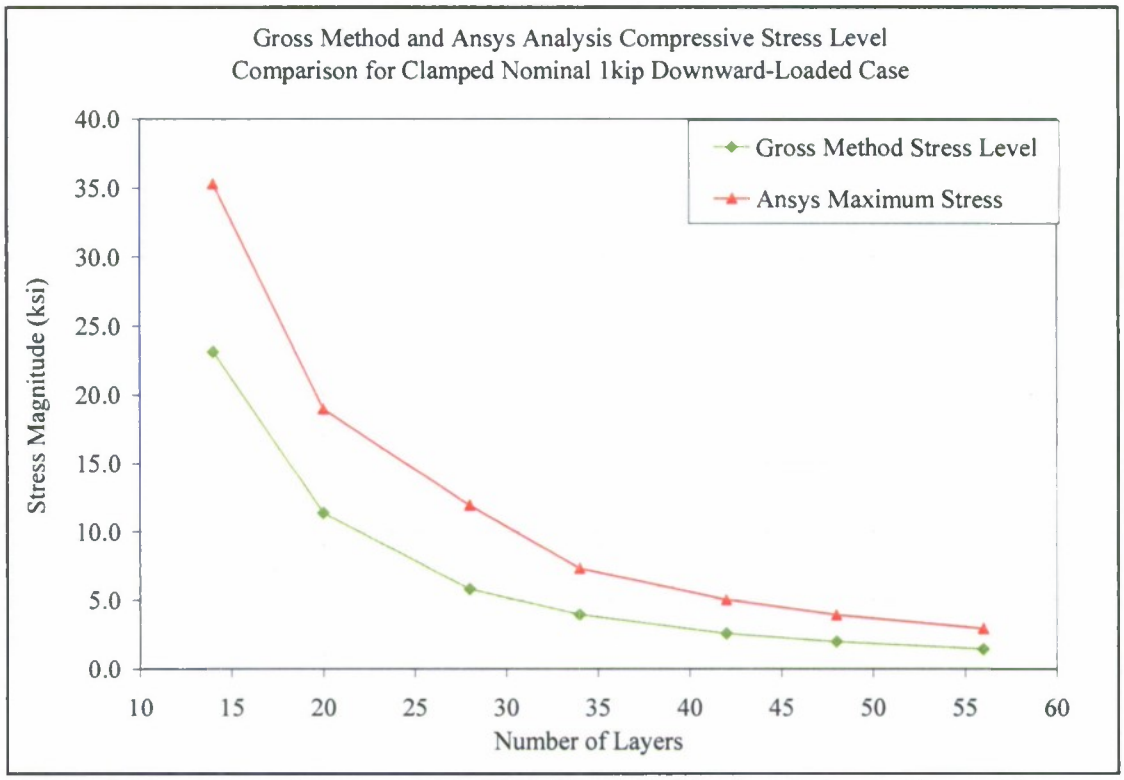

Figure 4.31 – Gross Method and ANSYS Clamped Maximum Stress Comparison

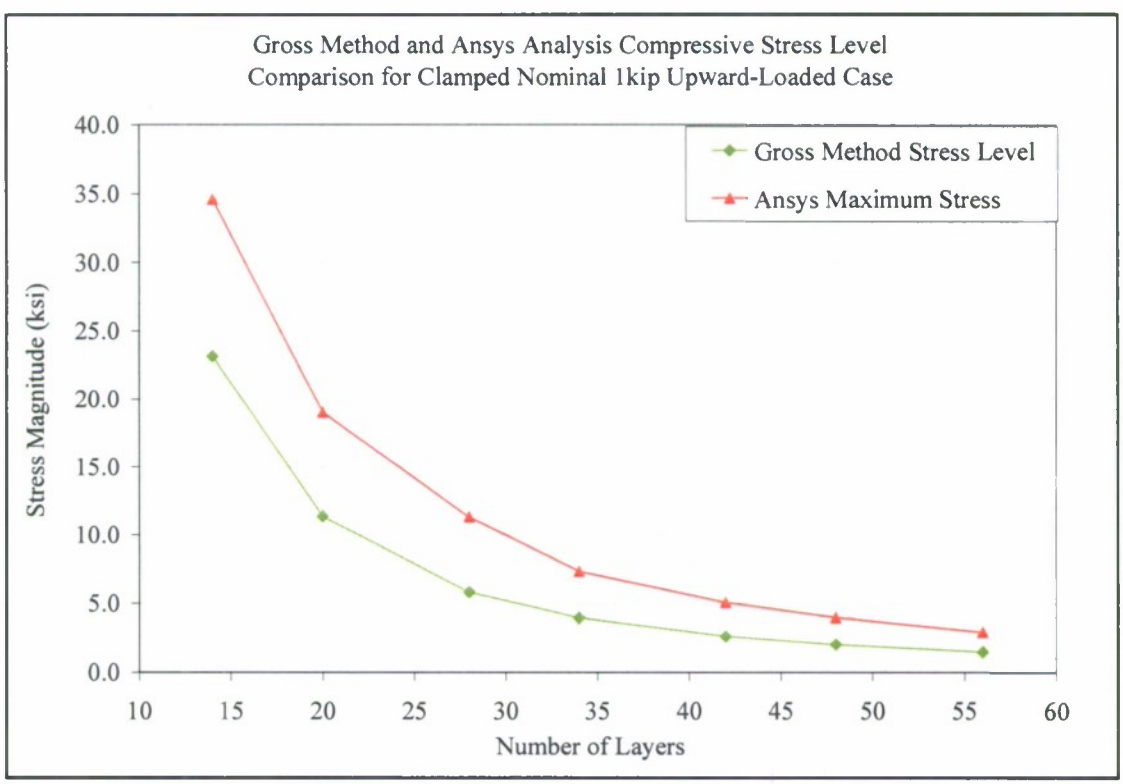

Figure 4.32 – Gross Method and ANSYS Clamped Maximum Stress Comparison

Laminate through-the-thickness ANSYS™ s σ_x stress plots for the 6, 28, and 48-ply thicknesses are shown for the case of nominal 1 kip downward load in Figures 4.33-4.35, respectively. In these plots, as well as those representing the upward load in Figures 4.39-4.41, the same general qualitative stress patterns that were seen with the bolted connection are apparent. The location where the stress magnitudes are obtained for all through-the thickness plots for the clamped model is shown in Figures 4.29 and 4.30, at the steel tee edge. The 6-ply plot in Figure 4.33 shows a slight shift of values toward the right side of the graph, signifying that magnitude of stress seen by the layers in tension is greater than those in compression. As with the bolted case, the degree of stress undergone by the layers in the 6-ply graph reaches unrealistic amounts; the middle, 0° layers are observed to reach 108 ksi. The level of stress, in general, diminishes as the

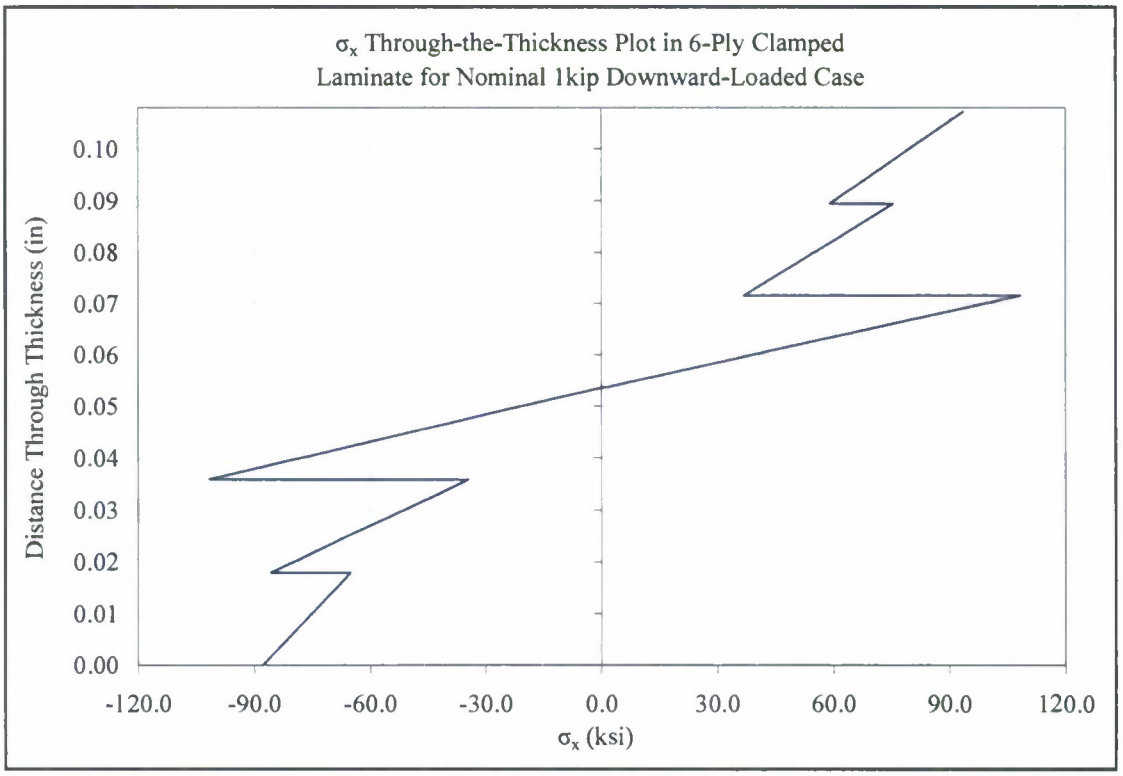

Figure 4.33 - Downward Loaded, Clamped 6-Ply σ_x Through-Thickness Plot

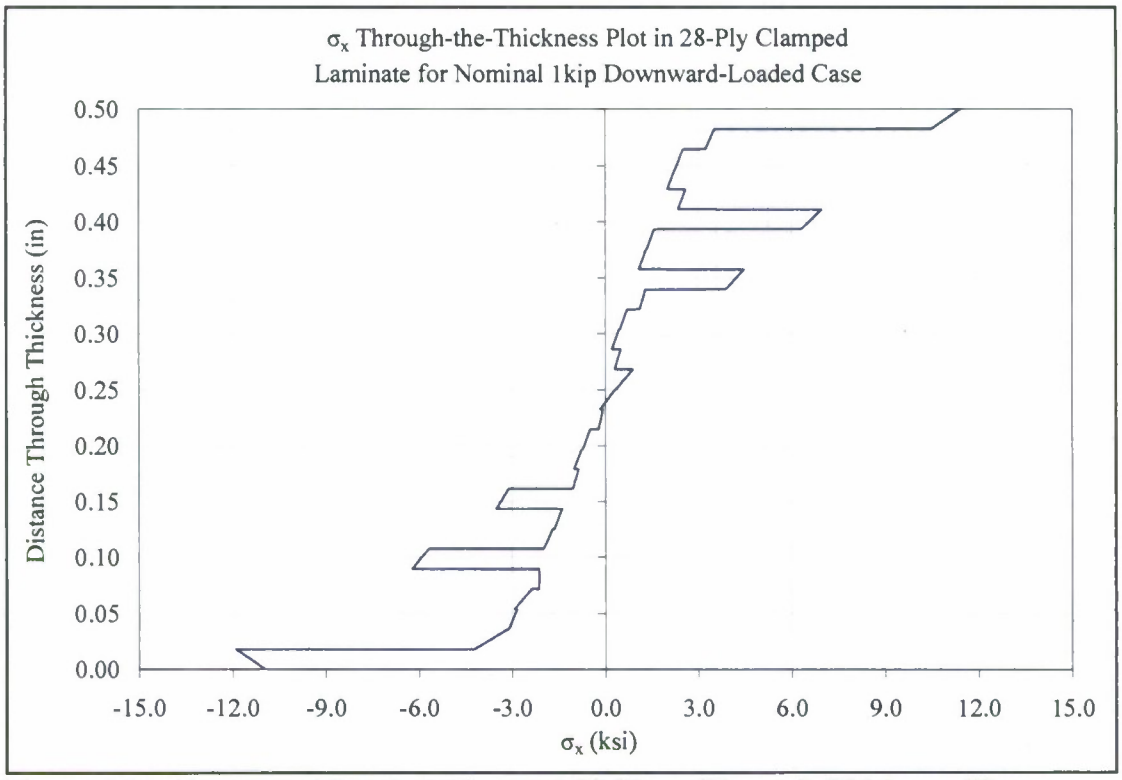

Figure 4.34 - Downward Loaded, Clamped 28-Ply σ_x Through-Thickness Plot

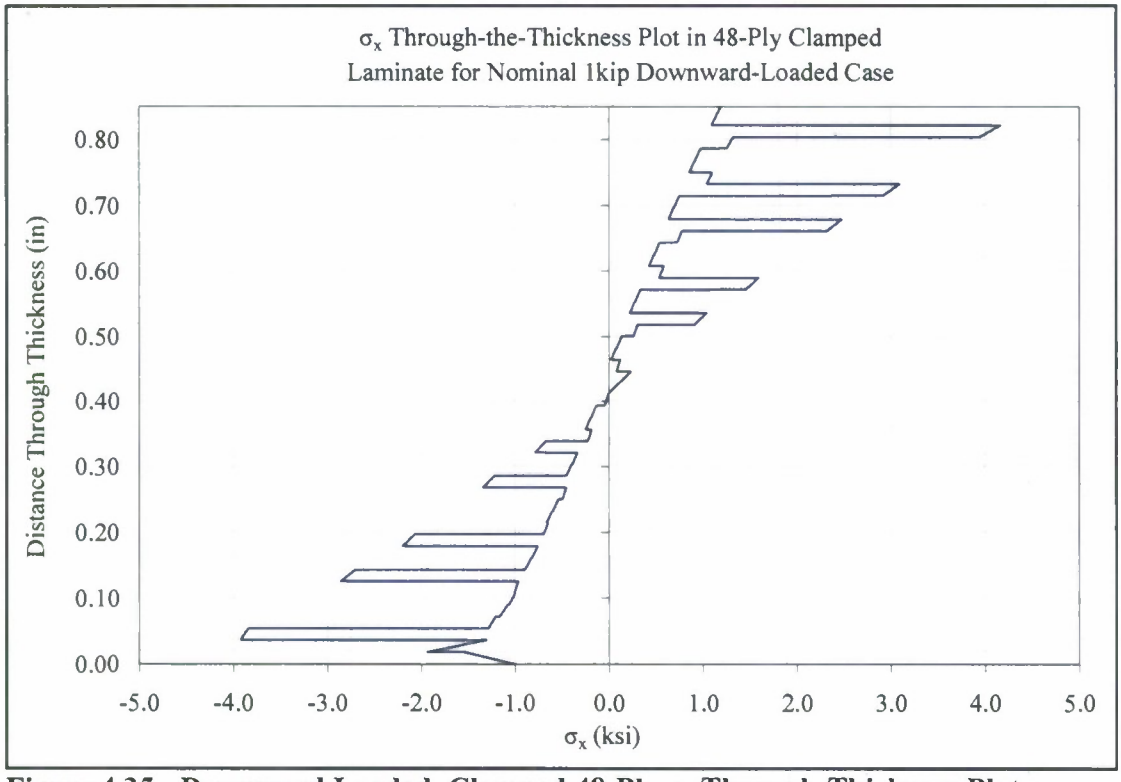

Figure 4.35 - Downward Loaded, Clamped 48-Ply σ_x Through-Thickness Plot

middle of the thickness is approached when looking at each layer separately in Figures 4.33-4.35. Yet in the 28-ply and 48-ply layups, the very bottom layer in each experiences the opposite effect.

Through-the-thickness ANSYS™ τ_{xy} stress plots for the 6, 28, and 48-ply layups are provided in Figures 4.36-4.38 when under a nominal 1 kip downward load. The 6-ply laminate in Figure 4.36 demonstrates negative, growing τ_{xy} stress values as the middle of the thickness is approached from the outer layers; interestingly the 28-ply and 48-ply composites show mostly positive stress. The 28-ply plot in Figure 4.37 shows negative τ_{xy} stress values for the top half of the thickness, as with the bolted model, and positive for the bottom half. In the 28-ply and 48-ply instances the magnitude of τ_{xy} stress reaches a maximum at the 3rd and 2nd layer from the bottom, respectively.

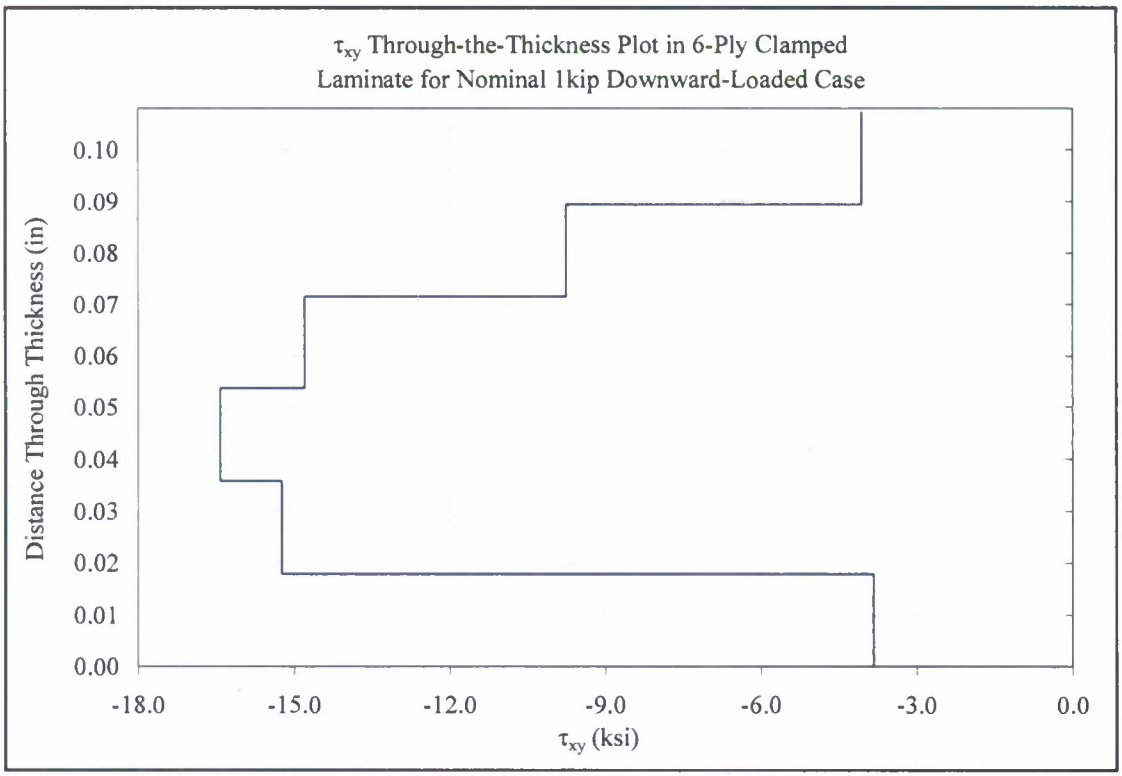

Figure 4.36 - Downward Loaded, Clamped 6-Ply τ_{xy} Through-Thickness Plot

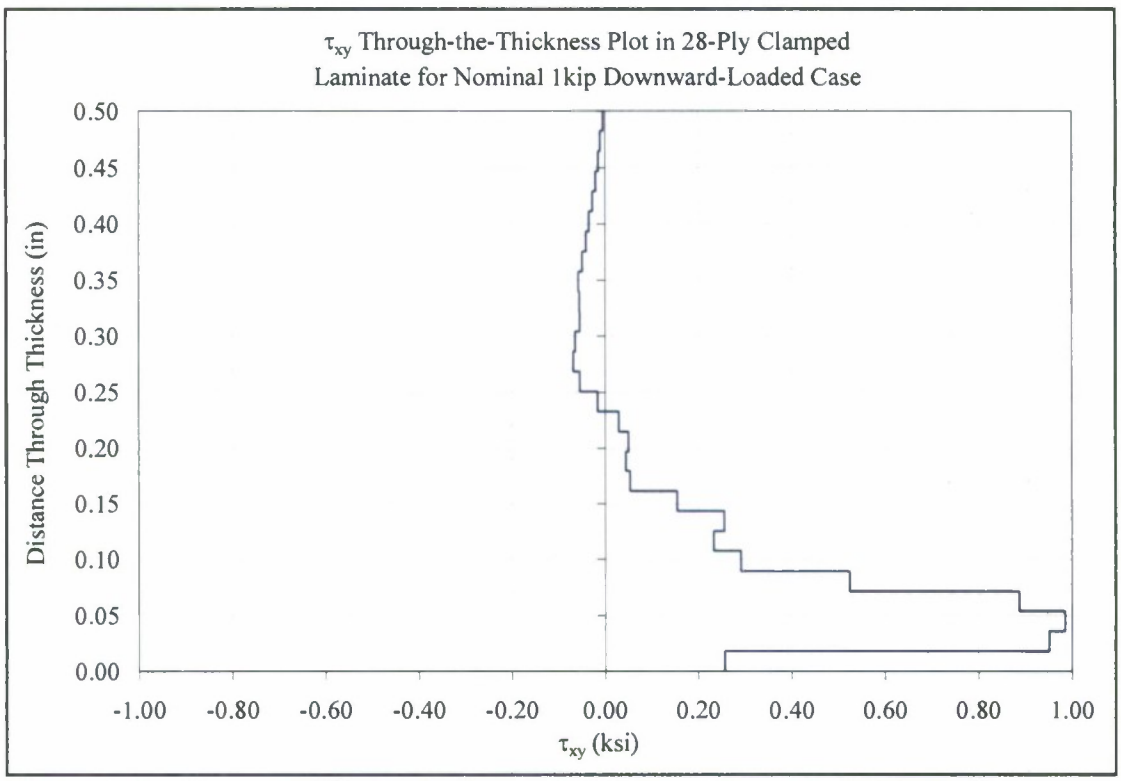

Figure 4.37 - Downward Loaded, Clamped 28-Ply τ_{xy} Through-Thickness Plot

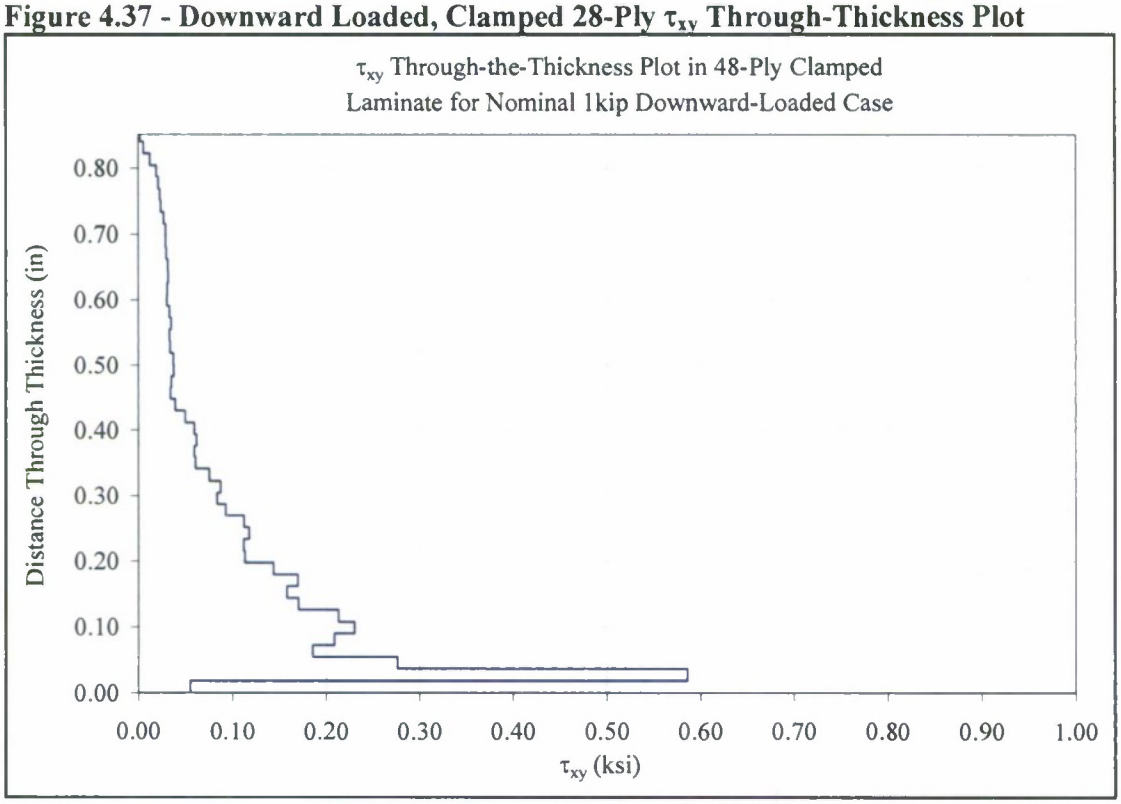

Figure 4.38 - Downward Loaded, Clamped 48-Ply τ_{xy} Through-Thickness Plot

ANSYS™ σ_x through-the-thickness plots in the 6, 28, and 48-ply thicknesses are shown for the case of nominal 1 kip upward load in Figures 4.39-4.41. In the 6-ply laminate, the value of σ_x reaches a maximum magnitude at about 108 ksi at the lower 0° layer. However in the same layup with the load being directed down, this occurs at the upper 0° ply, as is observed in Figure 4.33. This is true for the clamped configuration because upward and downward-bending stresses are much more alike than with the bolted case. In Figure 4.41, the very top layer in the 48-ply σ_x plot shows the same effect as was observed in the bottom layer for the downward-loaded model. The 28-ply instance in Figure 4.40, however, does not show this outcome, as is observed when the connection is loaded downward.

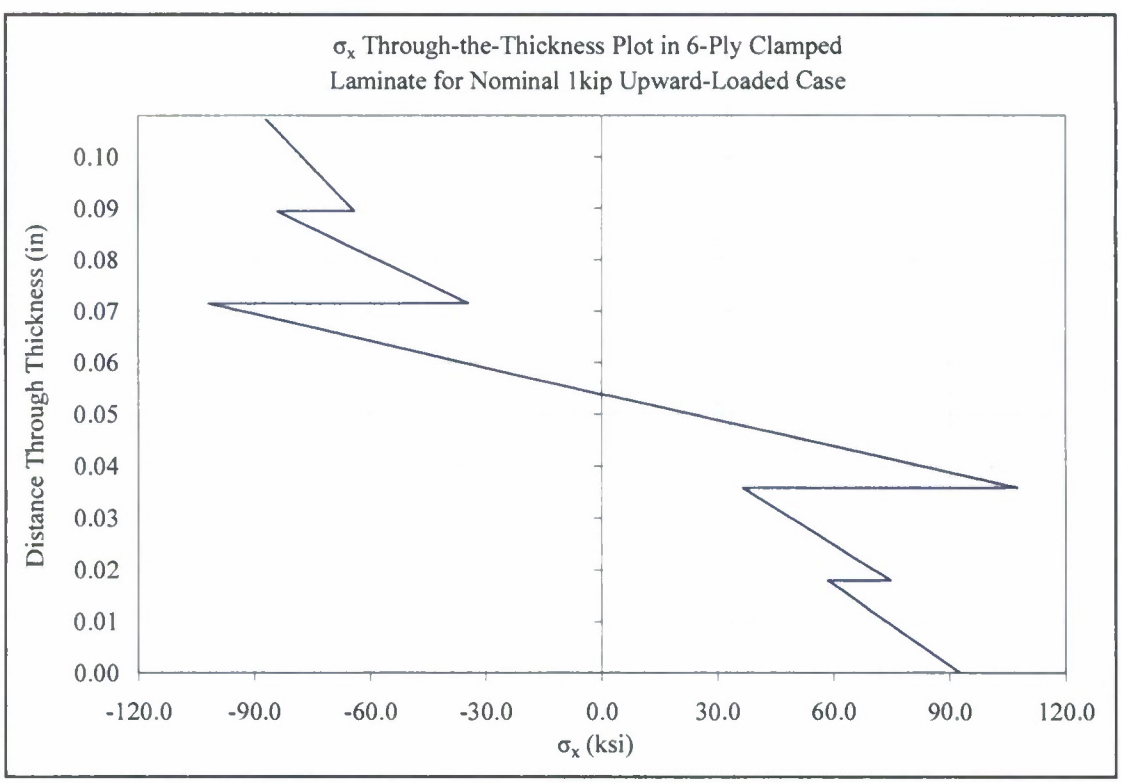

Figure 4.39 - Upward Loaded, Clamped 6-Ply σ_x Through-Thickness Plot

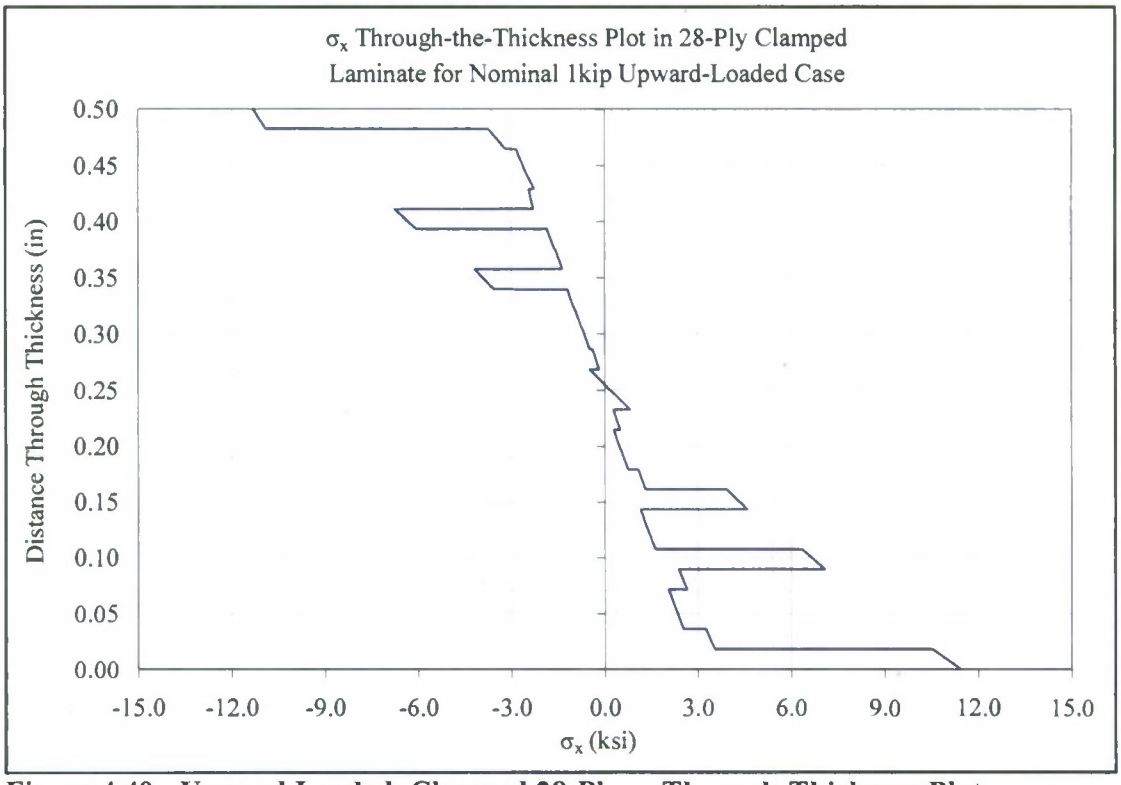

Figure 4.40 - Upward Loaded, Clamped 28-Ply σ_x Through-Thickness Plot

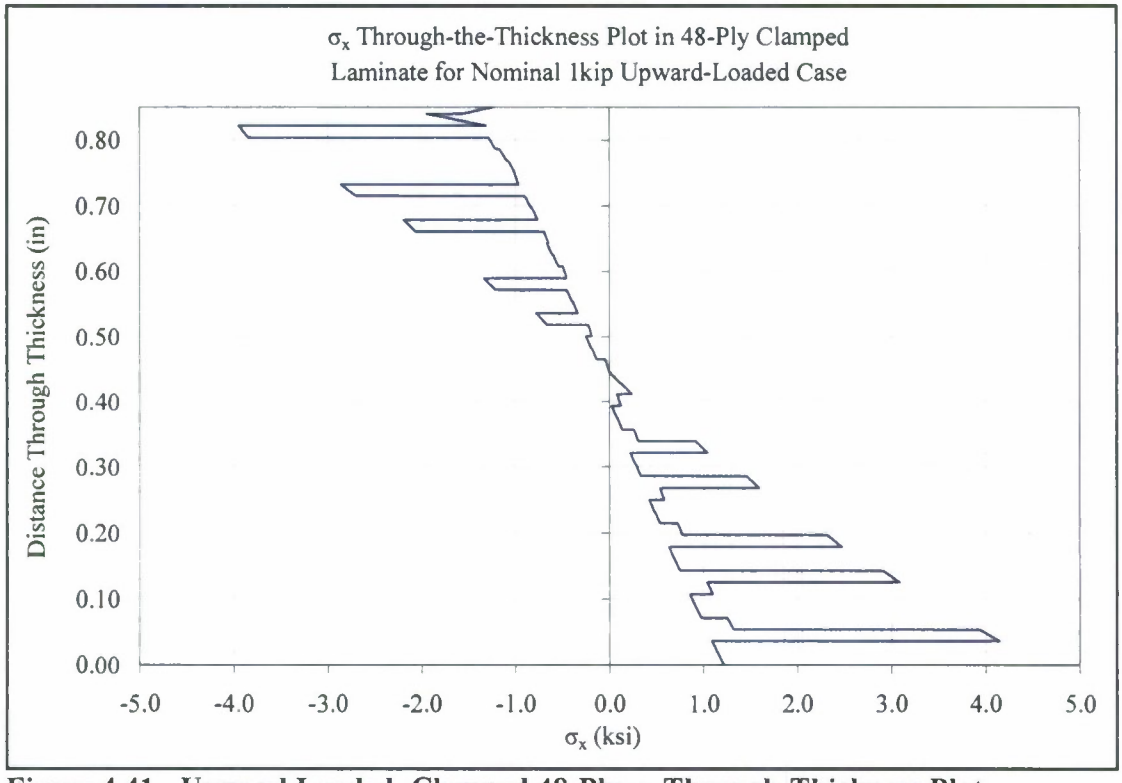

Figure 4.41 - Upward Loaded, Clamped 48-Ply σ_x Through-Thickness Plot

Through-the-thickness ANSYS™ τ_{xy} stress plots for the 6, 28, and 48-ply layups are provided in Figures 4.42-4.44 when under a nominal 1 kip upward load. The τ_{xy} stress values in the 6-ply case of upward load mimics that of load directed down, only they are opposite in sign. The 6-ply composite τ_{xy} stress plot displays positive values while the other two layups plots are comprised of negative stresses, as was observed in the instance of downward flexure in reverse fashion. The shear stress in the 28-ply case, provided in Figure 4.43, shows the same pattern as in downward load but only half the maximum magnitude; this occurs at the -45° layer, as also happens with the 48-ply laminate in Figure 4.44.

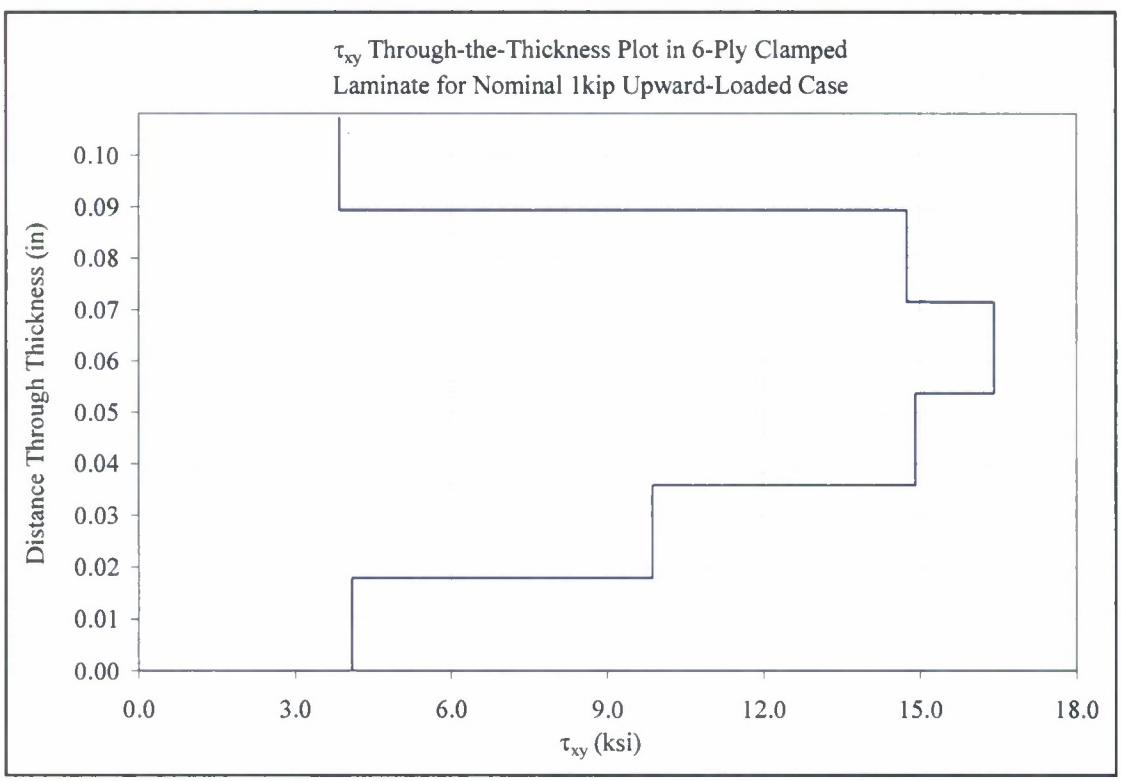

Figure 4.42 - Downward Loaded, Clamped 6-Ply τ_{xy} Through-Thickness Plot

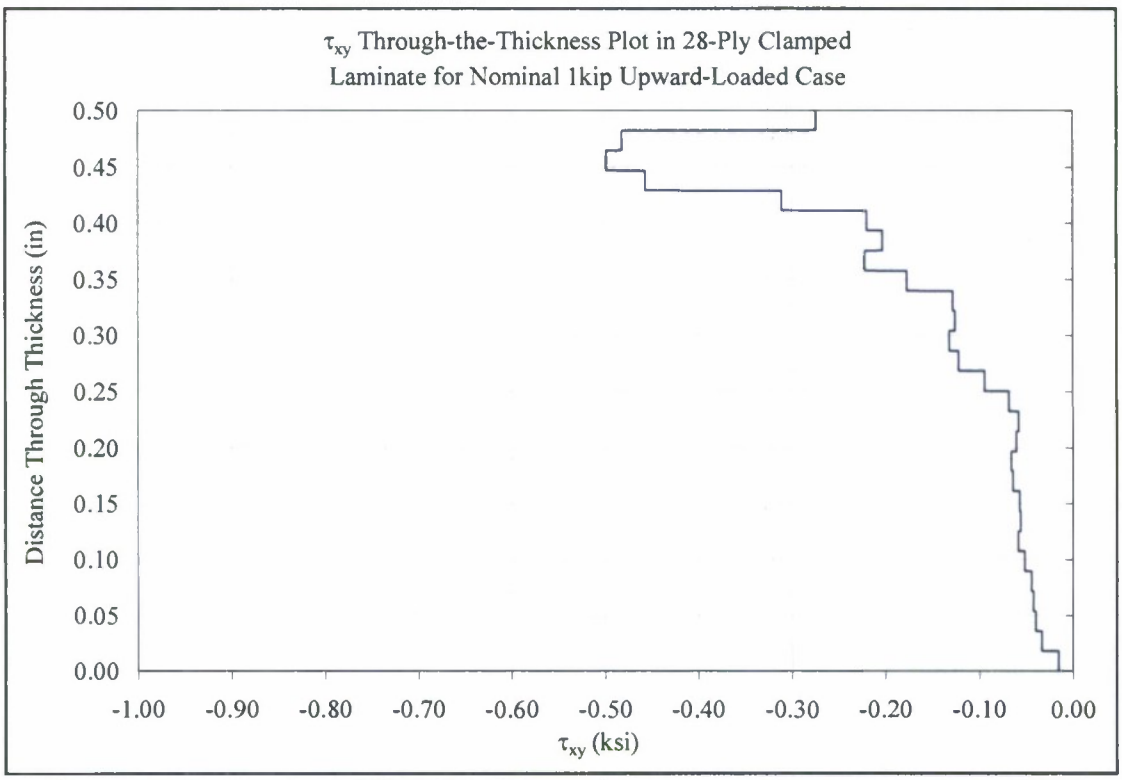

Figure 4.43 - Downward Loaded, Clamped 28-Ply τ_{xy} Through-Thickness Plot

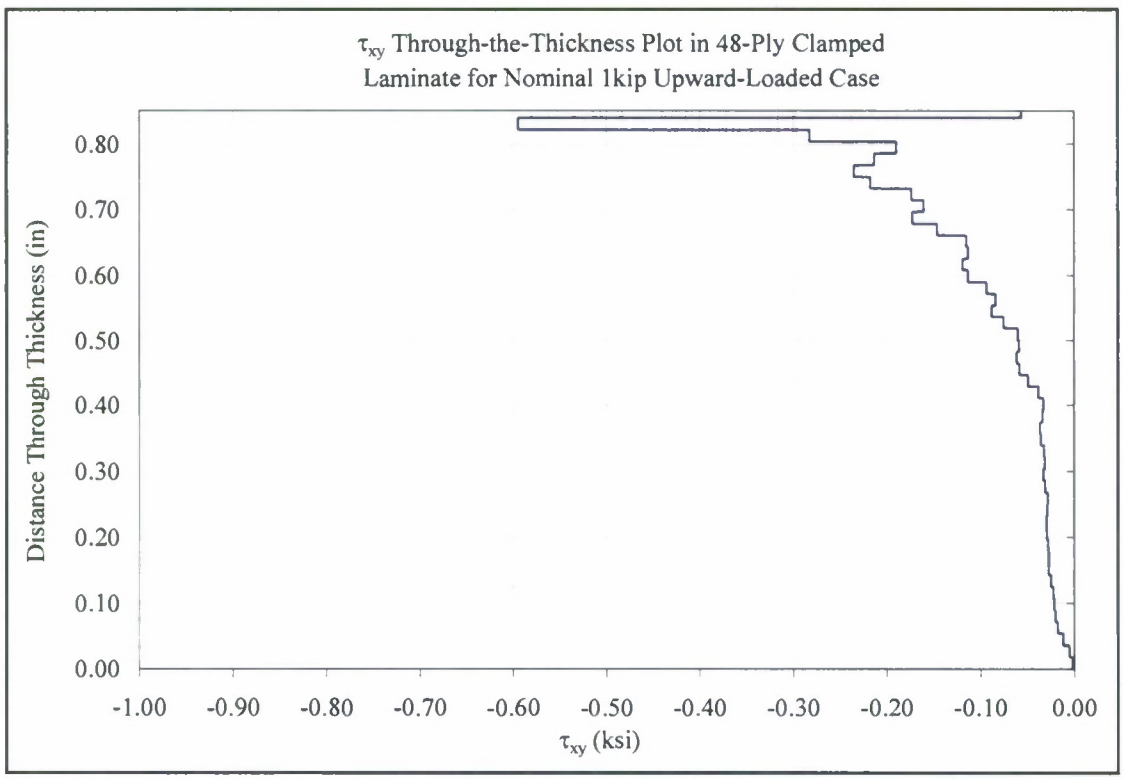

Figure 4.44 - Downward Loaded, Clamped 48-Ply τ_{xy} Through-Thickness Plot

4.2 Shell Analysis

This subsection will discuss the outcome of shell model results for the hybrid bolted configuration when loaded downward. The shell analysis has no direction dependencies so the downward case was used in the comparison. The shell model was constructed using orthotropic-composite and isotropic-metal shell elements to model the hybrid connection. The experimental and shell-analysis downward-deflection values are given in Table 4.13; both result sets are in good agreement, as is shown in Figure 4.45. The main purpose for a model of this form would be to implement it in a large global model of a ship structure. This analysis however is outside the scope of this project, and was already covered to a large degree by Kabche et al. (2006) and by Corriveau et al. (2008).

Table 4.13 – Shell Model and Experimental Bolted Downward-Flexure Deflections

Laminate Details		Downward Loaded	
Thickness (in)	# Plies	ANSYS Deflection (in)	Experimental Deflection (in)
0.1072	6	31.89313	-
0.25	14	1.92214	-
0.3572	20	0.78392	-
0.5001	28	0.345986	0.3736
0.6072	34	0.251091	-
0.7501	42	0.182319	0.23088
0.8573	48	0.1538692	0.1896
1.0002	56	0.12916	-

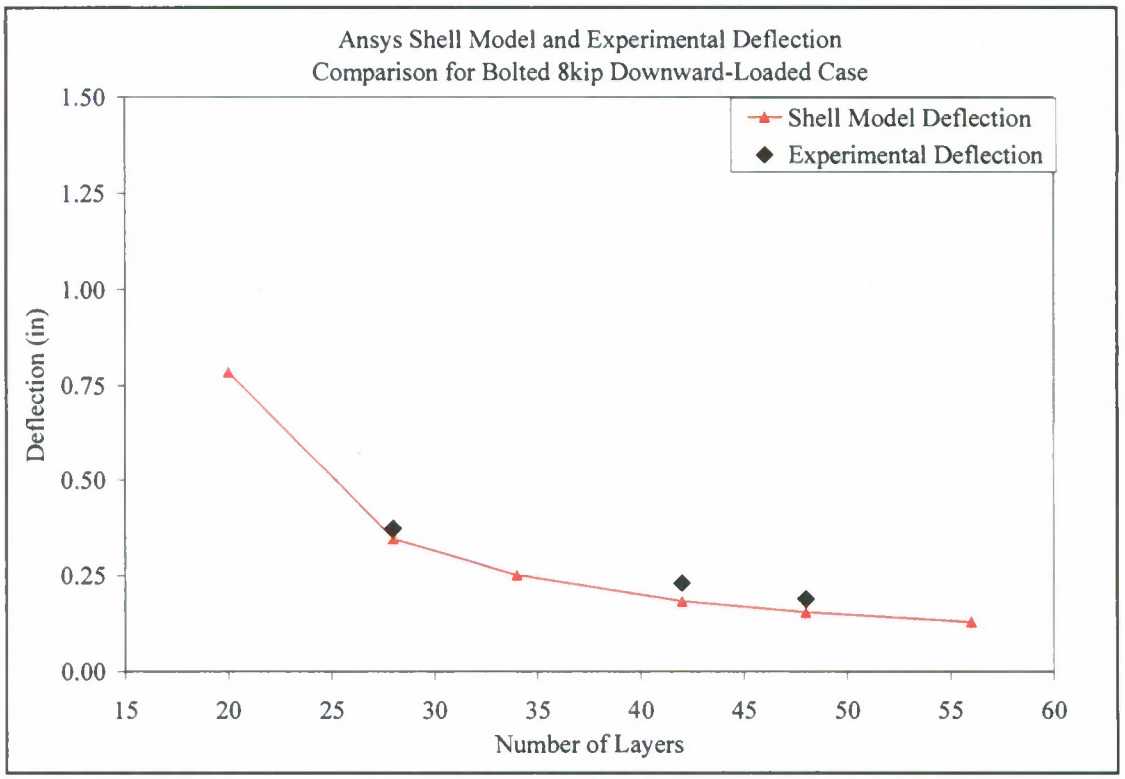

Figure 4.45 – Shell Model and Experimental Bolted Downward-Flexure Deflections

5. DISCUSSION, SUMMARY, & CONCLUSIONS

This section will discusses the fatigue test results analyzed using several different methods for computing stress levels. Methods include a simplified approach based upon isotropic mechanics theory to compute normal stress and shear stress as well as using results of 2-D plane strain finite element analysis to compute the stresses. This expression governing the fatigue response is taken in the form

$$N = A \cdot S^{-m} \qquad \text{(Eq. 5.1)}$$

where N is the number of cycles, S is the stress level at the location where failure occurs in the material, and m and A are obtained through statistical analysis. The following linear relation is obtained on a log-log scale by taking the logarithm of Equation 5.1:

$$\log(N) = -m\log(S) + \log(A) \qquad \text{(Eq. 5.2)}$$

Fatigue curves are dependent upon the experimental results and the method chosen for determination of the stress level, which inherently include the effects of stress concentrations and the composite material degradation response. The first method presented uses as simplified expression for the isotropic response of a bending beam to compute the peak stress at the outer fiber. The critical section is taken at the bolt line and the net section is used. The results of this computation are shown in Figure 5.1. The 42-ply curves are generated from data gathered by Corriveau et al. (2008). The current 28-ply tests results and the bolted/bonded tests are shown. Figure 5.2 uses the peak axial stress computed in ANSYS™ as the stress level. The stresses in Table 4.8 and 4.12 are scaled to the appropriate load level and plotted versus the number of cycles to failure on a log-log graph. In Figures 5.1 and 5.2 the plots are similar in appearance with the stress levels in Figure 5.2, computed by ANSYS™, but shifted higher. The 42-ply curves are below, and almost parallel to, the 28-ply layup data. Trendlines for each set of data are plotted on Figure 5.1 and shows that there is a thickness effect on fatigue life of the hybrid joint when the normal stress is used as the fatigue life predictor.

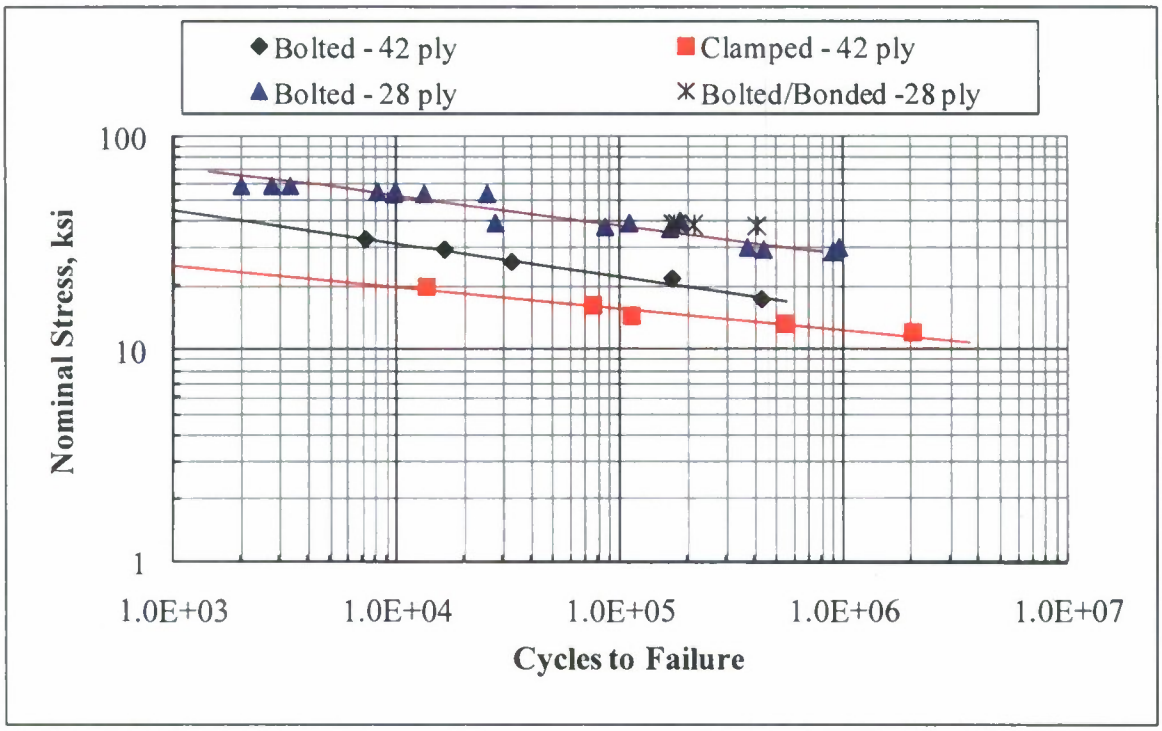

Figure 5.1 – Fatigue Data Plotted Using the Net Section Method and Simple Isotropic Stress Formula.

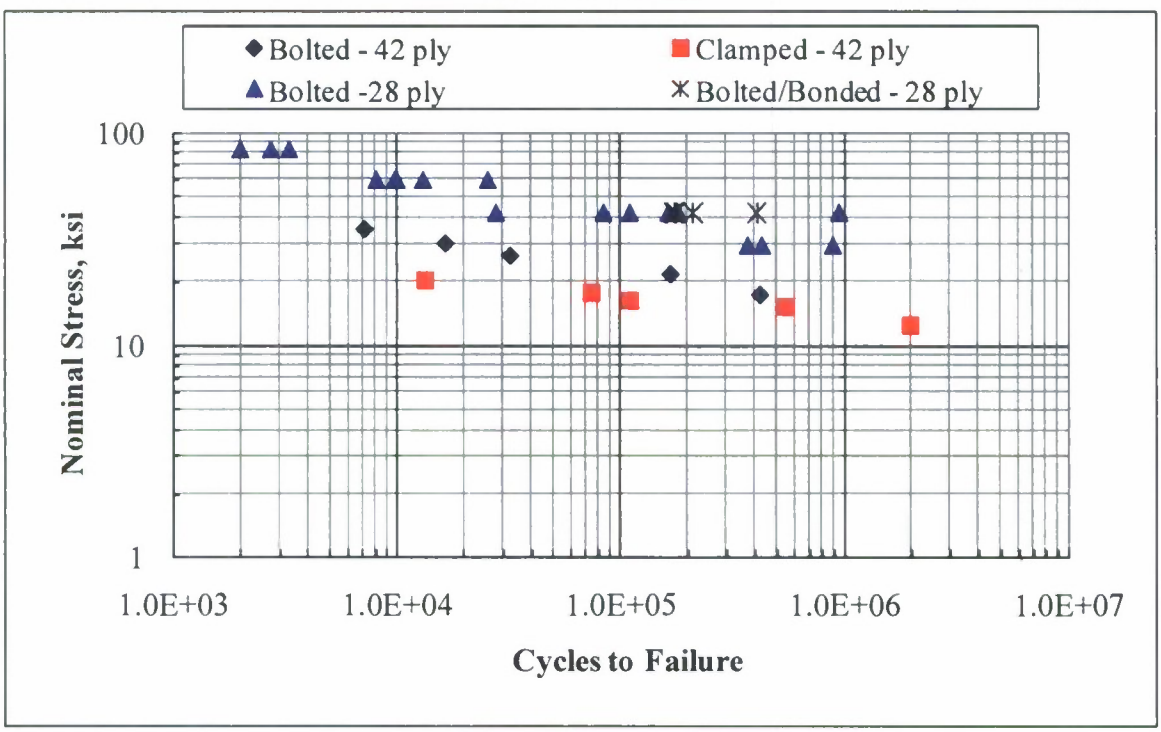

Figure 5.2 - Fatigue Data Plotted Using the ANSYS™ Computed Maximum Normal Stress.

Table 5.1 presents the fatigue constants for the straight line fit of the data as presented in Figure 5.1. The 28 ply adhesively bonded/bolted specimens were tested only at the +/-3.5 kip load level therefore fatigue constants are not computed for this data. In comparison, the geometric mean of the number of cycles to failure was found to be 140,400 cycles for the 28 ply bolted only specimens compared to 229,100 for the 28 ply bonded/bolted version at a +/- 3.5 kip fatigue load level. This demonstrates a measurable increase in fatigue life due to the bonding.

Table 5.1 – Fatigue Constants for Curve Presented in Figure 5.1

Case	m	Log(A)
Bolted 42 ply	6.37	13.58
Clamped 42 ply	9.85	16.82
Bolted 28 ply	7.19	16.42

Similar to uses of an approximate isotropic formula for computation of the normal stress, the shear stress can be used as a fatigue life predictor by using the simple formula for a rectangular isotropic beam where:

$$\tau_{max} = 1.5\frac{V}{A} \qquad \text{(Eq. 5.3)}$$

Where V is the shear force at the critical location and A is the actual area of the specimen. Figure 5.3 presents the result of using this formula as a stress predictor. In this case the results are bunched around a single straight line for the bolted specimens. Table 5.2 provides the fatigue life constants for the straight lines plotted in Figure 5.3 where the non bonded bolted joints are grouped together. In Figure 5.4, the maximum shear stress computed using the finite element analysis is used scaled from Tables 4.8 and 4.12. It is noted that the stress quantified in these tables is the average shear stress in the critical layer. Furthermore, the finite element model uses the nominal thickness, which does not include the thickness variation that occurred in specimen fabrication. Utilizing

the through the thickness shear stress as a failure indicator of the fatigue life of this connection may result in little or no thickness dependence. Further study using more representative composite models is recommended.

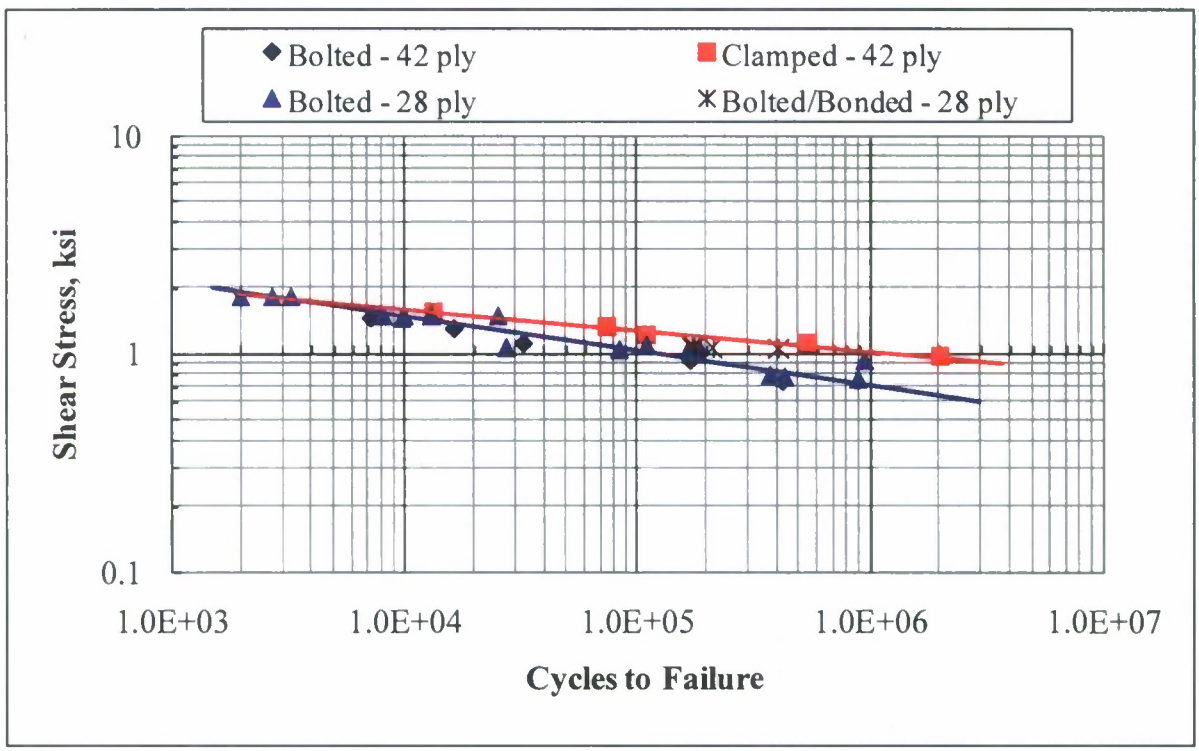

Figure 5.3 – Isotropic Peak τ_{xy} Values Used for Fatigue Data Prediction Curves

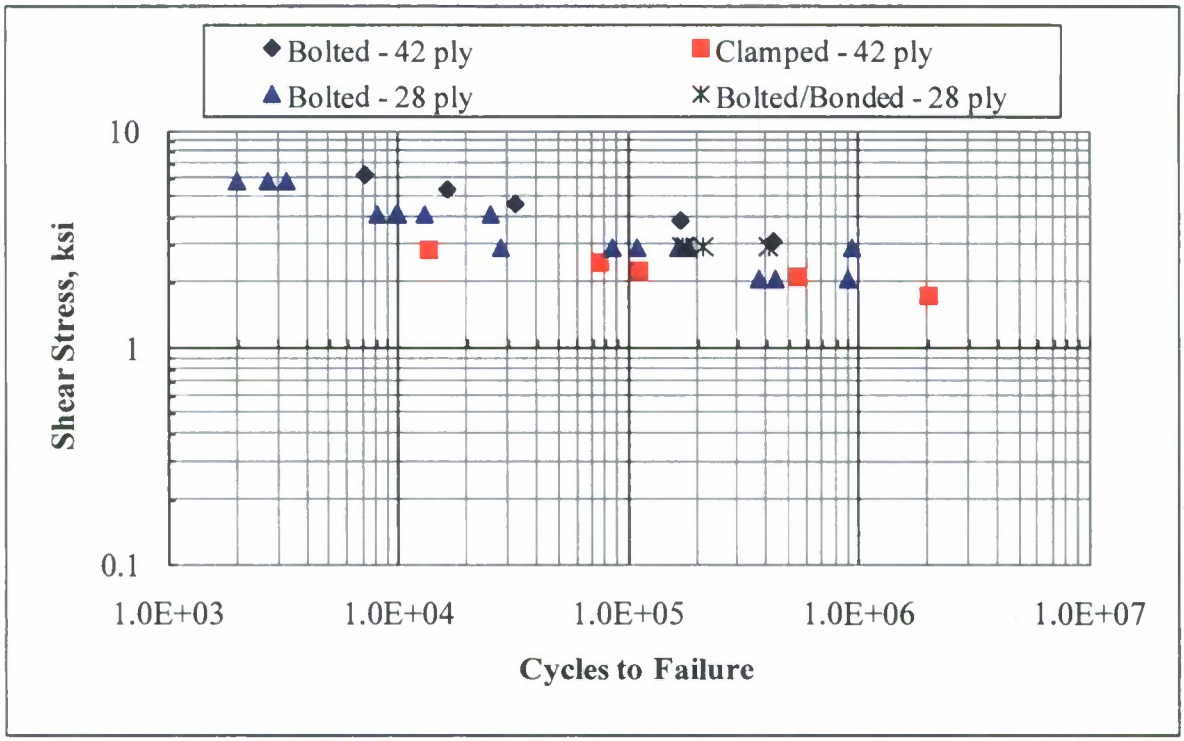

Figure 5.4 – Fatigue Data Plotted Using the ANSYS™ Computed Maximum Transverse Shear Stress, τ_{xy}

Table 5.2 – Fatigue Constants for Curve Presented in Figure 5.3

Case	m	Log(A)
42 and 28 ply Bolted Specimens	6.28	5.07
Clamped 42 ply	10.50	6.08

A clear mesh dependency is observed in the finite element analysis plane-strain procedure used, and making fatigue predictions by utilizing the actual magnitudes of stress which result from the model must be done with some consistent guidelines for handling the hot spot stress. Typical methods used for metal structures include use of the nominal stress method where stresses away from the hot spot are used as the predictor and different fatigue curves are given for different conditions and details. Hot spot methods can also be used where application of guidelines for mesh sizing, using stress away from the hot spot to predict values at the hot spot, and modeling the stress singularity location with a small radius eliminating the singularity are required. It is recommended that a hot-spot stress study be executed for the plain strain model, since stress singularities are present, as was visible in the plane-strain mesh study performed. If a predictive curve is going to be made with the procedure used in this document, it is crucial that the same mesh be used for all cases; otherwise the user runs the risk of miscalculating fatigue life substantially.

5.1 Summary

E-glass/epoxy vinyl ester laminate test articles of 28-ply and 48-ply thicknesses were fabricated for this work. In addition to work done by Corriveau et al. (2008), testing on 28-ply test articles was performed at various load amplitudes. One fatigue test was run with the 48-ply specimen at 6 kips, which failed in the steel tee at 195,000 cycles, and it was decided that this composite thickness was not a good match for the steel tee thickness in the connection, as the focus of this study was to investigate the fatigue response of the composite and not the steel part.

Finite element models were created using plane strain, shell, and 3-D modeling techniques. The shell method used a hybrid section to model the connection as previously developed by Kabche et al. (2006). The shell analysis does not capture joint details; however it works well for global analyses of large structures and in nominal stress approaches to fatigue. Several attempts were made at creating an accurate 3-D model of the joint. The higher level of difficulty involved in modeling and evaluating connection details in a solid analysis is evident. In lieu of the resource consuming 3-D analysis a 2-D approach was used for studying the effects of the connection geometry. Many of the connection details were captured in the 2-D plane strain model and contact elements were utilized for material interfaces. Composite layer interactions were captured by modeling each as a separate area, defining each ply orientation with the corresponding material properties. Using symmetry, the plane strain model was simplified by using known boundary conditions at the middle of the hybrid joint. Bolt clamp-up load, bolt stiffness, mesh size, and laminate thickness were varied and evaluated to determine their influence on response and stress of the connection in the plane strain analysis. A 2-D finite element analysis can be used to capture the important details of the connection response.

The analysis showed that bolt clamp-up load has a minor influence on response, but could contribute to error in comparison to the clamped joint deflection. The bolt stiffness was varied and evaluated over one degree of magnitude, and over this range the response was largely affected. A thorough study of the lower end of the bolt stiffness would only be necessary if composite fasteners were used instead of steel. Laminate thickness variation was found to largely define the magnitude of response and stress experienced in the hybrid joint. When the laminate thickness is reduced to 6-plies, large deformations result and making the deflections invalid for the range of loads applied. Isotropic stress calculation methods do not capture composite material response, but these calculations can provide an indication of the stress level for a fatigue evaluation.

Experimental tests on the 28-ply bolted connection were carried out at various fully-reversed load levels from +/- 7k to +/- 2.5k. The tests performed on the 28-ply thickness failed predominately at the bolt line, except for one 3.5 kip test which failed at the gripper

likely due to being contaminated with oil towards the end of the test.

5.2 Conclusion

Determination of stress level for fatigue life prediction was the main focus of this work. A 2-D plane strain analysis with contact is a robust method for analyzing the hybrid joint in detail. Utilizing this approach simplified the analysis when the variance of model parameters was needed. Shear stress may be a valid indicator of fatigue life in this hybrid connection; however more experimental data at different thicknesses is needed to confirm this claim. There is a good comparison between experimental and model deformation in the linear range. Nonlinear material effects were not included in the analysis, except for those which showed from the contact elements in the model. Future work on this project should include more testing of the bolted connection at other thicknesses and shear to moment ratios, especially at levels toward the lower end of the loading range. The fabrication and testing of embedded joints could also contribute to widening the scope of this research. Using FEA, studying the influence of more variables in a plane strain analysis such as the number of bolt rows, bolt diameter, steel tee thickness and composite modulus would also be beneficial.

REFERENCES

1. Alm, F. (1983) "GRP versus steel in ship construction", Naval Forces; V4(5), pp 82-86

2. ASTM D6507 – 00 (2005) "Standard Practice for Fiber Reinforcement Orientation Codes for Composite Materials", ASTM International, 100 Barr Harbor Drive, PO Box C700, West Conshohocken, PA, 19428-2959.

3. Barsoum, R.G. S. (2003) "Ships: Navy experts explain the newest materials and structural technologies", AMPTIAC; pp. 7-3: 52-61.

4. Black, S. (2003) "Fighting ships augment combat readiness with advanced composites", High Performance Composites; pp. 30-33.

5. Caccese, V. (2004), "Structural Material Testing Plan for Fire Resistant Ship Structures", Univ. of Maine Department of Mechanical Engineering, Report No. C2004-008-RPT-001, pp. 21.

6. Caccese, V., Vel, S., Grenestedt, J., Blomquist, P. (2005) "Structural Response of Hybrid Ship Connections Subjected to Fatigue Loads", Office of Naval Research Proposal, 2005.

7. Corriveau, D., Caccese, V., Vel, S. (2008) "Experimental investigation into the fatigue life of hybrid joints under fully reversed flexure loading", Univ. of Maine Department of Mechanical Engineering, Report No. C-2004-015-RPT-01, 151 p.p. June, 2008.

8. Fricke, W. (2002) "Evaluation of hot spot stresses in complex welded structures", Proceedings of The IIW fatigue seminar, Commission XIII, International Institute of Welding, Tokyo.

9. Fricke, W., Kahl, A. (2005) "Comparison of different structural stress approaches for fatigue assessment of welded ship structures", Marine Structures; 18; 473-488

10. Gurney, T.R., (1976) "Fatigue design rules for welded steel joints", The Welding Institute Research Bulletin; pp. 115-124

11. Harik, V.M., Bogetti, T.A. (2003) "Low cycle fatigue of composite laminates: A damage-mode-sensitive model", Journal of Composite Materials; 37; 7; pp. 597-610

12. Hyer, M.W. "Stress analysis of fiber-reinforced composite materials", Boston, MA: The McGraw-Hill Companies Inc., 1998 pp. 348-419.

13. Kabche, J.P., Caccese, V., Berube, K.A. (2006) "Testing and analysis of hybrid composite/metal connections and hull section for the MACH project", Univ. of Maine

Department of Mechanical Engineering, Report No. UM-MACH-RPT-01-01, 348 p.p. April, 2006.

14. Kendrick, A. (2005) "Effect of fabrication tolerance on fatigue life of welded joints", Ship Structure Committee, SSC-436, NTIS, Springfield, VA 22161

15. Makinen, K., Hellbratt, S.E., Olsson, K.A. (1988) "The development of sandwich structures for naval vessels," Mechanics of Sandwich Structures, Kluwer Academic Publishers, Netherlands, pp. 13-28

16. Mansour, A., Wirsching, P., White, G., Ayyub, B. (1996) "Probability based ship design: Implementation of design guidelines", Ship Structure Committee, SSC-392, NTIS, Springfield, VA 22161

17. Munse, W.H., Wilbur, T., Tellalian, M., Nicoll, K., Wilson, K. (1983) "Fatigue characterization of fabricated ship details for design", Ship Structure Committee, SSC-318, NTIS, Springfield, VA 22161

18. Shi, G., Lam, K.Y., Tay, T.E. (1998) "On efficient finite element modeling of composite beams and plates using higher-order theories and an accurate composite beam element," Composite Structures, Elsevier Science Ltd., pp. 159-165

19. Van Paepegem, W., Degrieck, J. (2001) "Tensile and compressive damage coupling for fully reversed bending fatigue of fibre-reinforced composites", Fatigue and Fracture of Engineering Materials and Structures; 25; 547-561

20. Van Paepegem, W., Degrieck, J. (2001) "Fatigue degradation modeling of plain woven glass/epoxy laminates", Composites: Part A; 32; 1433-1441

21. Whitworth, H.A., (2000) "Evaluation of the residual strength degradation in composite laminates under fatigue loading", Composite Structures, Elsevier Science Ltd., pp. 261-264

APPENDICIES

Appendix A: Intermediate Cyclic Test Graphs

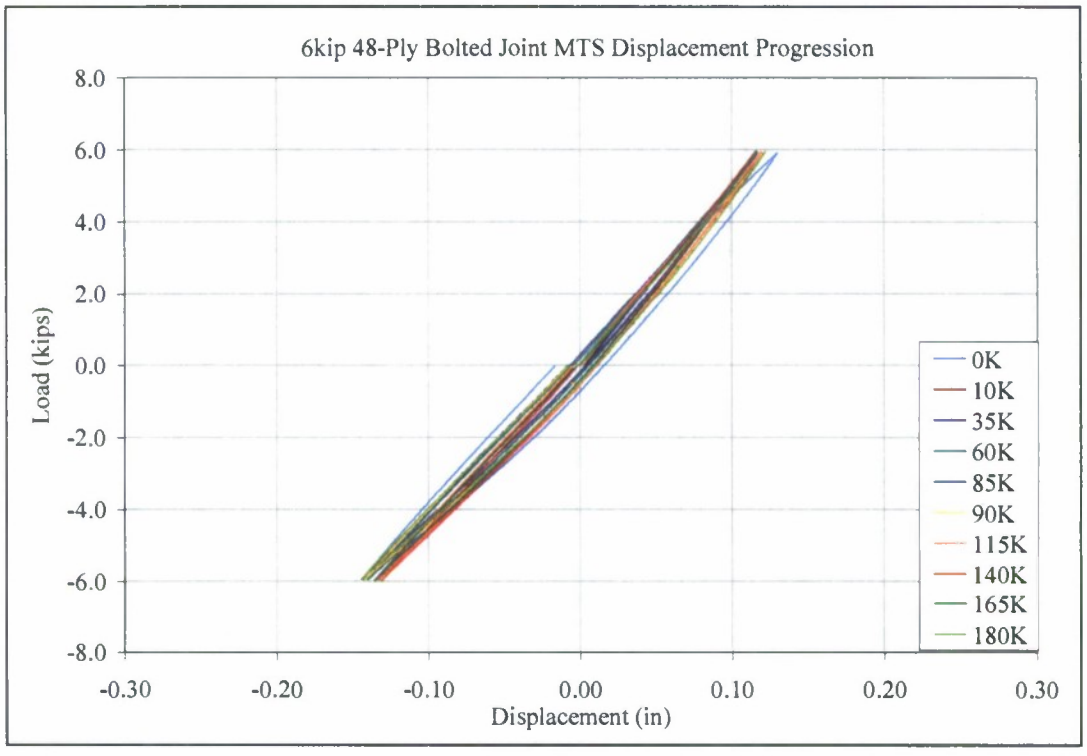

Figure A.1 - 6kip 48-Ply Bolted Cyclic Test MTS Displacement Progression

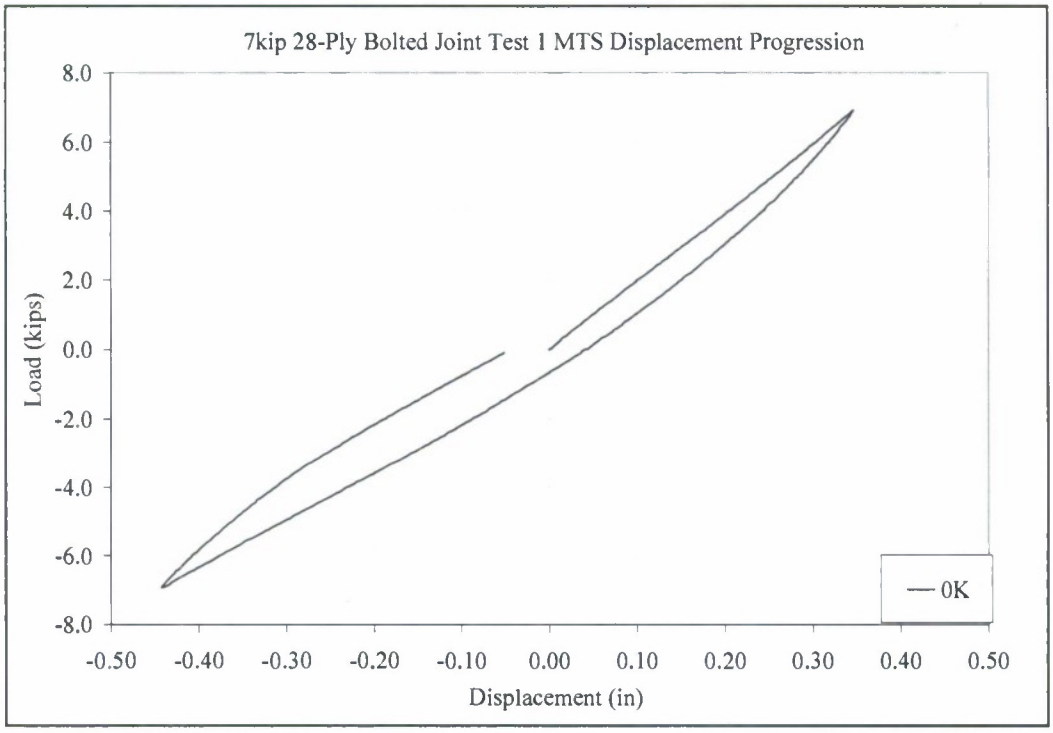

Figure A.2 - 7kip 28-Ply Bolted Cyclic Test 1 MTS Displacement Progression

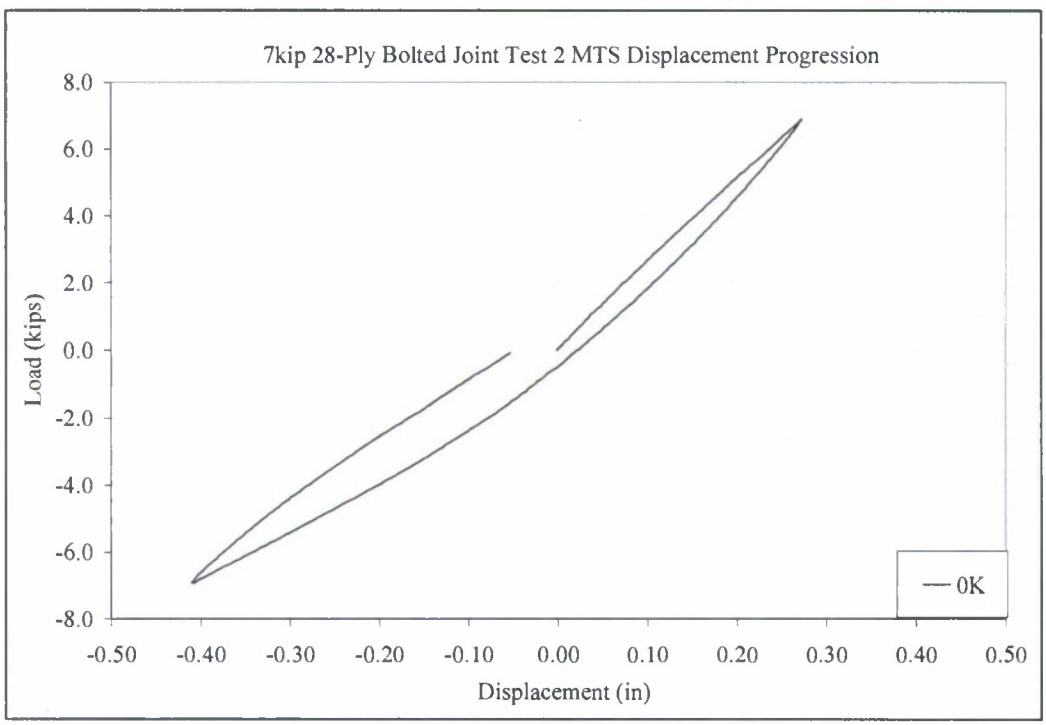

Figure A.3 - 7kip 28-Ply Bolted Cyclic Test 2 MTS Displacement Progression

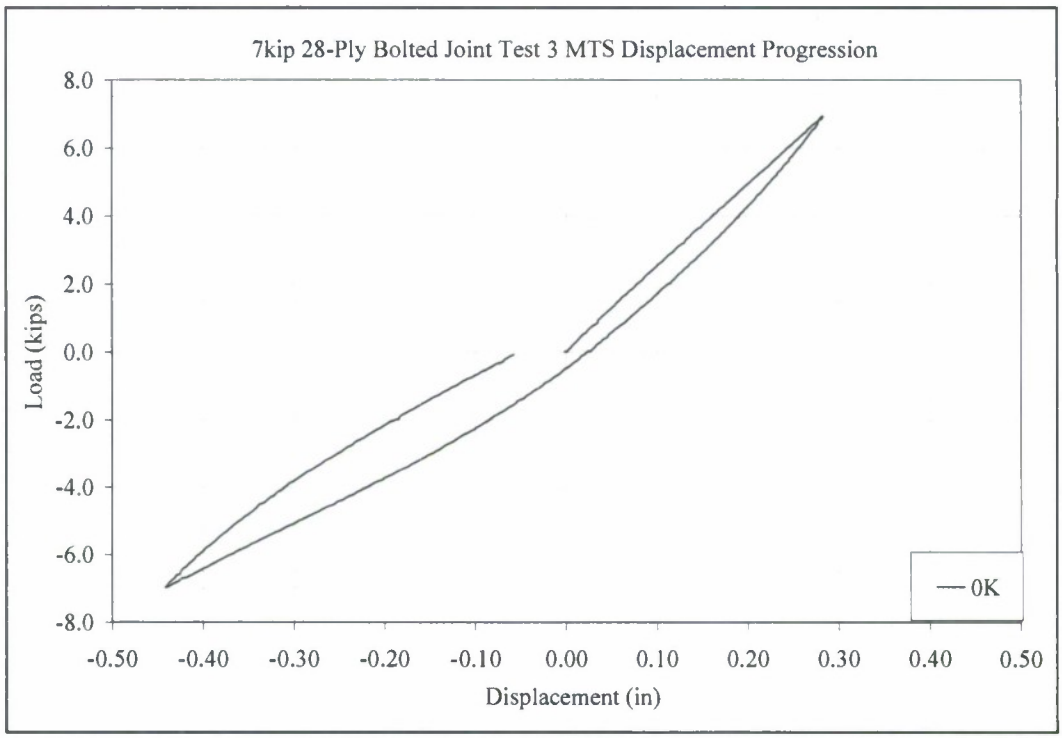

Figure A.4 - 7kip 28-Ply Bolted Cyclic Test 3 MTS Displacement Progression

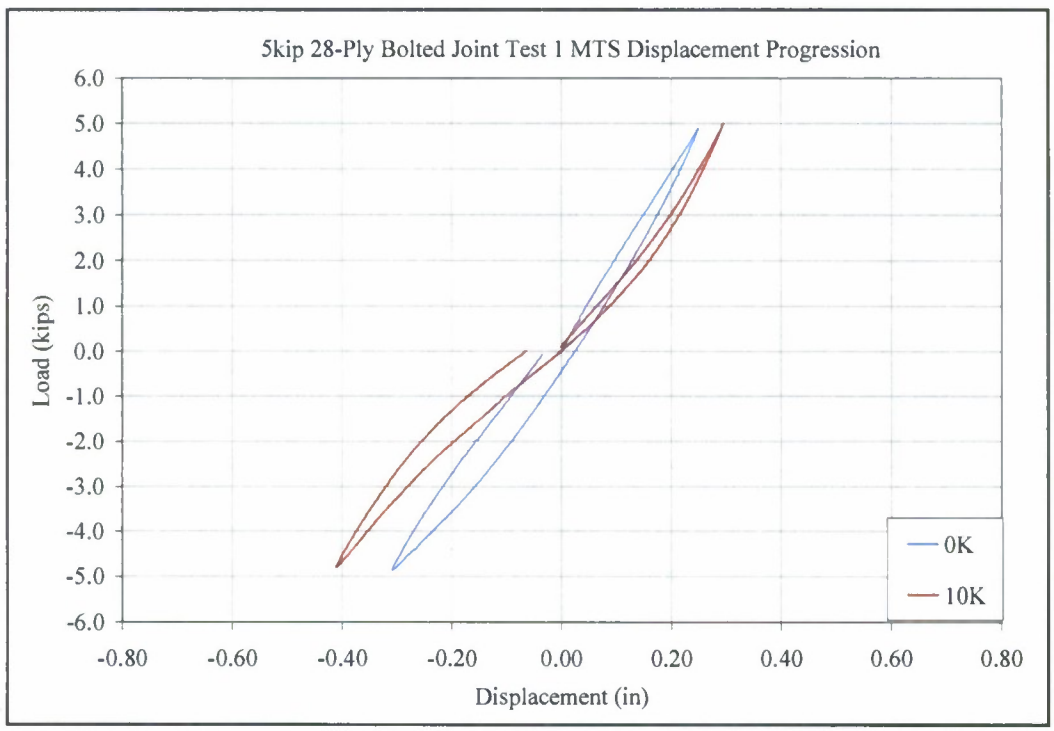

Figure A.5 - 5kip 28-Ply Bolted Cyclic Test 1 MTS Displacement Progression

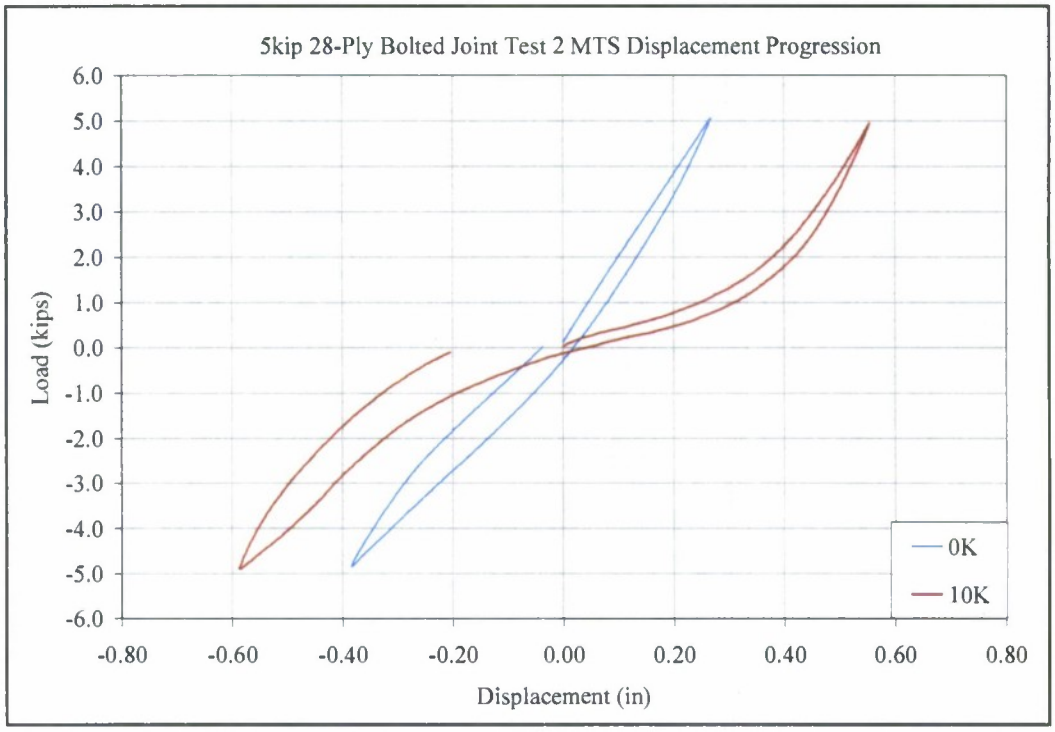

Figure A.6 - 5kip 28-Ply Bolted Cyclic Test 2 MTS Displacement Progression

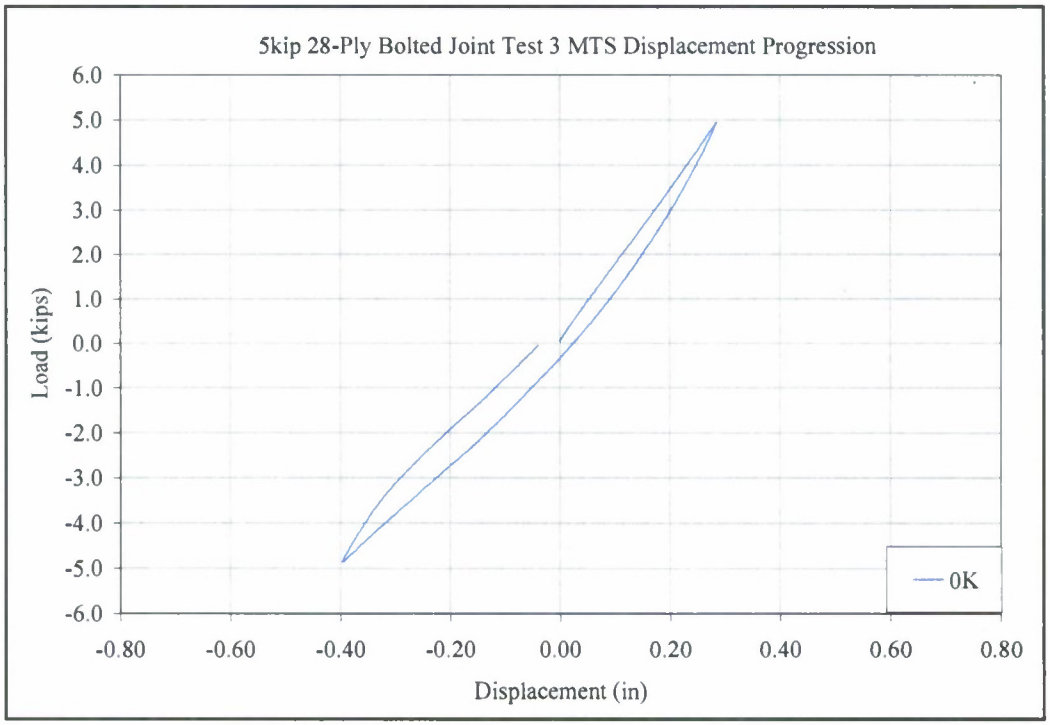

Figure A.7 - 5kip 28-Ply Bolted Cyclic Test 3 MTS Displacement Progression

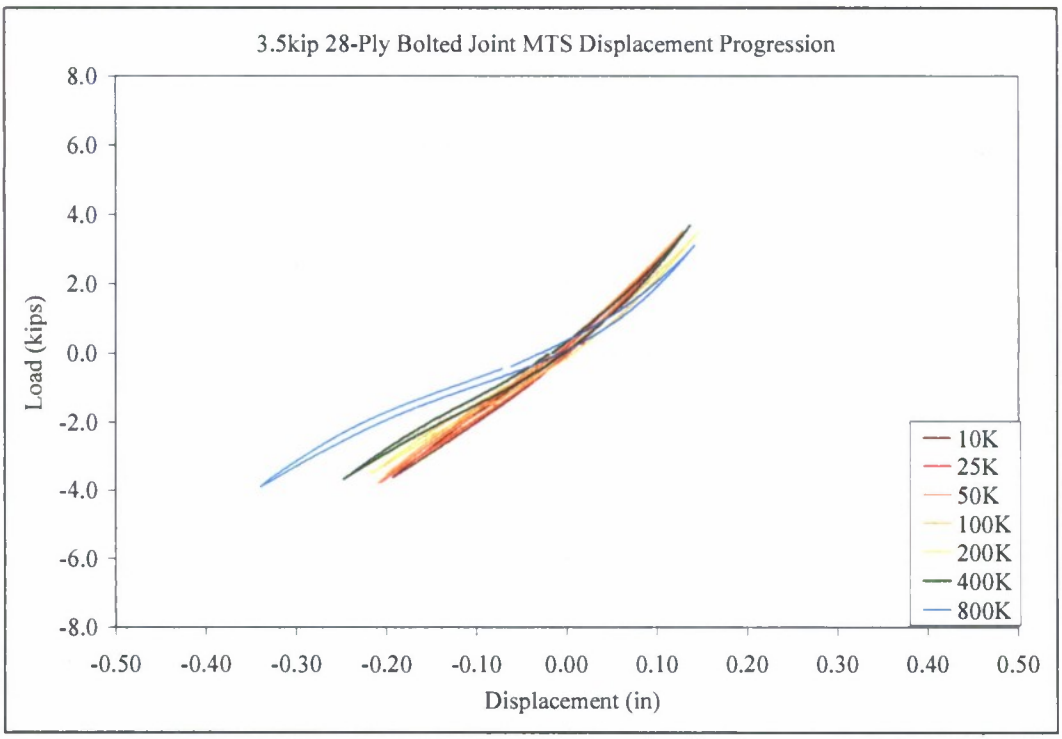

Figure A.8 – 3.5kip 28-Ply Bolted Cyclic Test MTS Displacement Progression

Appendix B: Composite Ply Orientations

Laminate Ply Orientations								
56-Ply Top	56-Ply Bottom	48-Ply	42-Ply	34-Ply	28-Ply	20-Ply	14-Ply	6-Ply
+45	90	+45						
-45	0	-45						
0	-45	0						
90	+45	90	+45					
-45	0	-45	-45					
+45	90	+45	0					
90	+45	90	90					
0	-45	0	-45	+45				
+45	90	+45	+45	-45				
-45	0	-45	90	0				
0	-45	0	0	90	0			
90	+45	90	+45	-45	90			
-45	0	-45	-45	+45	-45			
+45	90	+45	0	90	+45			
90	+45	90	90	0	90	+45		
0	-45	0	-45	+45	0	-45		
+45	90	+45	+45	-45	+45	0		
-45	0	-45	90	0	-45	90	-45	
0	-45	0	0	90	0	-45	0	
90	+45	90	+45	-45	90	+45	90	
-45	0	-45	-45	+45	-45	90	-45	
+45	90	+45	0	90	+45	0	+45	+45
90	+45	90	90	0	90	0	90	90
0	-45	0	90	90	0	90	0	0
+45	90	0	0	0	0	90	0	0
-45	0	90	90	0	90	0	90	90
0	-45	+45	0	90	+45	0	+45	+45
90	+45	-45	-45	+45	-45	90	-45	
		90	+45	-45	90	+45	90	
		0	0	90	0	-45	0	
		-45	90	0	-45	90	-45	
		+45	+45	-45	+45	0		
		0	-45	+45	0	-45		
		90	90	0	90	+45		
		+45	0	90	+45			
		-45	-45	+45	-45			
		90	+45	-45	90			
		0	0	90	0			
		-45	90	0				
		+45	+45	-45				
		0	-45	+45				
		90	90					
		+45	0					
		-45	-45					
		90	+45					
		0						
		-45						
		+45						

Appendix C: Clamped Case Solid Modeling Instructions

In order to reduce computation time for solving the model, it was decided that only a quarter of the actual fixture would be modeled, illustrated in Figure D.1 below, since there are two planes of symmetry in the model.

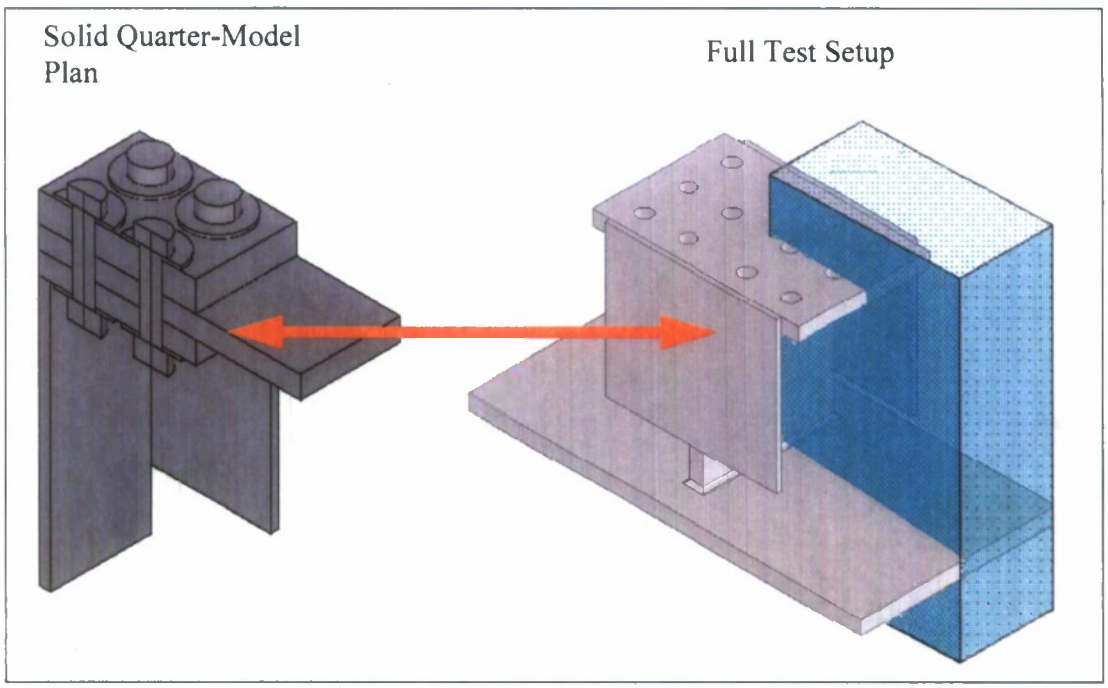

Figure C.1 – Solid Model Graphic

Step 1 –Choose a File Name and File Location:

a) Go to: **Utility Menu>File>Change Directory**. In the "*Browse for folder*" dialog box, choose a location for your file to be stored.

b) Go to: **File>Change Jobname.** In the "*Change Jobname*" dialog box, assign a file name for your model and check the "*New log and error file*" checkbox.

Step 2 –Choose Element Types:

It is necessary to define several elements for this analysis since we have a solid model with isotropic and orthotropic materials, bolts which need pretension elements, and

material interfaces that will need contact elements. All steel components were meshed using the SOLID92 element, shown below in Figure 3.27, which is a 3-D 10-noded structural solid and is well suited for irregular meshes. The composite plate was meshed using the 3-D 20-node SOLID186 brick element, shown in Figure 3.28, which can be defined as a solid or layered structure. To apply pretension in the bolts the PRETS179

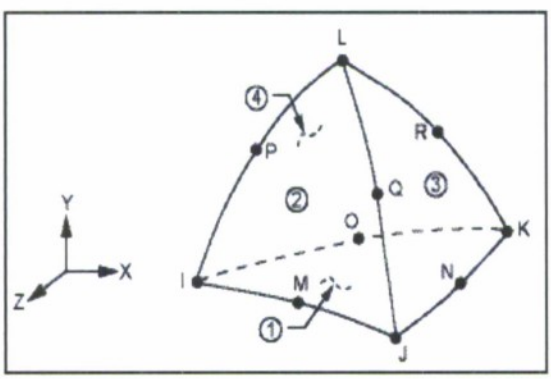

Figure C.2 –SOLID92 Element Geometry, ANSYS Inc. (2007)

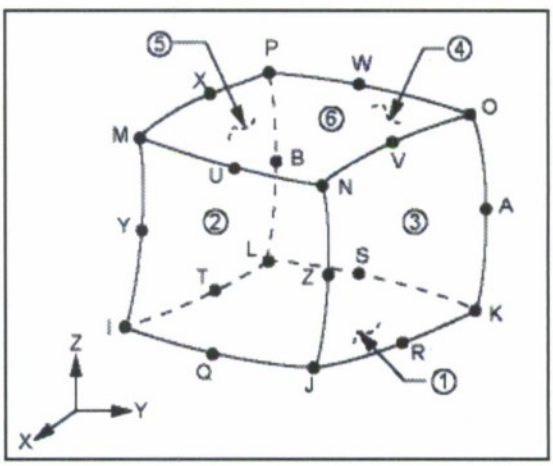

Figure C.3 –SOLID186 Element Geometry, ANSYS Inc. (2007)

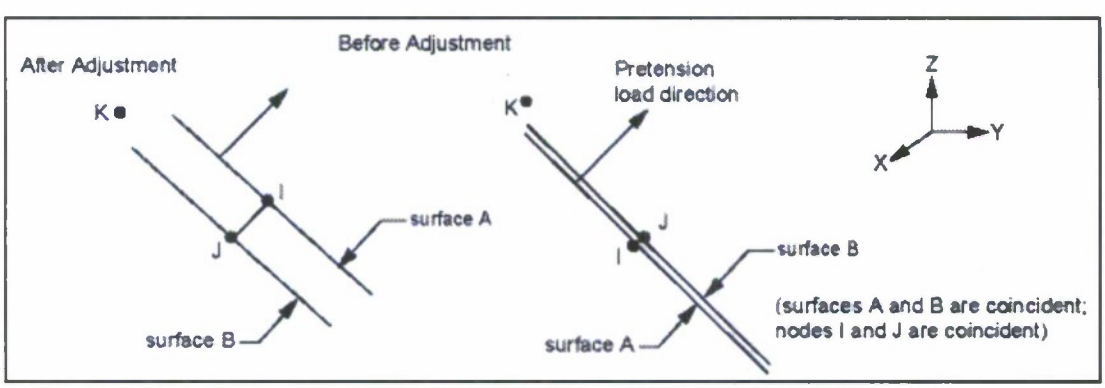

Figure C.4 –PRETS179 Element Geometry, ANSYS Inc. (2007)

element was used, shown in Figure 3.29, which has a single translation degree of freedom in a designated pretension direction and is inserted into an existing mesh. The contact between the composite plate and the steel components was modeled using CONTA174 and TARGE170 elements, and full descriptions of these can be found in the ANSYS

element library.

a) Using the same process for choosing elements as outlined in Step 2 of Section 3.1.1 in this paper, define SOLID92 and SOLID186 elements. The pretension and contact elements will be defined later on.

Step 3 – Assign Parameter Values:

a) Parameter values can be entered into ANSYS through the GUI by going to: **Utility> Menu>Parameters>Scalar Parameters**.

b) Define each of the parameter values as outlined in Table 3.1 below. To define a parameter value, for instance, enter "*stiffener x=4.375*" in the "*Scalar Parameters*" and click "*Accept*".

Step 4 – Assemble the Base Geometry:

What is designated to be the base assembly in this text is defined as three volumes in this model. These volumes are then added together using the **vadd** command.

a) Go to: Main Menu>Preprocessor>Modeling>Create>Volumes>Block>By 2 Corners & Z. This is the block command.

b) In the pop up window, enter the following for volume 1: "WP X "= 0, "WP Y" = 0, "Width" = midplate_x, "Height" = Half_Width_y, "Depth" = midplate_z.

c) For volumes 2 and 3, the working plane will be offset before each one is modeled so the local origin is at (x,y) = (0,0). Navigate to: **Utility Menu>WorkPlane>Offset WP to>XYZ Locations**.

d) In the dialog box enter the following offset values: "*0,0,midplate_z.*"

e) Generate volume 2 with the block command and enter: "WP X "= 0, "WP Y" = 0, "Width" = Ttop_x "Height" = Half_Width_y, "Depth" = Ttop_z

Table D.1 – Solid Model Parameters

Parameter Name	Value (inches	Description
stiffener_x	4.375	Stiffener plate width in x
stiffener_y	0.25	Stiffener plate thickness in y
stiffener_z	7.25	Stiffener plate hight in z
midplate_x	0.375	Midplate half thickness
midplate_z	9.0	Midplate hight in z
Half_Width_y	3.375	Halfwidth of fixture in y
Ttop_z	0.75	Top plate of T hight in z
Ttop_x	5.25	Top plate width in x
ClampPlate_z	1.0	Clamping plate hight in z
ClampPlate_x	5.25	Clamping plate width in x
Compo_x	8.25	Composite width in x
Compo_z	0.75	Composite hight in z
BoltDiam	0.75	Bolt shaft diameter
HeadDiam	1.125	Width across bolt head flats
Head_z	0.5	Basic head hight in z
NutDiam	1.125	Width across nut flats
Nut_z	0.641	Basic nut hight in z
Washer_OD	2.00	Washer Type A, Outer diameter
Washer_ID	0.812	Washer Type A, Inner basic diameter
Washer_z	0.134	Washer Type A, basic hight in z
ClearenceDiam	Washer_ID	Clearence holes through steel and composite

f) Repeat the working plane offset command with the following entry: "*0,Half_Width_y,-7*". The working plane is now located at the bottom corner of where volume 3 will be generated.

g) Generate volume 3 with the block command and enter: "WP X "= 0, "WP Y" = 0, "Width" = stiffener_x "Height" = stiffener_y, "Depth" = stiffener_z.

h) Now that volumes 1-3 have been generated, the working plane is returned to the

global origin via: **Utility Menu>WorkPlane>Offset WP to>global origin.**

i) The volumes comprising the base assembly have now been generated and can be added to a single volume. Go to: **GUI>Main Menu>Preprocessor>Modeling> Operate>Booleans>Add>Volumes**. Enter *all* in the dialog box. The base model, without bolt holes, has been created.

Step 5 –Create the Top Clamping Plate and Composite:

a) Generate what will be referred as volume 4, or the top clamping plate, by first offsetting the working plane, as was done before in step 4, by entering following coordinates: "*0,0,midplate_z+Ttop_z+ Compo_z* ".

b) Using the block command, enter the following for volume 4: "WP X " = 0, "WP Y" = 0, "Width" = ClampPlate_x, "Height" = Half_Width_y, "Depth" = ClampPlate_z.

c) Offset the working plane again, for the volume 5 (composite) generation, by entering: "*0,0,-Compo_z*".

d) Using the block command, create volume 5 by entering: "WP X "= 0, "WP Y" = 0, "Width" = Compo_x, "Height" = Half_Width_y, "Depth" = Compo_z.

e) In preparation for future steps the working plane is now realigned with the global coordinate system.

Step 6 –Create the Bolt Holes:

In order to generate the bolt holes, four cylindrical volumes have to be generated at the desired locations. Once these volumes are created they are subtracted from the base assembly, top clamping plate and composite. For each bolt hole the working plane will be offset such that it is located at the bottom of volume 2 in the z direction, as well as at the x and y locations of the bolt hole to be made. The following GUI command sequence will generate the four bolt holes H1 through H4:

a) Offset the working plane to: "*1.5,2.25,midplate_z*"

b) Go to: **Main Menu>Preprocessor>Modeling>Create> Volumes>Cylinder>Solid Cylinder.** In the dialog box enter *"WP X " = 0, "WP Y" = 0, "Radius" = ClearenceDiam/2, "Depth" = ClampPlate_z+2*Compo_z.*

c) Offset the working plane again with the coordinates: "*2.25,0,0*"

d) Generate the next cylindrical volume with the same entries as in b)

e) Offset the working plane by entering: "*0,-2.25,0*"

f) Generate the half cylinder volume by following: **Main Menu>Preprocessor> Modeling>Create>Volumes>Cylinder>Partial Cylinder.** In the dialog box enter *"WP X "= 0, "WP Y" = 0, "Rad-1" = 0, "Theta-1" =0, "Rad-2" = ClearenceDiam/2, "Theta-2" =180, "Depth" = ClampPlate_z+2*Compo_z.*

g) Offset the working plane by entering: "*-2.25,0,0*"

h) Repeat step f)

i) Now that the bolt hole volumes have been generated, they need to be subtracted from the model. Go to: **Main Menu>Preprocessor>Modeling>Operate>Booleans> Subtract>With Options> Volumes.**

j) Address the first pop up by selecting the volume that is being subtracted from, the base assembly volume, and click "*OK*". Address the second pop up by picking the volumes to be subtracted, the bolt hole volumes, and click "*OK*".

k) A new window will appear which has three drop down menus. Select the following:

Under "Intersect bndry will have", select "Shared entities"

Under "Base Volumes will be", select "Kept"

Under "Subtracted Volumes will be", select "Deleted"

l) In preparation for the following steps, return the working plane to the global origin.

Step 7 –Create the Bolt Head, Bolt Shaft, Nut, and Washer Volumes:

In this model the bolt head, shaft and the nut are three separate volumes that are glued together later on.

Bolt Shafts:

a) Offset the working plane to: "1.5,2.25,midplate_z-Washer_z"

b) Generate the first bolt shaft volume by following the path: **Main Menu> Preprocessor>Modeling>Create>Volumes>Cylinder>Solid Cylinder.** In the dialog box enter *"WP X "= 0, "WP Y"= 0, "Radius"= BoltDiam/2, "Depth"= 2*Washer_z+ 2*Compo_z+ ClampPlate_z.*

c) Offset the working plane by entering: "*2.25,0,0*", and repeat step b) for the second bolt shaft.

d) Offset the working plane by entering: "*0,-2.25,0*". Generate the third, half-cylinder bolt shaft volume by following: **Main Menu>Preprocessor>Modeling>Create> Volumes>Cylinder>Partial Cylinder.** In the dialog box enter: *"WP X " = 0, "WP Y" = 0, "Rad-1" = 0, "Theta-1" =0,"Rad-2" = BoltDiam/2, "Theta-2" =180, "Depth" = 2*Washer_z+2*Compo_z+ClampPlate_z.*

e) Offset the working plane by entering: "*-2.25,0,0*", and repeat step d) to create the fourth, half-cylinder bolt shaft volume.

Bolt Heads:

a) Offset the working plane by entering: "*0,0, 2*Washer_z+2*Compo_z+ClampPlate_z*"

b) Generate the first half-bolt head volume by following: **Main Menu>Preprocessor> Modeling>Create>Volumes>Cylinder>Partial Cylinder**. In the dialog box enter *"WP X " = 0, "WP Y" = 0, "Rad-1" = 0, "Theta-1" =0,"Rad-2" = HeadDiam/2, "Theta-2" =180, "Depth" = Head_z.*

c) Offset the working plane by entering: "*2.25,0,0*", and repeat step b) for the second

half-bolt head volume.

d) Offset the working plane by entering: "*0,2.25,0*". Generate the third-full cylindrical head volume by following: **Main Menu>Preprocessor>Modeling>Create>Volumes> Cylinder>Solid Cylinder.** In the dialog box enter *"WP X " = 0, "WP Y" = 0, "Radius" = HeadDiam/2, "Depth" = Head_z.*

j) Offset the working plane by entering: "*-2.25,0,0.*" Repeat step d) for the fourth-full cylindrical head volume. The washers on the top are created next.

Top Washers:

a) Offset the working plane by entering: "*0,0,- Washer_z*"

b) Generate the full washer volume by following **Main Menu>Preprocessor>Modeling>Create>Volumes>Cylinder>Solid Cylinder.** In the dialog box enter *"WP X " = 0, "WP Y" = 0, "Rad-1" = Washer_ID/2, "Theta-1" =0, "Rad-2" = Washer_OD/2, "Theta-2" =0, "Depth" = Washer_z.*

c) Offset the working plane by entering: "*2.25,0,0*"

d) Repeat step b)

e) Offset the working plane by entering: "*0,-2.25,0*"

f) Generate the half washer volume by following **Main Menu>Preprocessor> Modeling>Create>Volumes>Cylinder>Partial Cylinder.** In the dialog box enter *"WP X " = 0, "WP Y" = 0, "Rad-1" = Washer_ID/2, "Theta-1" =0, "Rad-2" = Washer_OD/2, "Theta-2" =180, "Depth" = Washer_z.*

g) Offset the working plane to: "*-2.25,0,0*"

Bottom Washers:

a) Offset the working plane by entering: "*0,0,-(2*Compo_z+ClampPlate_z)*"

b) Rotate the working plane about the x axis 180 degrees by following **Utility Menu>**

WorkPlane>Offset WP by Increments. In the pop up menu slide the angle setting all the way to the right (90 degrees per increment) and click twice on the +x button. This will align the positive z axis with the normal of the bottom washers. NOTE: Y-Values of work plane offset are now opposite in sign.

c) Generate the half washer volume by following **Main Menu>Preprocessor> Modeling>Create>Volumes>Cylinder>Partial Cylinder.** In the dialog box enter *"WP X " = 0, "WP Y" = 0, "Rad-1" = Washer_ID/2, "Theta-1" =0,"Rad-2" = Washer_OD/2, "Theta-2" =-180, "Depth" = Washer_z* (Theta-2 is negative here because of the working plane rotation).

d) Offset the working plane by entering:" *2.25,0,0"*

e) Repeat step c)

f) Offset the working plane by entering: "*0,-2.25,0"*

g) Generate the full washer volume by following **Main Menu>Preprocessor> Modeling>Create>Volumes>Cylinder>Solid Cylinder.** In the dialog box enter *"WP X " = 0, "WP Y" = 0, "Rad-1" = Washer_ID/2, "Theta-1" =0,"Rad-2" = Washer_OD/2, "Theta-2" =0, "Depth" = Washer_z.*

h) Offset the working plane by entering: "*-2.25,0,0"*

i) Repeat step g)

The Nuts:

a) Offset the working plane by entering: "*0,0,Washer_z"*

b) Generate the first full cylindrical nut volume by following: **Main Menu> Preprocessor>Modeling>Create>Volumes>Cylinder>Solid Cylinder.** In the dialog box enter *"WP X " = 0, "WP Y" = 0, "Radius" = NutDiam/2, "Depth" = Nut_z.*

c) Offset the working plane by entering: "*2.25,0,0"*

d) Repeat step b) for the second full cylindrical nut volume.

e) Offset the working plane by entering: *"0,2.25,0"*

f) Generate the third, half cylinder nut volume by following: **Main Menu>Preprocessor> Modeling>Create>Volumes>Cylinder>Partial Cylinder.** In the dialog box enter *"WP X " = 0, "WP Y" = 0, "Rad-1" = 0, "Theta-1" =0, "Rad-2" = NutDiam/2, "Theta-2" =-180, "Depth" = Nut_z.*

g) Offset the working plane by entering: *-2.25,0,0*

h) Repeat step f) for the fourth, half cylinder nut volume.

i) Realign the working plane with the global coordinate system by following **Utility Menu>WorkPlane>Align WP with>Global Cartesian.** The full model geometry is now complete and is shown in Figure D.2 below.

Step 7 –Glue Steel Volumes:

The Final step in generating the hybrid connection assembly is to glue all steel volumes to each other. The VGLUE command will join all coincident areas of the selected volumes, which means that they will share nodes and elements. This saves us from

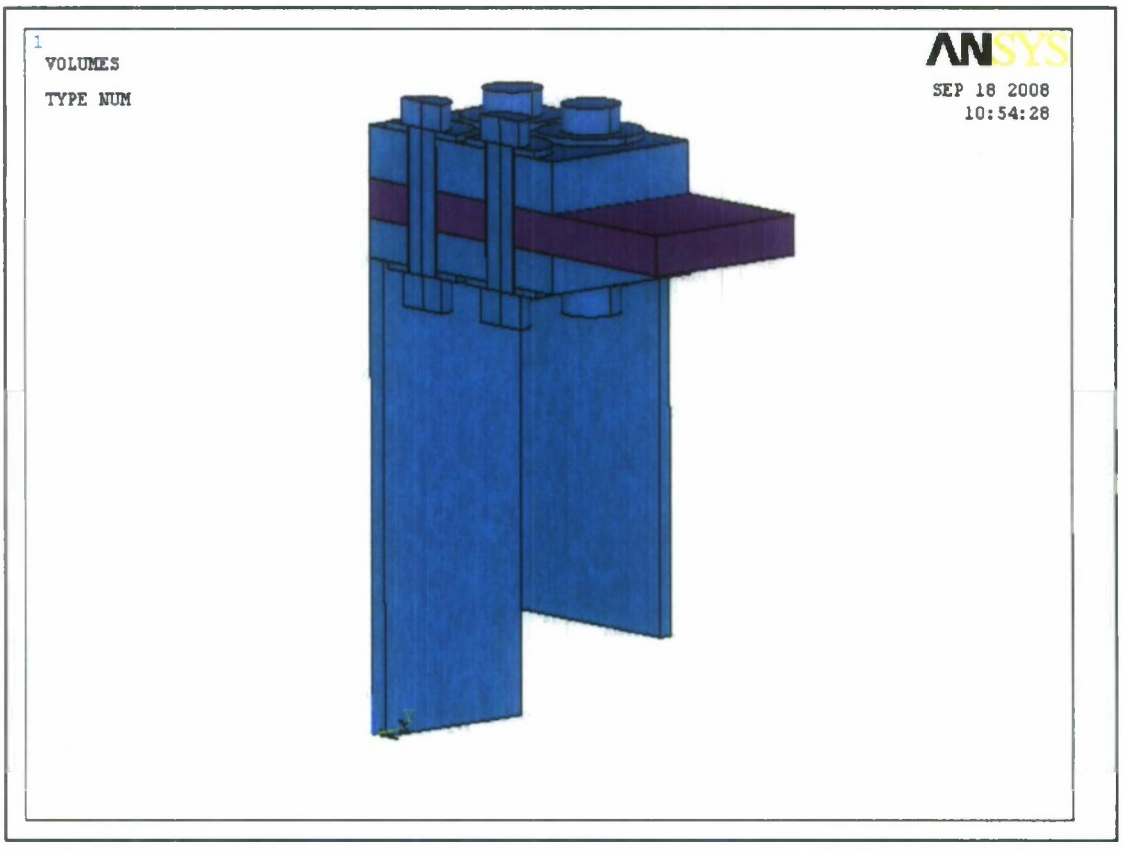

Figure C.5 – Full Quarter-Model Solid Clamped Geometry

having to generate contact pairs at each steel-steel interface.

a) Select all steel volumes by following **Utility Menu>Select>Entities.**

b) In the pop up menu's entity drop down menu, select: "*Volumes*". Leave the second drop down menu as is: "*By Num/Pick*". In the radio button list select the "*Unselect*" option and click **Ok**. Once the selection pop up is visible manually select the composite volume and click **Ok.** Now only the steel volumes are in the selected volume set.

c) To glue these volumes together follow **Main Menu>Preprocessor>Modeling> Operate>Booleans>Glue>Volumes.** In the selection pop up type "*all*". Now all coincident steel areas have been joined. In the command line, enter: "*allsel,allz*", which reselects all current components of the model, then navigate to: **Utility Menu>Plot> Replot**.

Step 8 – Meshing Steel Components:

Some of the areas making up the steel component volumes have to be conditioned for mesh errors not to occur. The element size values that are used in the following section were derived by simple trial and error. The sizes were altered until an error free mesh could be generated. Complete the following procedure:

a) Go to: **Utility Menu>Select>Entities.** In the Drop down menu select "*Volume*" and make sure the "*By Num/Pick*" and "*FromFull*" are also selected and click "*Ok*".

b) Select the following volumes: All bolt heads, all nuts and all washers

c) Go to: **Utility Menu>Plot>Replot.** (Now only the heads, nuts and washer should be displayed)

d) Main Menu>Preprocessor>Meshing>Mesh Tool. The mesh tool GUI will pop up

e) In the mesh tool GUI first set the following;

Under Element Attributes make sure that Global is selected and click "*set*"

In the Meshing Attributes GUI make sure that the element type is set to "*Solid92*", the material is set to "*1*", the real constants says "*none defined*" and finally that the element coordinate system is set to "*0*". If all applies then click "*Ok*".

In the mesh tool GUI under "*Size Control*", click the Global "*set*" button. In the Global Element Sizes GUI, enter 0.375 in the "*Size element edge length*" box and click "*Ok*".

Click the area size control "*set*" button. When the selection GUI pops up select the all outer areas making up the heads and nuts except the area in contact with the washers and then click "*Ok*". In the Element Size for the picked areas GUI enter 0.125 in the *Size* box and click *Ok*.

Click the area size control "*set*" button again and select the inside areas of the washers (inner cylindrical faces of the through hole) and click "*Ok*". In the Element Size for the picked areas GUI enter 0.0625 in the "*Size*" box and click "*Ok*".

Click the area size control "*set*" button again and select the areas between the inner cylindrical faces of the washer and the bolt shaft and click "*Ok*" (although the bolt shaft is not visible the thin area strip in question will be outlined and can be seen if magnified). In the Element Size for the picked areas GUI enter 0.0625 in the *Size* box and click "*Ok*". Close the mesh tool GUI by clicking "*Close*".

f) In the command line enter" *vsel,all*" to reselect all volumes and follow **Utility Menu>Plot>Replot.**

g) Follow **Utility Menu>Select>Entities.** In the Drop down menu select "*Volume*" and make sure the "*By Num/Pick*" and "*Unselect*" are also selected and click "*Ok*". Now select the Composite volume and click "*Ok*".

h) Go to: Utility Menu>Plot>Replot.

i) Reopen the mesh tool and make sure that under "*Mesh*" the following selections are active: The drop down menu selection should be set to "*Volume*", the shape should be set to "*Tet*" and "*free*" meshing should be active. If all applies then click "*Mesh*" and in the selection GUI type "*all*" in the command line.

j) During meshing you will see a warning message appear. To fix the elements in question, do the following. Go to: **Main Menu>Preprocessor>Meshing>Modify Mesh>Improve Tets>Volumes.** In the selection GUI type "*all*". When this is finished the improvement statistics will be displayed in a pop-up window. Close this window and follow: **Main Menu>Preprocessor>Meshing>Check Mesh>Individual Elements>Plot Warning/Error Elements**. If there were still faulty elements in the mesh, this command will plot them. In this case one degree of improvement takes care of the elements producing a warning so a pop up will say that there are no error elements to plot. Close the status message and type "*allsel,all*" in the command line, and follow: **Utility Menu> Plot>Elements.** The steel components are now meshed, as provided in Figure D.3.

Step 9 – Meshing Composite:

For this component only the global element size will be set. Complete the following

procedure:

Figure C.6 – Solid Clamped-Model Mesh of Steel Components

a) Go to: **Utility Menu>Select>Entities.** In the Drop down menu select "*Volume*" and make sure the "*By Num/Pick*" and "*FromFull*" are also selected and click "*Ok*".

b) Select the composite volume

c) Go to: Utility Menu>Plot>Replot

d) Go to: **Main Menu>Preprocessor>Meshing>Mesh Tool**, the mesh tool GUI will pop up. In the mesh tool GUI first set the following:

Under Element Attributes make sure that Global is selected and click "*set*"

In the Meshing Attributes GUI make sure that the element type is set to "*Solid186*", the material is set to *2*, the real constants says "*none defined*" and finally that the element

coordinate system is set to 0. Click *"Ok"*.

In the mesh tool GUI under Size Control, click the Global *"set"* button. In the Global Element Sizes GUI, enter 0.125 in the *"Size element edge length"* box and click *"Ok"*. Under *"Mesh"* the following selections have to be made: The drop down menu selection should be *"Volume"*, the shape should be set to *"Hex"* and *"sweep"* meshing should be active with *"Auto Src/Trg"* selected in the drop down menu. If all applies then click *"Sweep"* and in the selection GUI type *"all"* in the command line. The composite is now meshed, as well as the entire solid model, as seen in Figures D.4 and D.5.

Step 10 – Apply Pretension to Bolts:

To insert and load the pretension elements into the existing model do the following:

a) Go to: **Utility Menu>Select>Entities.** In the Drop down menu select *"Volume"* and make sure the *"By Num/Pick"* and *"FromFull"* are also selected and click *"Ok"*. Select

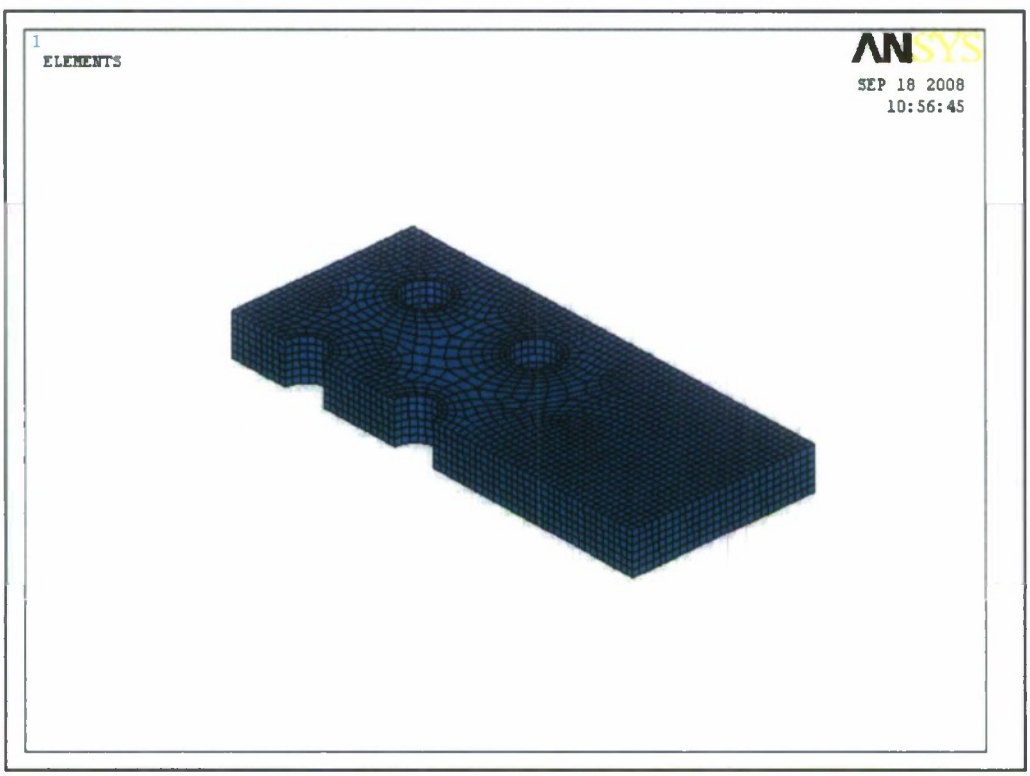

Figure C.7 – Composite Solid Model Mesh

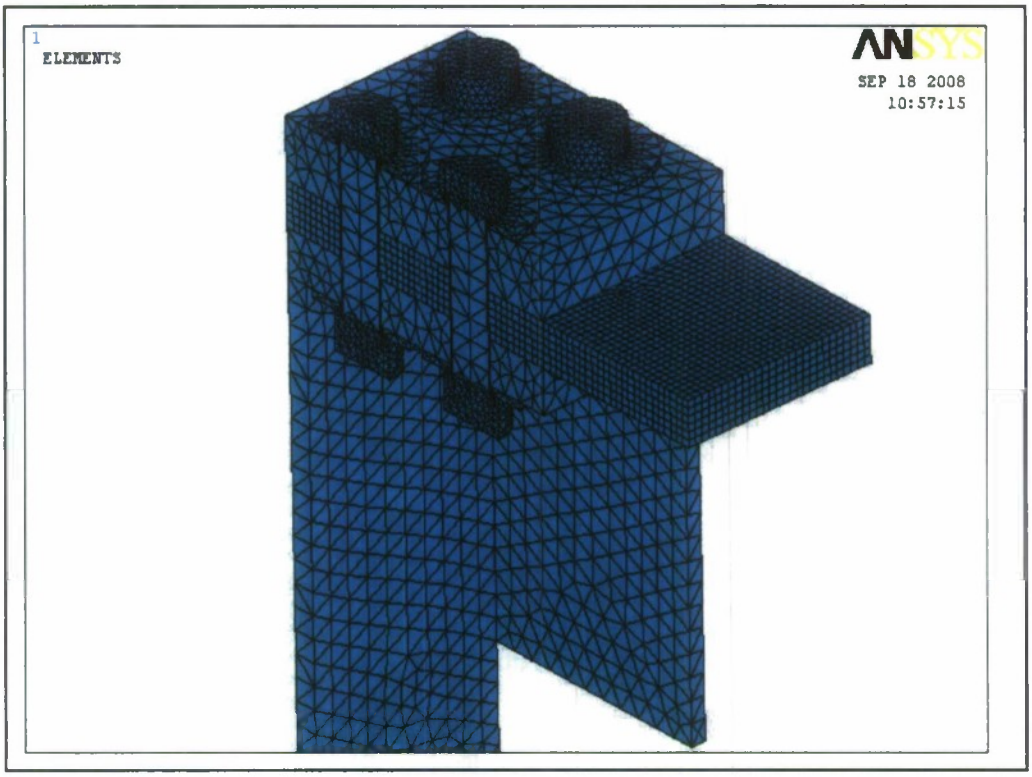

Figure C.8 – Complete Clamped Solid Model Mesh

the four bolt shaft volumes.

b) Go to: Utility Menu>Plot>Replot

c) Go to: **Main Menu>Preprocessor>Sections>Pretension>Pretension Mesh>With Options>Divide at Value>Elements in Volu.** Select the first volume, for example one of the half bolt shafts, and click "*Ok*" (You can only select one volume at a time).

d) Enter the following into fields in the Mesh Pretension Section GUI

Enter the following information in the dialog box and click "*Ok*":

NAME: Half_1

KCN: Global Cartesian

KDIR: Z-axis

VALUE: 10.25 (Z location of mid bolt shaft)

ECOMP: elems

e) Repeat this step for all bolt shafts, continually altering the NAME accordingly. Now the pretension sections have been generated and can be loaded in the solution phase.

Step 11 – Defining Contact for Material Interfaces:

The final preprocessor step is to generate contact pairs between the composite plate, the base assembly, and the clamping plate. Follow these steps to generate the contact pairs:

a) Open the "Contact Manager".

b) Click the "*Contact Wizard*" button in the Contact Manager GUI.

c) In the pop up GUI check the following:

Target Surface: "*Areas*"

Target Type: "*Flexible*"

d) Click "Pick Target".

e) Select the steel contact surfaces of the base assembly and the clamping plate and click "*Apply*". When the selection window closes and the wizard GUI reappears click "*Next*".

f) In the contact surface window check the following:

Contacts Surface: "*Areas*"

Contact Element Type: "*Surface-to-Surface*"

g) Click "Pick Contact".

h) Select the composite contact surfaces and click *"Apply"*. When the selection window closes and the contact wizard GUI reapers click *"Next"*.

i) Click "Optional Settings." Under the "Basic" tab select "Behavior of contact surface: Bonded".

j) Click *"Ok"* and then *"Create"*.

Step 12 – Solution Phase:

The model is now ready for the solution phase where boundary conditions and loads are applied. The first step is to define boundary conditions, so that the symmetry of the model about the two cut planes is accurate.

Symmetry Constraints:

a) Follow: Main Menu>Solution>Define Loads>Apply>Structural>Displacement> Symmetry B.C.>On Areas. Select all applicable areas and click *"Ok"*.

Displacement Constraints:

a) Follow: **Main Menu>Solution>Define Loads>Apply>Structural>Displacement> on Areas.** Select the narrow area at the very bottom of the base assembly. In the properties GUI, check the following:

DOFs to be constrained: *"All DOF"*

Apply as: "Constant value"

VALUE: 0

b) Click *"Ok"*. Now that the model is fully constrained, the pretension loads may be applied to the pretension sections.

Pretension Loading:

a) Follow: **Main Menu>Solution>Define Loads>Apply>Structural>Pretnsn Sectn.**

The pretension section load GUI will pop up with a listing of existing pretension sections. Make sure the first section in the list is highlighted (in this example it is "*Half_1*").

b) Under pretension load, check the following:

Apply at LS: 1

Force: 4000 (8000 in the case of full bolt shaft)

Lock at LS: 2

Click "*Apply*".

c) Select the next section in the list and repeat step b), changing the force value when applying the load to the full bolt shaft and when finished click "*Ok*". The bolts will now be preloaded in load step 1 and the pretension will be locked in load step 2 when the actual load is applied.

Solve Load Step 1:

a) Follow: Main Menu>Solution>Analysis Type>new Analysis. Check "*Static*"

b) Follow: **Main Menu>Solution>Solve>Current LS**. Click "*Ok*" in the pop up window, and this will solve load step 1. After the first load step has been solved, which can take on the order of 1 hour depending on the computer used, the actual load is applied and the model is resolved starting at the solution obtained in load step 1.

Restarting analysis at the end of LS 1:

a) Follow **Main Menu>Solution>Analysis Type>Restart**. In the pop up GUI set "*Restart from Load Step*" to 1.

b) Apply the actual force by following: **Main Menu>Solution> Define Loads>Apply> Structural>Force/Moment>On Nodes**. Select the all nodes at the top far edge of the composite plate and click **Ok**, all while noting the node count in the selection GUI. In the pop up window check the following:

"Lab Direction of force/mom": "FZ"

"Apply as": "Constant value"

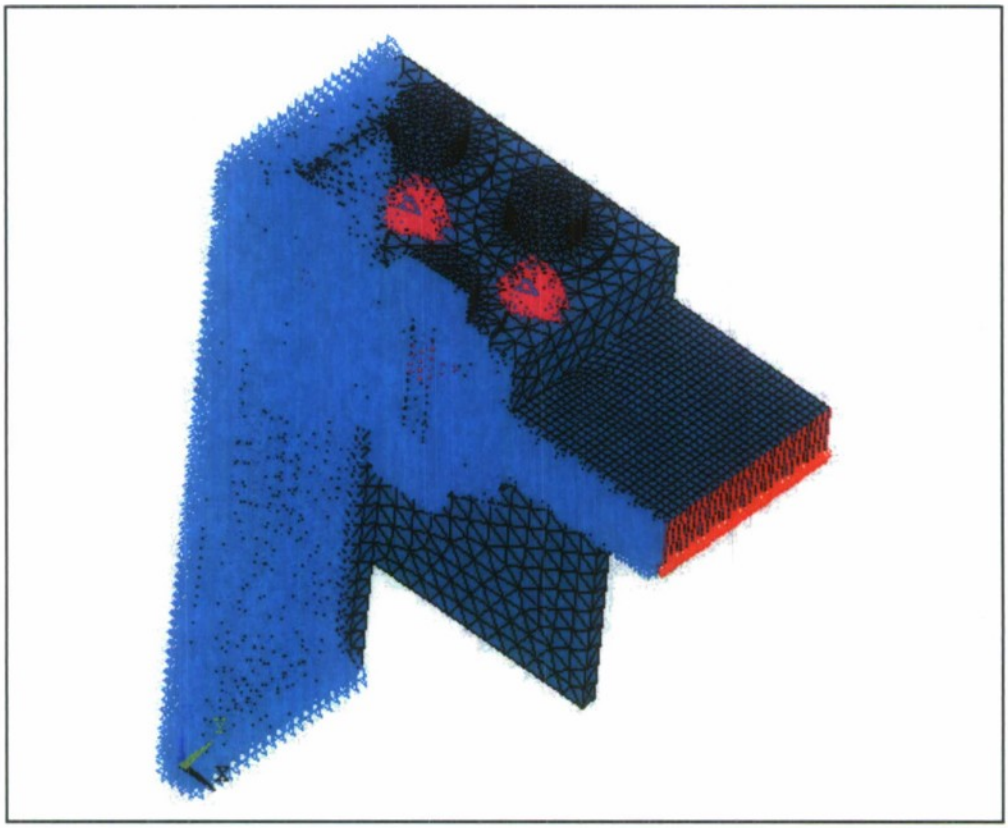

Figure C.9 – Clamped Model Showing Symmetry Constraints with Applied Load

"VALUE": "-2000/node_count" (in this case "node_count" = 55, "VALUE" = -36.36)

Once finished click *"Ok"*. Figure D.6 show the model with symmetric boundary condition constraints, as well as the applied external load. Now, follow: **Main Menu>Solution>Solve>Current LS**. Click *"Ok"* and let the program solve the second load step. Note: This load step could take a few hours to solve depending on the computer used, and once finished the model is complete.

REPORT DOCUMENTATION PAGE

Form Approved
OMB No. 0704-0188

PLEASE DO NOT RETURN YOUR FORM TO THE ABOVE ADDRESS.

1. REPORT DATE *(DD-MM-YYYY)*	2. REPORT TYPE	3. DATES COVERED *(From - To)*
31-August-2009	Project Report	1-Jun-2005 to 30-June-2009

4. TITLE AND SUBTITLE

FINITE ELEMENT ANALYSES AND EXPERIMENTAL TESTING OF HYBRID COMPOSITE/METAL JOINTS SUBJECTED TO FULLY REVERSED FLEXURE FATIGUE LOADING

5a. CONTRACT NUMBER

5b. GRANT NUMBER

N00014-05-1-0735

5c. PROGRAM ELEMENT NUMBER

6. AUTHOR(S)

Dow, Douglas
Caccese, Vincent
Vel, Senthil S.

5d. PROJECT NUMBER

5e. TASK NUMBER

5f. WORK UNIT NUMBER

7. PERFORMING ORGANIZATION NAME(S) AND ADDRESS(ES)

University of Maine
Office of Research and Sponsored Programs
5717 Corbett Hall
Orono, ME 04469-5717

8. PERFORMING ORGANIZATION REPORT NUMBER

C-2004-015-RPT-06

9. SPONSORING/MONITORING AGENCY NAME(S) AND ADDRESS(ES)

Office of Naval Research
Ballston Center Tower One
800 North Quincy St.
Arlington, VA 22217-5660

10. SPONSOR/MONITOR'S ACRONYM(S)

ONR

11. SPONSORING/MONITORING AGENCY REPORT NUMBER

12. DISTRIBUTION AVAILABILITY STATEMENT

Approved for Public Release, Distribution is Unlimited

13. SUPPLEMENTARY NOTES

14. ABSTRACT

The goal in this research is to accurately assess the fatigue life of hybrid composite/metal connections focusing upon bolted joints used in removable panels. Experimental testing was performed in flexure fatigue as part of this effort and is essential for fatigue life evaluation. In addition, analytical studies were performed using finite element analysis. Existing finite element modeling software offers a robust method for assessing the structural integrity of proposed hybrid connections. Ansys, a finite element modeling program, was used to study the response of two hybrid connection configurations subjected to fully-reversed flexure fatigue loading. A through-the-thickness stress investigation at critical locations in the connection was developed. Variables in the hybrid connection were altered in a parametric study and effects on flexibility and stress were observed. Through the use various models, a method for predicting the fatigue life in hybrid joints is proposed.

15. SUBJECT TERMS

Hybrid Structures; Fatigue; Bolted Connections; Composites.

16. SECURITY CLASSIFICATION OF:			17. LIMITATION OF ABSTRACT	18. NUMBER OF PAGES	19a. NAME OF RESPONSIBLE PERSON
a. REPORT	b. ABSTRACT	c. THIS PAGE			Vincent Caccese
U	U	U	UU	170	19b. TELEPONE NUMBER *(Include area code)* (207) 581-2131

Standard Form 298 (Rev. 8-98)
Prescribed by ANSI-Std Z39-18